3-19-2004

Chemical Investigation of Three Antarctic Marine Sponges

Young Chul, Park
University of South Florida

Chemical Investigation of Three Antarctic Marine Sponges

by

Young Chul Park

A dissertation submitted in partial fulfillment
of the requirements for the degree of
Doctor of Philosophy
Department of Chemistry
College of Arts and Sciences
University of South Florida

Major Professor: Bill J. Baker, Ph.D
Robert Potter, Ph.D
Edward Turos, Ph.D
Abdul Malik, Ph.D

Date of Approval:
March 19, 2004

Keywords: marine natural products, tryptophan catabolism,
chemical defense, Antarctic invertebrates, erebusinone

DEDICATION

This dissertation is dedicated to my wife Jung Sook, who never fails to remind me how every day is most precious. I would also like to dedicate this work to my daughter, Yei Ryun and my son, Min Jun.

I would like to dedicate this work to my dear parents, who gave me their love and patience. I would also like to dedicate this work to my father-in-law and my mother-in-law, for their patience and understanding on the value of education. Without their support, love, and patience, there is no way I could possibly have accomplished this.

ACKNOWLEDGMENTS

First and foremost, I would like to acknowledge my adviser, Dr. Bill J. Baker. This dissertation would not have been possible without his assistance and financial support. He has taught, inspired, and challenged me throughout this process. I would like to thank Jill Baker, for her concern towards my family.

I would like to thanks Dr. James B. McClintock and Dr. Charles D. Amsler at the University of Alabama at Birmingham for the field and laboratory assistance. I would like to thank Dr. Steven Mullen at the University of Illinois at Urbana-Champaign, for the mass spectral data. Also I would like to thank Dr. Maya. P. Singh from Wyeth Pharmaceuticals and Dr. Fred Valeriote from Ford hospital for their bioactivity data.

Finally, I would like to acknowledge my committee members, Dr. Robert Potter, Dr. Edward Turos and Dr. Abdul Malik, for their encouragement and guidance. Last but not the least I would like to thank Dr. Baker's students who have given me assistance in many ways.

TABLE OF CONTENTS

LIST OF FIGURES

LIST OF TABLES

LIST OF SCHEMES

LISTS OF ABBREVIATIONS

Ac_2O	acetic anhydride
$[\alpha]$	specific rotation = $100\alpha/lc$
$BH_3S(CH_3)_2$	dimethylsulfide borane
BnBr	benzylbromide
Boc_2O	di-*tert*-butyldicarbonate
BuLi	butyllithium
BuOH	butanol
CaH_2	calcium hydride
$CDCl_3$	deuterated chloroform
CF_3COOH	trifluoroacetic acid
CH_2Cl_2	dichloromethane
CH_3CN	acetonitrile
$CoCl_2$	cobalt chloride
C18	octadecyl bonded silica
δ	chemical shifts
DEPT	distortionless enhancement by polarization transfer
DMSO-d_6	deuterated dimethylsulfoxide
EtOAc	ethylacetate
EtOH	ethanol
ε	the molar extinction coefficient in UV spectroscopy
gCOSY	gradient correlation spectroscopy

gHSQC	gradient heteronuclear single quantum correlation
gHMBC	gradient heteronuclear multiple bond connectivity
HRFAMS	high resolution fast atom bombardment mass spectrometry or spectrum
HREIMS	high resolution electron impact mass spectrometry or spectrum
HRESIMS	high resolution electrospray ionization mass spectrometry or spectrum
HCl	hydrochloric acid
HPLC	high performance liquid chromatography
IR	infrared
J	coupling constant
$^{n}J_{CH}$	n-bond hydrogen to carbon correlation (n = 2, 3 or 4)
$^{n}J_{HH}$	n-bond hydrogen to hydrogen correlation (n = 2, 3 or 4)
K_2CO_3	potassium carbonate
KOH	potassium hydroxide
$LiAlH_4$	lithium aluminum hydride
LREIMS	low resolution electron impact mass spectrometry or spectrum
LRESIMS	low resolution electrospray ionization mass spectrometry or spectrum
LRFAMS	low resolution fast atom bombardment mass spectrometry or spectrum
λ_{max}	the wavelength at which maximum absorption occurs
MeOH	methanol
MeOH-d_4	deuterated methanol
MTPA-Cl	α-methoxy-α–(trifluoromethyl)phenylacetyl chloride
$MgSO_4$	magnesium sulfate
m/z	mass/charge for mass spectrometry

$NaHCO_3$	sodium bicarbonate
$NaBH_4$	sodium borohydride
Na_2SO_4	sodium sulfate
$Na_2S_2O_3$	sodium thiosulfate
NMR	nuclear magnetic resonance
Pd	palladium
ROESY	rotating-frame overhauser enhancement spectroscopy
S_N2	bimolecular nucleophilic substitution
THF	tetrahydrofuran
TOCSY	total correlation spectroscopy
UV	ultraviolet

Chemical Investigation of Three Antarctic Marine Sponges

Young Chul Park

ABSTRACT

This thesis describes the chemical investigation of three marine sponges from Antarctica and the total syntheses of natural products erebusinone (**12**) and its derivative, erebusinonamine (**52**). Investigation of the yellow Antarctic marine sponge *Isodictya setifera* resulted in the isolation of two secondary metabolites, purine analog (**32**) and 3-hydroxykynurenine (**24**). Chemical investigation of *Isodictya setifera* led to the isolation of six secondary metabolites which included 5-methyl-2-deoxycytidine (**25**), uridine (**28**), 2-deoxycytidine (**31**), homarine (**37**), hydroxyquinoline (**33**), 3-hydroxykynurenine (**24**). The latter two compounds were found to be intermediates of tryptophan catabolism in crustaceans. From the Antarctic marine sponge *Isodictya antractica* ceramide analog (**39**) was isolated and its chemical structure was assigned by a combination of spectroscopic and chemical analyses. Stereochemistry was determined by modified Mosher's method. Erebusinone (**12**), a yellow pigment isolated from the Antarctic marine sponge *Isodictya erinacea* has been implicated in molt inhibition and mortality against the Antarctic crustacean amphipod, *Orchomene plebs*, possibly serving as a precursor of a xanthurenic acid analog.

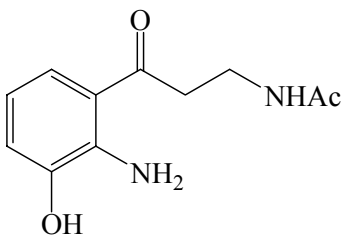

Erebusinone (**12**)

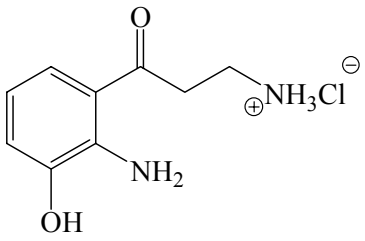

Erebusinonamine (**52**)

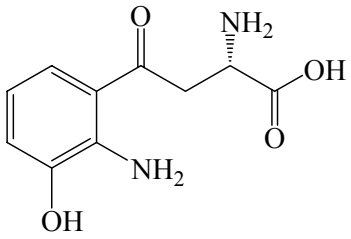

3-Hydroxykynurenic acid (**24**)

Thought to act as a 3-hydroxykynurenine 24 mimic, erebusinone (**12**) may be involved chemical defense.[1] This appears to be the first example in the marine realm of an organism utilizing tryptophan catabolism to modulate molting as a defensive mechanism. To further investigate the bioactivity and ecological role of erebusinone (**12**), the synthesis of this pigment was carried out in an overall yield of 44% involving seven steps which were economical and convenient. Erebusinonamine (**52**) was also similarly synthesized in eight steps with an overall yield of 45%.

Reference

1. Moon B. H.; Park Y. C.; McClintock J. B.; Baker B. J., *Tetrahedron* **2000**, *56*, 9057-9062.

Chapter 1. INTRODUCTION

1.1. A Brief History of Natural Products

Natural products of terrestrial plants have been utilized for many purposes such as medicines, euphoria and hunting. The use of crude natural products to treat cancer has a long history, recorded at least as far back as the Ebers papyrus in 1550 B. C.[1] The origin of traditional Chinese medicine also dates back to around 2500 B. C.[2] With the origin of organic and biological chemistry in the 19th century, chemists and biologists began the investigation of bioactive compounds in order to identify the individual active ingredients from the terrestrial plants, freshwater, and marine organisms.

The study bioactive plant compounds such as morphine, strychnine, atropine, quinine and colchicine was begun in the early 1800's. However, the structures of these secondary metabolites were not elucidated until a century.[3] The invention of advanced instrumentation tools, such HPLC (high performance liquid chromatography) and NMR (nuclear magnetic resonance) spectrometers enabled the characterization of minute quantities of secondary metabolites such as maitotoxin and taxol.[4-6]

1.2. Marine Natural Products Chemistry

Marine organisms have been investigated by natural products chemists for the past 40 years. Many of the secondary metabolites produced are both complex and quite

distinct from terrestrial natural products. Marine natural products chemistry has evolved from being the source of a handful of chemical curiosities 20 years ago to being one of the most productive areas of natural products research.[7-9] The oceans and seas have been the focus of considerable attention for their biological resources. Marine organisms have evolved under markedly distinctive chemical and physical conditions from terrestrial plants and animals.[10] Oceanic marine organisms are of scientific interest for two major reasons. First, they constitute a major share of the Earth's biological resources.[11] Second, marine organisms often possess unique structures, metabolic pathways, reproductive systems, and sensory and chemical defense mechanisms,[12,13] because they have adapted to environmental conditions which have high biodiversity. Their range encompasses the cold polar Arctic and Antarctic seas at low temperature, the warm water tropics and the bright shallow waters to the great pressures of the deep ocean floor. Yet the potential of this domain as the basis for new biotechnology resources such as drug discovery remains largely underexplored. Recent improvements in underwater life-support systems, however, have facilitated the collection of organisms from previously unexplored regions of the oceans. Many bioactive chemicals from the marine environment have been isolated and characterized.[14-31] Same hold great promise for useful biotechnological applications, such as development of a wide range of pharmaceutical compounds, medical research materials, agricultural products and processes, novel energy sources and bioremediation techniques.[32,33] With knowledge of these factors, several marine invertebrates and microorganism groups have been noted for their potential for new drug discovery.[33,34] Many marine invertebrates such as algae, corals, sponges and ascidians (tunicates) use

highly evolved chemical compounds for purposes such as reproduction, communication, and protection against predation, infection, and competition.[11] These bioactive chemical compounds may have antibiotic, anti-inflammatory, antiviral, cytotoxic, antitumor or antifungal properties. Secondary metabolites, which are not needed by the organism for basic or primary metabolic processes such as food digestion, energy storage, or metabolism, are believed to confer some evolutionary advantage because many marine invertebrates living in densely populated habitats are non-motile, have primitive immune systems, and are found symbiotic relationships with microorganisms.[35,36]

Natural product chemists have been interested in sponge-microbe symbioses because of the possibility that the diverse, bioactive chemical structures found in sponges might be produced by microorganisms. More natural products have been reported from sponges[37] than from any other marine invertebrate phylum, and many of the most promising pharmaceuticals and agents for cell biological research were isolated from sponges.[37] Marine sponges belong to the phylum *Porifera* and are actually simple cell aggregates, which are usually referred to as the most undeveloped multicellular animals.[14-31] In contrast, ascidians belong to the phylum *Chordata*, which encompasses all vertebrate animals, including mammals. As much as 40% of the cell mass of sponges, ascidians and other marine macroorganisms could be composed of prokarytic organisms.[38,39]

The first isolation of a secondary metabolite from a marine organism was Tyrian purple (6,6'-dibromoindigotin) (**1**) from a marine mollusk. Identified in 1901,[7,40]

Tyrian purple (**1**) was also the first marine natural product to be used for commercial applications.

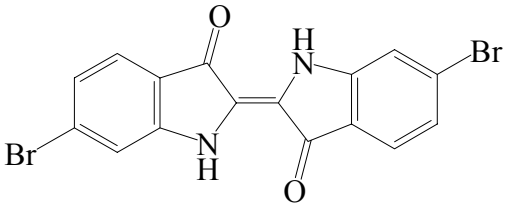

Tyrian Purple (**1**)

The marine environment became the focus of natural products drug discovery research because of its relatively unexplored biodiversity compared to terrestrial environments. The potential for marine natural products as pharmaceuticals was introduced by the pioneering work of Bergmann in 1950's which led to the discovery of Ara-A (**2**)[41] and Ara-C (**3**),[42] the only two marine derived pharmaceuticals that are clinically available today. The anticancer drug cytosine arabinoside (Ara-C) (**3**) is used to treat acute myelocytic leukemia.[43] The antiviral drug adenine arabonoside (Ara-A) (**2**) is used for the treatment of herpes virus infections.[44,45]

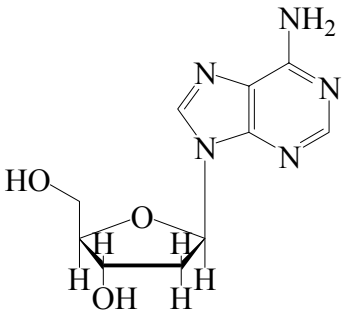

Ara-A (**2**)
Adenine Arabinoside
(Vidarbine)

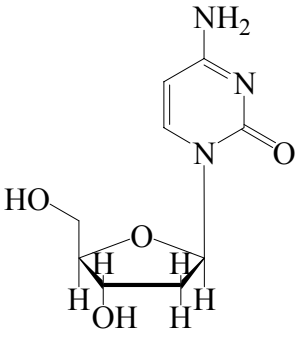

Ara-C (**3**)
Cytosine Arabinoside
(Cytarabine)

Both are derived from nucleosides isolated from a shallow water marine sponge *Cryptotethya crypta* collected off the coast of Florida.

The cytotoxic macrolide bryostantin (**4**), isolated from the bryozoan *Bugula neritina*, was found to have anticancer activity against murine P388 lymphocytic leukemia *in vitro* cell line.[46] It is now in clinical trials for the treatment of leukemias, lymphomas, melanoma and solid tumors.[47,48]

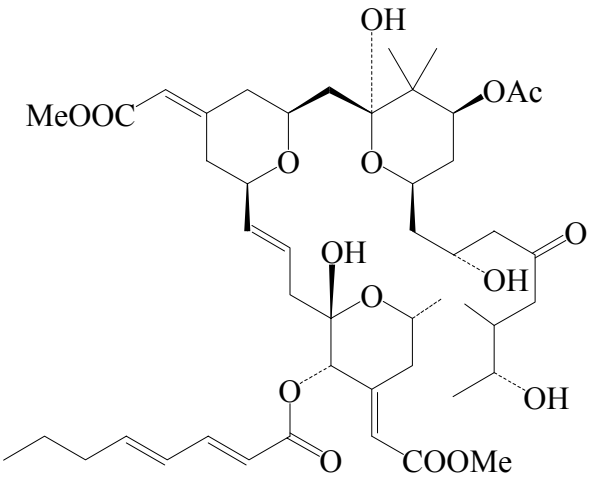

Bryostatin (**4**)

Another example of an important marine natural products include ecteinascidin 743 (**5**), a secondary metabolite displaying strong anticancer activity, which was first isolated from the mangrove tunicate, *Ecteinascidia turbinata* in 1990.[50, 51]

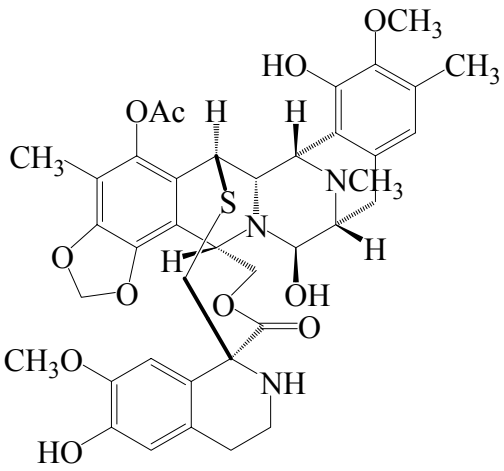

Ecteinascidin 743 (**5**)

Marine prostaglandins, first discovered in a gorgonian have since been isolated from other invertebrates and from red algae.[53] Punaglandins,[52] which are halogenated antitumor eicosanoids, were isolated from the octocoral *Telesto riisei*. These punaglandins (**6**, **7**) are characterized by C-12 oxygen and unprecedented C-10 chlorine functions and inhibit L1210 leukemia cell proliferation with an IC_{50} values in the range of 0.02 μg/mL.[54, 55]

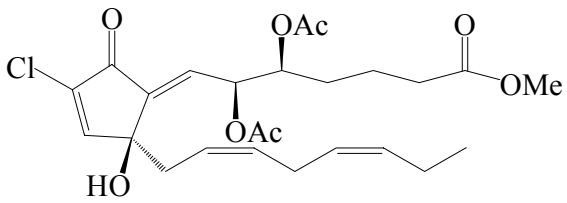

Punaglandin 3 (**6**)

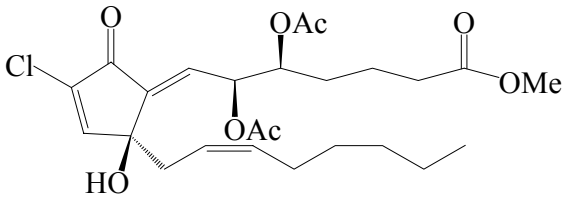

Punaglandin 4 (**7**)

Papuamine (**8**), an antifungal pentacyclic alkaloid from the marine sponge *Haliclona sp.,* a thin, red, encrusting sponge, is formally derivable from a C_{22} unbranched hydrocarbon and 1,3-diaminopropane and inhibits the growth of the fungus *Trichophyton mentagrophytes*.[56]

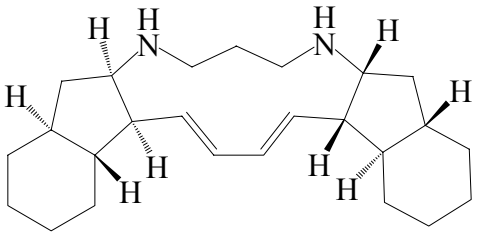

Papuamine (**8**)

Spongia tubulifera found in the Florida Keys contains two types of toxins. The spongianolids, exemplified by spongianolide A-F (**9**,**10**) and kuropongin (**11**) are a series of cytotoxic sesterterpenes which display potent MCF-7 mammary tumor cell inhibition activity, inhibition of protein kinase C and antibiotic activity, displaying 5 mm zones of inhibition at 100 μg/disk toward a host of antibiotic tester strains.[57]

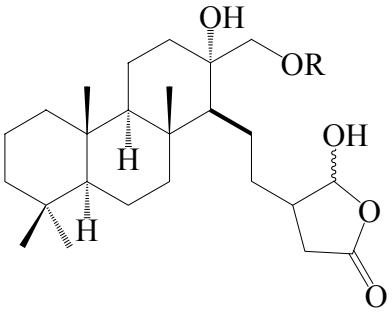

Spongianolides A - B (**9**)

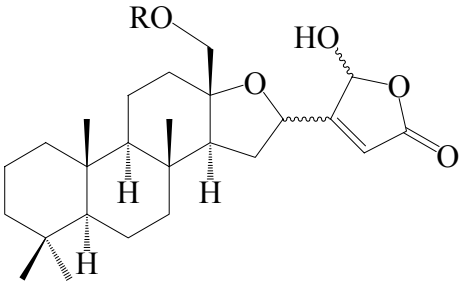

Spongianolides C - F (**10**)

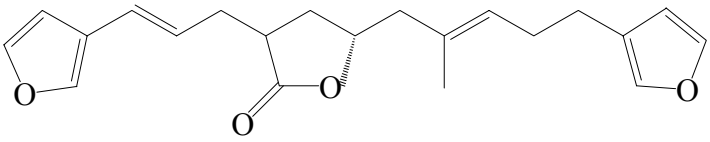

Kurospongin (**11**)

Marine sponges are among the most prolific sources of diverse chemical compounds with therapeutic potential. Of the more than 5000 chemical compounds derived from marine organisms, more than 30 percent have been isolated from sponges.[49]

1.3. Antarctic Marine Natural Products

The Antarctica marine benthos has diverse and abundant biological and ecological communities. For 20 million years the Antarctica benthos has had physically unique, isolated environments and ecology. These factors provide a basis to study the chemical and biological interactions such as competition and predation. Secondary metabolites from Antarctica have recently begun to be studied and they have been found to display unique biological activities such as cytotoxic, antimicrobial, antifungal, and antiviral properties. This may result from unique functional roles for Antarctic species.[58]

On the benthos of McMurdo Sound, Antarctica, sponges are found to occupy 55% of the surface area.[59] The sea star *Perknaster fuscus* and the amphipod *Orchomene plebs* are predominant and voracious sponge predators. We reported that the bright yellow marine sponge *Isodictya erinacea* is a conspicuous member of the sponge community on the McMurdo Sound and suggested that despite a lack of physical protection such as spicules, *I. erinacea* is chemically defended against predator *O. plebs*.[60,61]

Secondary metabolites, erebusinone (**12**), erinacine (**13**) were isolated from *I. erinacea*. Erebusinone (**12**) displayed molt inhibition leading to increased mortality in the predator amphipod, *Orchomene plebs*, serving as the first example in the marine realm of molt inhibition as a chemical defense mechanism. Erinacine (**13**) has shown

cytotoxcity (LD_{50} 50 μg/mL) against L5178Y mouse lymphoblastoid cells and displayed chemical deterrence toward the sea star *Perknaster fuscus.* [60,61,62]

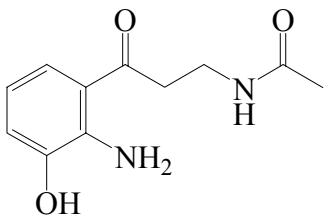

Erebusinone (**12**)

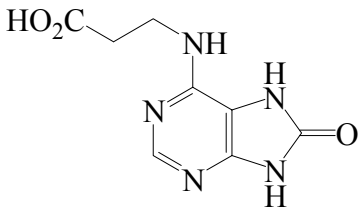

Erinacean (**13**)

Sponges of the genus *Latrunculia apicalis* have been chemically studied. Ichthyotoxic and cytotoxic agents have been reported from the Red Sea *Latrunculia magnifica*[63] and South Pacific *Latrunculia* species.[64] Discohabdin C (**14**) and G (**15**), imino-quinone pigments having antibiotic and cytotoxic activity and influencing sea star (*Perknaster fuscus*) feeding behavior were isolated from the Antarctic sponge *Latrunculia apicalis* Ridley and Dendy from McMurdo Sound.[65] Variolin A (**16**) is unusual cytotoxic alkaloid, has been isolated from the bright red sponge *Kirkpartrickia variolosa*.[66]

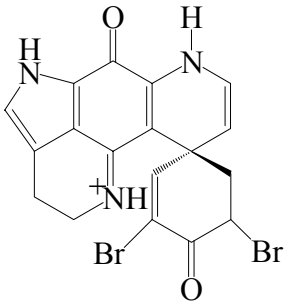

Discorhabdin C (**14**)

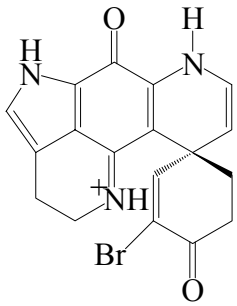

Discorhabdin G (**15**)

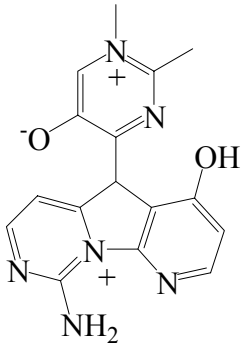

Variolin A (**16**)

Rhapsamine (**17**), a linear C28 polyene substituted by terminal 1,3-diaminoglycerol groups was isolated from the Antarctic sponge *Leucetta leptorhapsis* from the Ross sea. It was found to have potent cytotoxicity displaying LC_{50} of 1.8 μM in the KB nasopharyngeal cell line.[67]

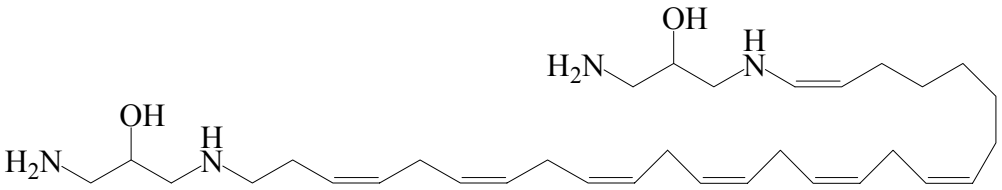

Rhapsamine (**17**)

Secondary metabolites, membranolide (**18**), 9, 11-dihydrogracillin (**19**) and an isoquinoline pigment (**20**) were isolated from the bright yellow Antarctic sponge *Dendrilla membranosa*. The isoquinoline pigment, 4,5,8 trihydroxyquinoline-2-carboxylic acid displayed antibacterial activity against the marine bacteria *Vibrio angullarum* and *Beneckea harveyii B-392*.[68,69]

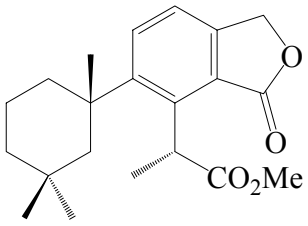

Membranolide (**18**)

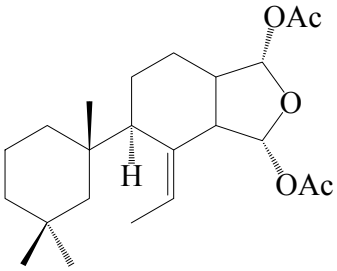

9,11-Dihydrogracilin A (**19**)

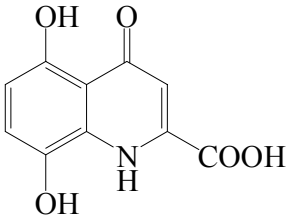

Isoquinoline pigment (**20**)

1.4. Research Objectives

Antarctic marine organisms have evolved differently under markedly distinctive chemical and physical conditions compared to terrestrial plants and animals. To study its chemical and ecological relationships of marine organisms in Antarctica, we have investigated three marine sponges. The benthos of McMurdo Sound is characterized by extensive sponge communities with spongevorous. Previously we reported that the secondary metabolite, erebusinone from *Isodictya erinacea* has been implicated in molt inhibition and mortality against an Antarctic crustacean, *Orchomene plebs*, perhaps serving as precursor of a xanthurenic acid analog.[61] With our previous metabolite profile, biological activities and ecological implications, we suggest that the Antarctic sponge, *Isodictya setifera* may have similar chemical defense mechanisms. To further investigate the chemical ecology of Antarctic sponges, we studied three Antarctic marine sponges, *Isodictya erinacea*, *Isodictya setifera*, and *Isodictya antarctica*. We also synthesized the natural product, erebusinone (**12**) and its derivative, erebusinonamine (**52**).

Chapter 2. CHEMICAL INVESTIGATION OF ANTARCTIC MARINE SPONGE *ISODICTYA ERINACEA*

2.1 Introduction

The marine sponge *Isodictya erinacea* (Topsent, 1916) (Family Esperiopsidae) is a conspicuous member of the Antarctic benthos which appears to be free of predation despite its lack of structural protection elements such as spicules (Figure 1).

Figure 1. *Isodictya erinacea* collected from at Erebus Bay, Ross Island, Antarctica (Photograph supplied by Bill J. Baker, University of South Florida)

We have previously reported that *I. erinacea* is chemically defended against the major Antarctic sponge predator, the sea star *Perknaster fuscus* and the isolation of

secondary metabolites, erebusinone (**12**), erinacean (**13**), 1,9-dimethylguanine (**21**), 7-methyladenine (**22**). Erebusinone, a yellow pigment is a tryptophan catabolite and appears to protect the sponge from crustacean predation by inhibition of molting in predatory amphipods. In the course of our continuing search for secondary metabolites possessing ecological and biological significance, *I. erinacea* has been further studied.[60, 61,70]

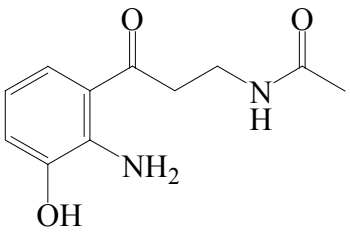

Erebusinone (**12**)

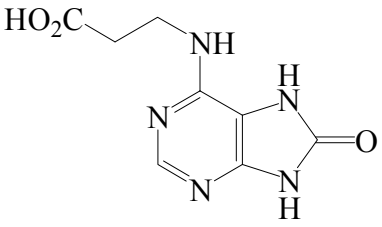

Erinacean (**13**)

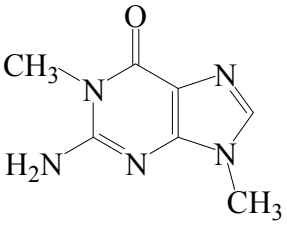

1,9-Dimethylguanine (**21**)

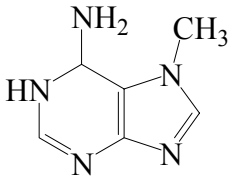

7-Methyladenine (**22**)

2.2 Extraction and Isolation of Secondary Metabolites

The chemical investigation of *Isodictya erinacea* collected from Erebus Bay on the western coast of Ross Island, Antarctica resulted in the isolation and structure elucidation of two compounds, purine (**23**) and 3-hydroxykynurenine (**24**)

The wet sample of *Isodictya erinacea* was extracted (Scheme 1) with MeOH at 7 ˚C. After concentration, the residue was subjected to Sephadex LH-20® column chromatography with MeOH/CH_2Cl_2 (1:1) to provide five fractions. Fraction 4 was subjected to C18 column chromatography with a MeOH/CH_2Cl_2 gradient system to give additional fractions. The first fraction 8 was chromatographed on silica gel to give 4 fractions. Fraction 11 (Scheme 1) was further chromatographed on silica gel yielding a purine analog (**23**) (68 mg, 0.0068% dry wt). Fraction 12 (104 mg) was chromatographed on silica gel to give 3-hydroxykynurenine (**24**) (13.5 mg, 0.00135% dry wt) (Scheme 1).

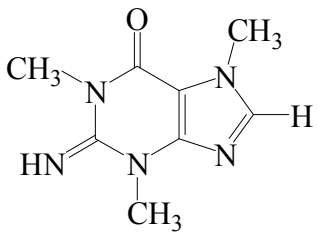

(**23**)

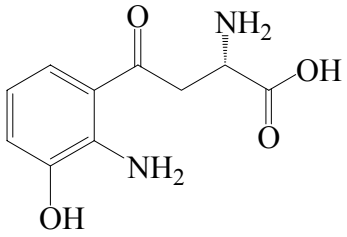

(**24**)

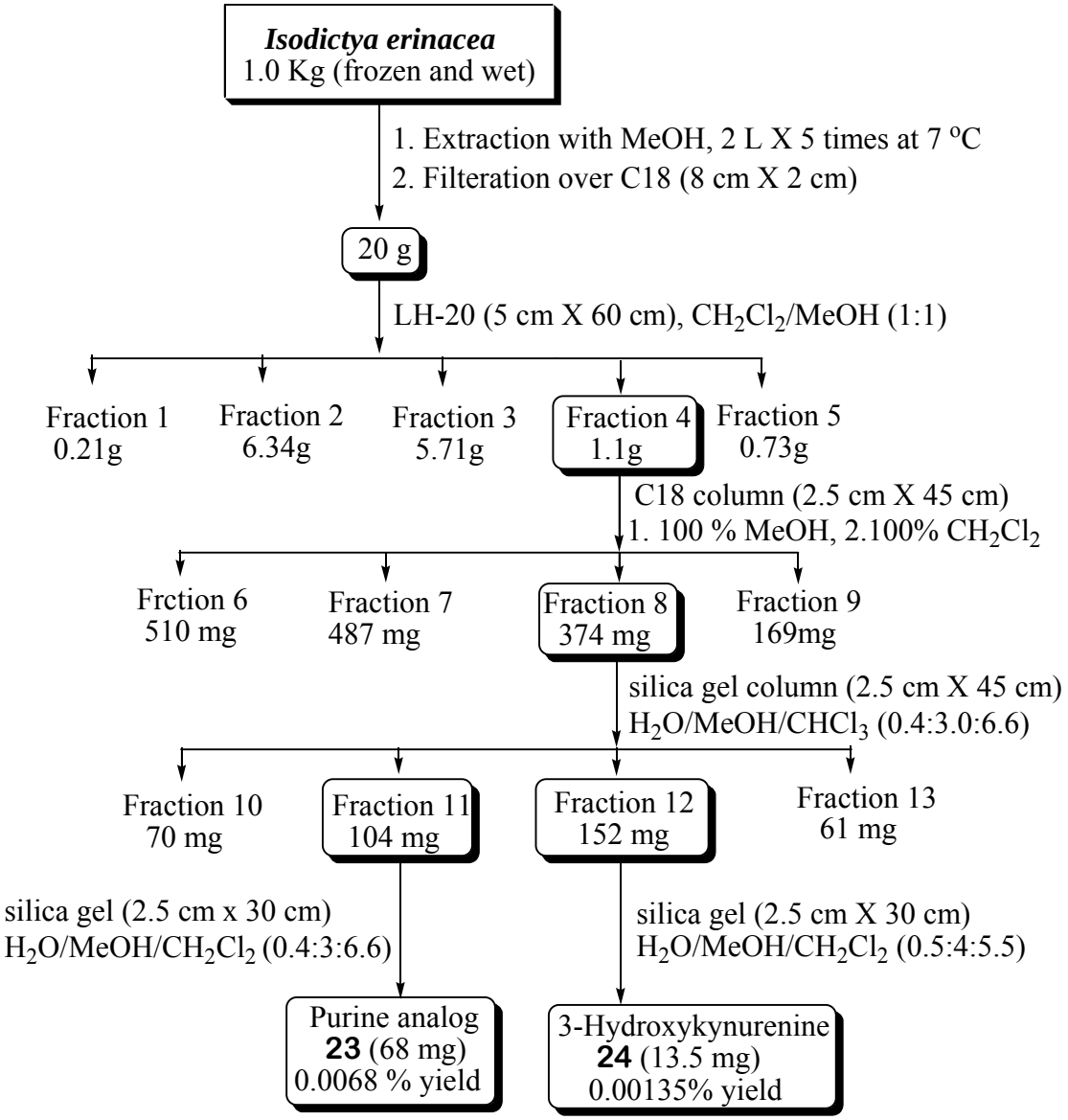

Scheme 1. Isolation of purine analog **23** and 3-hydroxykynurenine **24**.

2.3 Characterization of Purine analog (23)

From fraction 11, purine analog **23** was obtained as a pale brown solid and assigned the molecular formula $C_8H_{11}N_5O$, as deduced by HREIMS (observed *m*/*z* 193.0959, calculated 193.0964). The ^{1}H NMR spectrum (Figure 2) of purine analog (**23**) in DMSO-d_6 contained four signals at δ 3.36, δ 3.61, and δ 3.88 which suggested methyl protons bearing nitrogen and an aromatic methine at δ 8.17 with one exchangeable proton signal at δ 3.4. The ^{13}C NMR spectrum (Figure 3) showed three methyl groups at δ 33.4, 32.2, 29.3, one methine at δ 143.6 and four quaternary carbons at δ 152.5, 151.3, 148.2, 106.9.

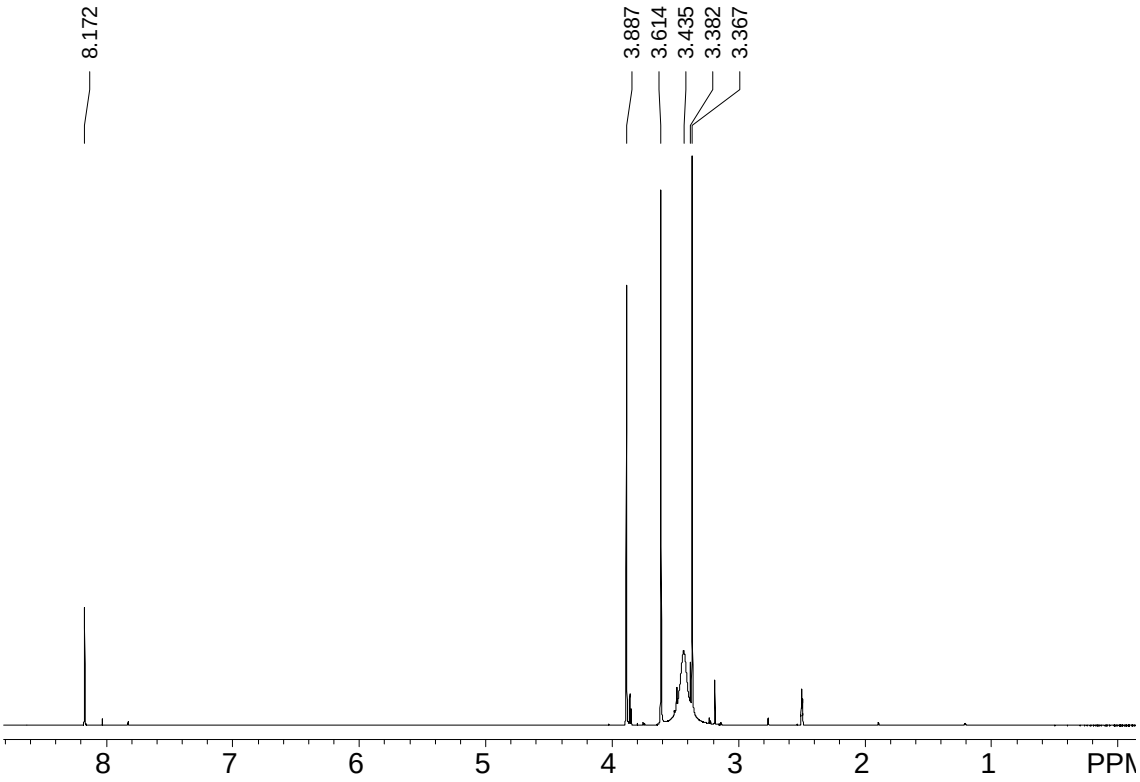

Figure 2. ^{1}H NMR spectrum of purine analog (**23**) (500 MHz, DMSO-d_6).

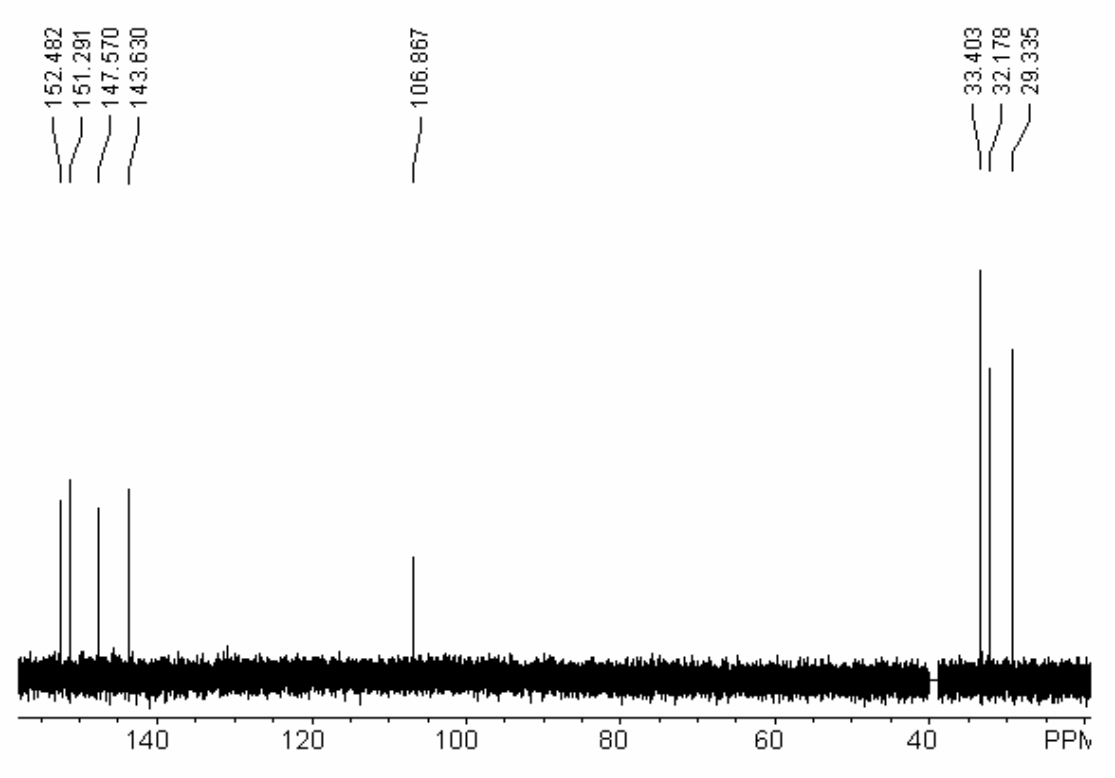

Figure 3. ^{13}C NMR spectrum of purine analog (**23**) (125 MHz, DMSO-d_6).

The IR spectrum of **23** showed one carbonyl stretching absorption band at 1715 cm^{-1}, a C=N stretching absorption band at 1641 cm^{-1} and NH stretching absorption bands at 3303 cm^{-1}. The basic chemical skeleton of this purine analog (**23**) was established by a gHMBC (gradient **H**eteronuclear **M**ultiple **B**ond **C**onnectivity) in DMSO-d_6 as shown in (Figure 4). Three methyl proton signals bearing nitrogen revealed connectivity (Figure 5) from N-1-CH_3 to C-2 (δ151.3) and C-6 (δ152.5); from N-3-CH_3 to C-2 (δ151.3) and C-4 (δ147.6); from N-7-CH_3 to C-5 (δ106.9) and C-8 (δ143.6) and one methine proton bearing carbon signal showed HMBC three-bond correlations with two quaternary carbons at C-5 (δ106.9) and C-8 (δ143.6). Table 1 provides a summary of NMR spectroscopic data.

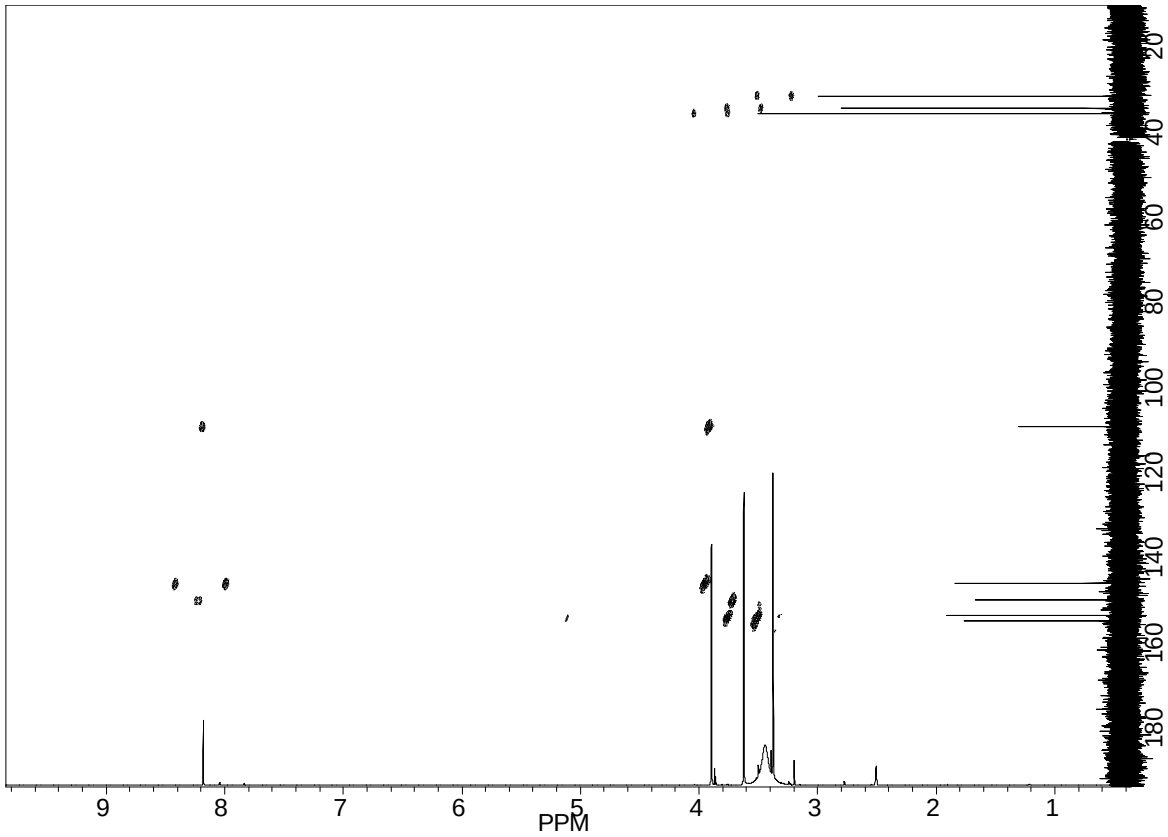

Figure 4. HMBC spectrum of purine analog (**23**) (500 MHz, DMSO-d_6).

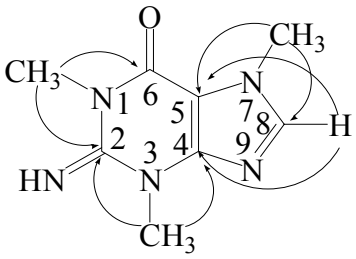

Figure 5. Key gHMBC correlations observed in purine analog (**23**).

Table 1. NMR data of purine analog (**23**) (DMSO-d_6)
(^{13}C, 125 MHz; ^{1}H NMR 500 MHz)

position	^{1}H(δ)	^{13}C(δ)	gHMBC
N-1-Me	3.36 (3.42)[a]	29.3 (27.8)[a]	C2, C6
C-2		151.3 (151.7)	
N-3-Me	3.61 (3.66)	32.2 (30.6)	C2, C4
C-4		147.6 (147.2)	
C-5		106.9 (106.8)	
C-6		152.5 (152.2)	
N-7-Me	3.88 (3.95)	33.4 (32.4)	C5, C8
C-8		143.6 (142.9)	
C-8-H(1H)	8.17 (8.14)		C4, C5
N-9			

[a] Chemical shifts (δ) measured in MeOH-d_4 (^{13}C, 75 MHz; ^{1}H NMR 250 MHz)

The UV spectrum of purine analog (**23**) showed at λ_{max} 210 nm and 268 nm, which is similar to absorption properties of known compounds 1,3,7-trimethylguanine [UV (MeOH) λ_{max} 213 nm and 288 nm][71] and 1,3,7-trimethylisoguanine [UV (MeOH) λ_{max} 214 nm and 288 nm].[72] The mass spectrum of purine analog **23** and its 1-, 3-, and 7- methyl derivatives have been analyzed in detail.[73] In the LREIMS spectrum of purine analog (**23**) (Scheme 2), fragments at *m/z* 178.1 $[M-NH]^+$ and *m/z* 164.1 $[M-CHO]^+$ were observed. The fragments of *m/z* 138.1 $[M-HNCNCH_3]^+$ due to the loss of methyl cyanamide at $[M-55]^+$, which then sequentially loses CO (*m/z* 109), HCN (*m/z* 82.1) as were reported in an N-1-methylated isoguanine purine[73] as the most characteristic mode of decomposition of this compound. Scheme 2 illustrates these fragmentations

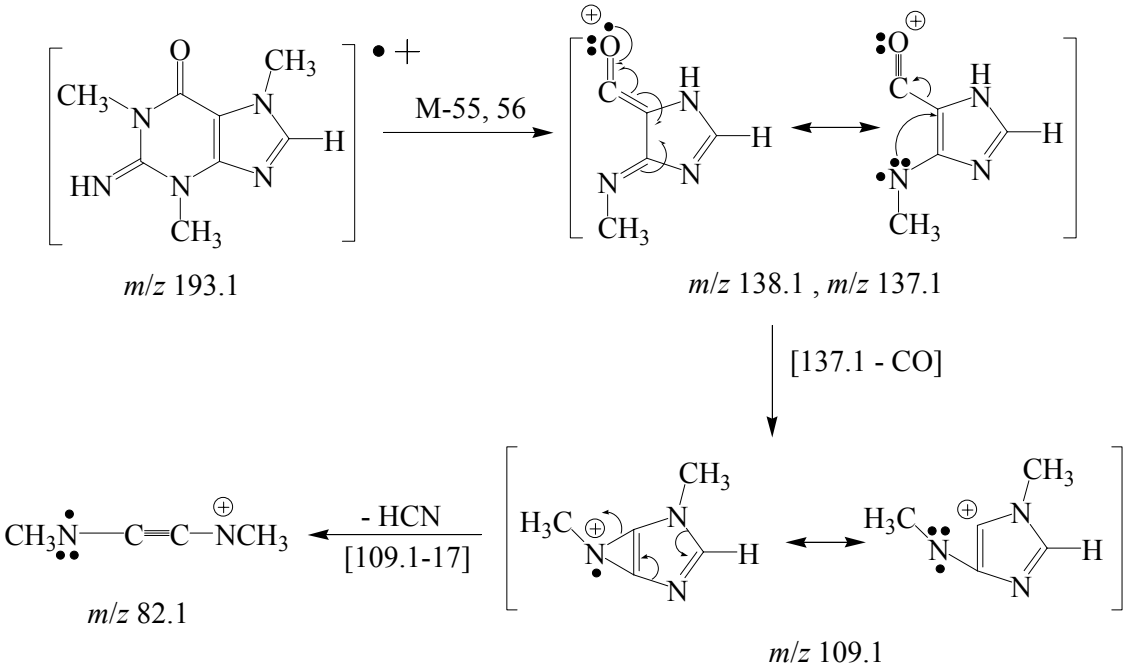

Scheme 2. Proposed fragmentations of purine analog **23**.

2.4 Characterization of 3-Hydroxykynurenine (24)

3-Hydroxykynurenine (**24**) was obtained as a bright yellow powder ($C_{10}H_{12}N_2O_3$) and was soluble in DMSO and MeOH. The UV absorption in MeOH showed λ_{max} 234, 273, 381 nm. The compound displayed a classic ^{1}H NMR (Figure 6) pattern for a 1, 2, 3-trisubstituted aromatic ring with signals at δ7.26 (1H, dd, J = 1.2, 8.2 Hz), δ 6.79 (1H, dd, J = 1.3, 7.5 Hz), and δ 6.45 (1H, t, J = 8.2 Hz) in MeOH-d_4. The three aliphatic protons were observed including one methine at δ 3.98 (1H, dd, J = 2.7, 9.0 Hz), two methylene protons at δ 3.70 (1H, dd, J = 2.5, 18.6 Hz) and δ 3.47 (1H, dd, J = 9.5, 18.5 Hz). The ^{1}H NMR spectrum of aromatic proton chemical shifts of 3-hydroxykynurenine (**24**) was similar to that of erebusinone (**12**) (Figure 7) in MeOH-d_4.

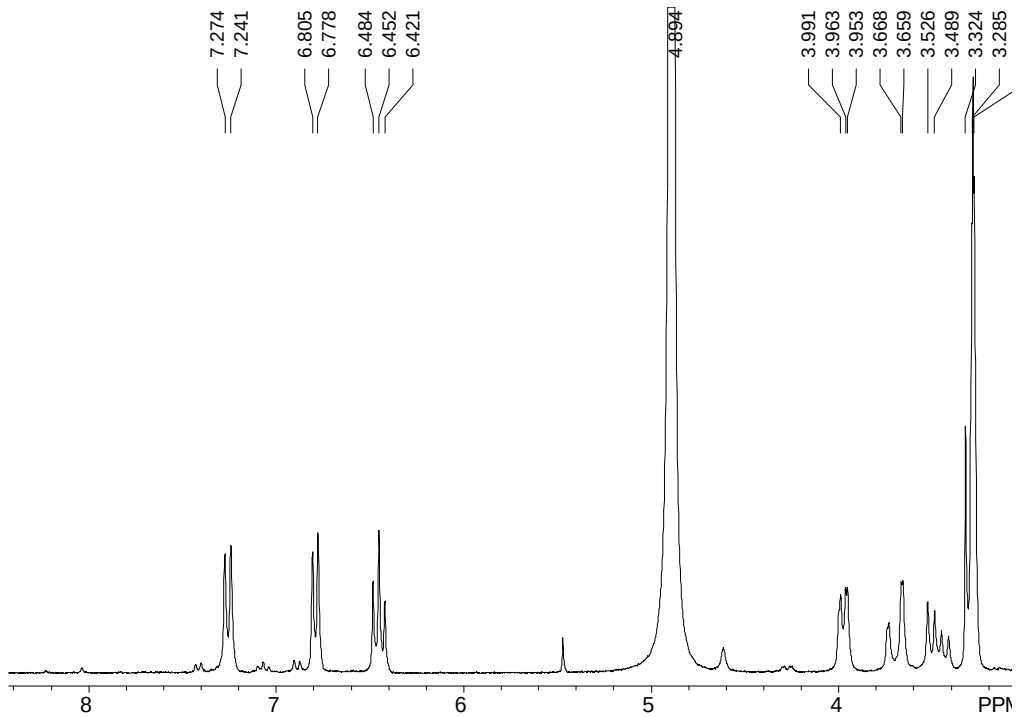

Figure 6. ^{1}H NMR spectrum of 3-hydroxykynurenine (**24**) (250 MHz, MeOH-d_4).

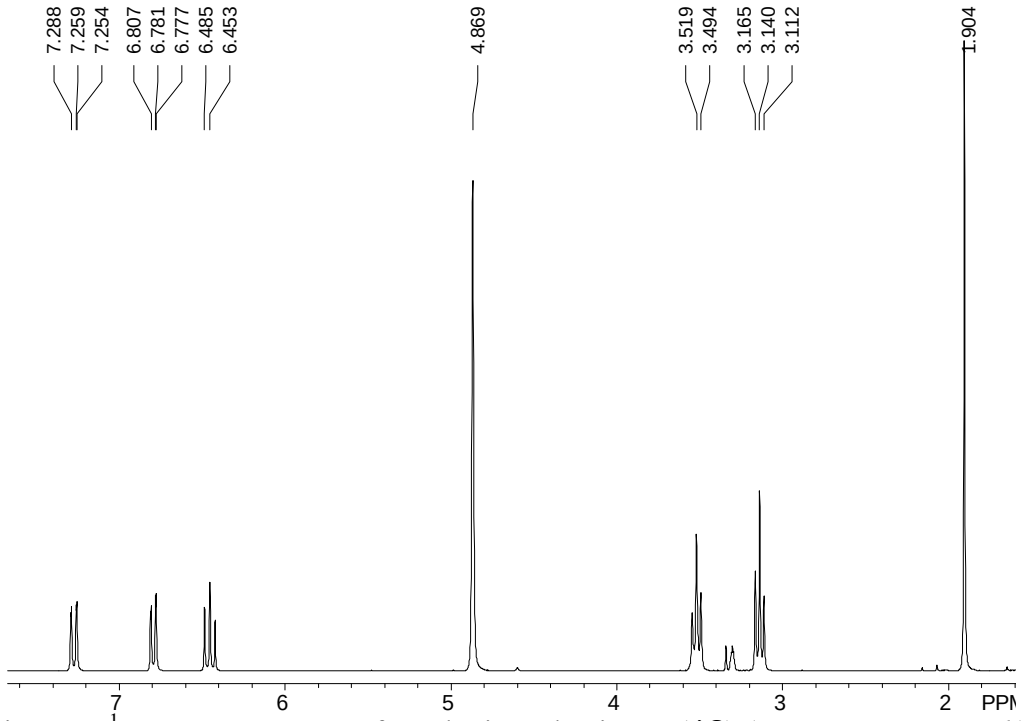

Figure 7. ^{1}H NMR spectrum of synthetic erebusinone (**12**) (250 MHz, MeOH-d_4).

The ^{13}C NMR spectrum (Figure 8) indicated the presence of ten carbons; six aromatic carbons at δ 145.5, 141.6, 121.6, 117.4, 117.1, 114.6, two carbonyl carbons at δ 170.3 and δ 200.0 and two aliphatic carbons at δ 50.5 and δ 41.1. The structure of 3-hydroxykynurenine (**24**) was deduced by analysis 2D NMR techniques [gCOSY (gradient **CO**rrelation **S**pectroscop**Y**), gHSQC (gradient **H**eteronuclear **S**ingle **Q**uantum **C**orrelation), and gHMBC)] (Figure 9, 10).

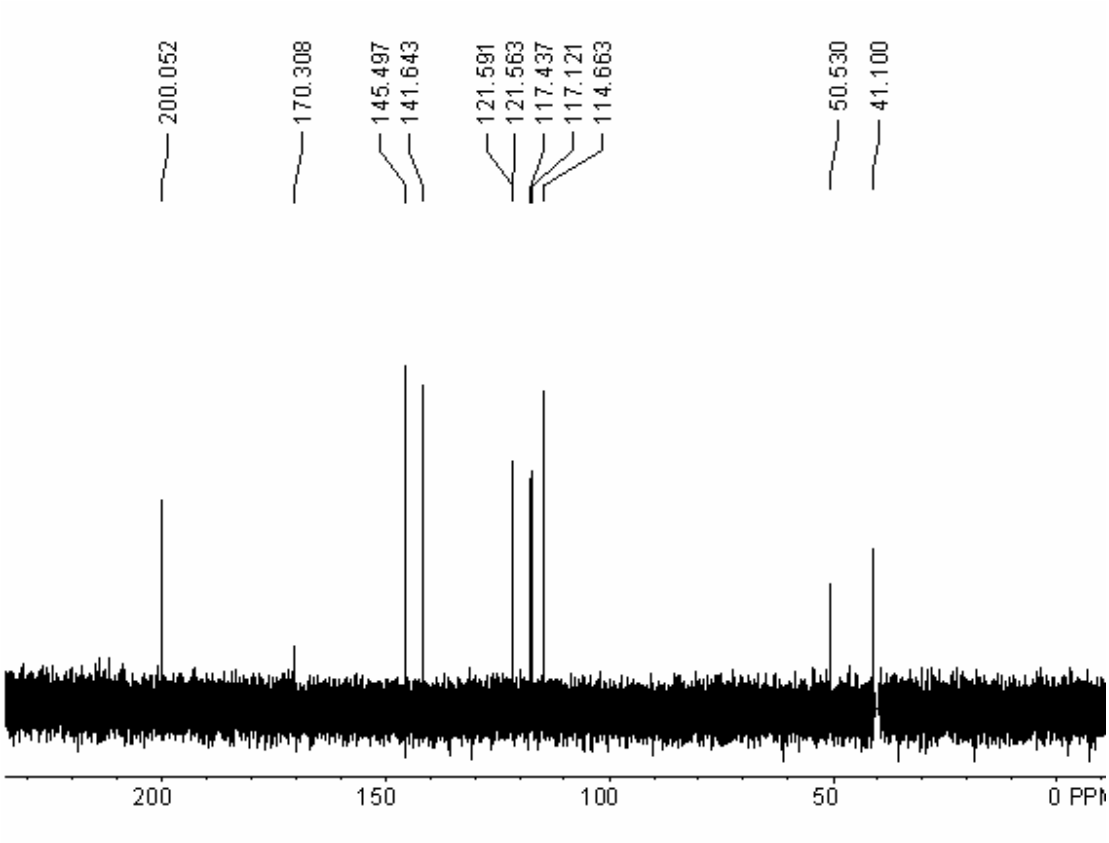

Figure 8. ^{13}C NMR spectrum of 3-hydroxykynurenine (**24**) (125 MHz, DMSO-d_6).

In the gHSQC experiment, mutual cross-peaks were observed between the aromatic protons at δ 7.19 (H-1), 6.85 (H-2), 6.40 (H-4) to carbons at δ 121.6, 117.4, and 114.6, respectively. Also, in the gHMBC spectrum (Figure 9) (Table 2), long range couplings ($^2J_{CH}$/ $^3J_{CH}$) were observed between δ 7.12 (H-1) and C-12 (δ 200.0), C-10 (δ

145.5), C-9 (δ 141.6), C-8 (δ 117.1), and C-2 (δ 117.4) indicating the presence of the benzene ring (Figure 10).

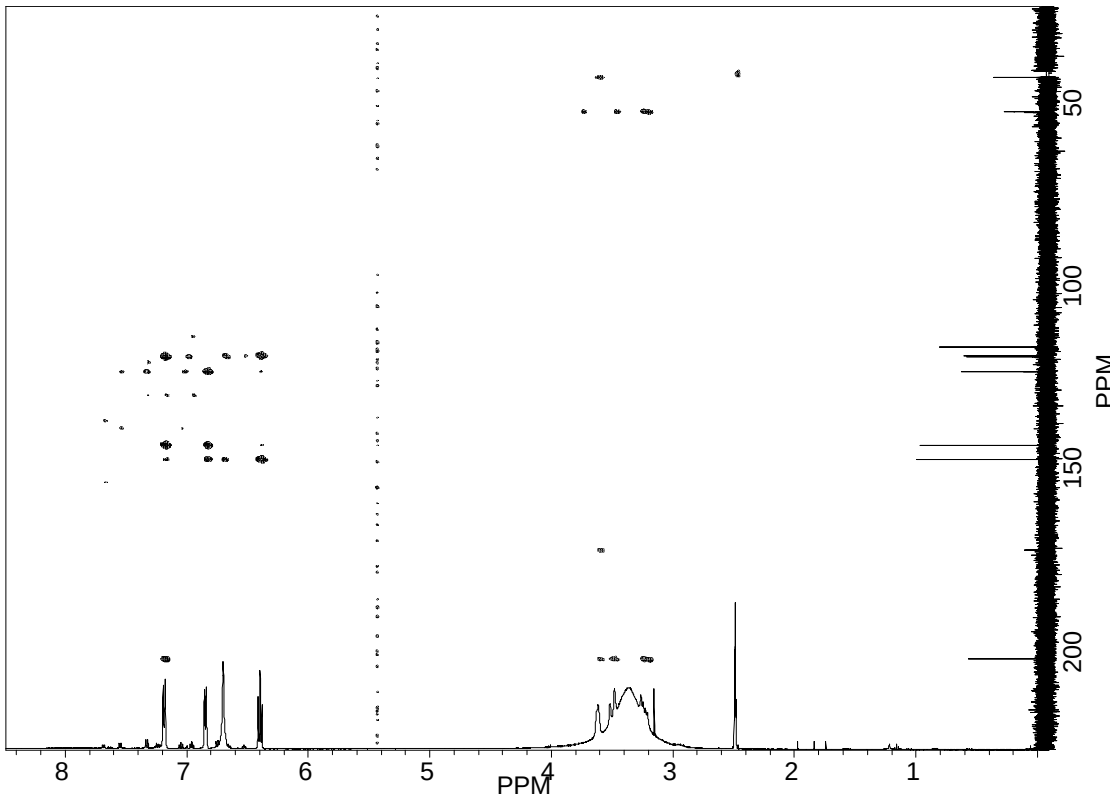

Figure 9. gHMBC spectrum of 3-hydroxykynurenine (**24**) (500 MHz, DMSO-d_6).

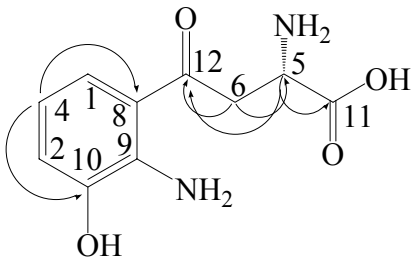

Figure 10. Key gHMBC correlations observed in 3-hydroxykynurenine (**24**).

Table 2. NMR data of 3-hydroxykynurenine (**24**) (DMSO-d_6) (^{13}C, 125 MHz; ^{1}H, 500 MHz)

	^{1}H (δ)[a]	^{13}C(δ)	gHMBC
1	7.19 (1H, d, *J* = 8.2 Hz)	121.6	C12, C10, C9, C8, C2
2	6.85 (1H, d, *J* = 7.6 Hz)	117.4	C10, C9, C1
3	6.70 (2H, s)		C10, C8
4	6.40 (1H, t, *J* = 8.0 Hz)	114.6	C10, C8
5	3.62 (1H, d, *J* = 7.8 Hz)	50.5	C12, C11, C6, C7
6	3.50 (1H, dd, *J* = 2.3, 18.1 Hz)	41.1	C12, C5
7	3.24 (1H, dd, *J* = 8.6, 17.5 Hz)	41.1	C12, C5
8		117.1	
9		141.6	
10		145.5	
11		170.3	
12		200.0	

[a] ^{1}H NMR (250 MHz, MeOH-d_4) δ 3.46 (1H, dd, *J* = 9.5, 18.5 Hz), 3.70 (1H, dd, *J* = 2.5, 18.7 Hz), 3.97 (dd, *J* = 2.5, 9.7 Hz), 6.45 (t, *J* = 8.2 Hz), 6.79 (d, *J* = 7.5 Hz), 7.26 (d, *J* = 8.2 Hz)

The 3-hydroxykynurenine (**24**) displayed an optical rotation $[\alpha]^{25}_{D}$ -47.6° (*c* = 0.17, MeOH) which is similar to that reported $[\alpha]^{25}_{D}$ -45° [(*c* = 0.9, MeOH)][74,75] suggesting absolute stereochemistry at position C-5 of our isolate to be the *S* configuration. The UV spectrum of compound **24** observed in λ_{max} 234, 273, 381 nm in MeOH (pH = 7) was similar to previously reported absorption values, λ_{max} 224, 266, 370 nm (0.005 M HCl) from literature.[74]

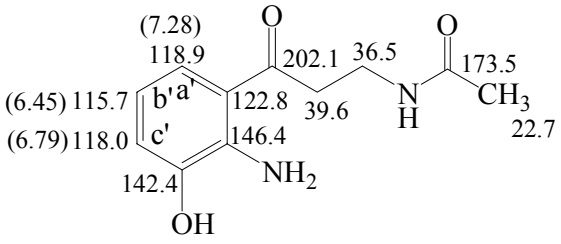

Erebusinone (**12**)

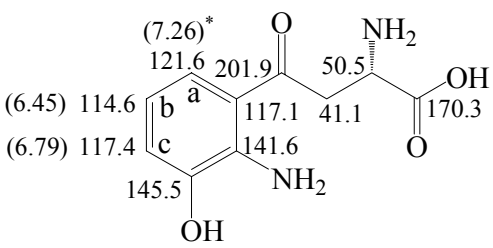

3-Hydroxykynurenine (**24**)

Figure 11. Assigned NMR data of erebusinone[61] and 3-hydroxykynurenine (MeOH-d_4, ^{1}H NMR 250 MHz; ^{13}C NMR, 75, 125 MHz) * ^{1}H chemical shifts.

Chapter 3. CHEMICAL INVESTIGATION OF ANTARCTIC MARINE SPONGE *ISODICTYA SETIFERA*

3.1 Introduction

The Antarctic marine sponge *Isodictya setifera* Topsent (family Esperiopsidae) (Figure 12) has received attention due to its bioactive metabolites which were isolated from the sponge-associated with bacterial strain *Pseudomonas aerugenosa*, which showed strong antibacterial activity.[76] Although the chemistry of the *I. setifera* sponge-associated bacterium has been reported,[77,78] the secondary metabolites of the sponge have not been reported.

Figure 12. *Isodictya setifera* collected from Bahia Paraiso, Palmer Station, Antartica (Photograph supplied by Bill J. Baker, University of South Florida).

3.2 Extraction and Isolation of Secondary Metabolites

In continuation of our study of *Isodictya setifera*, sponges were collected by SCUBA diving at the Bahia Paraiso shipwreck on the coast near Palmer station, Antarctica, and chemically studied, resulting in the isolation of six compounds, 5-methyl-2'-deoxycytidine (**25**), uridine (**27**), 2-deoxycytidine (**30**), hydroxyquinoline (**33**), 3-hydroxykynurenine (**24**), and homarine (**37**).

The freeze–dried sample of *Isodictya setifera* was exhaustively extracted with MeOH at room temperature (Scheme 2). After concentration, the crude extract was partitioned with hexane, MeOH, H_2O and BuOH. The BuOH soluble material was subjected to Sephadex LH-20® column chromatography (5 cm X 60 cm) with MeOH to provide seven fractions. Fraction 12 was further subjected to normal phase column chromatography with MeOH/CH_2Cl_2 and CH_3CN (acetonitrile)/H_2O and followed by reversed phase HPLC with a cyano-derivatized column using a gradient CH_3CN/H_2O to give pure compounds which are 5-methyl-2'-deoxycytidine (**25**, 3.0 mg, 0.0007% dry wt), uridine (**28**, 2.0 mg, 0.0005% dry wt), 2'-deoxycytidine (**31**, 1.5 mg, 0.0003% dry wt), hydroxyquinoline (**33**, 1.8 mg, 0.0004% dry wt), 3-hydroxykynurenine (**24**, 1.7 mg, 0.0004% dry wt), and homarine (**37**, 2.0 mg, 0.0005% dry wt).

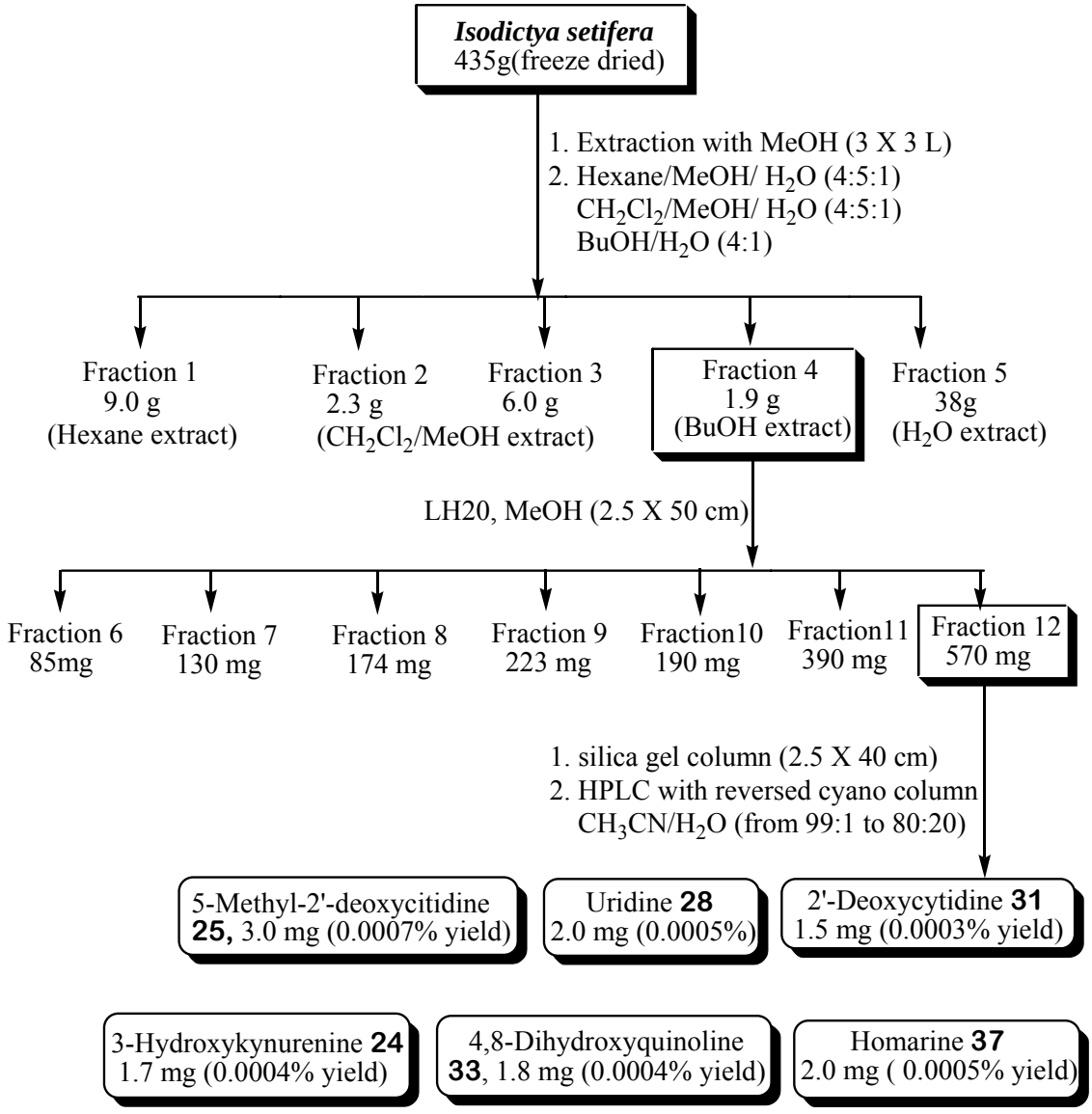

Scheme 3. Isolation of nucleosides, 3-hydroxykynurenine, 4, 8-dihydroxyquinoline, and homarine.

3.3 Characterization of 5-Methyl-2'-deoxycitidine (25)

The ^{1}H NMR spectrum (Figure 13) of 5-methyl-2'-deoxycitidine (**25**) showed typical chemical shifts of nucleosides, including the presence of one olefinic methine group (δ 7.83), three aliphatic mithine groups (δ 6.30. 4.42, 3.92), two aliphatic methylene groups (δ 3.78, 2.25) and one methyl group (δ 1.89). The ^{13}C NMR spectrum (Figure 14) showed ten carbon signals corresponding to one methyl (δ 11.3), two methylenes (δ 61.7, 40.0), four methines (δ 136.7, 87.4, 85.1, 71.0), and three quaternary carbons (δ 165.3, 151.2, 110.3) based on analysis by the gHSQC spectrum.

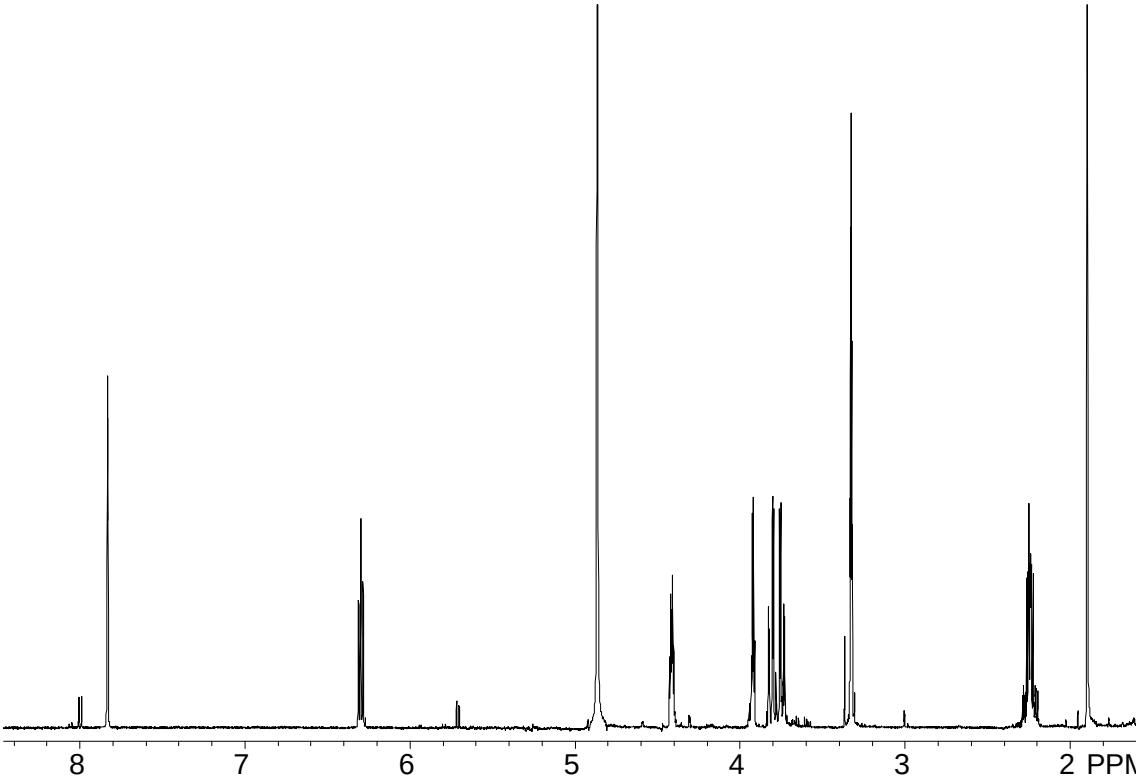

Figure 13. ^{1}H NMR spectrum of 5-methyl-2'-deoxycitidine (**25**) (500 MHz, MeOH-d_4).

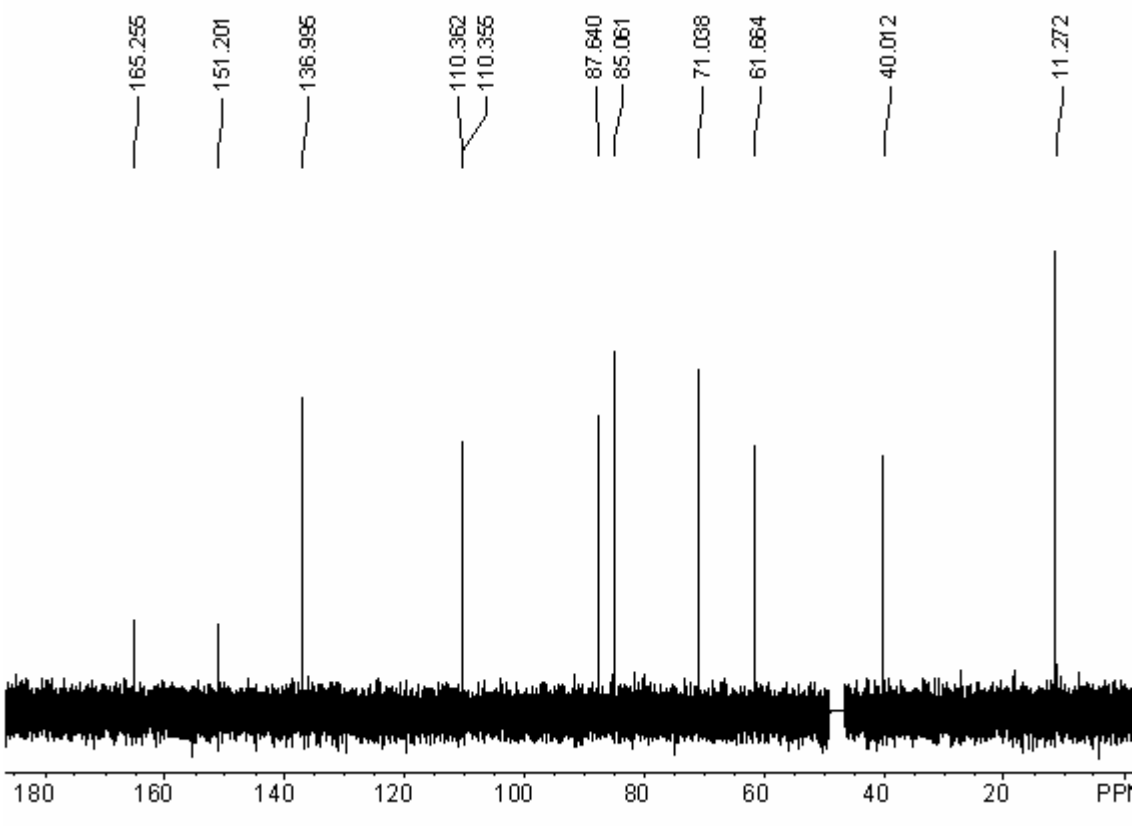

Figure 14. ^{13}C NMR spectrum of 5-methyl-2'-deoxycitidine (**25**) (125 MHz, MeOH-d_4).

First, the partial structure (**a**) of 5-methyl-2'-deoxycitidine was established using a gCOSY (Table 3) (Figure 15) experiment. The olefinic methine at δ 7.83 (1H, s, H-1) showed allylic coupling with the methyl protons at δ 1.89 (3H, s, H_3-7). A second partial structure (**b**) was evidenced by the aliphatic methines at δ 6.30 (1H, t, J = 6.8 Hz, H-2') coupled with neighbor methylene protons at δ 2.25 (2H, m, H-3') which were in turn correlated with methines at δ 4.42 (1H, m, H-4'). The methine at δ 4.42 (H-4') showed 1, 3-correlations with methines at δ 3.92 (1H, q, J = 3.4, H-5') and δ 2.25 (2H, m, H-3'). The methine at δ 3.92 (H-5') showed correlations with one methine at δ 4.42 (H-4') and one methylene at δ 3.81 (1H, dd, J = 3.2, 12.5 Hz, H_a-6') and 3.74 (1H, dd, J = 3.5, 11.8 Hz, H_b-6'). The methylene protons at δ 3.81 (H_a-6') and 3.74 (H_b-6')

showed correlation with one methine at δ 3.92 (H-5') and W-coupling with the methine at δ 4.42 (H-4'), completing partial structure (**b**).

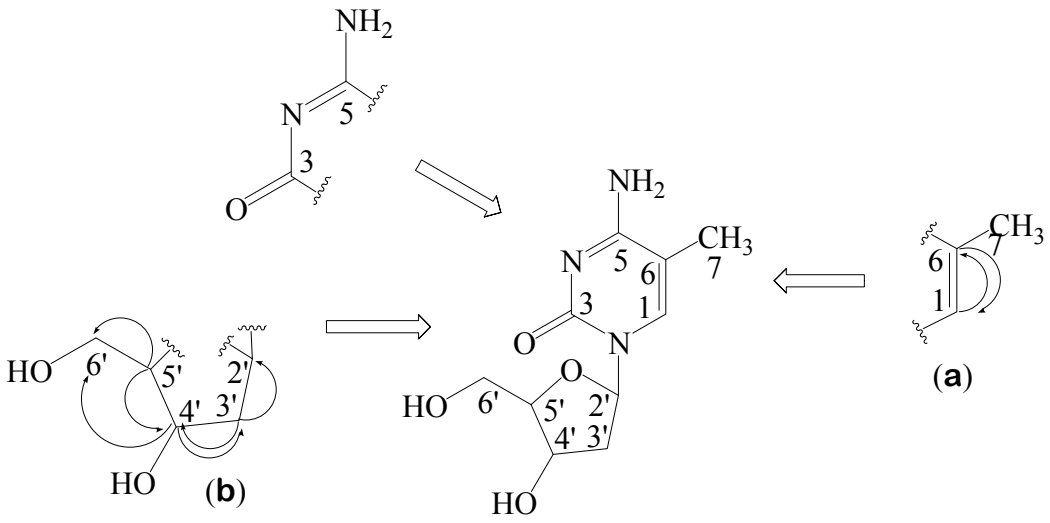

Figure 15. gCOSY correlations of **25.**

A methine proton at δ 7.83 (H-1) showed $^{2}J_{CH}/^{3}J_{CH}$ correlations in the gHMBC spectrum (Figure 16) to C-2' (δ 85.1), and C-7 (δ 11.3) as well as with three quaternary carbons C-6 (δ 110.4), C-3 (δ 151.2), and C5 (δ 165.3) supporting a pyrimidine moiety. The methine proton (H-2') at δ 6.30 showed $^{3}J_{CH}$ correlation to C-1 (δ 136.7) and a quaternary carbon at δ 151.20 (C-3). The methylene protons (H_2-3') showed $^{2}J_{CH}/^{3}J_{CH}$ correlations to C-2' (δ 85.1), C-4' (δ 71.1), and C-5' (δ 87.6) supporting a sugar moiety. These data established the structure of 5-methyl-2'-deoxycytidine (**25**) (Figure 17).

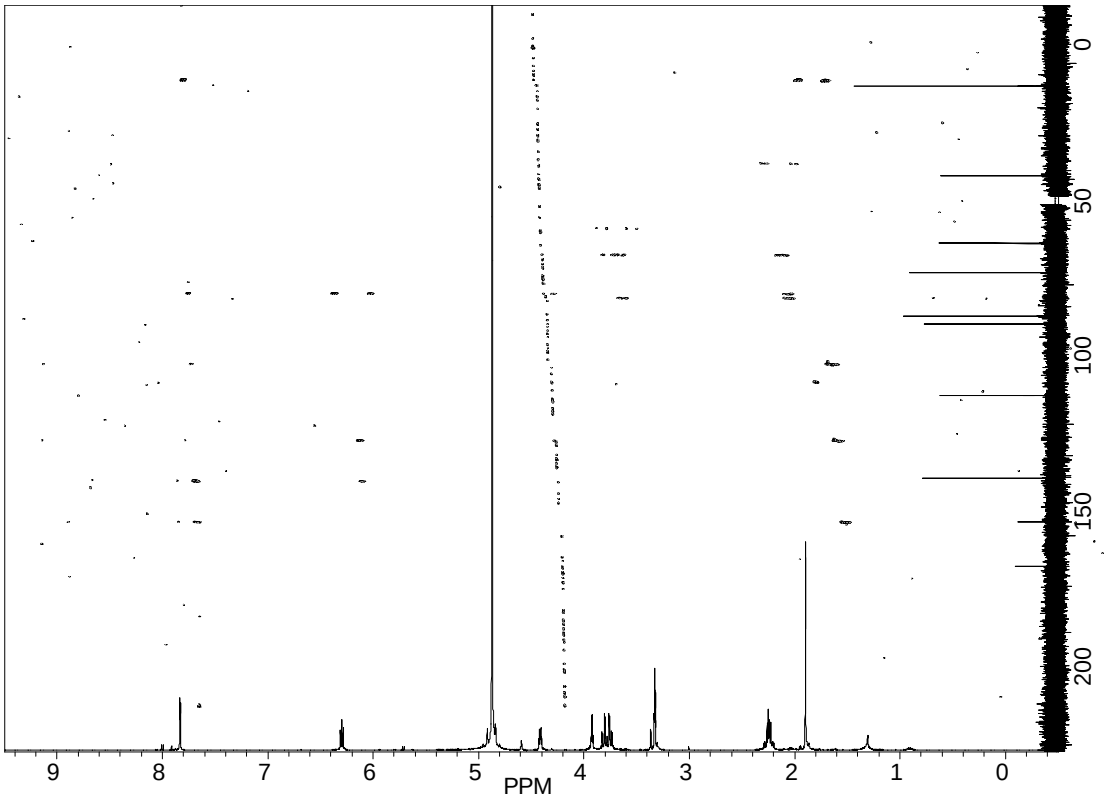

Figure 16. gHMBC spectrum of 5-methyl-2'-deoxycytidine (**25**) (500 MHz, MeOH-d_4).

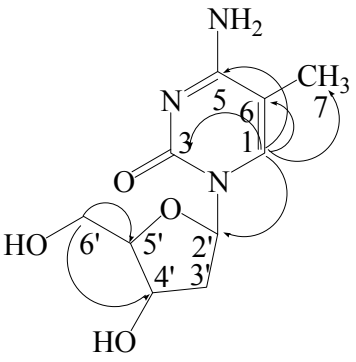

Figure 17. Key gHMBC correlations observed in 5-methyl-2'-deoxycitidine (**25**).

Table 3 . NMR data of 5-methyl-2'-deoxycytidine (**25**) (MeOH-d_4) (^{13}C, 125 MHz; ^{1}H, 500 MHz)

position	^{1}H (δ)	^{13}C (δ)	gCOSY	gHMBC
1	7.83 (1H, s)	136.7 (CH)	H7	C3, C5, C6, C7, C2'
3		151.2 (C)		
5		165.3 (C)		
6		110.4 (C)		
7	1.89 (3H,s)	11.3 (CH_3)	H1	C5, C6, C1
2'	6.30 (1H, t, J = 6.8Hz)	85.1 (CH)	H3'	C3, C1
3'	2.25 (2H, m)	40.0 (CH_2)	H2', H4'	C2', C4', C5'
4'	4.42 (1H, m)	71.0 (CH)	H3', H5'	C2', C5'
5'	3.92 (1H, q, J = 3.4 Hz)	87.6 (CH)	H4', H6'	C3'
6'	3.81 (1H, dd, J = 3.2,12.5 Hz)	61.7 (CH_2)	H6'	C4', C5'
	3.74 (1H, dd, J = 3.5,11.8 Hz)	61.7 (CH_2)	H6'	C4', C5'

The chemical shifts of 5-methyl-2'-deoxycytidine (**25**) from the current study was compared with the literature and Aldrich Library of NMR spectra.[79,80] All assigned chemical shifts by ^{1}H NMR and gCOSY are similar those of published (Figure 18).

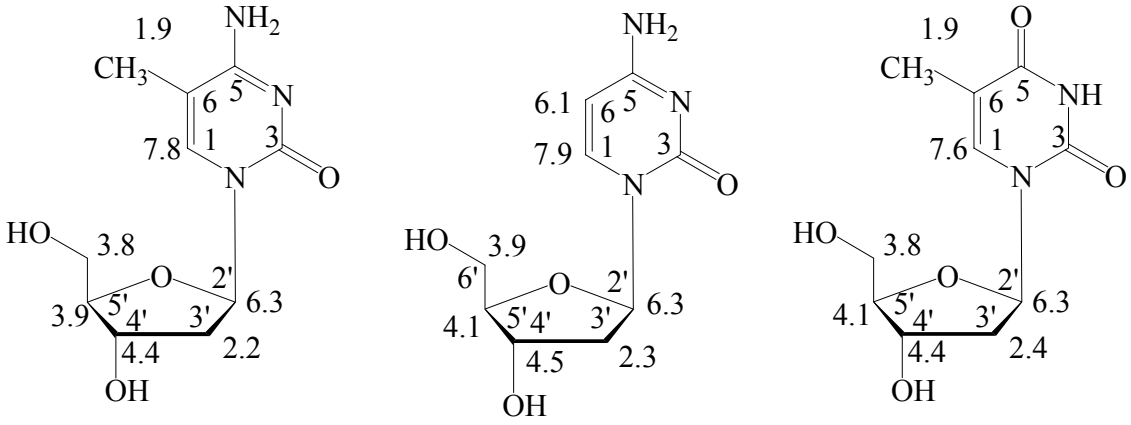

Figure 18. Assigned ^{1}H NMR chemical shifts (δ) of 5-methyl-2-deoxycytidine **25** (500 MHz, DMSO-d_6) from the current study data, 2-deoxycytidine **26**[80] and thymidine **27**[80] (60 MHz, D_2O).

3.4 Characterization of Uridine (28)

The ^{1}H NMR spectrum (Figure 19) of uridine (**28**) is similar to that of 5-methyl-2'-deoxycytidine (**25**) except for the absence of the methyl group at δ 1.89.

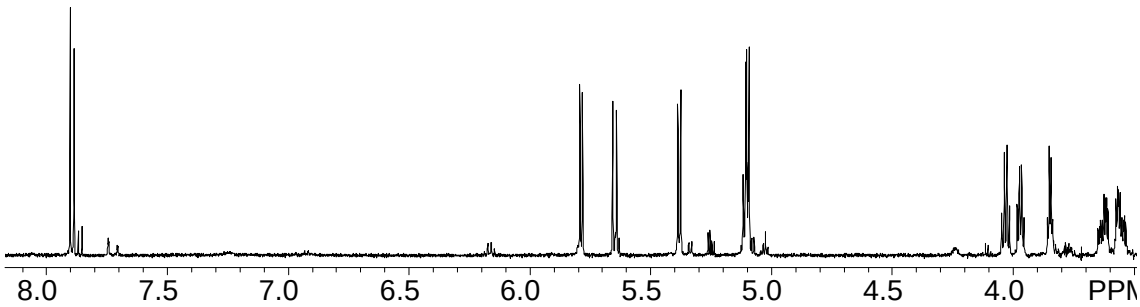

Figure 19. The ^{1}H NMR spectrum of uridine (**28**) (500 MHz, DMSO-d_6).

The ^{1}H-^{1}H gCOSY (Figure 20) of uridine (**28**) displayed 3 spin systems that include two olefinic methine groups (δ 7.88, 5.64), four aliphatic methine groups (δ 5.77, 4.01, 3.95, 3.83) and contiguous with one methylene group (δ 3.61, 3.54). The aliphatic methines at δ 5.77 (H-2') coupled with its neighboring proton at δ 4.01 (H-3'), which was in turn correlated with δ 3.95 and with one exchangeable proton. The methine at δ 3.95 (H-4') showed further correlation ($^{3}J_{HH}$) with δ 3.83 (H-5') and one exchangeable proton at δ 5.10 (H-4"). The methine at δ 3.83 (H-5') showed additional correlation ($^{3}J_{HH}$) with the methylene protons (H-6') at δ 3.61 and 3.54 which showed further vicinal correlation ($^{2}J_{HH}$).

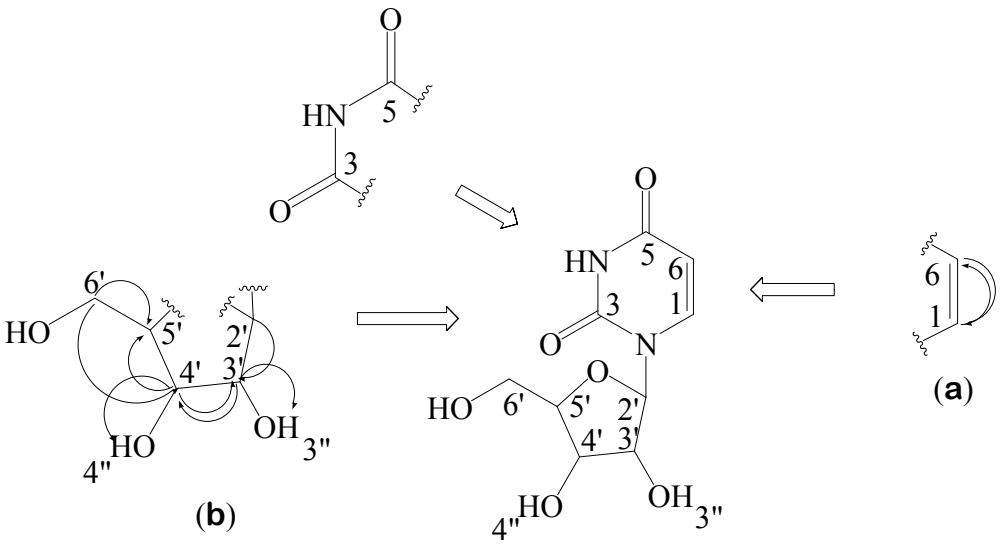

Figure 20. gCOSY correlation of **28.**

The ^{13}C NMR spectrum (Figure 21) displayed nine carbon signals. In the gHSQC experiment, mutual cross-peaks ($^{1}J_{CH}$) were observed between the aromatic protons at δ 7.88 (H-1) and 5.64 (H-6) to carbons at δ 141.4 and δ 102.4, respectively. Also, in the gHMBC spectrum (Figure 22), cross-peaks ($^{2}J_{CH}$/ $^{3}J_{CH}$) were observed between δ 7.88 (H-1) and C-5 (δ 163.8), C-3 (δ 151.4), C-6 (δ 102.4) and C-2' (δ 88.3) (Figure 23) (Table 4).

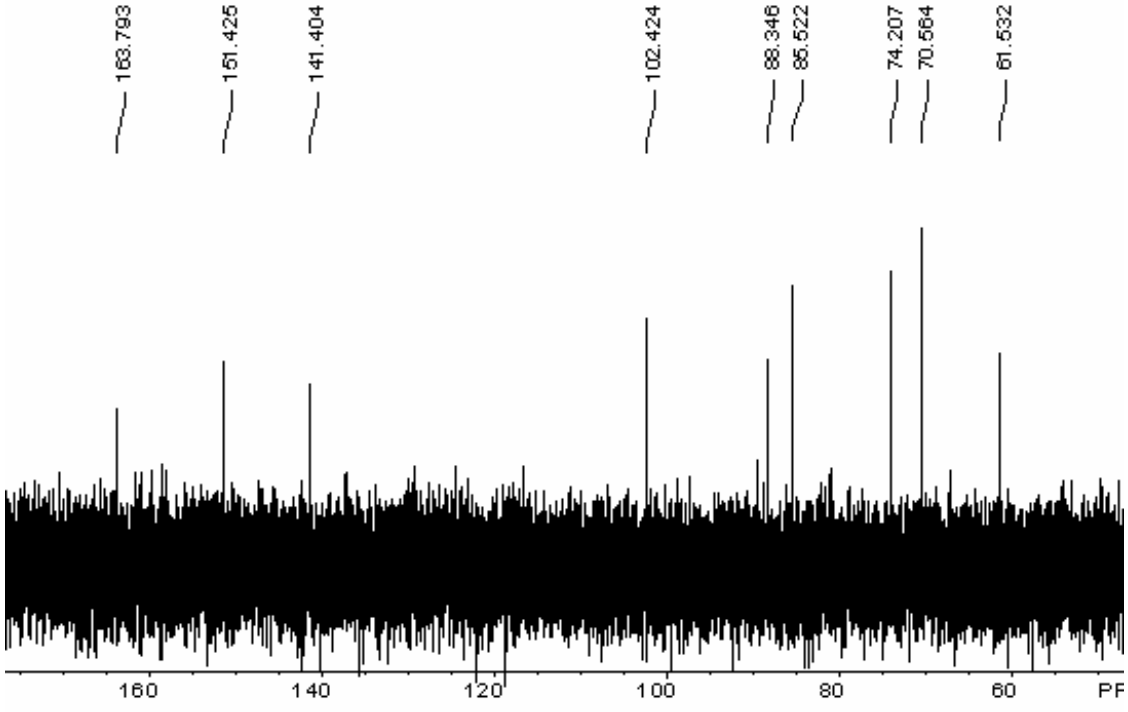

Figure 21. The ^{13}C NMR spectrum of uridine (**28**) (500 MHz, DMSO-d_6).

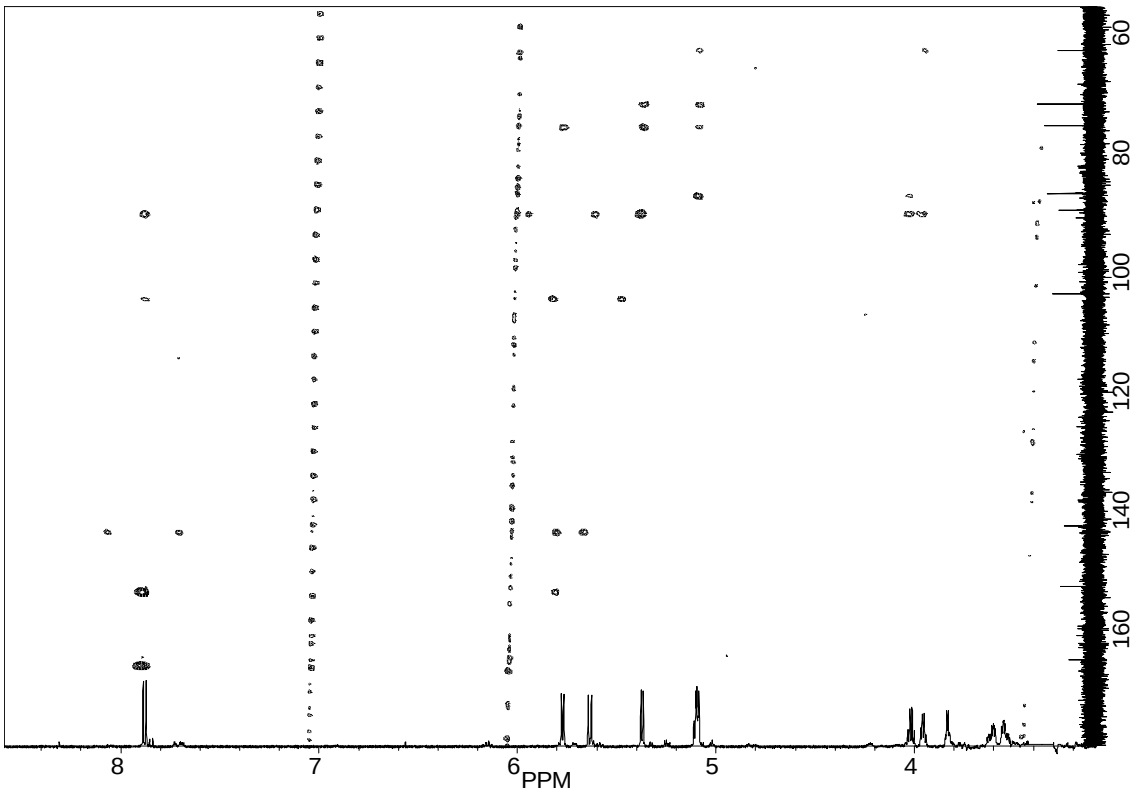

Figure 22. The gHMBC spectrum of uridine (**28**) (500 MHz, DMSO-d_6).

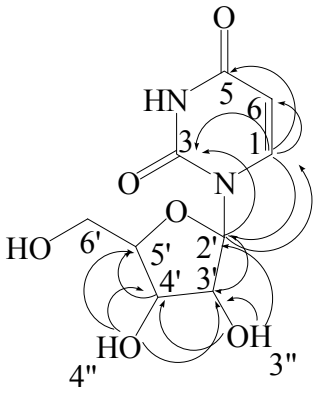

Figure 23. Key gHMBC correlations observed in uridine (**28**).

Table 4. NMR data of uridine (**28**) (DMSO-d_6) (^{13}C, 125 MHz; ^{1}H, 500 MHz)

position	^{1}H (δ)	^{13}C (δ)	gCOSY	gHMBC
1	7.88 (1H, d, *J* = 7.9 Hz)	141.4 (CH)	H6	C3, C5, C6, C2'
3		151.4 (C)		
5		163.8 (C)		
6	5.64 (1H, d, *J* = 8.3 Hz)	102.4 (CH)	H1	C1
2'	5.77 (1H, d, *J* = 5.8 Hz)	88.3 (CH)	H3'	C3, C1, C3'
3'	4.01 (1H, q, *J* = 5.4 Hz)	74.2 (CH)	H2', H4', H3"	C2', C5'
4'	3.95 (1H, q, *J* = 4.6 Hz)	70.5 (CH)	H3', H5', H4"	C2', C5'
5'	3.83 (1H, q, *J* = 3.3 Hz)	85.5 (CH)	H6', H4'	
6'	3.61 (m, 1H)	61.5 (CH)	H5', H4"	
	3.54 (m, 1H)	61.5 (CH)	H5', H4"	
3"	5.37 (1H, d, *J* = 5.9 Hz)		H3'	C2', C3', C4'
4"	5.10 (1H, m)		H4'	C3', C4', C5'

The natural compound uridine (**28**) [70] was previously isolated from *Isodictya erinacea* and characterized structure by 2D NMR. In the current study, the isolated uridine **28** displayed two aromatic methines on the pyrimidine ring at δ 7.88 (H-1, *J* = 7.9 Hz) and 5.64 (H-6, *J* = 8.3 Hz), which were identical to chemical shifts (Figure 23)

and coupling constant previously reported [δ 7.86 (H-1, J = 8.1 Hz) , δ 5.66 (H-6, J = 8.1 Hz)] Comparison of reported ^{1}H NMR data of uridine (Figure 24) showed the difference of chemical shifts attributed by solvent effect.

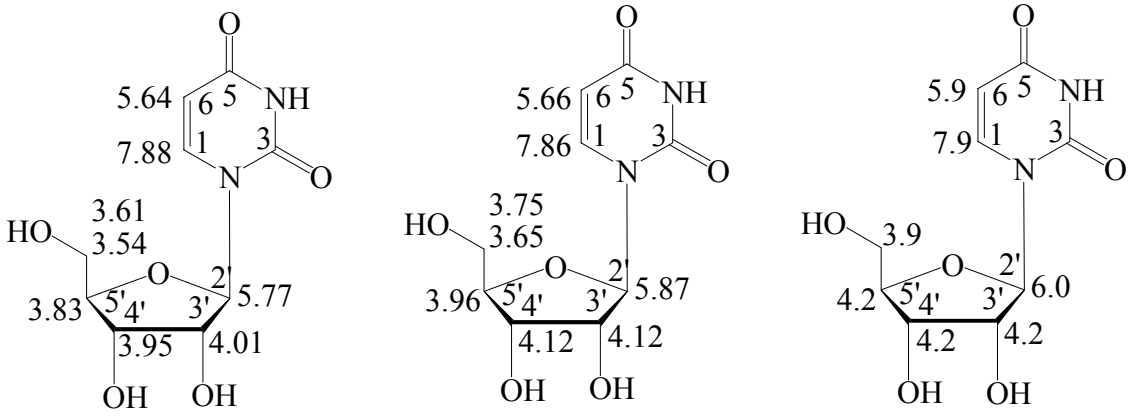

Figure 24. Assigned ^{1}H NMR chemical shifts (δ) of uridine (**28**) (500 MHz, DMSO-d_6) from the current study, previous reported uridine (**29**)[70] (360 MHz, MeOH-d_4) and uridine **30**[81] (60 MHz, D_2O+NaOD).

3.5 Characterization of 2'-Deoxycytidine (31)

2'-Deoxycytidine (**31**) was obtained as a pale brown solid. The ^{1}H NMR spectrum displayed (Figure 25) three spin systems including two olefinic methine groups at δ 7.84 (1H, d, J = 8.1 Hz, H-1), and 5.63 (1H, d, J = 8.1 Hz, H-6), as well as four aliphatic methine groups at δ 6.14 (1H, t, J = 6.2 Hz, H-2'), 4.27 (1H, m, H-4'), 3.77 (1H, m, H-5') coupled to two methylene groups at δ 3.55 (2H, m, H_2-6'), and 2.08 (2H, m, H_2-3') (Figure 26). The aliphatic methines at δ 6.14 (H-2') coupled with

neighboring methylene protons at δ 2.08 (H_2-3') which were correlated with two methines at δ 4.27 (H-4') and 3.77 (H-5').

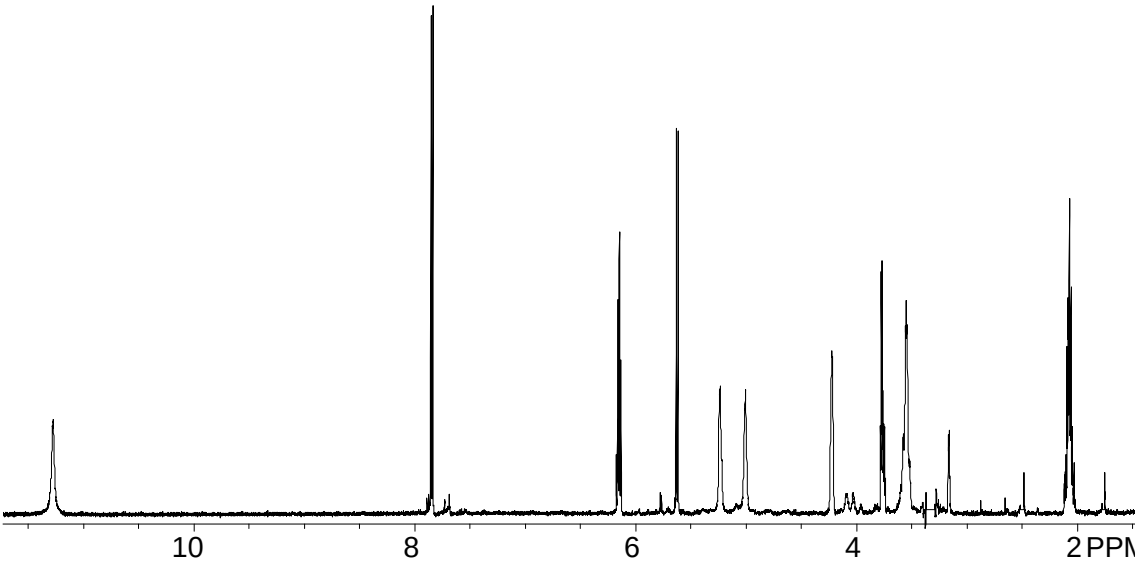

Figure 25. ^{1}H NMR spectrum of 2'-deoxycytidine (**31**) (500 MHz, DMSO-d_6).

The methine at δ 4.27 (H-4') showed 1,3 correlation ($^3J_{HH}$) with one methine at δ 3.77 (H-5'), one methylene at δ 2.08 (H-3') and with one exchangeable proton attached on the position at δ 5.23 (H-4").

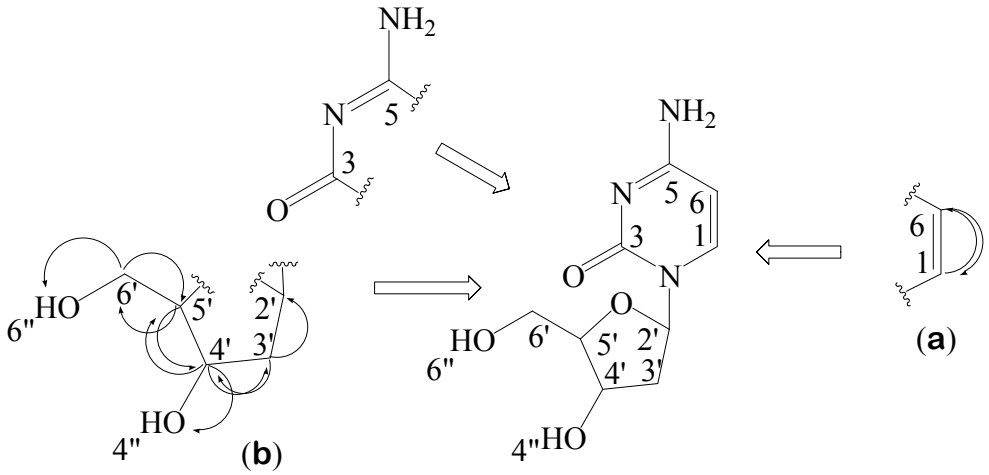

Figure 26. gCOSY correlations of **31.**

The methine at δ 3.77 (H-5') showed correlations ($^3J_{HH}$) with one methine at δ 4.27 (H-4') and one methylene at δ 3.55 (H-6'). The methylene protons at δ 3.55 (H_2-6') also showed 1,3 correlation ($^3J_{HH}$) with one methine at δ 3.77 (H-5') and with one exchangeable proton at δ 5.00 (H - 6").

The ^{13}C NMR spectrum (Figure 27) showed nine carbons including one carbonyl carbon at δ 151.1. The positions of two quaternary carbons δ 151.1 (C-3) and 163.8 (C-5) were confirmed by correlation ($^2J_{CH}$/ $^3J_{CH}$) with two methine protons at δ 7.84 (H-1) and δ 5.63 (H-6) by the gHMBC experiment as shown in Figure 28. The methylene protons (H-3') on furan ring also showed correlations ($^2J_{CH}$/ $^3J_{CH}$) (Table 5) with three methine carbons at δ 84.8 (C-2'), 71.1 (C-4'), and 88.0 (C-5') (Figure 29).

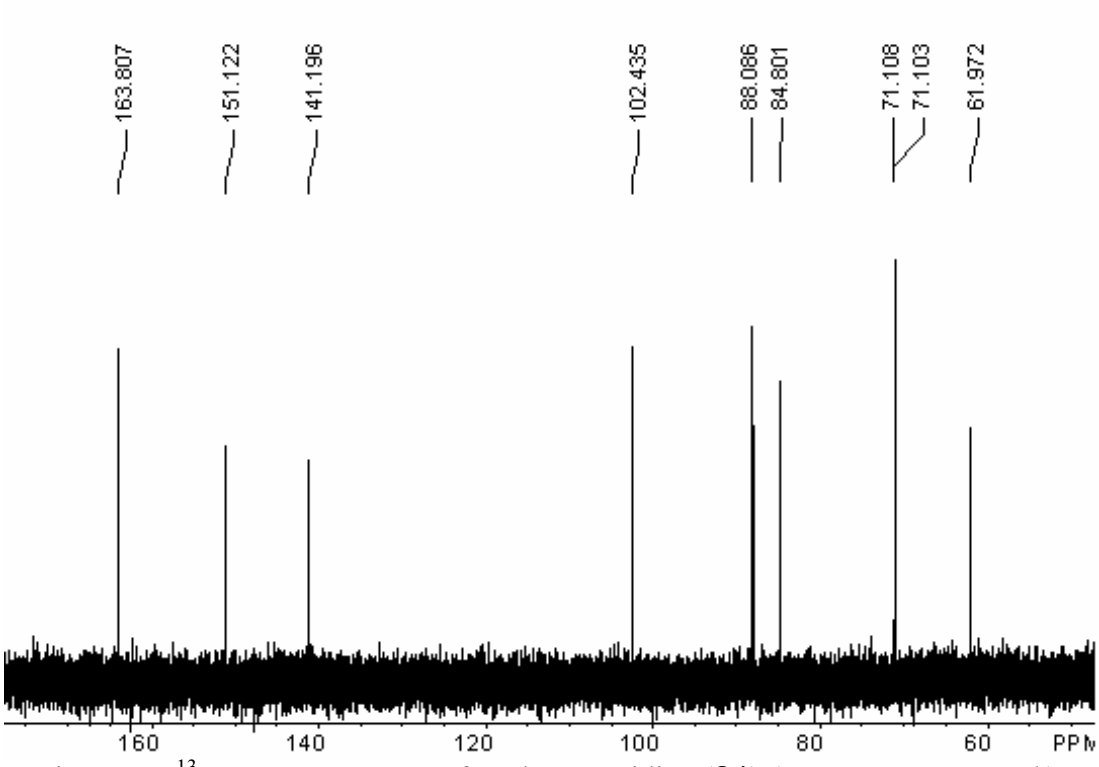

Figure 27. ^{13}C NMR spectrum of 2'-deoxycytidine (**31**) (125 MHz, DMSO-d_6).

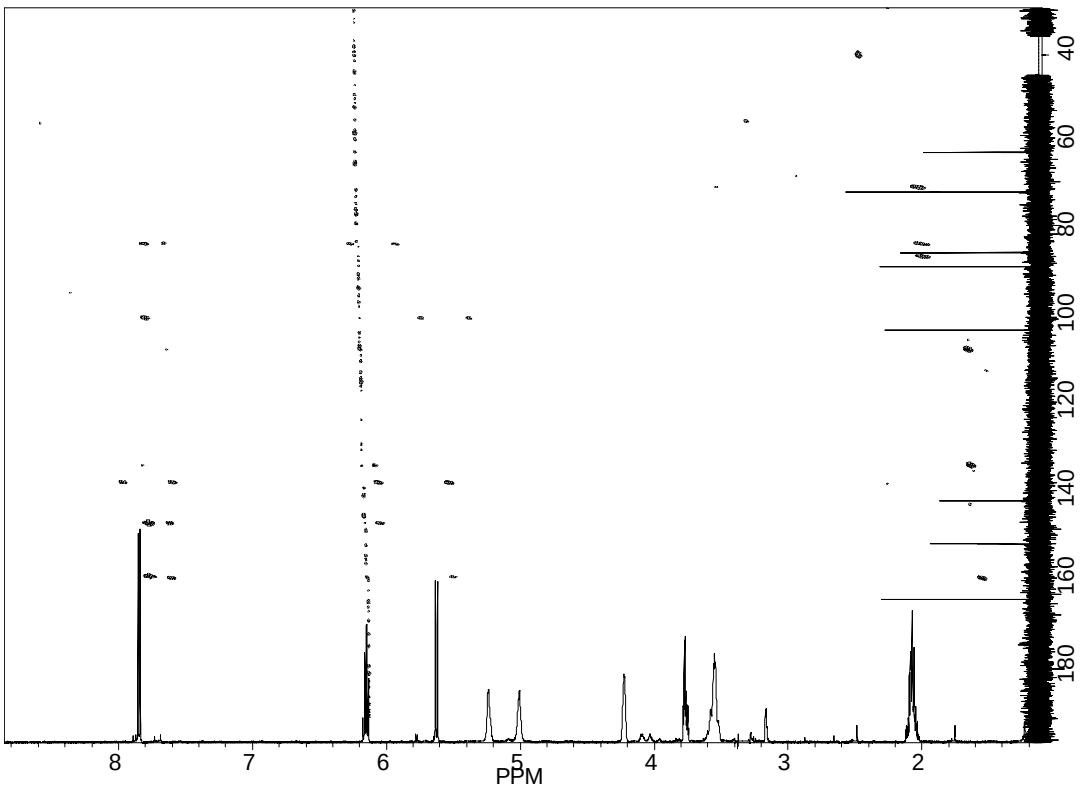

Figure 28. gHMBC spectrum of 2-deoxycytidine (**31**) (500 MHz, DMSO-d_6).

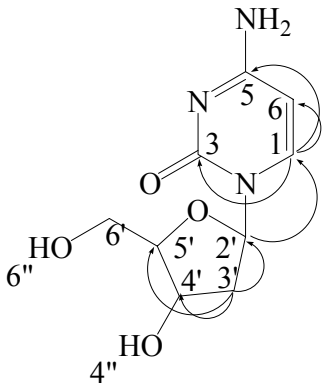

Figure 29. Key gHMBC correlations observed in 2'-deoxycytidine (**31**).

Table 5. NMR data of 2'-deoxycytidine (**31**) (DMSO-d_6) (^{13}C, 125 MHz; ^{1}H, 500 MHz)

position	^{1}H (δ)	^{13}C (δ)	gCOSY	gHMBC
NH_2	11.27 (s, 1H)			
1	7.84 (1H, d, J = 8.1 Hz)	141.2 (CH)	H6	C12, C11
3		151.1 (C)		
5		163.8 (C)		
6	5.63 (1H, d, J = 8.1 Hz)	102.4 (CH)	H1	C12, C2
2'	6.14 (1H, t, J = 6.1Hz)	84.8 (CH)	H3'	C11, C2
3'	2.08 (m,2H)	40.2 (CH_2)	H2', H4'	C8, C3, C7
4'	4.27 (m, 1H)	71.1 (CH)	H5', H3',H4"	
5'	3.77 (m, 1H)	88.0 (CH)	H4', H6'	
6'	3.55 (m, 2H)	61.9 (CH_2)	H5', H6"	
4"	5.23 (br,s, 1H)		H4'	
6"	5.00 (br,s, 1H)		H6'	

2-Deoxycytidine (**31**) was isolated previously from the marine sponge *Isodictya erinacea* and characterized structure by 2D NMR.[70] The ^{1}H NMR data were compared with the current compound (**31**), previous compound (**32**) and authentic 2-deoxycytine (**26**). In the current study (**31**), two aromatic methines attached to the pyrimidine ring of 2-deoxycytidine are found at δ 7.88 (H-1, J = 8.1 Hz) and 5.64 (H-6, J = 8.1 Hz), which is identical to chemical shifts and coupling constant from the authentic sample (Figure 30), compound (**31**) [δ 7.86 (H-1, J = 8.1 Hz) , 5.66 (H-6, J = 8.1 Hz)].[71,75] The difference in chemical shifts is attributed to solvent effect.

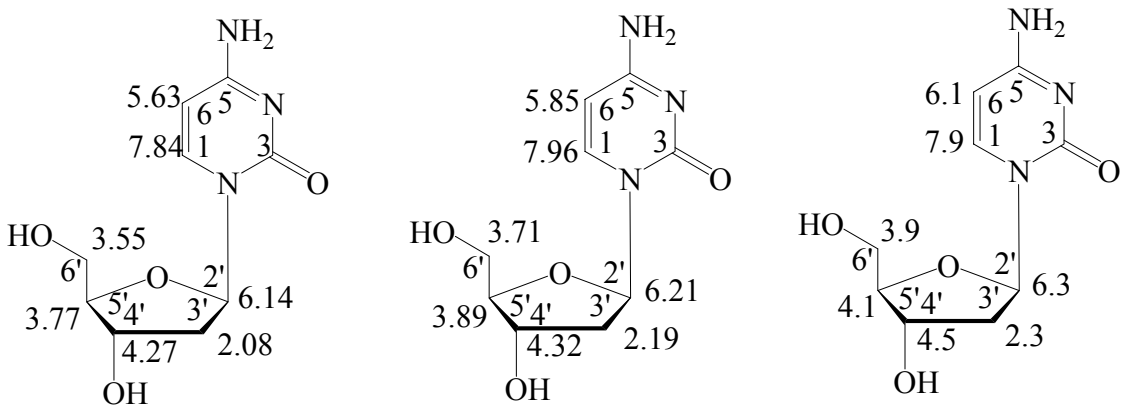

Figure 30. Assigned ^{1}H NMR chemical shifts (δ) of natural 2-deoxycytidine (**31**) (500 MHz, DMSO-d_6), previously isolated 2-deoxycytidine (**32**) [70] (360 MHz, MeOH-d_4) and authentic sample (**26**) [80] (60 MHz, D_2O+NaOD).

3.6 Characterization of 4, 8-Dihydroxyquinoline (33)

4, 8-Dihydroxyquinoline (**33**) was obtained as an amorphous powder. The structure elucidation, complete proton and carbon assignment were achieved by DEPT, gCOSY, gHSQC, and gHMBC techniques. The ^{1}H NMR spectrum (Figure 31) of 4,8-dihydroxyquinoline showed chemical shifts of a classic pattern for a 1,2,3-trisubstituted aromatic ring at δ 7.49 (1H, dd, J = 8.0, 1.0, 1.5 Hz), 7.09 (1H, t, J = 7.8 Hz), 7.04 (1H, dd, J = 7.7 , 1.5 Hz) and pyridine moiety at δ 7.72 (1H, d, J = 7.2 Hz), 6.0 (1H, d, J = 7.2 Hz). The ^{13}C NMR spectrum (Figure 32) of 4, 8-dihydroxyquinoline (**33**) displayed nine aromatic carbons assigned with gHSQC indicating that five methine cabons (δ 139.4, 123.6, 115.4, 114.8, 109.2) and four quaternary carbons (δ 177.8, 147.8, 131.1, 127.4).

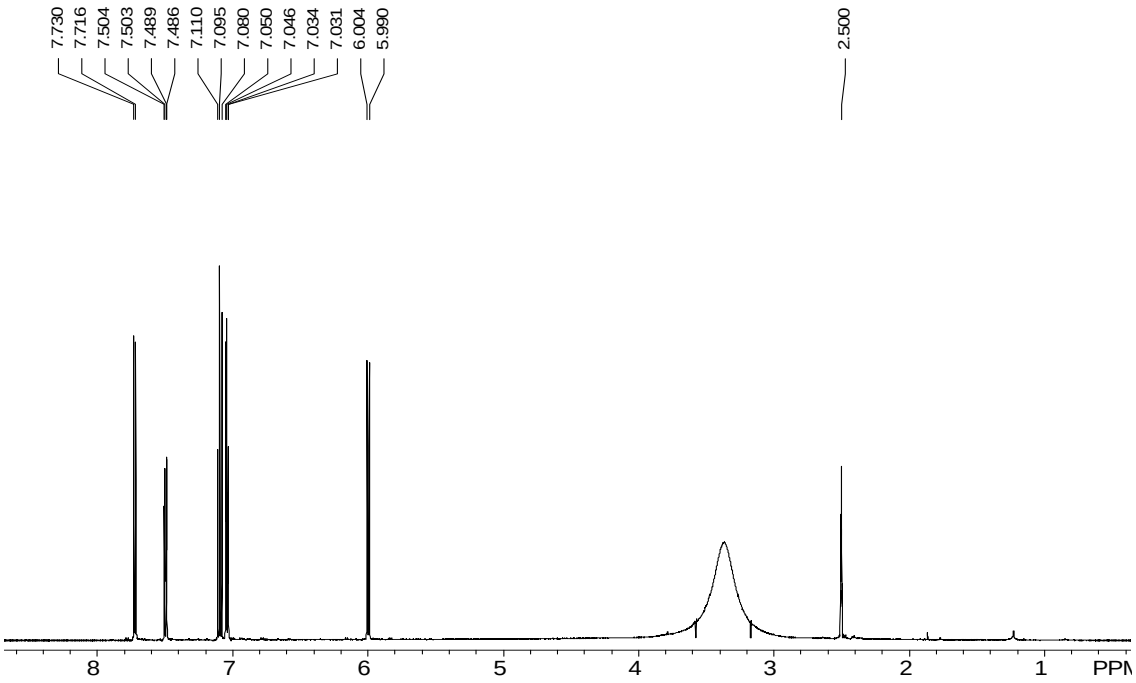

Figure 31. ^{1}H NMR spectrum of 4, 8-dihydroxyquinoline (**33**) (500 MHz, DMSO-d_6).

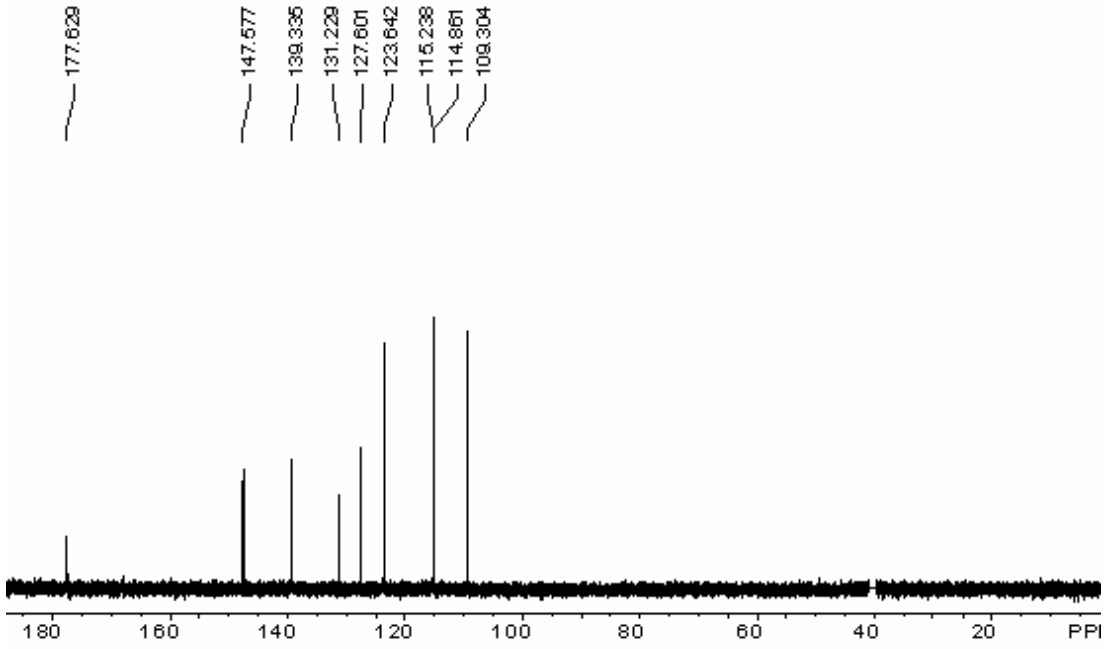

Figure 32. ^{13}C NMR spectrum of 4, 8-dihydroxyquinoline (**33**) (125 MHz, DMSO-d_6).

In the gHMBC spectrum (Figure 33), correlations ($^2J_{CH}$/ $^3J_{CH}$) between proton and carbon were observed that the aromatic proton at H-1 (δ 7.72) to C-9 (δ 177.8), C-7 (δ 131.1), and C-5 (δ 109.2) and H-5 (δ 6.00) to C-9 (δ 177.8), C-6 (δ 127.4), and C-1 (δ 139.4). A benzene moiety was evident in the gHMBC experiment (Figure 34) based on correlations ($^2J_{CH}$/ $^3J_{CH}$ / $^4J_{CH}$) of H-2 (δ 7.50) to C-8 (δ 147.8), C-7 (δ 131.1), C-3 (δ 123.6), and C-4 (δ 114.8) while H-3 (δ 7.09) correlated with C-8 (δ 147.8), C-7 (δ 131.1), C-6 (δ 127.4), C-4 (δ 114.8) and C-2 (δ 115.4).

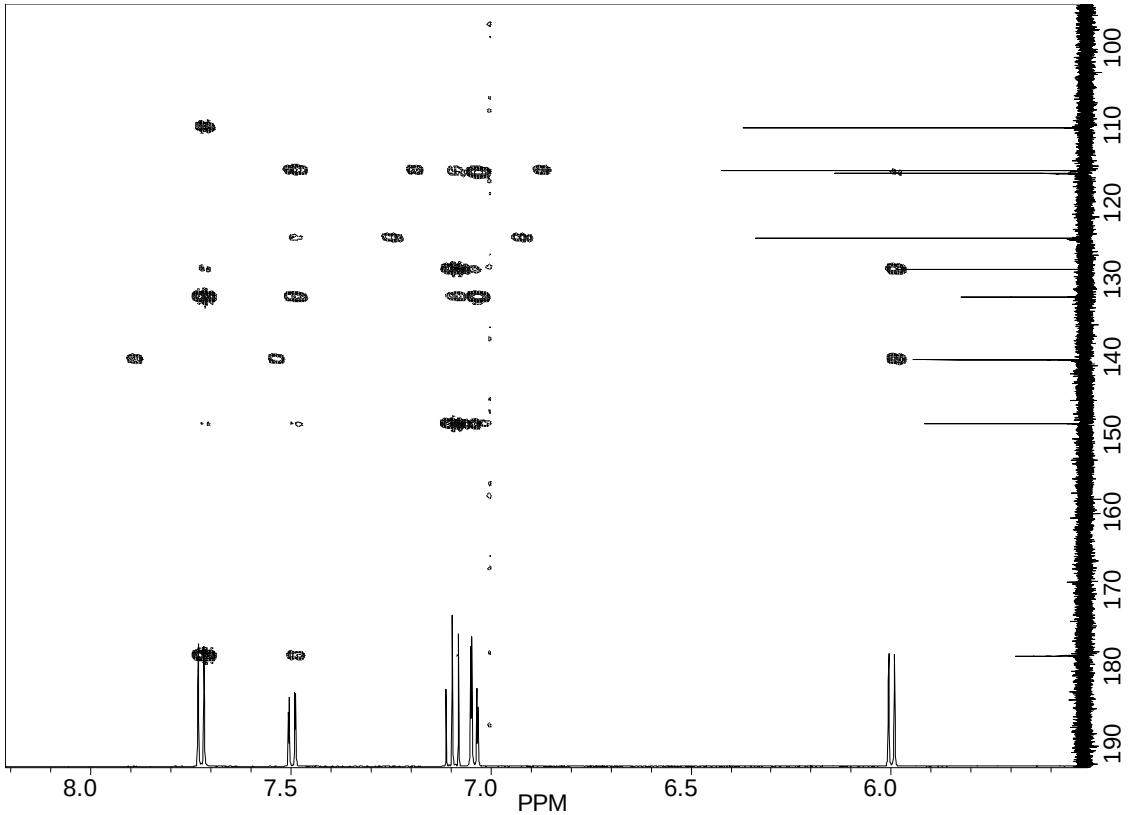

Figure 33. gHMBC spectrum of 4, 8-dihydroxyquinoline (**33**) (500 MHz, DMSO-d_6).

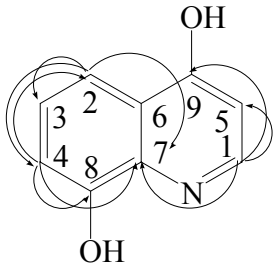

Figure 34. Key gHMBC correlations observed in 4, 8-dihydroxyquinoline (**33**).

Table 6. NMR data of 4, 8-dihydroxyquinoline (**33**) (DMSO-d_6)
(^{13}C, 125 MHz; ^{1}H, 500 MHz)

	^{1}H (δ)	^{13}C (δ)	gCOSY	gHMBC
1	7.72 (1H, d, *J* = 7.2 Hz)	139.4 (CH)	H5	C9, C7, C6, C5
2	7.50 (1H, dd, *J* = 1.4, 7.9 Hz)	115.4 (CH)	H3, H4	C9, C8, C7, C3, C4
3	7.09 (1H, t, *J* = 7.7 Hz)	123.6 (CH)	H2, H4	C8, C7, C6, C4, C2
4	7.04 (1H, dd, *J* = 1.5, 7.7 Hz)	114.8 (CH)	H3, H2	C8, C7, C6, C2
5	6.00 (1H, d, *J* = 7.3 Hz)	109.2 (CH)	H1	C9, C6, C7, C1
6		127.4 (C)		
7		131.1 (C)		
8		147.8 (C)		
9		177.8 (C)		

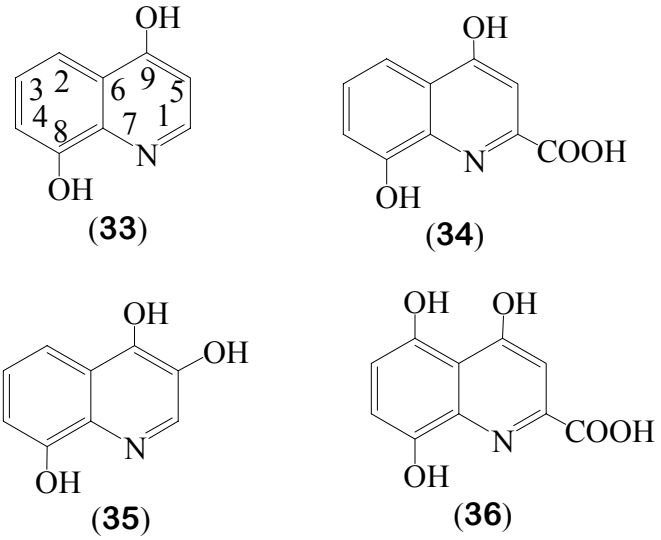

Figure 35. Secondary metabolites of quinoline derivatives.

Quinoline derivatives including quinoline (**34**), 4,5,8-trihydroxyquinoline-2-carboxylic acid (**35**) are known secondary metabolites isolated from sponges *Dendrilla membranosa* and the genus *Verogia*[69] and are suggested to be intermediates of tryptophan catabolism (Figure 35). The chemical shifts of isolated 4,8-dihydroxyquinoline (**33**) were compared relative to known quinoline derivatives **34, 35**[69] and xanthurenic acid **36** from the Aldrich Library of NMR spectra.[82] The quaternary C-9 at δ 177.8 in 4, 8-dihydroxyquinoline (**33**) showed a similar chemical shift with quaternary C-9 at δ 183.6 in trihydroxyquinoline carboxylic acid (**36**).[69]

3.7 Characterization of Homarine (37)

Homarine (N-methyl picolinic acid) (**37**) was isolated as pale brown solid. The ^{1}H NMR spectrum of homarine (Figure 36) showed four methine groups at δ 8.72 (d, J = 6.0 Hz), 8.42 (t, J = 7.9 Hz), 7.90 (dd, J = 1.3, 7.8 Hz), 7.85 (t, J = 6.9 Hz) and one methyl group at δ 4.28 (s).

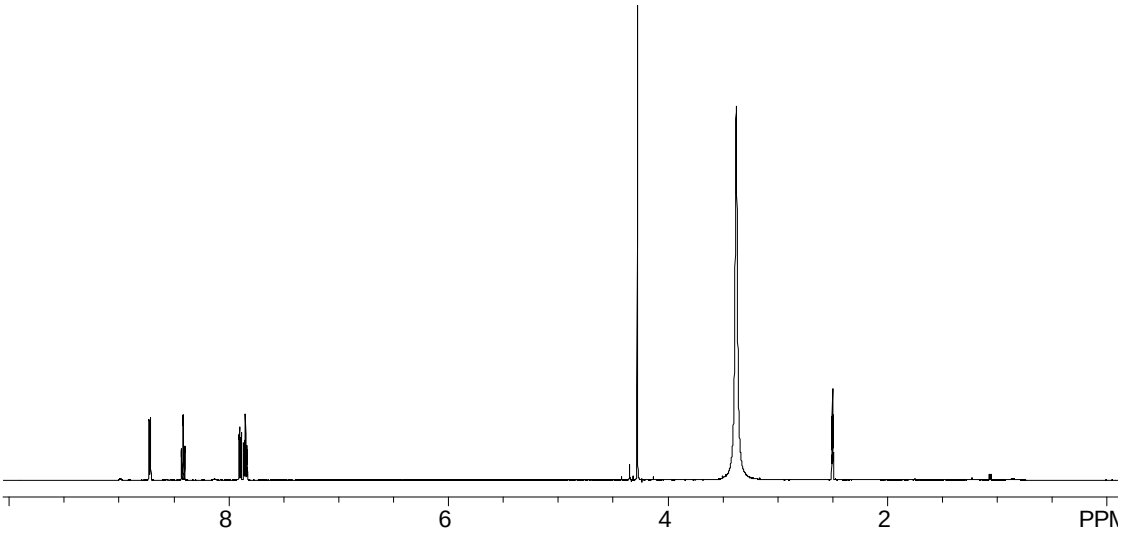

Figure 36. ^{1}H NMR spectrum of homarine (**37**) (500 MHz, DMSO-d_6).

In the ^{13}C NMR spectrum (Figure 37), the five carbons of the pyridine ring resonated at δ 156.7, 145.7, 145.0, 126.9, 125.5, the quaternary carbon of carboxylic acid resonated at δ 161.8 and the carbon of methyl bearing nitrogen was seen at δ 46.5.

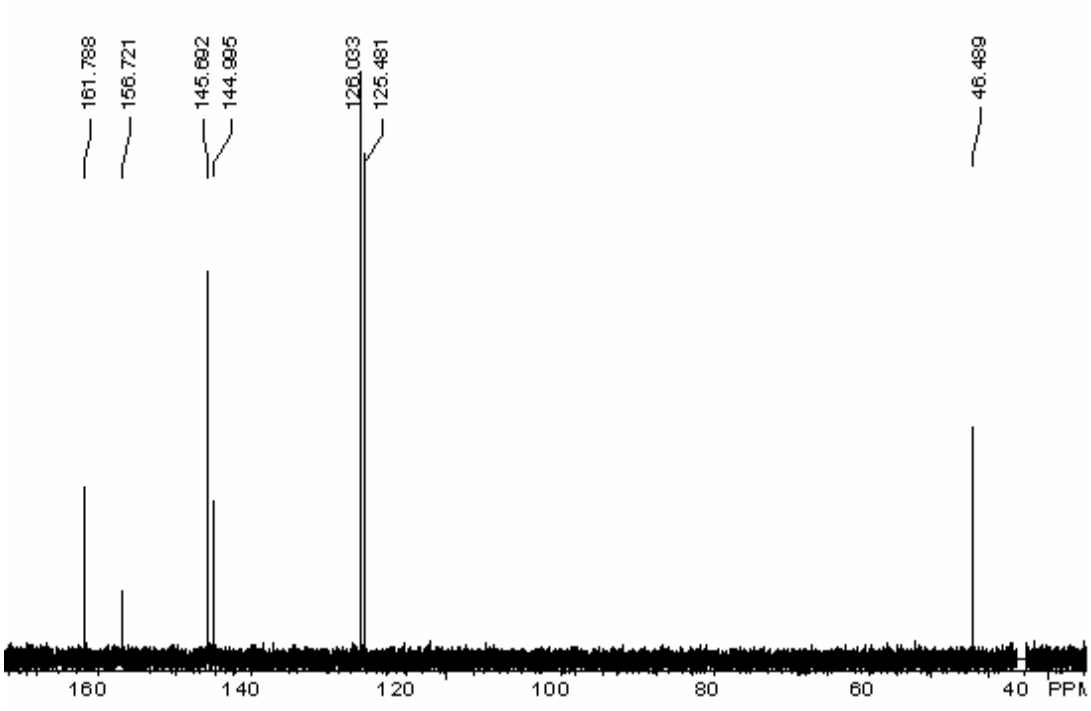

Figure 37. ^{13}C NMR spectrum of homarine (**37**) (125 MHz, DMSO-d_6).

In the gHMBC spectrum (Figure 38), correlations (Table 7) ($^2J_{CH}$/ $^3J_{CH}$) from the aromatic proton at H-1 (δ 8.72) to C-2 (δ 145.7), C-6 (δ 156.7), C-4 (δ 125.5), C-5 (δ 46.5), and H-2 (δ 8.42) to C-1 (δ 145.0), C-6 (δ 156.7). H-3 (δ 7.90) correlated to C-4 (δ 125.5), C-6 (δ 156.7), and C-7 (δ 161.8) and H-4 (δ 7.85) correlated with C-1 (δ 145.0), and C-3 (δ 126.0), H_3-5 (δ 4.26) to C-1 (δ 145.0), and C-6 (δ 156.7). Thus, the structure of homarine was deduced by gCOSY and gHMBC (Figure 39).

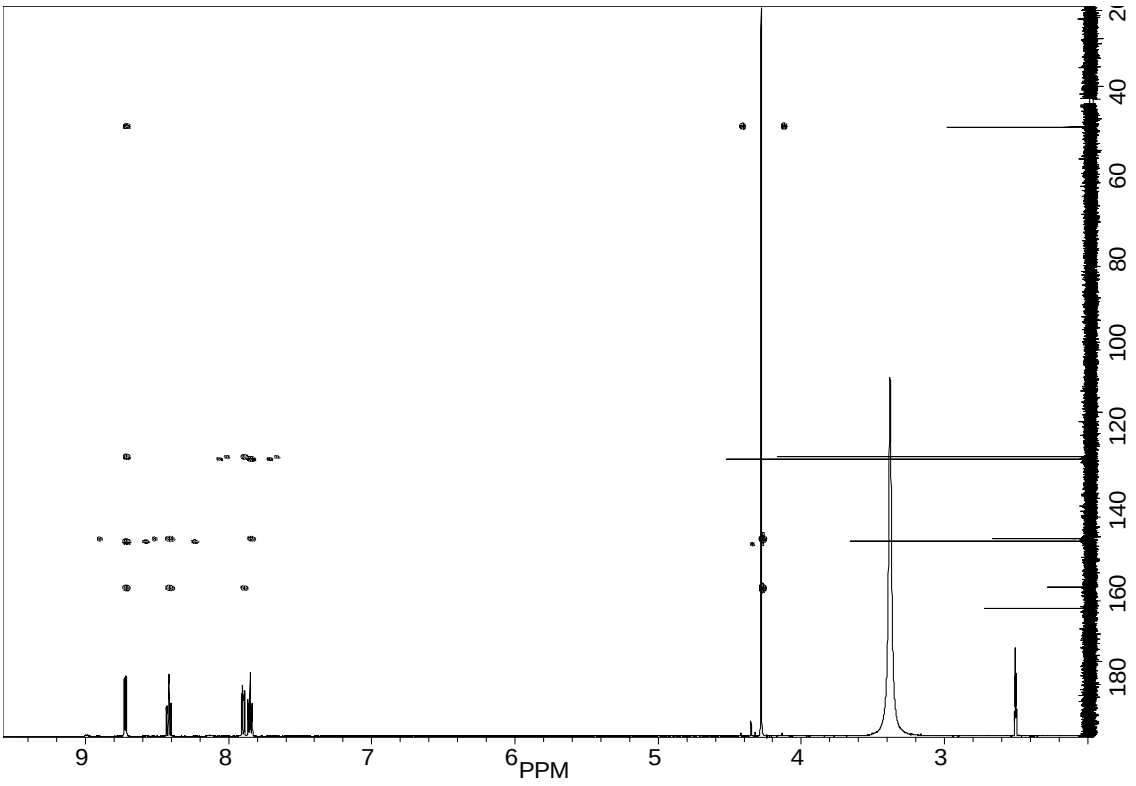

Figure 38. The gHMBC spectrum of homarine (**37**) (500 MHz, DMSO-d_6).

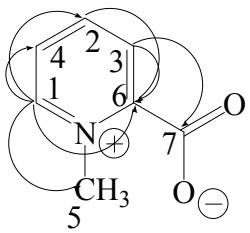

Figure 39. Key gHMBC correlations observed in homarine (**37**).

Table 7. NMR data of homarine (**37**) (DMSO-d_6) (^{13}C, 125 MHz; ^{1}H, 500 MHz)

position	^{1}H (δ)	^{13}C (δ)	gCOSY	gHMBC
1	8.72 (1H, d, J = 6.0 Hz)	145.0 (CH)	H2, H4	C2, C6, C4, C5
2	8.42 (1H, t, J = 7.9 Hz)	145.7 (CH)	H3, H4	C1, C6
3	7.90 (1H, dd, J = 1.3, 7.8 Hz)	126.0 (CH)	H2	C4, C6, C7
4	7.85 (1H, t, J = 6.9 Hz)	125.5 (CH)	H1, H2, H3	C1, C3
5	4.28 (3H, s)	46.5 (CH_3)		C1, C6
6		156.7 (C)		
7		161.8 (C)		

Homarine was isolated from *Dendrilla membranosa* and showed feeding deterrence to the Antarctic seastar *Odonataster validus*[83] and suggested chemical interactions between sponge and sea stars.[83] The feeding deterrence of homarine also was reported Antarctic mollusk *Marseniopsts mollis* against seastars.[84] The chemical shifts of homarine **37** were compared with authentic ^{1}H NMR spectrum data (Figure 40) from the Aldrich Library of NMR spectra[85] and suggest homarine. The difference in chemical shifts is attributed to solvent effect.

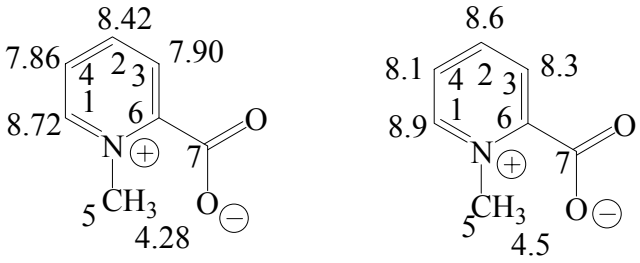

(**37**) (**38**)

Figure 40. Assigned ^{1}H NMR chemical shifts (δ) of natural homarine (**37**) (500 MHz, DMSO-d_6), and authentic sample (**38**)[85] (60 MHz, D_2O).

Chapter 4. CHEMICAL INVESTIGATION OF ANTARCTIC MARINE SPONGE *ISODICTYA ANTARCTICA*

4.1 Extraction and Isolation of Secondary Metabolite

The sponge *Isodictya antarctica* (Figure 41) was collected by SCUBA diving on the shipwreck Bahia Paraiso near Palmer station, Antarctica. The freeze-dried sample of *Isodictya antarctica* was first extracted with methanol at room temperature (Scheme 4).

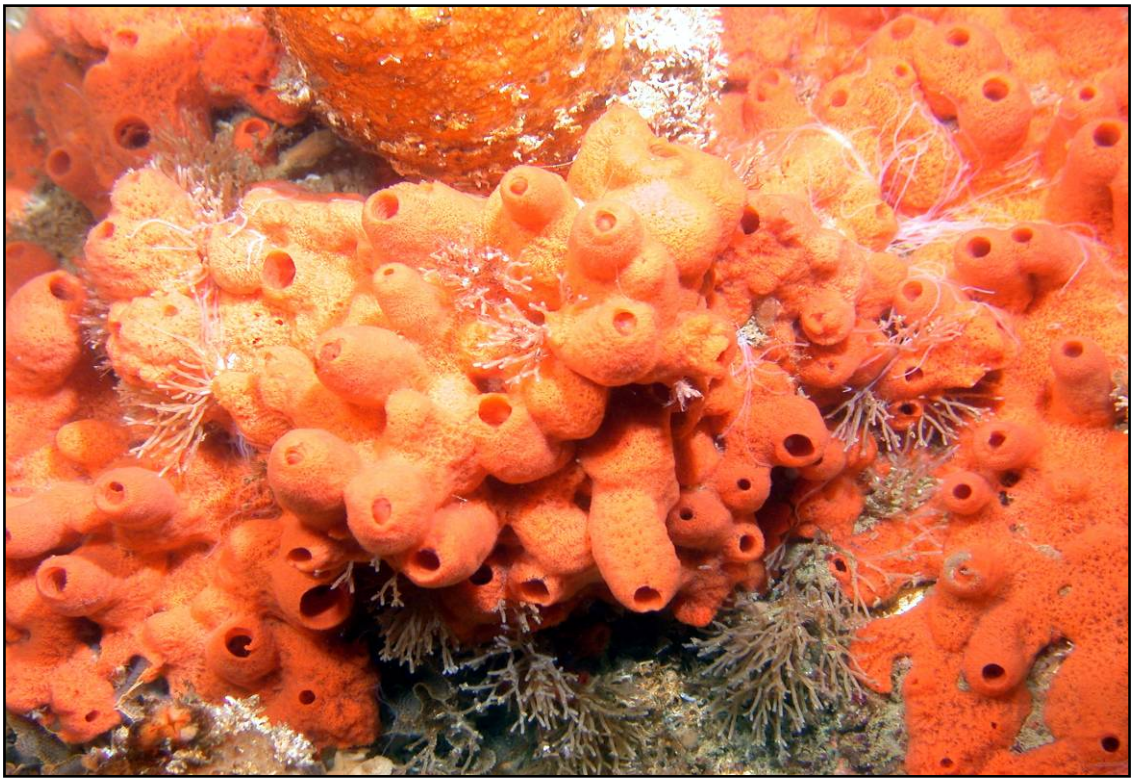

Figure 41. *Isodictya antarctica* collected from Bahia Paraiso, Palmer Station, Antartica (Photograph supplied by Bill J. Baker, University of South Florida).

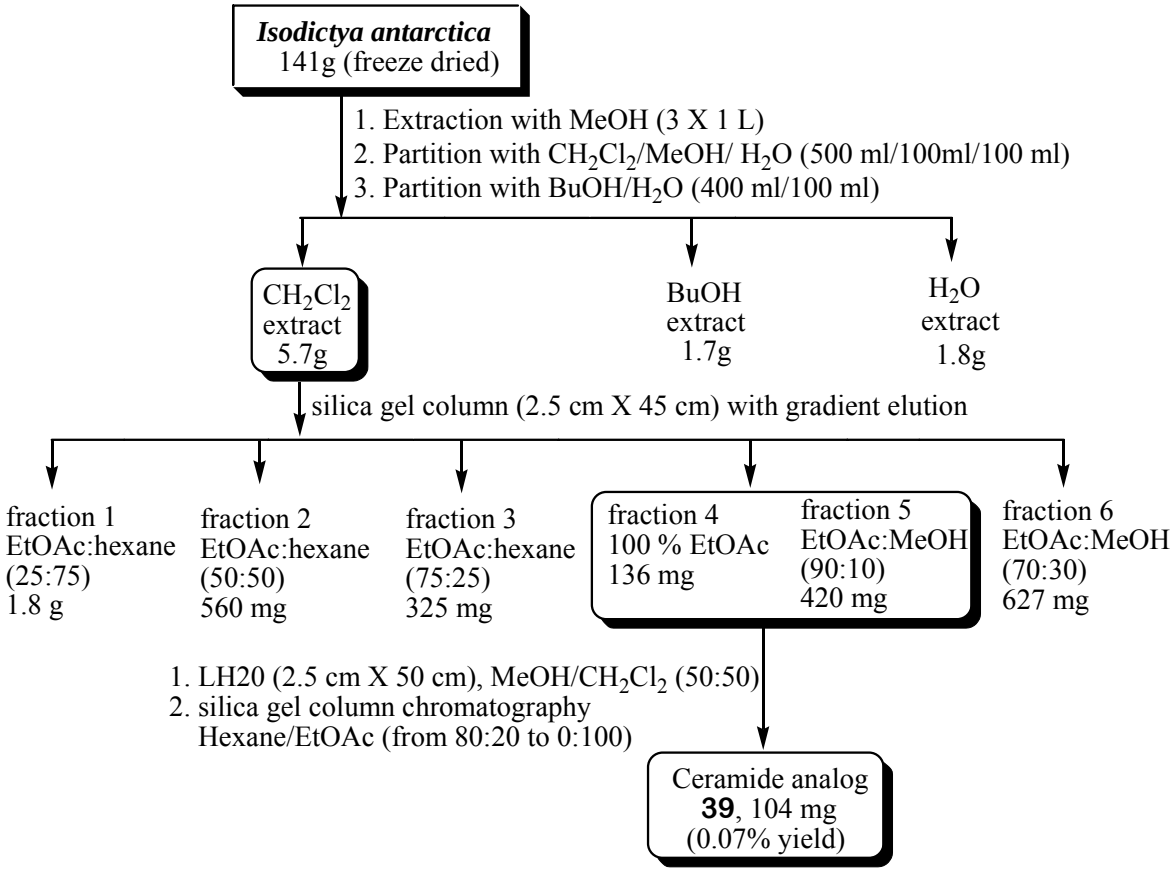

Scheme 4. Isolation of ceramide analog (**39**).

After concentration, the crude extract was partitioned with CH_2Cl_2, MeOH, and BuOH. The CH_2Cl_2 soluble material was initially chromatographed on silica gel with gradient elution (from EtOAc/hexane to EtOAc/MeOH) to afford six fractions. After combining fraction 4 and fraction 5, the resulting fraction was subjected to Sephadex LH-20® column chromatography and then further purified by silica gel column chromatography to afford a ceramide analog (**39**) (104 mg, 0.07% dry wt).

4.2 Characterization of Ceramide analog (39)

Ceramide analog (**39**) was obtained as a colorless amorphous solid. The HRESIMS showed the $[M + H]^+$ ion peak at *m/z* 664.6599 (calculated 664.6607) corresponding to the molecular formula $C_{43}H_{85}NO_3$. The IR spectrum showed absorptions at 3300 cm^{-1} for a hydroxyl group, 1642 cm^{-1} for a carbonyl. The ^1H NMR spectrum (Figure 42) displayed a large number of methylene groups at δ 1.28. The connectivities of the aliphatic moiety were determined by gCOSY, TOCSY and the $^1J_{CH}$ connectivities were assigned by gHSQC.

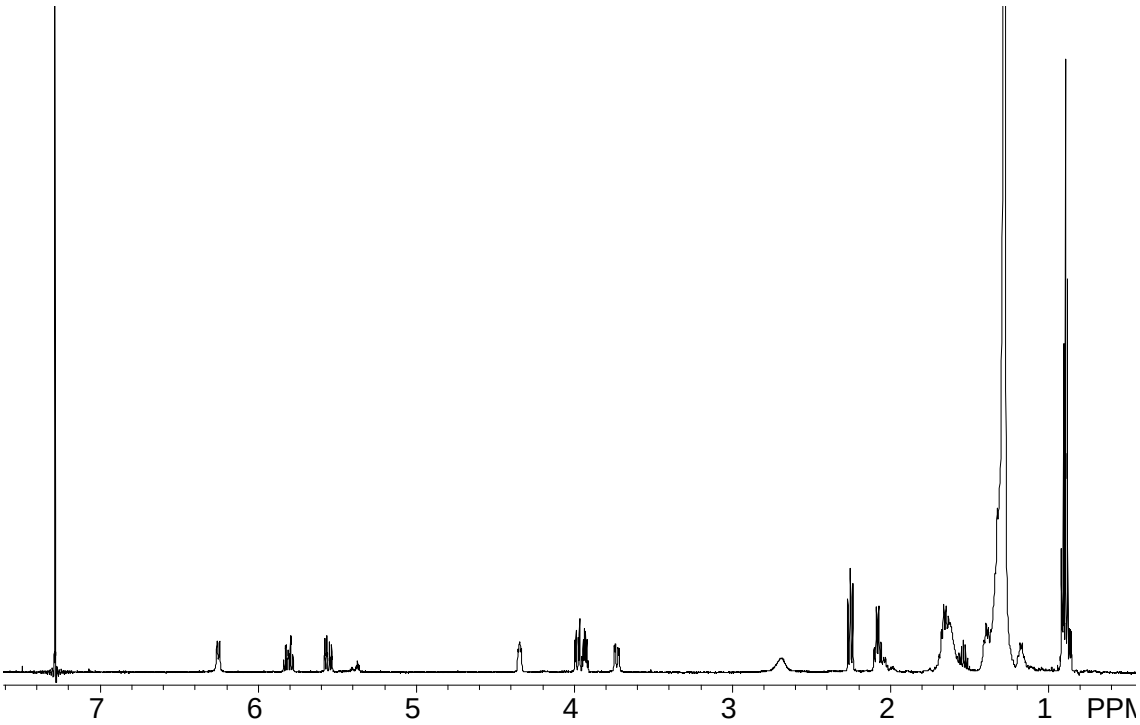

Figure 42. ^1H NMR spectrum of ceramide analog (**39**) (500 MHz, $CDCl_3$).

A substructure is represented by the nonequivalent methylene proton (H-1) signals at δ 3.97 (dd, *J* = 3.8, 11.0 Hz) and 3.71 (dd, *J*= 3.3, 11.3 Hz), two olefinic proton signals at δ 5.80 (H-5) (dt, *J* = 7.4, 15.5 Hz) and δ 5.54 (H-4) (dd, *J* = 6.6, 15.6 Hz) and two methine protons at δ 4.34 (H-3) (t, *J* = 5.0 Hz) and δ 3.91 (m, H-2). The large coupling constants (*J* = 15.5, 15.6 Hz) of two methine protons at δ 5.80 and 5.54 revealed the (*E*) configuration of the double bond. The gCOSY and TOCSY (**TO**tal **C**orrelation **S**pectroscop**Y**) experiments (Figure 43) confirmed the coupling of an amide proton (δ 6.24) with the methine proton at δ 3.91 (1H, m, H-2), as well as with the methylene proton (H_2-1) signals at δ 3.97 (1H, dd, *J* = 3.8, 11.0), 3.71 (1H, dd, *J* = 3.3, 11.3) and methine signal at δ 4.34 (1H, t, *J* = 5.0, H-3). The methylene proton at δ 2.02 (2H, m, H-6) also showed the coupling with methine signal at δ 5.54 (H-4) and 4.34 (H-3). Thus the ^{1}H, ^{13}C NMR (Figure 44), gCOSY, TOCSY, gHSQC, and gHMBC experiments led to confirm the partial structure (**a**) of ceramide analog (**39**).

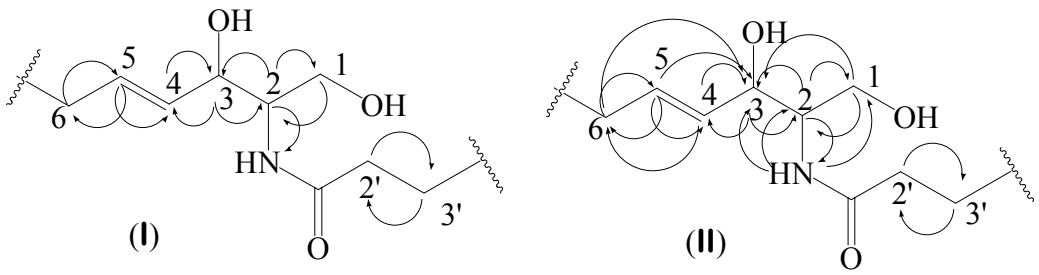

Figure 43. Key gCOSY (**I**) and TOCSY (**II**) correlations in partial structure (**a**).

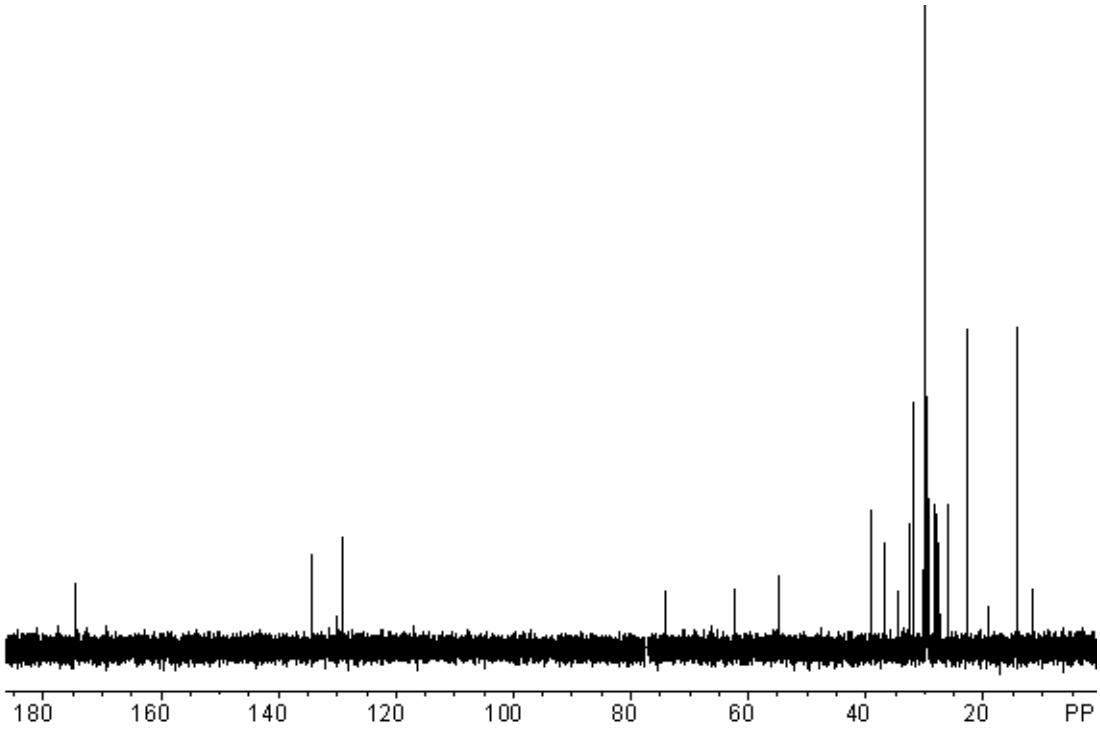

Figure 44. ^{13}C NMR spectrum of ceramide analog (**39**) (125 MHz, $CDCl_3$).

The DEPT (**D**istortionless **E**nhancement by **P**olarization **T**ransfer)-135 (Figure 45) and 90 (Figure 46) data showed five methine carbon groups at δ 134.2, 129.1, 74.2, 54.9, 28.2 and three methyl carbons at δ 22.9, 22.8 indicating terminal isopropyl group and δ14.3. The partial gHMBC data (Table 8) revealed correlations (Figure 47, 48) from amide proton (δ 6.24) to the methine carbons at δ 74.2 (C-3), 55.0 (C-2) and the methylene carbon at δ 62.4 (C-1) along with quaternary carbonyl carbon at δ 174.5 (C-1').

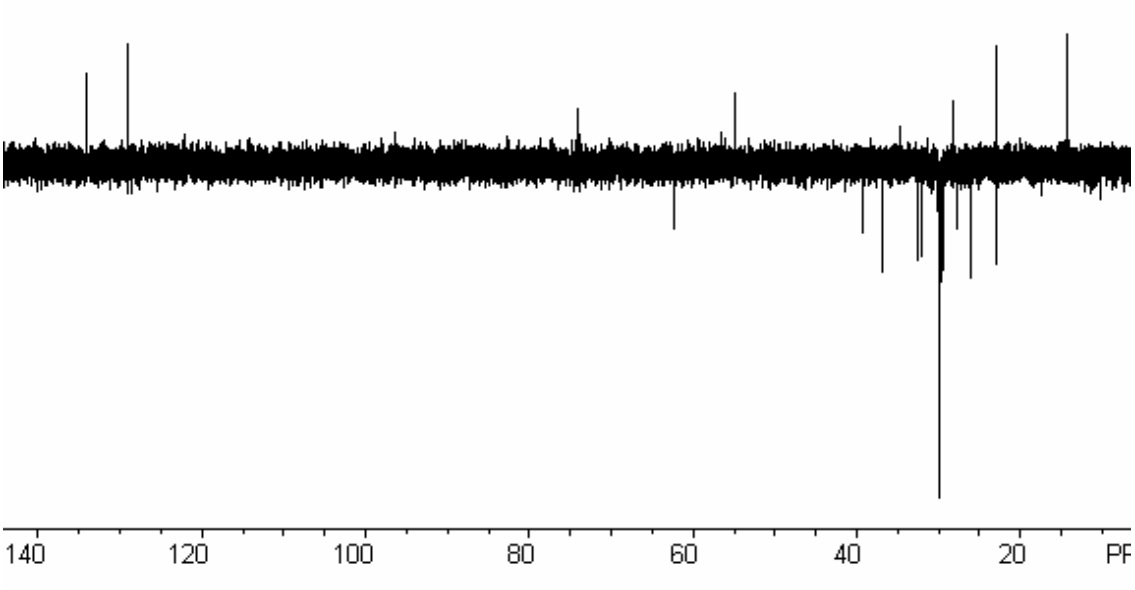

Figure 45. DEPT-135 spectrum of ceramide analog (**39**) (125 MHz, $CDCl_3$).

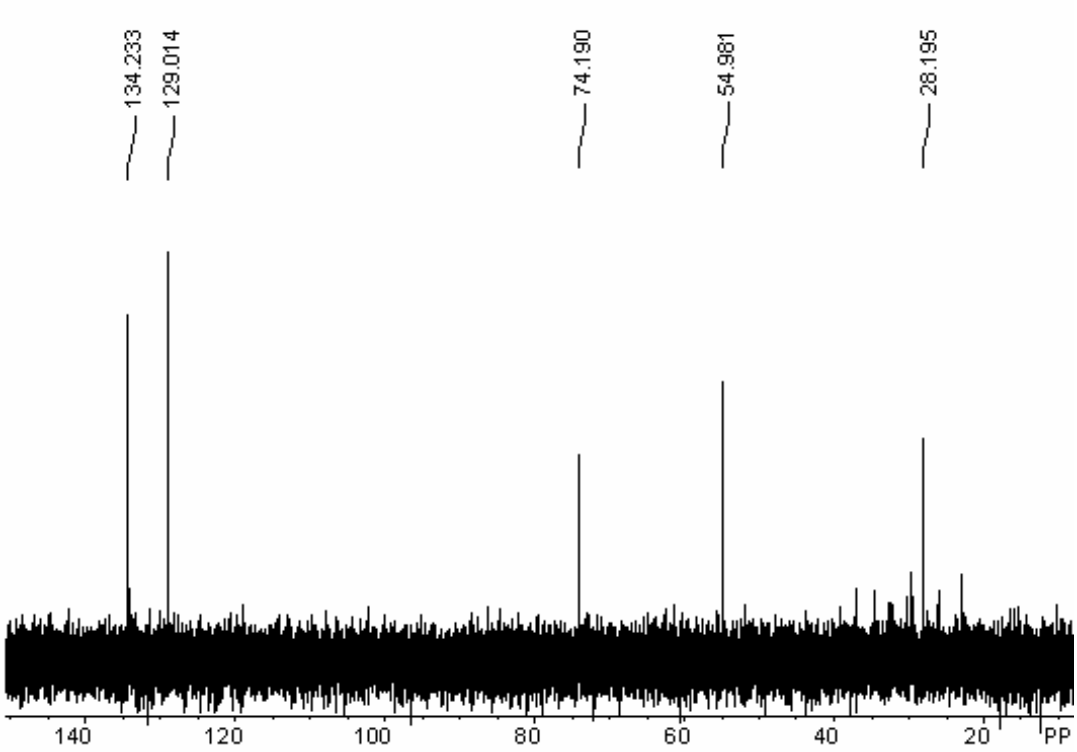

Figure 46. DEPT-90 spectrum of ceramide analog (**39**) (125 MHz, $CDCl_3$).

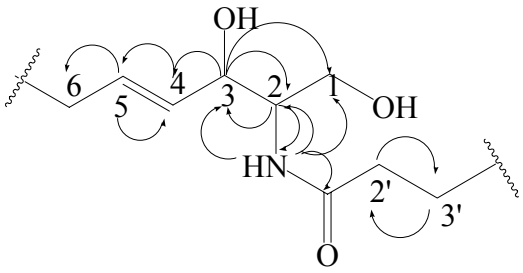

Figure 47. Key gHMBC correlations observed in partial structure (**a**) of ceramide analog (**39**) (125 MHz, $CDCl_3$).

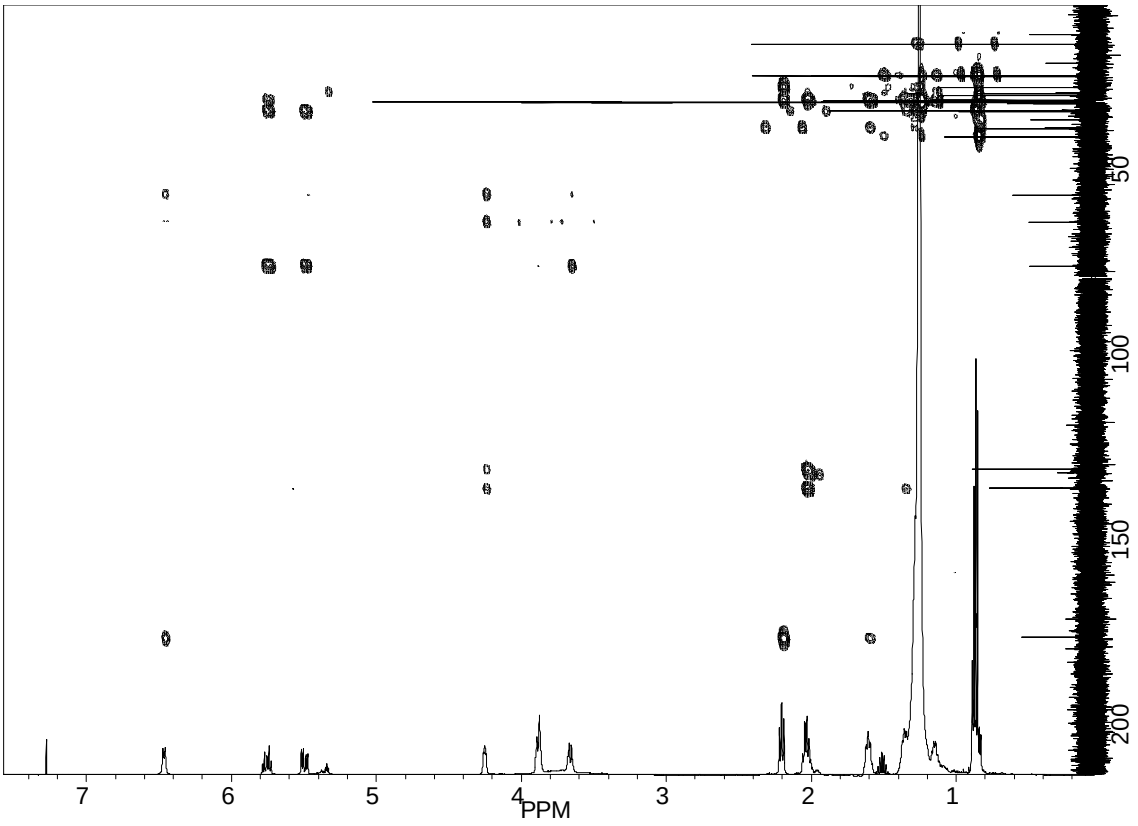

Figure 48. gHMBC spectrum of ceramide analog (**39**) (500 MHz, $CDCl_3$).

Table 8. NMR data of partial structure (**a**) ($CDCl_3$) (^{13}C, 125 MHz; ^1H, 500 MHz)

	^1H (δ, *J*, Hz)	^{13}C (δ)	gCOSY	TOCSY	gHMBC
1	3.97 (1H, dd, 3.8, 11.0)	62.4 (CH_2)	H2	H2, H3, NH	C2, C3
	3.71 (1H, dd, 3.3, 11.3)		H2	H2, H3, NH	
2	3.91 (1H, m)	54.9 (CH)	H3, NH	H1, H4, H5	C4, C1'
3	4.34 (1H, t, 5.0)	74.2 (CH)	H2, H4	H1, H2, H4, H5, H6, NH	C1, C2, C4, C5
4	5.54 (1H, dd, 6.6, 15.6)	129.1 (CH)	H3, H5	H3, H5, H6 H7, NH	C2, C3, C6
5	5.80 (1H, dt, 7.4, 15.5)	134.2 (CH)	H4, H6	H3, H4, H6 H7	C3, C6
6	2.02 (2H, m)	32.6 (CH_2)	H5, H7	H3, H4, H5	C4, C5, CH_2
1'		174.5 (C)			
2'	2.24 (2H, t, 7.5)	37.0 (CH_2)	H3'	H3', CH_2	C1', C3', CH_2
3'	1.60 (2H, m)	26.0 (CH_2)	H2'	H2', CH_2	C1', C2', CH_2
NH	6.24 (1H, d, 7.7)		H2	H1, H2, H3 H4, H5, H6	C1, C2, C3, C1'

To determine the number of methylene carbons of ceramide analog (**39**), the natural product ceramide analog was subjected to methanolysis (Scheme 5) with 1.25 M HCl - MeOH for 20 hr under mild reflux and then partitioned into petroleum ether and MeOH layers.

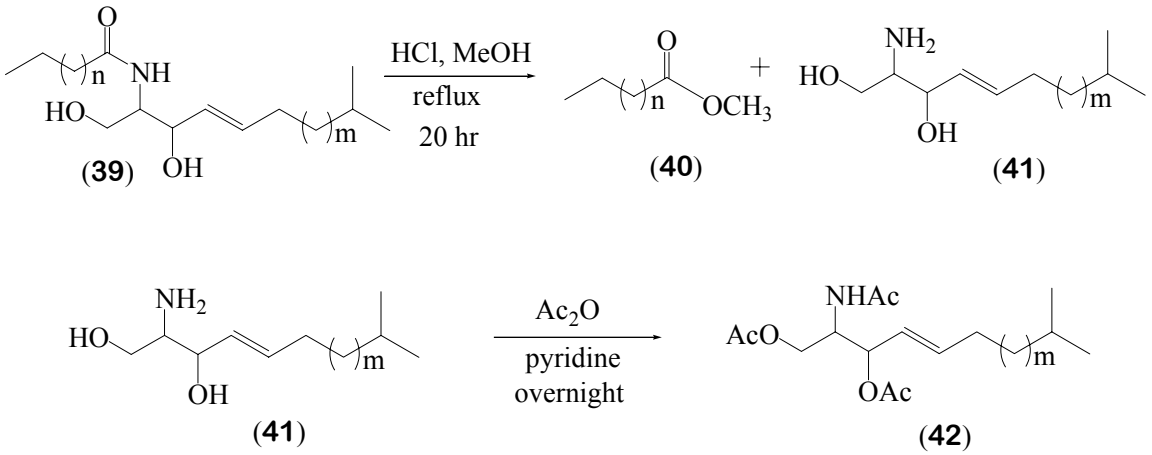

Scheme 5. Methanolysis and protection reactions of ceramide analog (**39**).

The MeOH layer was treated with acetic anhydride to give the protected compound (**42**). The ^{1}H NMR spectrum (Figure 49) of compound (**40**) in the petroleum ether layer displayed typical fatty ester moiety with methoxy proton at δ 3.59 and provided single terminal methyl proton at δ 0.81 (3H, t, J = 6.7 Hz). The ^{13}C NMR spectrum (Figure 50) showed quaternary carbonyl carbon at δ 174.6 indicating an ester unit. The molecular formula of compound **40** was determined by HREIMS as $C_{25}H_{50}O_2$ (observed m/z 382.3804, calculated 382.3811) indicating a C24 *n*-nervonic acid moiety.

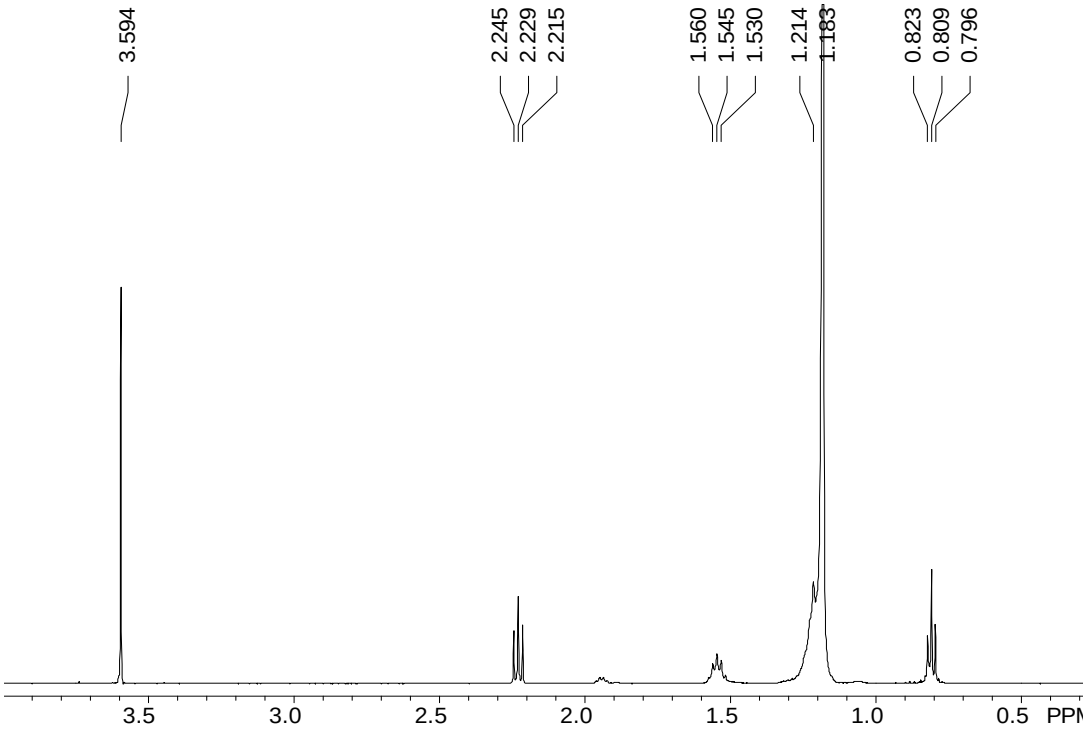

Figure 49. ^{1}H NMR spectrum of methyl ester (**40**) (500 MHz, $CDCl_3$).

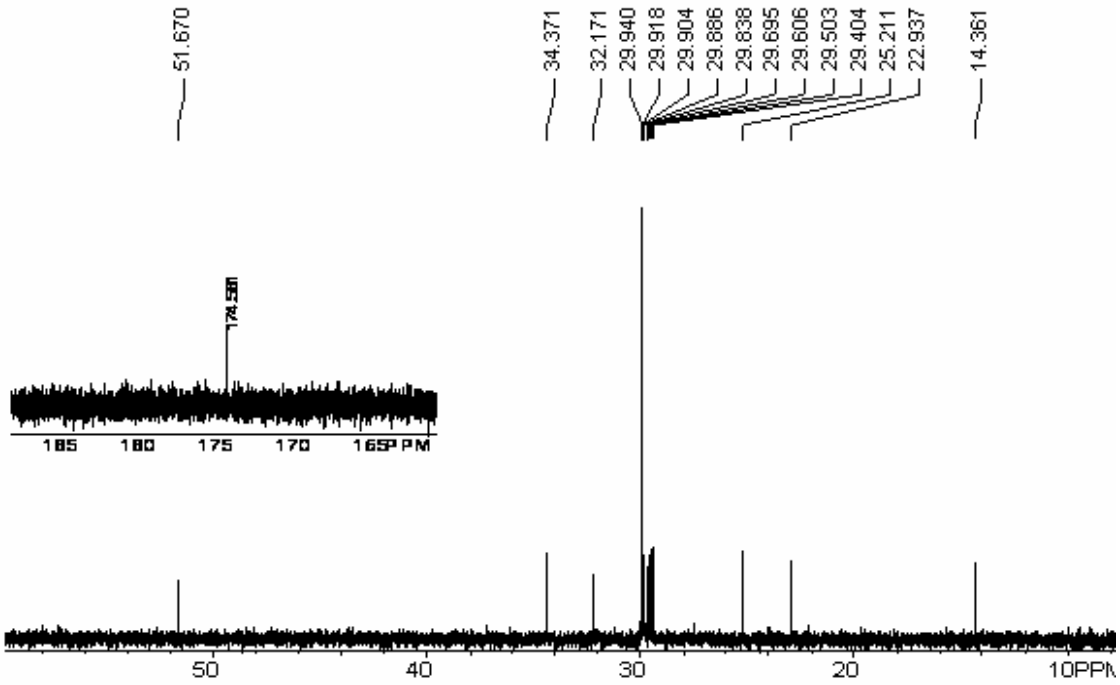

Figure 50. ^{13}C NMR spectrum of methylester **40** (125 MHz, $CDCl_3$).

The ^{1}H NMR spectrum (Figure 51) of protected acetylated aminodiol **42** showed three acetoxy methyl groups at δ 2.10, 2.09, 2.01 along with isopropyl unit at δ 0.87 (6H, d, J = 6.3 Hz) and the ^{13}C NMR spectrum (Figure 52) displayed two esters and one amide carbonyls at δ 171.2, 170.2, and 169.8. The HRESIMS data of compound **42** displayed an ion peak at m/z 440.3372 $[M + H]^+$ (calculated m/z 440.3376) corresponding to the molecular formula $C_{25}H_{45}NO_5$.

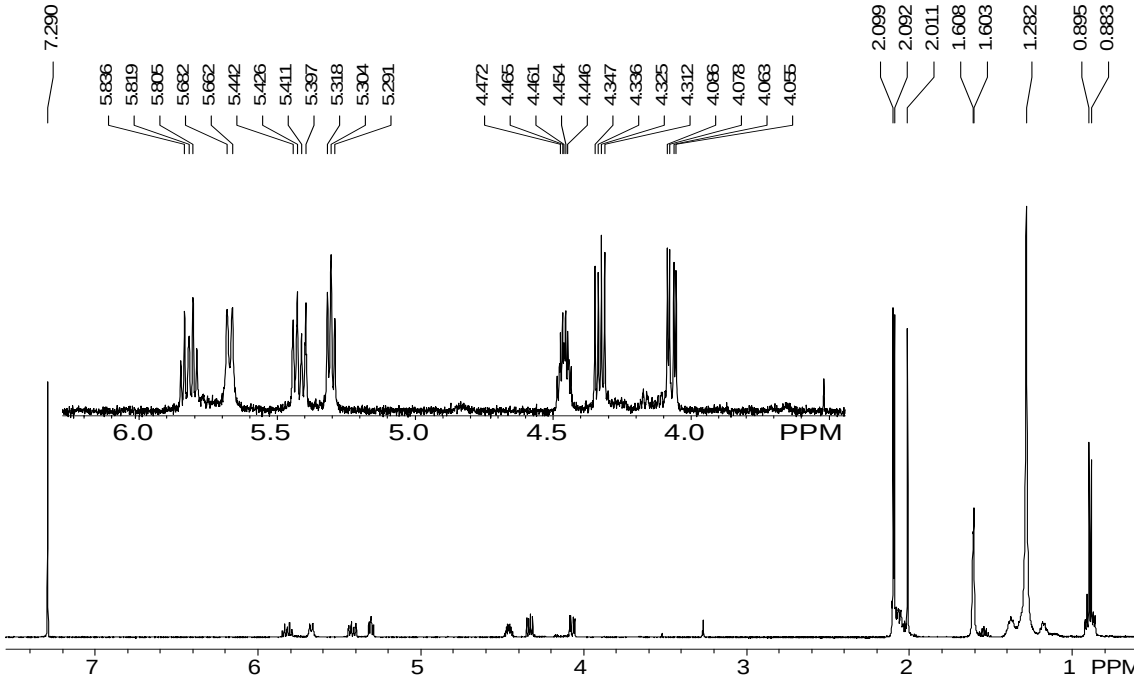

Figure 51. ^{1}H NMR spectrum of acetylated aminodiol (**42**) (500 MHz, $CDCl_3$).

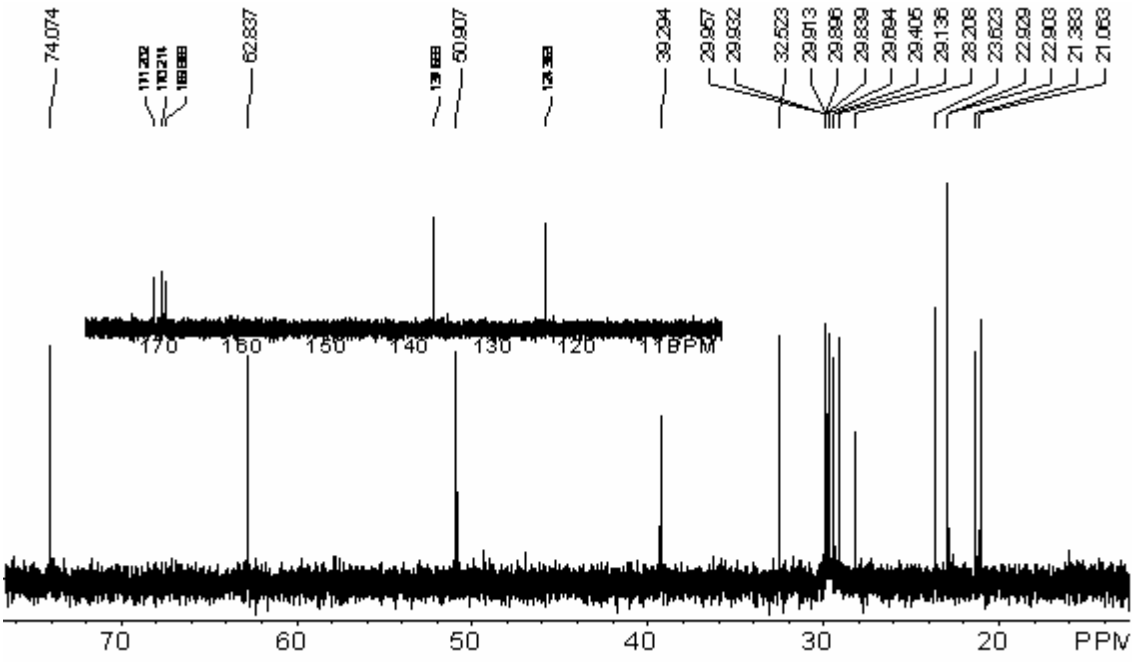

Figure 52. ^{13}C NMR spectrum of acetylated aminodiol (**42**) (125 MHz, $CDCl_3$).

4.3 Determination of Stereochemistry

The modified Mosher's method was used for the determination of absolute stereochemistry of ceramide analog (**39**) at C-3 using a MTPA-Cl [α-methoxy-α-(trifluoromethyl)phenylacetyl chloride].[86] The most important factor of modified Mosher's method is the difference in steric bulkiness of the substitutions of the two β- and β'-carbons. The steric repulsion between the phenyl group of MTPA moiety and the β-substitutions is essential to bring about the Δδ of the CF_3 (^{19}F NMR) or OMe (^{1}H NMR) of the (*R*) – and (*S*) - MTPA esters which is then used to determine the absolute stereochemistry. However, some erroneous predictions of absolute stereochemistry have reported using the original Mosher's method,[87] due to the β- or β'-substituents of certain compounds being placed far away from the MTPA moiety or other substituents (γ-, δ-, ε- positions) having a greater steric interaction with the MTPA groups.[86, 87] The modified Mosher's method uses the same principles as the initial Mosher's method, however these assigned values must meet certain conditions before the absolute stereochemistry can be confidently assigned.[86,88] Thus, the modified method is generally more reliable than initial Mosher's method. However, there were some reports incorrect absolute stereochemistry assignments using this technique on secondary alcohols with the hydroxyl group located in crowded environments.[86] If a molecule has a less steric crowding or hindrance around hydroxyl group, the preferred conformation of the MTPA ester should be obtained, and the modified Mosher's method will give the correct absolute configuration. This preferred orientation consists of the carbinyl proton, ester carbonyl and trifluoromethyl groups of the MTPA ester all

lie in the same plane (Figure 53). In this orientation, protons ($H_{A,B,C}$) of an (*R*) – MTPA ester should have an upfield ^{1}H NMR chemical shift compared to the protons ($H_{X,Y,Z}$) of (*S*) – MTPA ester due to the anisotropic effect of the MTPA phenyl rings (Figure 54). This shielding effect of the phenyl group has assumed to alter the chemical shifts of proton from the ring.[86,89] With the modified Mosher's method, after the determination of the Δδ values ($\Delta\delta = \delta_S - \delta_R$) for the particular compound, a molecular model is constructed and then confirmed that all the assigned protons with positive and negative Δδ values are actually found on the right and left sides of the MTPA plane, respectively (Figure 54).

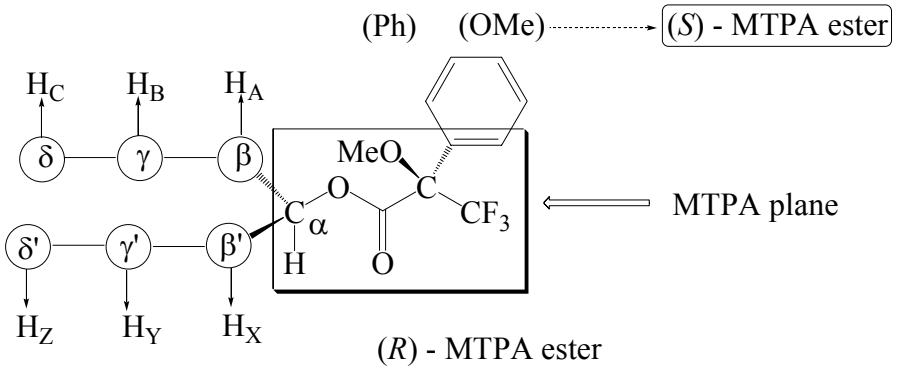

Figure 53. The MTPA plane of the (*R*) – MTPA and (*S*) – MTPA esters of a secondary alcohol.

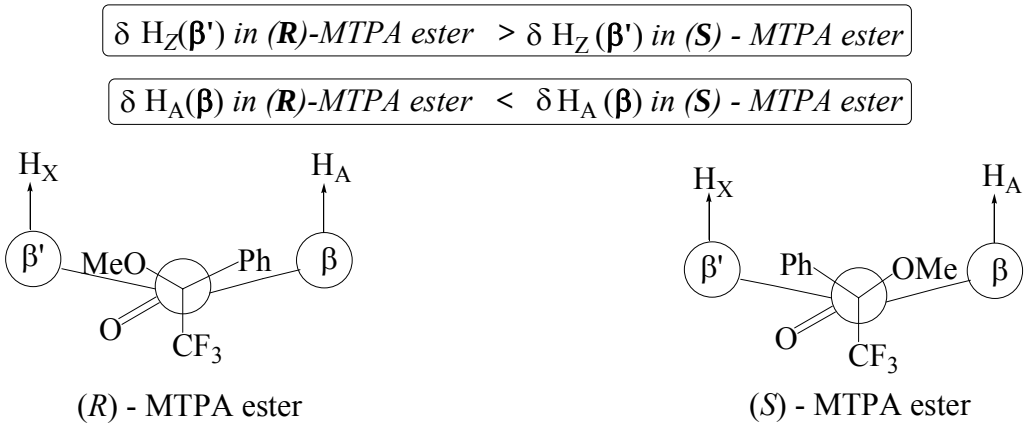

Figure 54. Configurational correlation model for (*R*) and (*S*) – MTPA esters.

The absolute values of the $\Delta\delta = \delta_S - \delta_R$ for each proton should be proportional to the distance from the MTPA moiety due to the diamagnetic effect of the benzene ring of the MTPA to the particular proton (Figure 55). When these conditions are satisfied, the MTPA model indicates the correct absolute stereochemistry.

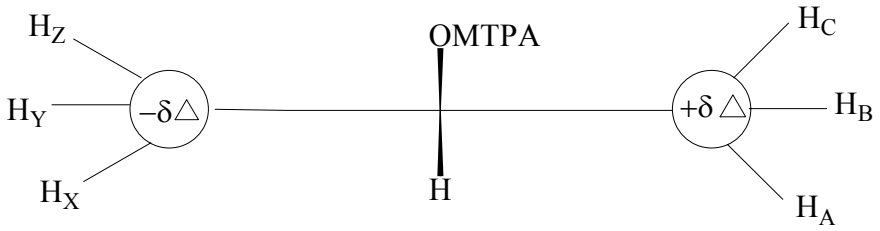

Figure 55. MTPA ester model to determine the absolute configurations of secondary alcohols ($\Delta\delta = \delta_S - \delta_R$) by the modified Mosher's method assignment.

After construction of a simple molecular model, the ceramide analog (**39**) was subjected to esterification with (*R*) – MTPA-Cl and (*S*) – MTPA-Cl in the presence of pyridine (Scheme 6).

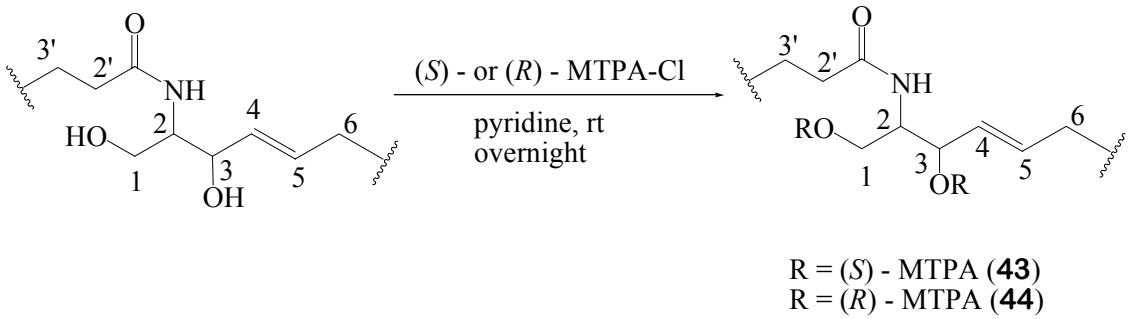

Scheme 6. MTPA reactions with ceramide analog (**39**).

The MTPA esters were chromatographed by normal phase silica gel with EtOAc/hexane (5:95). The absolute stereochemistry of ceramide analog (**39**) was confirmed using ^{1}H NMR spectra (Figure 56 and 57) and gCOSY analysis (Table 9 and

10). All proton signals for both (*S*) – MTPA ester (**43**) and (*R*) – MTPA ester (**44**) were assigned and ^{1}H NMR chemical shift differences ($\Delta\delta = \delta_S - \delta_R$) (Figure 58) were determined for neighboring protons.

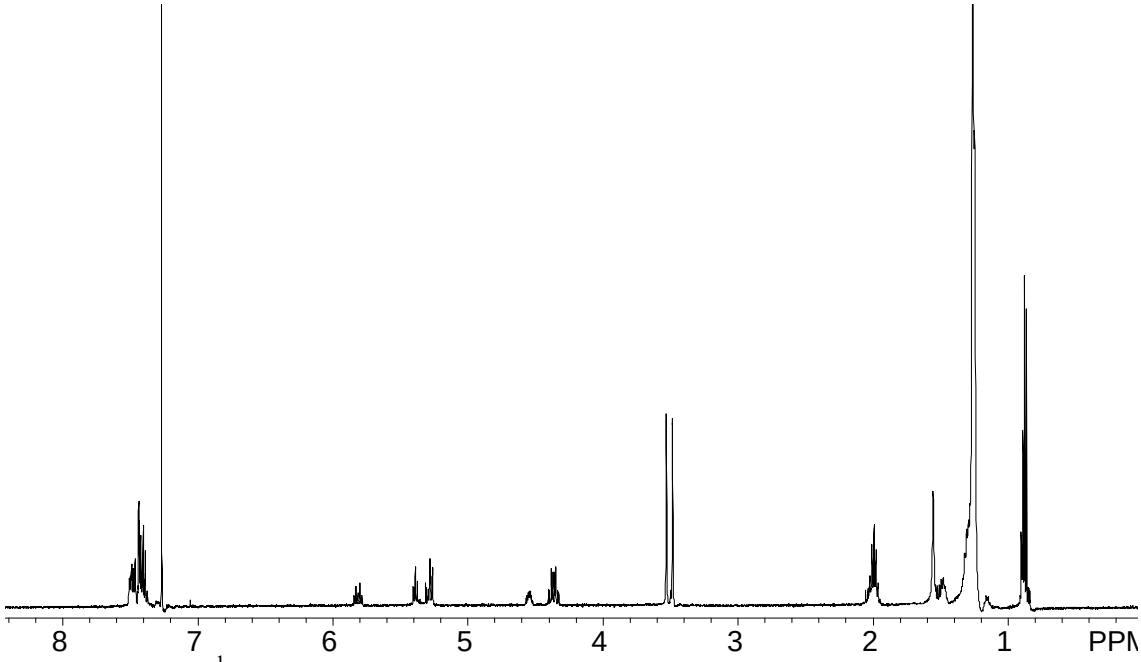

Figure 56. ^{1}H NMR spectrum of (*S*) – MTPA ester (**43**) (500 MHz, $CDCl_3$).

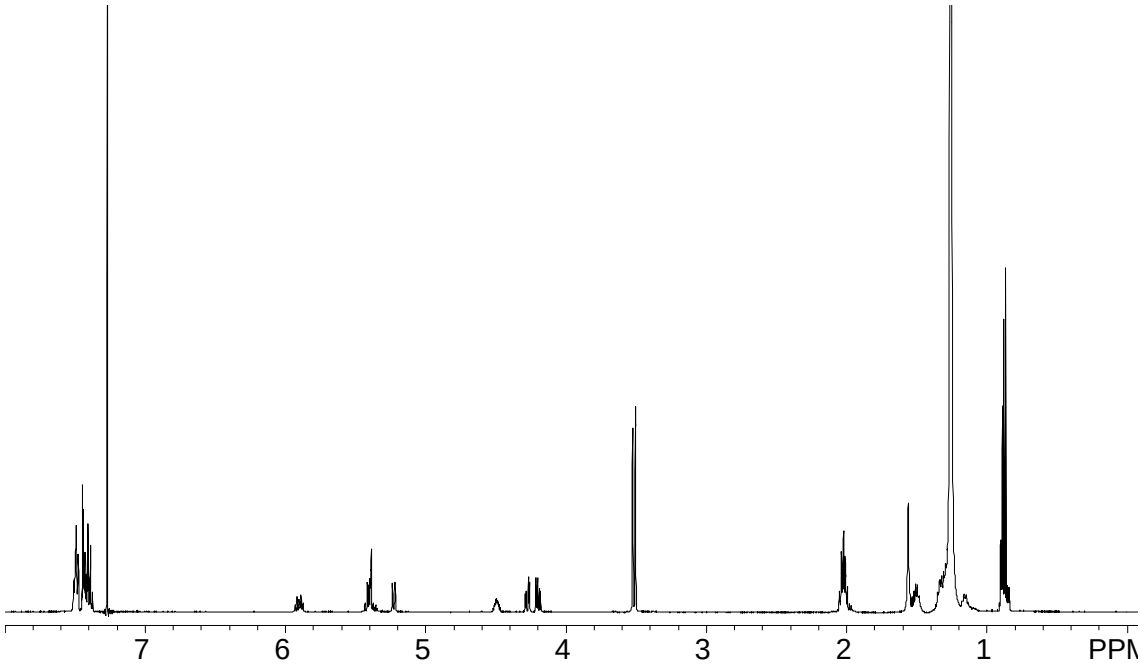

Figure 57. ^{1}H NMR spectrum of (*R*) – MTPA ester (**44**) (500 MHz, $CDCl_3$).

Table 9. NMR data of (*S*)-MTPA ester (**43**) ($CDCl_3$)
(^{13}C, 125 MHz; ^1H NMR 500 MHz)

	$^1H(\delta)$	gCOSY
1	4.39 (1H, dd, *J* = 5.2, 11.6 Hz) 4.34 (1H, dd, *J* = 4.0, 11.8 Hz)	H2
2	4.55 (1H, m)	H1, H3, NH
3	5.39 (1H, t, *J* = 7.8 Hz)	H2, H4
4	5.29 (1H, m)	H2, H3, H5
5	5.81 (1H, dt, *J* = 7.9, 13.4 Hz)	H4, H6
6	2.01 (2H, m)	H4, H5
2'	1.99 (2H, t, *J* = 8.0 Hz)	H3'
3'	1.49 (2H, m)	H2'
NH	5.27 (1H, d)	H2

Table 10. NMR data of (*R*)-MTPA ester (**44**) ($CDCl_3$)
(^{13}C, 125 MHz; ^1H NMR 500 MHz)

	$^1H(\delta)$	gCOSY
1	4.27 (1H, dd, *J* = 3.6, 11.5 Hz) 4.20 (1H, dd, *J* = 5.5, 11.3 Hz)	H2
2	4.49 (1H, m)	H1, H3, NH
3	5.42 (1H, t, *J* = 8.5 Hz)	H2, H4
4	5.39 (1H, m)	H2, H3, H5
5	5.90 (1H, dt, *J* = 5.5, 14.6 Hz)	H4, H6
6	2.02 (2H, m)	H4 ,H5
2'	2.02 (2H, m)	H3'
3'	1.51 (2H, m)	H2'
NH	5.23 (1H, d)	H2

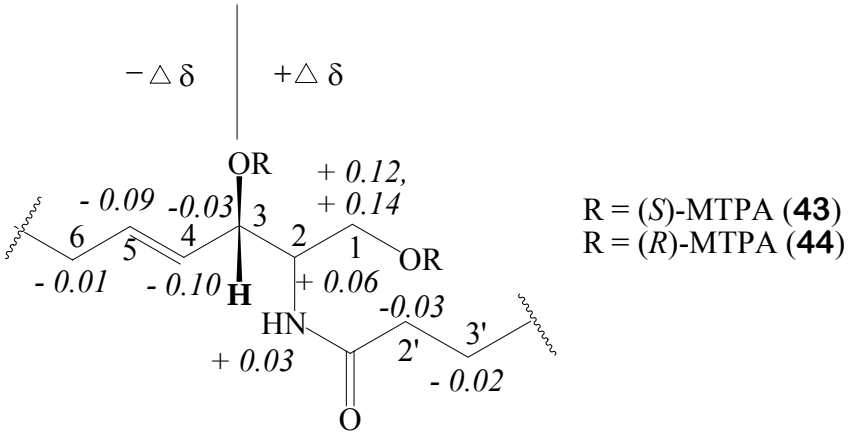

Figure 58. Δδ values ($\delta_S - \delta_R$) of the MTPA esters **43** and **44** in $CDCl_3$.

An MTPA molecular model was constructed with the - Δδ protons on the right and + Δδ protons on the left side of the MTPA plane (Figure 59). After checking that the Δδ values were qualitatively proportional to the distance from the MTPA moiety, the substituents about the chiral centre indicated priority by the Cahn-Ingold-Prelog rules.[90] The results, shown in Figure 59, established that the absolute stereochemistry of C-3 was 3*S* configuration.

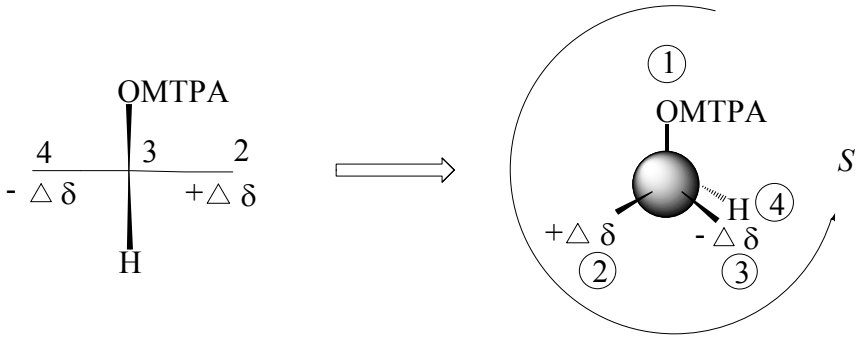

Figure 59. Model to determine the absolute configuration of the cearamide analog (**39**) MTPA esters.

The relative stereochemistry of C-2 was determined with Chem3D software from Cambridge Soft Corporation. The carbon-2 was assumed to have *R* configuration and carbon-3 to have *S* configuration. The dihedral angles (Figure 60) of H-2 (C-2), H-3 (C-3), and H-4 (C-4) were obtained from Chem3D with minimized energy condition by computational calculations. The possible proton-proton dihedral angles showed 173˚ between H-3 and H-2, 163˚ between H-3 and H-4. The relative dihedral angles suggested that H-3 was located in *anti* configuration between H-4 and H-2 and the possible coupling constant ($^{1,3}J_{HH}$) should be triplet multiplicity. The relative dihedral angles showed 91˚ indicating *gauch* form between H-2 and H-1a, 147˚ indicating *anti* form between H-2 and H-1b suggesting that H-2 is multiplet.

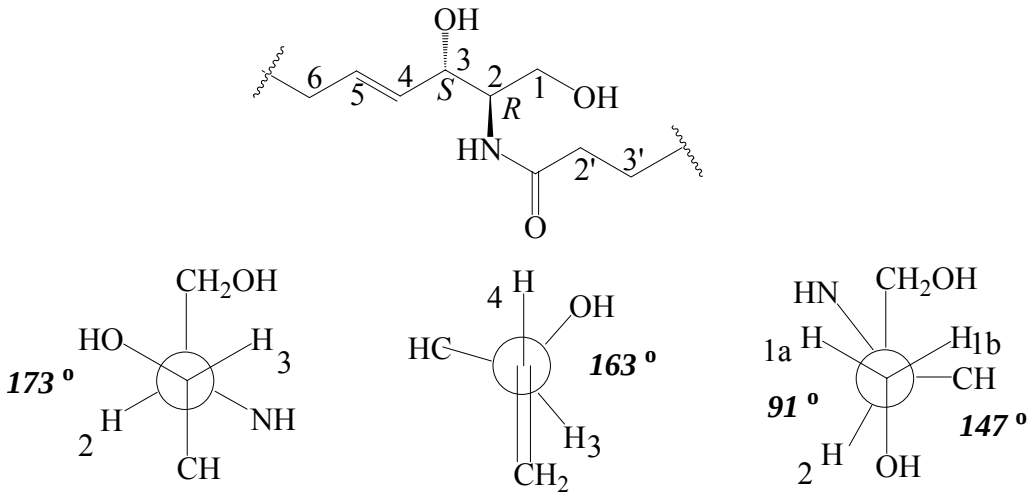

Figure 60. Dihedral angles of H-3, H-4 proposed with 3 (*S*) and 2 (*R*) of ceramide analog (**39**).

When the carbon-2 was assumed to have *S* configuration, the possible proton-proton dihedral angles (Figure 61) calculated by Chem3D showed 63˚ between H-3 and H-2, 166˚ between H-3 and H-4.

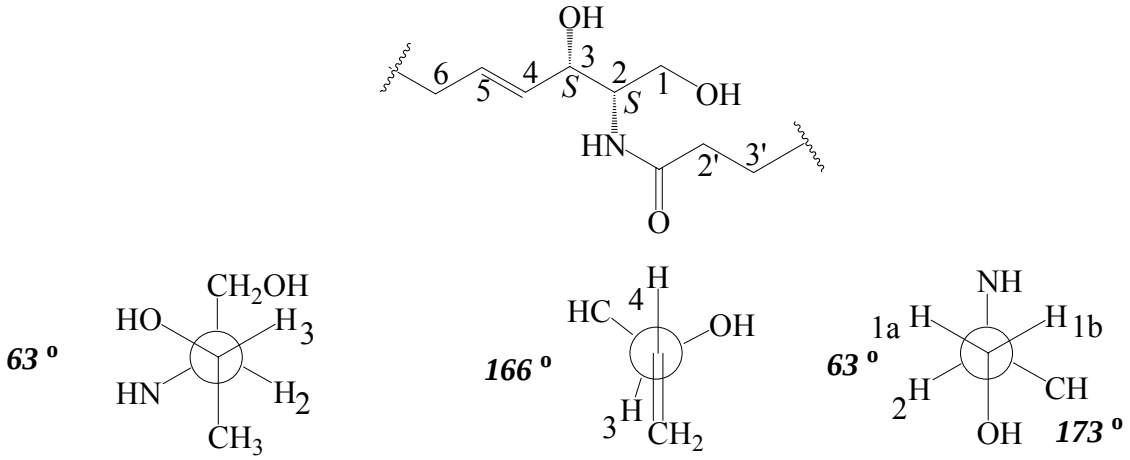

Figure 61. Dihedral angles of H-3, H-4 proposed with 3 (*S*) and 2 (*S*) in ceramide analog (**39**).

The dihedral angle showing 63˚ suggested a *gauche* arrangement between H2 and H3 and the dihedral angle showing 166˚ suggested an *anti* arrangement between H3 and H4. Therefore, H3 when assumed as 3*S* and 2*S* configurations has to display two different multiplicities which are doublet and doublet, however the actual multiplicity of

C-3 in ceramide analog (**9**) is triplet ($^{1,3}J_{HH}$ = 4.9 Hz) between H-3 and H-6. The relative dihedral angles also showed 63˚ indicating *gauch* form between H-2 and H-1a, 173˚ anti form between H-2 and H-1b suggesting that H-2 is multiplet. Thus C-3 (*S*) and C-2 (*R*) are favorable configurations than C-3 (*S*) and C-2 (*S*) in ceramide analog (**9**) by Chem3D. The relative configuration (Figure 62) of C-6 is suggested to be *R* and C-3 (*S*) indicates triplet multiplicity of H-3.

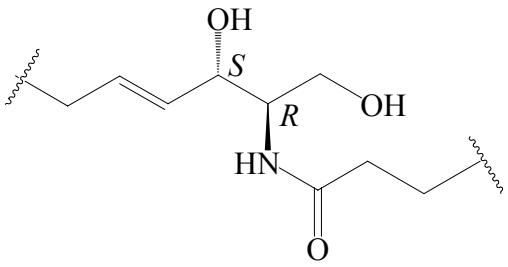

Figure 62. Relative stereochemistry of ceramide analog (**39**).

The Chem 3D models with C-3 in *S* configurations and C-2 in *R* configuration showed almost the same dihedral angle between H-2 and H-4 which are 173˚ and 163˚. This indicates that H-3 is not a double-doublet, but a triplet. However, theoretically the coupling constant ($^{1,3}J_{HH}$) of H-3 between two protons, H-2 and H-4 with dihedral angles, 163˚ and 173˚ should be above $^{1,3}J_{HH}$ = 5 Hz. The Mosher's method and the Chem3D models are showing that C-3 is in the *S* configuration and C-2 is in *R*-configuration. Also, the acetylated aminodiol **42** showed that H-4 is a triplet with coupling constant with $^{1,3}J_{HH}$ = 6.6 Hz. The dihedral angle between H-2 and H-3 in this product is also the same as that in ceramide analog (**39**). Except for the coupling constants in ceramide, all the other models are showing as C-3 (*S*) and C-2 (*R*) rather than C-3 (*S*) and C-2 (*S*). Hence, the relative configuration of C-2 is suggested to be *R* configuration from the results of Chem3D and C-3 (*S*) indicates triplet multiplicity of

H-3 from the Mosher's method. From the mass spectrometric data of ceramide analog (**39**), methanolysis reaction, and Mosher's method, the chemical structure of ceramide analog (**39**) was suggested in Figure 63 with Table 11.

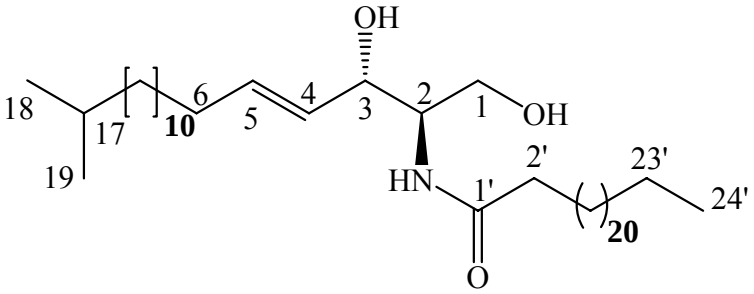

Figure 63. Ceramide analog (**39**).

Table 11. NMR data of ceramide analog (**39**) ($CDCl_3$) (^{13}C, 125 MHz; ^1H, 500 MHz)

	^1H (δ, *J*, Hz)	^{13}C (δ)	gCOSY	TOCSY	gHMBC
1	3.97 (1H, dd, 3.8, 11.0)	62.4 (CH_2)	H2	H2, H3, NH	C2, C3
	3.71 (1H, dd, 3.3, 11.3)		H2	H2, H3, NH	
2	3.91 (1H, m)	54.9 (CH)	H3, NH	H1, H4, H5	C4, C1'
3	4.34 (1H, t, 5.0)	74.2 (CH)	H2, H4	H1, H2, H4, H5, H6, NH	C1, C2, C4, C5
4	5.54 (1H, dd, 6.6, 15.6)	129.1 (CH)	H3, H5	H3, H5, H6 H7, NH	C2, C3, C6
5	5.80 (1H, dt, 7.4, 15.5)	134.2 (CH)	H4, H6	H3, H4, H6, H7	C3, C6
6	2.02 (2H, m)	32.6 (CH_2)	H5, H7	H3, H4, H5, H7	C4, C5, CH_2
7	1.40 (2H, m)	27.9 (CH_2)	H6, H8	H3, H4, H5, H6	C6, CH_2
8-15	1.28 (16H, m)				
16	1.17 (2H, m)	39.8 (CH_2)	H17	H17, H18, H19	C17, C18, C19, CH_2
17	1.54 (1H, heptet, 6.7)	28.2 (CH)	H16, H18 H19	H16, H18, H19	C16, C18, C19
18	0.88 (3H, d, 6.8)	22.9 (CH_3)	H16, H17	H16, H17	C16, C17
19	0.88 (3H, d, 6.8)	22.8 (CH_3)	H16, H17	H16, H17	C16, C17
1'		174.5 (C)			
2'	2.24 (2H, t, 7.5)	37.0 (CH_2)	H3'	H3', CH_2	C1', C3', CH_2
3'	1.60 (2H, m)	26.0 (CH_2)	H2'	H2', CH_2	C1', C2', CH_2
4'- 23'	1.28 (34H, m)				
24'	0.90 (3H, t, 7.0)	14.3 (CH_3)	H23'	H23', CH_2	
NH	6.24 (1H, d, 7.7)		H2	H1, H2, H3, H4 H5, H6	C1, C2, C3, C1'

Chapter 5. TOTAL SYNTHESIS OF THE NATURAL PRODUCT EREBUSINONE AND EREBUSINONAMINE

5.1 Introduction.

The Antarctic benthos is characterized by a dominant sponge community. Sponge predators include sea stars, nudibranchs and amphipods, though some sponge species appear to lack predation. Our own chemical ecological investigations of Antarctic invertebrates led to us to investigate the sponge *Isodictya erinacea* (Topsent, 1916) (Family Esperiopsidae), collected in McMurdo Sound, Antarctica, because *I. erinacea* appeared to be free of predation despite its lack of structural protection elements such as spicules.[59] *I. erinacea* was found to elaborate a host of secondary metabolites bearing cytotoxicity and ecological activities.[60, 61] We have documented molt-inhibition activity of sponge extracts toward the sympatric amphipod *Orchomene plebs*, a common predator of McMurdo Sound sponges. In laboratory assays carried out at McMurdo Station, amphipods were fed diets composed of either nutritionally rich control agar pellets or the same pellets to which an ecologically relevant (i.e., on a volume/volume basis relative to that found in the sponge) sponge extract had been added; the sponge extracts were substantially enriched with erebusinone (**12**), a yellow pigment we had previously isolated from the sponge. [61]

We monitored food consumption, molt events and mortality. Feeding was vigorous in both groups of amphipods as control and experimental (erebusinone-

enriched) diets. Over the 4 week experiment, the consumption and mortality of amphipods (Figure 64) were significantly higher in erebusinone-enriched diet and molt events significantly reduced; leading us to suggest that erebusinone interferes with molting in *O. Plebs* leading to premature mortality (Figure 65).

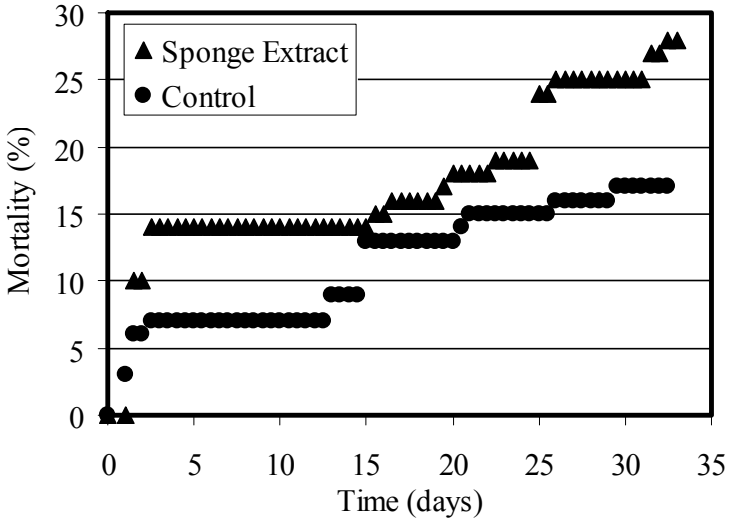

Figure 64. Occurrence of mortality in *O. plebs* fed erebusinone in their diet.

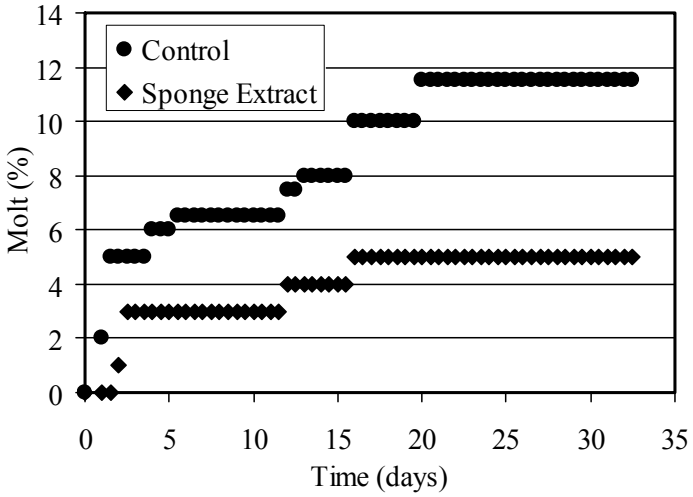

Figure 65. Occurrence of molting in *O. plebs* fed erebusinone in their diet.

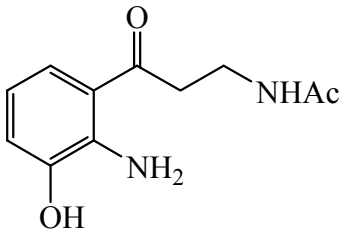

Erebusinone (**12**)

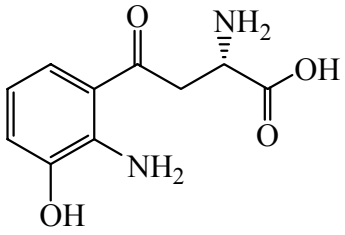

3-Hydroxykynurenic acid (**24**)

Molt inhibition as a chemical defense mechanism has not previously been documented in marine systems. We believe that erebusinone (**12**) is acting as a 3-hydroxykynurenine (**24**) mimic. 3-Hydroxykynurenine is a tryptophan catabolite intermediate in the biosynthesis of xanthurenic acid, a quinoline alkaloid inhibitor of the cytochrome P450 oxidase responsible for oxidizing ecdysone (Figure 66) to 20-hydroxyecdysone, the latter of which is the molt regulator of crustaceans (Figure 67, 68).[74,91] To further investigate the bioactivity and ecological role of erebusinone, we have carried out the synthesis of the yellow pigment, erebusinone.

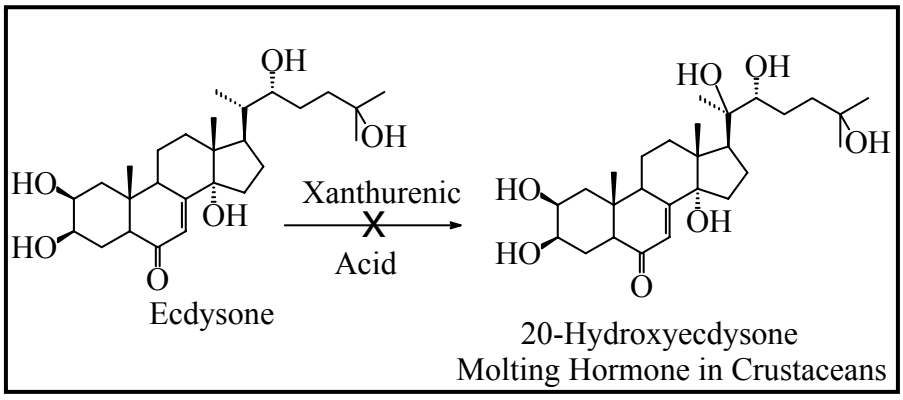

Figure 66. Ecdysone metabolism.

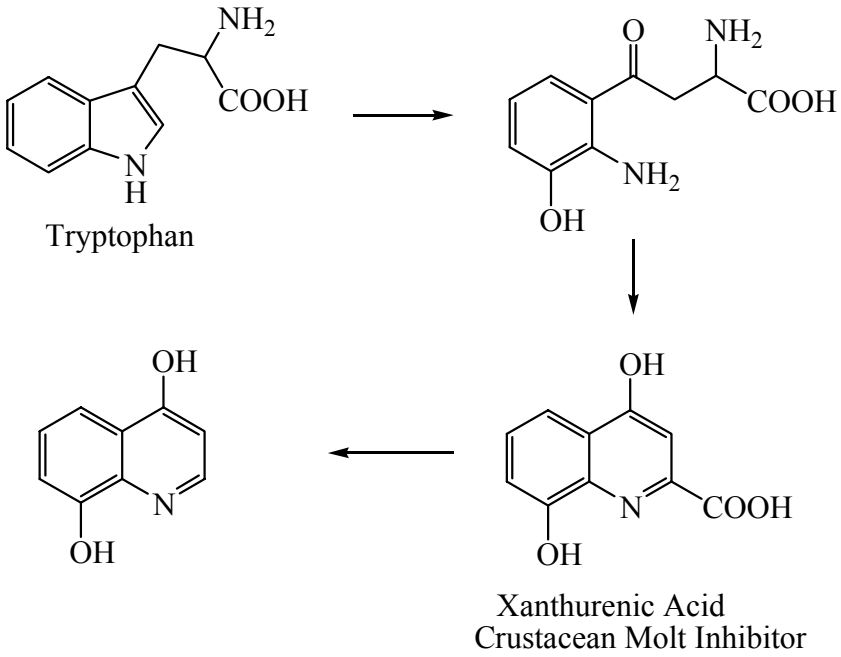

Figure 67. Tryptophan Catabolism.

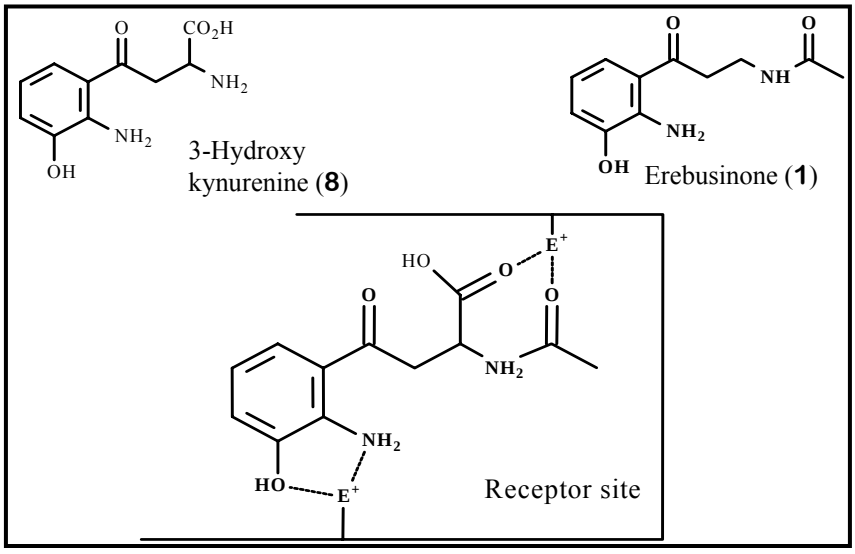

Figure 68. Overlay of erebusinone (**12**) with 3-hydroxykynurenine (**24**) in a hypothetical receptor.

5.2 Synthesis of Erebusinone (12)

The yellow pigment from the Antarctic sponge *Isodictya erinacea*, erebusinone has been implicated in molt inhibition and mortality against Antarctic crustacean amphipods, perhaps serving as a precursor of a xanthurenic acid analog. Our interest in erebusinone bioactivity led us to develop the synthesis, which we have achieved in an overall yield of 44% involving seven steps. The synthetic pathway also features an economical and efficient preparation of erebusinone.

5.3 Results and Discussion

We developed a convenient and efficient total synthetic strategy of erebusinone (**12**). As shown in Scheme 7, we initially pursued the synthesis of the 3-benzyloxy-2-nitrobenzylbenzoate (**46**) using 3-hydroxy-2-nitro benzoic acid (**45**) as a starting material. Benzyl bromide treatment with solid K_2CO_3[92] in dry DMSO at ambient temperature gave the dibenzyl ester (**46**) in 95% yield.

To elaborate the side chain, we envisioned that the extension of aliphatic carbon chains could be achieved by lithium acetonitrile generated *in situ* by the treatment of acetonitrile and n-butyllithium.[93] The treatment of lithium acetonitrile with dibenzyl ester **46** through direct S_N2 substitution provided a 90% yield of the resulting ketontrile **47**. To prepare amino alcohol **49**, we had to establish the reduction conditions for the conversion of the nitrile to amine. At this stage, our initial attempts of sequential

reduction of ketone and nitrile proved to be more difficult than we had expected. Numerous attempts to perform reduction of **47** and **48** with $LiAlH_4$, $NaBH_4$ with $CoCl_2$,[94,95] and hydrogenation failed.[96] However we finally achieved a successful reduction to afford amino alcohol **49** in a two step procedure by $NaBH_4$ and dimethylsulfide borane (BH_3SMe_2).[97] The reduction of compound **48** with 2.0 equiv of aqueous sodium borohydride ($NaBH_4$) afforded the corresponding intermediate **48** in 95 % yield, which was further treated with 2.4 equiv of BH_3SMe_2 in refluxing dry THF, providing the desired hydroxyl amine **49** in 76% overall yield via two-step reduction sequence involving ketone reduction of **47** and nitrile reduction of **48**.

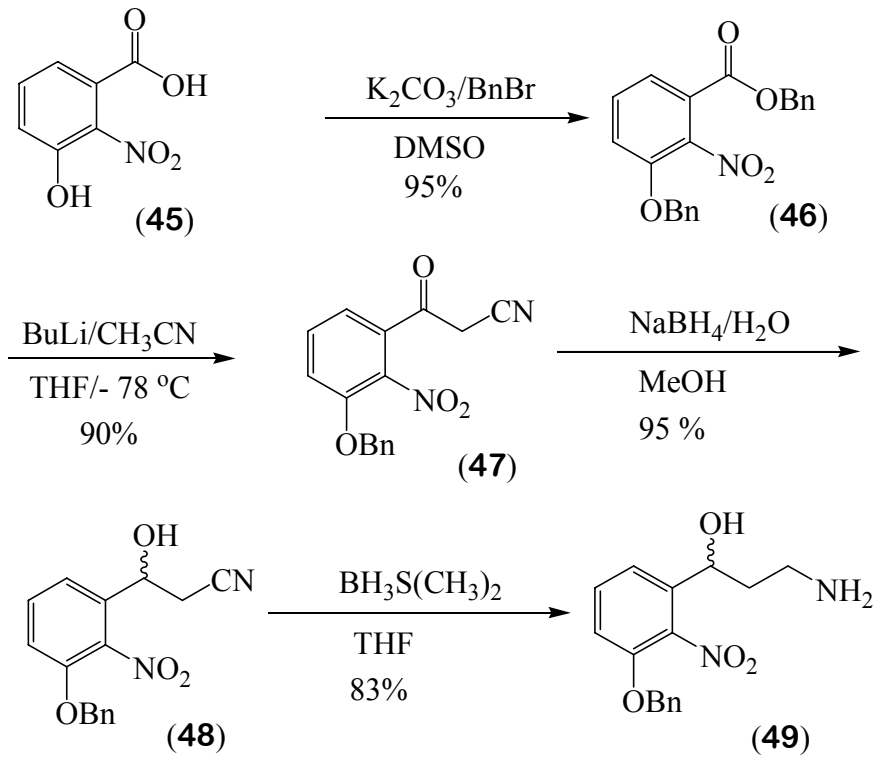

Scheme 7. Synthetic route to erebusinone precursor **49**

The selective protection reaction (Scheme 8) of the intermediate **49** was carried out by the selective protection of the primary amine[98] with 1.2 equiv of acetic

anhydride in the presence of triethylamine in dry dichloromethane at ambient temperature providing 82% yield of the protected acetylamide **50**. Oxidation of secondary alcohol **50** by Dess-Martin oxidation[99] led to the formation of the desired the ketone **51** in 90 % yield.

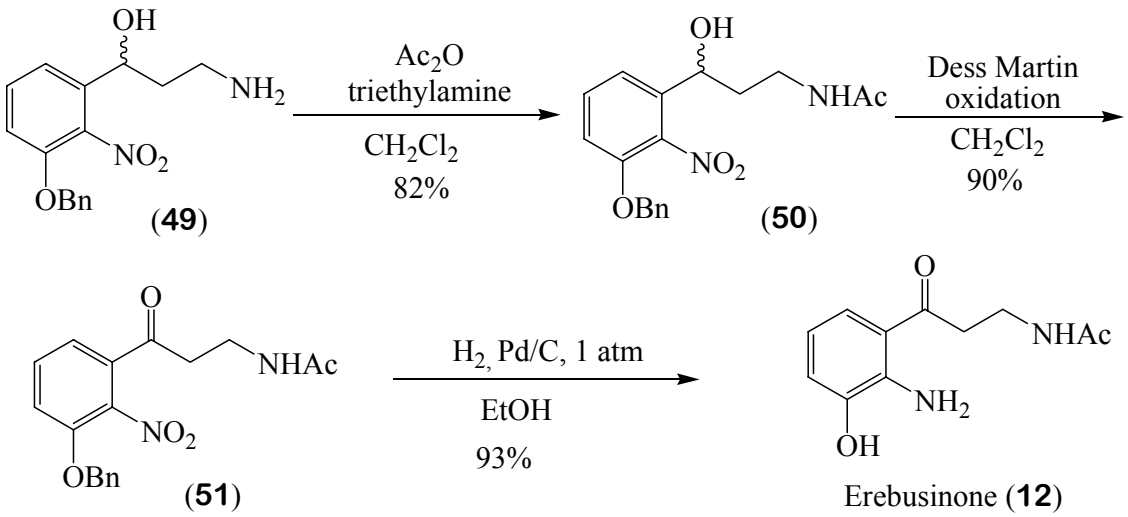

Scheme 8. Synthetic route from erebusinone precursor **49** to erebusinone (**12**).

To complete the synthesis of erebusinone **12**, we needed to remove the protected benzyl group and reduce the nitro group. For the purpose of this study, we considered that the intermediate **51** had to be converted into erebusinone **12** in a one-pot reaction. Exposure of **51** in absolute ethanol to Pd/C (10%)[96] at ambient temperature under a hydrogen atmosphere (1 atm) worked well with mild conditions leading to erebusinone **12** in 93% yield (Scheme 8).

In summary, we have developed a highly convenient synthetic pathway of erebusinone (**12**) providing an overall 44% yield. To further evaluate the biological activities of erebusinone (**12**) and its analogs, the explored synthetic method should

hold promise for the preparation of various structural types of erebusinone congeners with potential molt inhibition activity. We have envisioned analogs of erebusinone with different substitution patterns on the aromatic ring, with differing side chain lengths, and with additional oxidation levels.

5.4 Synthesis of Erebusinonamine (52)

The utility of our synthesis of erebusinone (**12**), besides being brief and high-yielding, is the opportunity to afford its analogue synthesis. Our ongoing research focuses on the preparation of analogues and the evaluation of the potential role of these compounds as molt inhibitors. Analogues with different substitution patterns on the aromatic ring, with differing side chain lengths, and with additional oxidation levels are envisioned. The synthesis of erebusinononamine (**52**), the deacetylated terminal amine was the first erebusinone analog synthesis attempted.

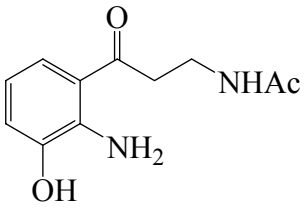

Erebusinone (**12**)

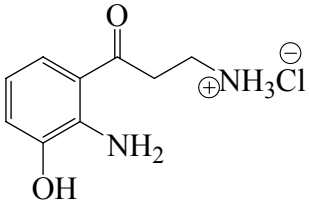

Erebusinonamine (**52**)

5.5 Results and Discussion

In our previous study, the synthesis of erebusinone (**12**) was achieved and the synthesis of erebusinonamine (**52**) was pursued from an intermediate of erebusinone, hydroxylamine (**49**). Erebusinonamine (**52**) was synthesized following the reaction sequence depicted in Scheme 8. Hydroxylamine **49** was reacted with di-*tert*-butyl dicarbonate (Boc_2O)[100] to afford the *tert*-BOC carbamate **53** in 100% yield and then followed by Dess-Martin oxidation to give compound **54** in 80% yield. The deprotection of *t*-BOC group[101] was achieved in the presence **55** with HCl (1.25 M) to afford precursor of erebusinonamine in 100% yield. Finally, erebusinonamine (**52**) was prepared by reaction of **55** with Pd/C[96] under 3.5 atm in 90% yield.

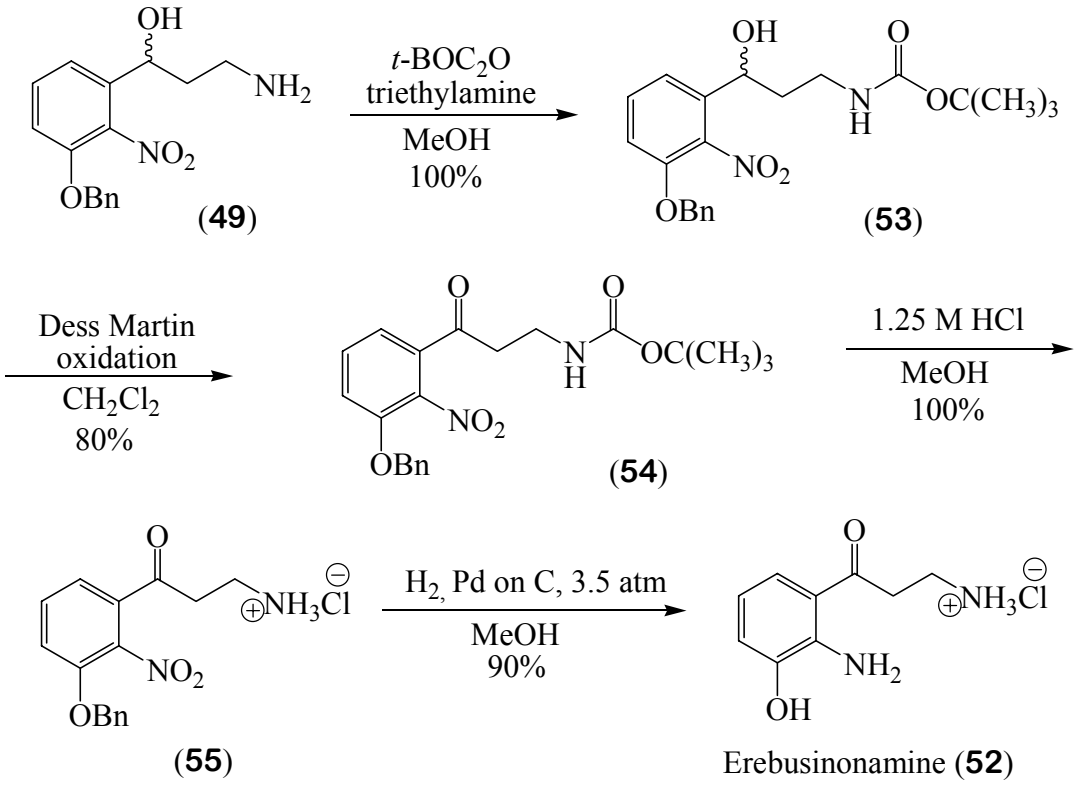

Scheme 9. Synthetic route of erebusinonamine (**52**) from erebusinone precursor **49**.

Chapter 6. BIOASSAY OF PURE COMPOUNDS

Bioassays for the pure compounds were done at Wyeth Pharmaceuticals and also at Marine Natural Products Lab at University of South Florida. Antimicrobial activities were carried out with the isolated compounds purine analog (**23**), ceramide analog (**39**), synthetic compounds, erebusinone (**12**) and erebusinonamine (**52**) using standard disk diffusion method against two gram-positive bacteria, *Staphylococcus aureus* (Sa, strain 375) and *Staphylococcus* meth resistant (Sa, strain 310), against one gram-negative bacteria *Escherichia faecium* van resistant (Ef, strain 379), and against a fungus *Candida albicans* (Ca, strain 54).[102] Assay plates were prepared by pouring 125 mL volume of agar medium (tempered at 50°C) inoculated with an overnight broth culture of the test organisms. Sample concentrations of 100 µg in 10 µL aliquots were spotted onto agar surface and the plates were incubated at 37°C for 24-48 h. The zones of growth inhibition were measured from the edge of the disk to the edge of the clear inhibition zone in mm, respectively. Control disks were treated with solvent alone (MeOH or $CHCl_3$).

Table 12 . Antimicrobial activity of pure compounds (100 µg/disk) using the disk diffusion assay (Zone of Inhibition in mm)

	Sa375	Sa310	Ef379	Ca54
Purine analog (**23**)	0	0	0	0
Ceramide analog (**39**)	7	7	6	9
Synthetic erebusinone (**12**)	0	0	0	0
Erebusinonamine (**52**)	8	8	6	10

Sa375: *Staphylococcus aureus*, Sa310: *Staphylococcus* meth resistant, Ef379: *Escherichia faecium* van resistant, Ca54: *Candida albicans*

The purine analog (**23**) did not show considerable antimicrobial activity. Ceramide analog (**39**) showed modest antimicrobial activity against *Staphylococcus aureus* (Sa, strain 375), *Staphylococcus* meth resistant (Sa, strain 310), *Escherichia faecium* van resistant (Ef, strain 379) and *Candida albicans* (Ca, strain 54). Erebusinonamine (**52**) showed relatively better activity against *Candida albicans* (Ca, strain 54) than *Staphylococcus aureus* (Sa, strain 375), *Staphylococcus* meth resistant (Sa, strain 310) and *Escherichia faecium* van resistant (Ef, strain 379). Erebusinone (**12**) did not show considerable antimicrobial activity. Erebusinone (**12**) is presently being tested for insecticidal activity.

Chapter 7. DISCUSSION

Isodictya erinacea has been found to produce unusual molt inhibitor precursor analog erebusinone (**12**), purine derivatives (**13**, **21**, **22**, **23**) and nucleosides metabolites and exhibits an unusual chemical defense role against a major sponge predator, the sea star *Perkanster fuscus*, as well as the amphipod *Orchomene plebs*.[60,61] Our chemical and ecological investigations of the Antarctic invertebrates led us study the marine sponges, *Isodictya erinacea*, *Isodictya setifera* and *Isodictya antarctica.*

Isodictya erinacea was found to produce an unusual N-methylated purine analog **23** and 3-hydroxykynurenine (**24**), the precursor of molting inhibitor xanthurenic acid. N-methylated purine base analogues previously reported including from various sponges, 1,9-dimethyl-6-imino-8-oxopurine from *Hymeniacidon sanguinea*,[103,104] 1,3,7-trimethylguanine from *Latrunculia brevis*,[71] herbipoline (7,9-dimethylguanidium salt) and 1-methyl adenine from *Geodia gigas*, [105] longamide (3,7-dimethylisoguanine) from *Agelas lingissima*,[106] 1,3-dimethylisoguanine from *Amphimedon viridis*,[107] mucronatine (2-methoxy-3-methylisoguanine) from *Styphnus mucronatus*.[108] The purine 1,3,7-trimethylisoguanine was also isolated from the Ascidian *Pseudodistoma cereum*.[72]

Chemical investigation of *Isodictya setifera* led to the isolation of known secondary metabolites, homarine (**37**), 5-methyl-2-deoxycytidine (**25**), uridine (**28**), 2'-deoxycytidine (**31**), 4, 8-dihydroxyquinoline (**33**), 3-hydroxykynurenine (**24**), of

which the latter two are known biosynthetic intermediates of tryptophan catabolism in crustaceans. The first discovery of purine and nucleosides were isolated from the marine sponge *Cryptothethya crypta* by Bergmann and co-workers in the 1950's.[41,42,109,110] The modified unusual halogenated nucleosides also isolated from sponges and algae.[111-115] Therefore, marine sponges are well known as source of nucleosides and purine derivatives.

Among the potential ecological roles of the sponges ion the Antarctic benthos, previously we reported that the secondary metabolite, erebusinone (**12**) from *Isodictya erinacea* has been implicated in molt inhibition and mortality against an Antarctic crustacean, *Orchomene plebs*, perhaps serving as a precursor of xanthurenic acid analog. We documented significant molt inhibition activity against common sponge predator crustacean amphipods.[60,61] The secondary metabolites, 4,8-dihydroxyquinoline (**33**), 3-hydroxykynurenine (**24**), from the Antarctic sponge *I. setifera*, are known to participate in the regulatory pathway of crustacean molting via tryptophan catabolism.[60,61] This appears to be the first example in marine realm that sponges produce tryptophan catabolism intermediates to that interfere molting in *O. plebs* for chemical defense. According to our previous metabolite profile, biological activities and ecological implications, we believe species of the genus *Isodictya* is distinctive in producing biosynthetically unique and various secondary metabolites and suggest that *I. setifera* and *I. erinacea* may play a role in chemical defense.

Chemical investigation of *I. antarctica* was found to produce ceramide analog which showed antimicrobial activity against *Staphylococcus aureus*, *Staphylococcus meth* resistant, *Escherichia faecium* van resistant and *Candida albicans*. A variety of ceramide derivatives have been reported from marine sponges.[116-118] Relative stereochemistry of ceramide analog (**39**) was assigned by Mosher's method and Chem3D.[86]

We have developed mild, simple, and efficient synthetic methods for erebusinone (**12**) and erebusinonamine (**52**) in excellent yields from 3-hydroxy-2-nitro benzoic acid (**45**) and we also optimized each synthetic conditions of erebusinone (**12**) and erebusinonamine (**52**) from 1 to 20 gram. The bioassays of synthetic natural product, erebusinone (**12**) did not show antimicrobial activity but, erebusinonamine (**52**) showed moderate antimicrobial activity against *Staphylococcus aureus*, *Staphylococcus* meth resistant, *Escherichia faecium* van resistant and *Candida albicans*. The ecological and biological assays of these compounds as molt inhibitors are currently under investigation.

Chapter 8. EXPERIMENTAL

8.1 General Procedure.

Flash column chromatography was performed on EM Science normal phase Silica gel 60 (200 – 400 mesh). Thin layer chromatography (tlc) was carried out using Whatman normal phase Silica gel 60Å Partisil® K6F, reversed phase Silica gel 60Å Partisil® KC18F, and $CNF_{254}s$ plates 0.25 mm thickness. There were visualized by spraying with 5% phosphomolybdic acid in EtOH and heating and 2 % ninhydrin in BuOH/acetic acid (95:5). HPLC (high performance liquid chromatography) was performed on Waters 510 equipped with a Waters 490E programmable multiwavelength UV detector at 254 nm and Shimadzu LC-8A equipped with a multisolvent delivery system connected to a Shimadzu SPD-10A UV-VIS tunable absorbance detector and/or an Alltech ELSD 2000 using a YMC-Pack® ODS-AQ C-18 analytical column, a Waters prepLC® (25 mm X 30 cm) C-18 column for reversed phase, or Waters Sphereclone®(250 X 10 mm) for normal phase. Infrared (IR) spectra were obtained with Nicolet Avatar 320FT-IR in solid state. Ultraviolet-Visible (UV) experiments were measured on a Hewlett-Packard 8452A diode array UV/Vis spectrometer. High resolution mass spectra ESI-MS (negative or positive mode), EI-MS (negative or positive mode) and CI-MS were obtained on Micromass 70-VSE spectrometer at the University of Illinois. Optical rotation was determined on a Rudolph Research Analytical AUTOPOL® IV with a sodium lamp (589 nm) and 0.5 dm cell. ^{1}H NMR

and ^{13}C NMR spectra were recorded at 250 MHz and 75 MHz, respectively on a Bruker AMX-250 or 500 MHz and 125 MHz, respectively on a Varian INOVA-500. ^{1}H and ^{13}C NMR chemical shifts are listed relative to $CDCl_3$ (δ 7.27), MeOH-d_4 (δ 3.31), or DMSO-d_6 (δ 2.50) and (δ 77.00), (δ 49.00), or (δ 39.50) respectively. The ^{13}C resonance multiplicities were determined by DEPT experiments. ^{1}H-^{1}H correlations were determined by using gCOSY and TOCSY experiments optimized coupling constant (J_{HH} of 7 Hz). One bond connectivities ($^{1}J_{CH}$) of ^{1}H-^{13}C were determined via the 2-D proton-detected gHSQC experiment. The interpulse delays were optimized for average $^{1}J_{CH}$ of 120 MHz. Two- or three-bond heteronuclear multiple-bonds ($^{3}J_{CH}/^{2}J_{CH}$) were recorded via the 2D proton detected gHMBC experiment optimized for a long range coupling constant (J_{CH} of 7 Hz). Unless otherwise specified, materials were purchased from commercial suppliers and used without further purification. Low-temperature baths of –78 ˚C and – 40 ˚C were obtained with an immersion cooler bath using acetone and CH_3CN with dry ice (CO_2). THF was distilled from sodium and benzophenone immediately before use. CH_2Cl_2 and CH_3CN were distilled from CaH_2 under argon and triethylamine from KOH. Moisture-sensitive reactions were conducted in oven or flame-dried glassware under and argon atmosphere. Unless otherwise noted, all organic layers were dried with over either anhydrous Na_2SO_4 or $MgSO_4$ and concentration of all solutions was accomplished by a rotary evaporator at water aspirator pressures. Melting points were uncorrected.

8.2 Isolation of Secondary Metabolites from *Isodictya erinacea*

A specimen of *Isodictya erinacea* was collected by using SCUBA diving (-20 - 30 m) at Erebus Bay on the western coast of Ross Island, Antarctica in summer 1999. The freshly collected marine sponge was frozen in liquid nitrogen immediately to prevent degradation of the pigment. A voucher specimen has been deposited in a – 70 ˚C freezer at the Department of Chemistry, University of South Florida. The body of *I. erinacea* is yellow or light brown both inside and outside, and the surface is globular and spiny.

The marine sponge (1.0 kg, wet) which was kept frozen until use was exhaustively extracted with MeOH (2L X 5 times) at 7 ˚C. After concentration, the extract was re-dissolved with MeOH to remove salt. The residual fraction (20g) was subjected to Sephadex LH-20® column chromatography (5 cm X 60 cm) with CH_2Cl_2/MeOH (1:1) to provide 5 fractions. Fraction 4 (1.1g) was further subjected to C18 column chromatography (2.5 X 45 cm) with a MeOH/CH_2Cl_2 (100:0 → 0:100) gradient system to give four fractions. Fraction 8 (374 mg) was chromatographed on silica gel column (2.5 cm X 45 cm) with H_2O/MeOH/$CHCl_3$ (0.4:3.0:6.6) to provide 4 fractions. Purine analog (**23**) (0.0068 %, 68 mg) was obtained from fraction 11 (104 mg) on silica gel column (2.5 cm X 30 cm) with H_2O/MeOH/CH_2Cl_2 (0.4:30:66). Fraction 12 was chromatographed on silica gel (2.5 cm X 30 cm) eluting with H_2O/MeOH/CH_2Cl_2 (0.5:4:5.5) to yield 3-hydroxykynurene (**24**), fraction 20 (0.00135%, 13.5 mg) (Scheme 1).

8.2.1 Spectral data of Purine analog (23)

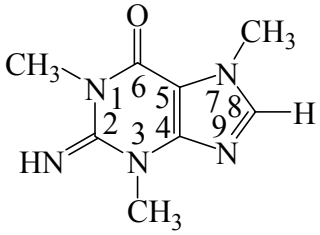

1,3,7-Trimethylisoguanine: a pale brown crystal; mp decomposed at 230 ˚C ; IR ν_{max} 3303, 3241, 3089,1715, 1641, 1567, 1026 cm^{-1}; UV (MeOH) λ_{max} (log ε) 210 (2.02), 268 (0.75) nm; ^{1}H NMR (DMSO-d_6, 500 MHz): δ 8.17 (s, 1H, H-8), 3.88 (s, 3H, N-7-C*H*$_3$), 3.61 (s, 3H, N-3-C*H*$_3$), 3.36 (s, 3H, N-1-C*H*$_3$); ^{13}C NMR (DMSO-d_6, 125 MHz) 152.5 (s, C-6), 151.3 (s, C-2), 147.6 (s, C-4), 143.6 (d, C-8), 106.9 (s, C-5), 33.4 (q, N-7-C*H*$_3$), 32.2 (q, N-3-C*H*$_3$), 29.3 (q, N-1-C*H*$_3$); HREIMS m/z 193.0959 (calcd for $C_8H_{11}N_5O_1$, 193.0964), LREIMS *m/z* [M^+] 193.1 (100 %), [M-NH]$^+$ 178.1, [M-CHO]$^+$ 164.1 (20 %), [M-HNCNCH$_3$]$^+$ 138.1 (12 %), [M-CO]$^+$ 109.0 (30 %), [M-HCN]$^+$ 82.1 (24 %).

8.2.2 Spectral data of 3-Hydroxykynurenine (24)

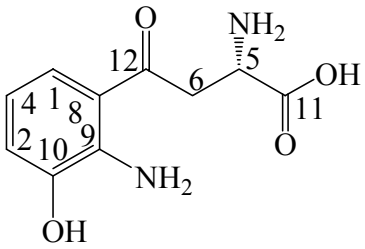

3-Hydroxykynurenic acid; bright yellow solid; $[\alpha]^{25}_{D}$ -47.6° (*c* = 0.17, MeOH); IR ν_{max} 3339, 2981,1685, 1611, 1533, 1275 cm^{-1}; UV (MeOH) λ_{max} (log ε) 234 (1.06), 273 (0.36), 381 (0.21) nm; ^{1}H NMR (DMSO-d_6, 500 MHz) δ 7.19 (1H, d, *J* = 8.2 Hz, H-1), 6.85 (1H, d, *J* = 7.6 Hz, H-2), 6.40 (1H, t, *J* = 8.0 Hz, H-4), 3.62 (1H, d, *J* = 7.8 Hz, H-5), 3.50 (1H, dd, *J* = 2.3, 18.1 Hz, H-6), 3.24 (1H, dd, *J* = 8.6, 17.5 Hz); ^{13}C NMR (DMSO-d_6, 125 MHz) δ 200.0 (s, C-12), 170.3 (s, C-11), 145.5 (s, C-10), 141.6 (s, C-9), 121.6 (d, C-1), 117.4 (d, C-2), 117.1 (s, C-8), 114.6 (d, C-4), 50.5 (d, C-5), 41.1 (t, C-6).

8.3 Isolation of Secondary Metabolites from *Isodictya setifera*

The marine sponge *Isodictya setifera* was collected by using SCUBA from Bahia Paraiso on the coast near Palmer station, Antartica at depths of 40-50 m on 28 Jan 2003. The marine sponge, *Isodictya setifera* (435g, freeze dried) was first extracted with methanol (3L X 3 times) at room temperature. After concentration, the crude extract was partitioned with hexane/MeOH/H_2O (400 mL/500 mL/100 mL). The hexane layer was separated and concentrated to give a crude extract (9.0 g) and aqueous layer was partitioned with CH_2Cl_2/MeOH/H_2O (400 mL/500 mL/100 mL) and the organic layer was separated and concentrated to give CH_2Cl_2/MeOH extract (8.3 g). The aqueous layer was extracted with BuOH which gave a BuOH extract (1.9 g) and the aqueous extract was concentrated to provide the H_2O extract (38g). BuOH extract (1.9g) was subjected to Sephadex LH-20® column (5 cm X 60 cm) with MeOH to provide seven fractions. Fraction 12 (570 mg) was further subjected to normal phase silica gel column (2.5 X 45 cm) with a MeOH/CH_2Cl_2 (0:100 → 30:70) and CH_3CN/H_2O (100:0 → 80:20) and followed by HPLC with reversed cyano column using AcCN/H_2O (99:1 → 80:20) to give pure compounds which are 3-hydroxykynurenine (**24**) (1.7 mg, 0.0004% yield), 5-methyl-2'-deoxycytidine (**25**) (3 mg, 0.0007% yield), uridine (**28**) (2.0 mg, 0.0005% yield), 2'-deoxycytidine (**31**) (1.5 mg, 0.0003% yield), 4,8-dihydroxyquinoline (**33**) (1.8 mg, 0.0004% yield), homarine (**37**) (2.0 mg, 0.0005% yield) (Scheme 3).

8.3.1. Spectral data of 5-Methyl-2'-deoxycytidine (25)

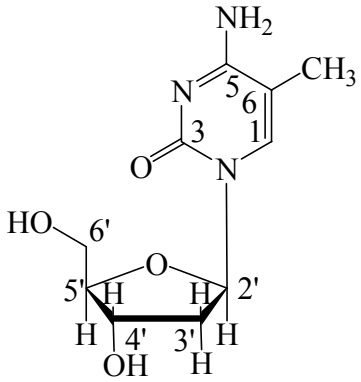

5-Methyl-2'deoxycytidine; white solid: $[\alpha]^{25}_{D}$ +5.3° (*c* = 0.15, MeOH); IR ν_{max} 2918, 1688, 1469, 1236, 1090 cm^{-1}; UV (MeOH) λ_{max} (log ε) 209 (0.88), 268 (0.83) nm; ^{1}H NMR (MeOH-d_4, 500 MHz) δ 7.83 (1H, s, H-1), 6.30 (1H, t, *J* = 6.8 Hz, H-2'), 4.42 (1H, m, H-4'), 3.92 (1H, q, *J* = 3.4, H-5'), 3.81 (1H, dd, *J* = 3.2, 12.5 Hz, H_a-6'), 3.74 (1H, dd, *J* = 3.5, 11.8 Hz, H_b-6'), 2.25 (2H, m, H-3'), 1.89 (3H, s, H-7); ^{13}C NMR (MeOH-d_4, 125 MHz) δ 165.3 (s, C-5), 151.2 (s, C-3), 136.7 (d, C-1), 110.4 (s, C-6), 87.6 (d, C-5'), 85.1 (d, C-2'), 71.0 (d, C-4'), 61.7 (t, C-6'), 40.0 (t, C-3'), 11.3 (q, C-7).

8.3.2. Spectral data of Uridine (28)

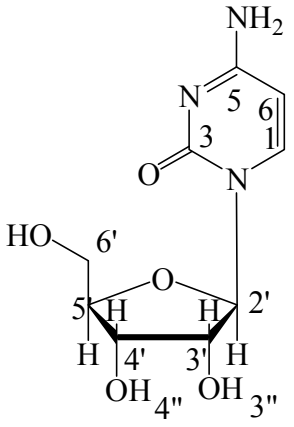

5-Methyl-2'deoxycytidine; white solid: $[\alpha]^{25}_{D}$ 0° (*c* = 0.1, MeOH); IR ν_{max} 2984, 2902, 1687, 1235, 1207, 1089 cm^{-1}; UV (MeOH) λ_{max} (log ε) 209 (1.01), 265 (0.56) nm; ^{1}H NMR (DMSO-d_6, 500 MHz) δ 7.88 (1H, d, *J* = 7.9 Hz, H-1), 5.77 (1H, d, *J* = 5.8 Hz, H-2'), 5.64 (1H, d, *J* = 8.3 Hz, H-6), 5.37 (1H, d, *J* = 5.9 Hz, H-3"), 5.10 (1H, m, H-4"), 4.01 (1H, q, *J* = 5.4 Hz, H-3'), 3.95 (1H, q, *J* = 4.6 Hz, H-4'), 3.83 (1H, q, *J* = 3.3 Hz, H-5'), 3.61 (1H, m, H_a-6'), 3.54 (1H, m, H_b-6'); ^{13}C NMR (DMSO-d_6, 500 MHz): δ 163.8 (s, C-5), 151.4 (s, C-3), 141.4 (d, C-1), 102.4 (d, C-6), 88.3 (d, C-2'), 85.5 (d, C-5'), 74.2 (d, C-3'), 70.5 (d, C-4'), 61.5 (t, C-6').

8.3.3. Spectral data of 2'-Deoxycytidine (31)

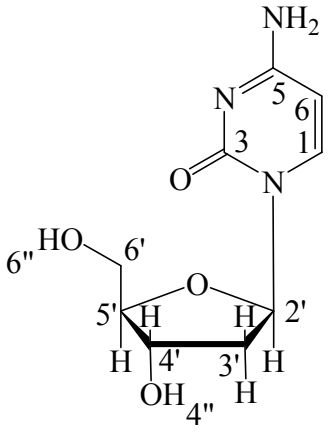

2'-Deoxycytidine; white solid: $[\alpha]^{25}_{D}$ +7.1° (*c* = 0.07, MeOH); IR ν_{max} 2977, 2917, 1685, 1235, 1089 cm^{-1}; UV (MeOH) λ_{max} (log ε) 209 (0.75), 265 (0.65) nm; ^{1}H NMR (DMSO-d_6, 500 MHz) δ 11.27 (2H, br s, NH_2), 7.84 (1H, d, *J* = 8.1 Hz, H-1), 6.14 (1H, t, *J* = 6.2 Hz, H-2'), 5.63 (1H, d, *J* = 8.1 Hz, H-6), 5.23 (1H, br s, OH-4"), 5.00 (1H, br s, OH-6"), 4.27 (1H, m, H-4'), 3.77 (1H, m, H-5'), 3.55 (2H, m, H-6'), 2.08 (2H, m, H-3'); ^{13}C NMR (DMSO-d_6, 125 MHz) δ 163.8 (s, C-5), 151.1 (s, C-3), 141.2 (d, C-1), 102.4 (d, C-6), 88.0 (d, C-5'), 84.8 (d, C-2'), 71.1 (d, C-4'), 61.9 (t, C-6'), 40.2 (t, C-3').

8.3.4. Spectral data of 4, 8-Dihydroxyquinoline (33)

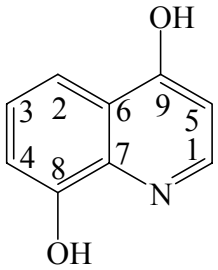

4,8-Dihydroxyquinoline; white solid: IR ν_{max} 2976, 1574, 1525, 1285, 1235, 1089 cm^{-1}; UV (MeOH) λ_{max} (log ε) 227 (1.2), 263 (0.3), 325 (0.4) nm; ^{1}H NMR (DMSO-d_6, 500 MHz) δ 7.72 (1H, d, J = 7.2 Hz, H-1), 7.50 (1H, dd, J = 1.4, 7.9 Hz, H-2), 7.09 (1H, t, J = 7.7 Hz, H-3), 7.04 (1H, dd, J = 1.5, 7.7 Hz, H-4), 6.00 (1H, d, J = 7.3 Hz, H-5); ^{13}C NMR (DMSO-d_6, 125 MHz) δ 177.8 (s, C-9), 147.8 (s, C-8), 139.4 (d, C-1), 131.1 (s, C-7), 127.4 (s, C-6), 123.6 (d, C-3), 115.4 (d, C-2), 114.8 (d, C-4), 109.2 (d, C-5).

8.3.5. Spectral data of Homarine (37)

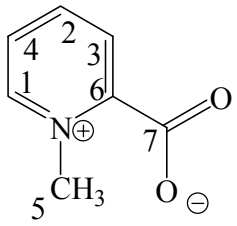

Homarine; white solid: IR ν_{max} 2976, 1652, 1610, 1373, 1235, 1089 cm^{-1}; UV (MeOH) λ_{max} (log ε) 206 (0.8), 280 (0.6); ^{1}H NMR (DMSO-d_6, 500 MHz) δ 8.72 (1H, d, J = 6.0 Hz, H-1), 8.42 (1H, t, J = 7.9 Hz, H-2), 7.90 (1H, dd, J = 1.3, 7.8 Hz, H-3), 7.85 (1H, t, J = 6.9 Hz, H-4), 4.28 (3H, s, N-CH_3); ^{13}C NMR (DMSO-d_6, 125 MHz) δ 161.8 (s, C-7), 156.7 (s, C-6), 145.7 (d, C-2), 145.0 (d, C-1), 126.0 (d, C-3), 125.5 (d, C-4), 46.5 (q, C-5).

8.4 Isolation of Secondary Metabolite from *Isodictya antarctica*

The marine sponge *Isodictya antarctica* was collected by using SCUBA on the Bahia Paraiso on the coast near Palmer station, Antartica 2001. A voucher specimen was freeze dried in the laboratory of marine natural products laboratory in the department chemistry at University of South Florida.

The marine sponge, *Isodictya antarctica* (141g, freeze dried) was first extracted with methanol (1L X 3 times) at room temperature. After concentration, the crude extract (10g) was partitioned with CH_2Cl_2/MeOH/H_2O (500 mL/100 mL/ 100 mL). The organic layer was separated and concentrated to give CH_2Cl_2 extract (5.7 g). An aqueous layer was partitioned with BuOH/H_2O (400 mL/100 mL). The BuOH layer was separated and concentrated to give BuOH extract (1.7 g). An aqueous layer was concentrated to provide H_2O extract (1.8 g). The CH_2Cl_2 extract (5.7 g) was subjected to normal phase silica gel (2.5 X 45 cm) with EtOAc/hexane (25:75 → 100:0) and EtOAc/MeOH (90:10 → 70:30) to give six fractions. Fraction 4 and fraction 5 (556 mg) was combined and subjected over Sephadex LH-20® column (5 cm X 60 cm) with MeOH/CH_2Cl_2 (1:1) followed by silica gel with EtOAc/hexane (20:80 → 100:0) to give ceramide analog (**39**) (104 mg, 0.07% yield) (Scheme 4).

8.4.1 Spectral data of Ceramide analog (39)

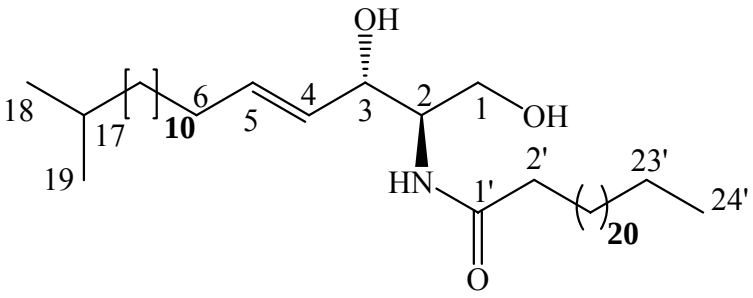

Ceramide analog; white solid: $[\alpha]^{25}_{D}$ -7.3˚ (*c* = 0.165, $CHCl_3$); mp 73 ˚C; IR ν_{max} 3300, 2916, 2849, 1642, 1615, 1547, 1466 cm^{-1}; UV ($CHCl_3$) λ_{max} (log ε) 243 (0.3) nm; ^1H NMR ($CDCl_3$, 500 MHz) δ 6.24 (1H, d, *J* = 7.7 Hz, N*H*), 5.80 (1H, dt, *J* = 7.4, 15.5 Hz, H-5), 5.54 (1H, dt, *J* = 6.6, 15.6 Hz, H-4), 4.34 (1H, t, *J* = 5.0 Hz, H-3), 3.97 (1H, dd, *J* = 3.8, 11.0 Hz, H-1_a), 3.71 (1H, dd, *J* = 3.3, 11.3 Hz, H-1_b), 3.91 (1H, m, H-2), 2.24 (2H, t, *J* = 7.5 Hz, H-2'), 2.02 (2H, m, H-6), 1.60 (2H, m, H-3'), 1.54 (1H, heptet, *J* = 6.7 Hz, H-17), 1.40 (2H, m, H-7), 1.28 (16H, m, H – (8-15)), 1.28 (34H, m, H - (4'-23')), 1.17 (2H, m, H-16), 0.90 (3H, t, *J* = 7.0 Hz, H-24'), 0.88 (3H, d, *J* = 6.8 Hz, H-18), 0.88 (3H, d, *J* = 6.8 Hz, H-19); ^{13}C NMR ($CDCl_3$, 125 MHz) δ 174.5 (s, C-1'), 134.2 (d, C-5), 129.19 (d, C-4), 74.2 (d, C-3), 62.4 (t, C-1), 54.9 (d, C-2), 39.8 (t, C-16), 37.0 (t, C-2'), 32.6 (t, C-6), 29.9 (t, C8-15, C4'-23'), 28.2 (d, C-17), 27.9 (t, C-7), 26.0 (t, C-3'), 22.9 (q, C-18), 22.8 (q, C-19), 14.3 (q, C-24'); LRFABMS *m/z* 664.5 $[M + H]^+$, HRESIMS as $C_{43}H_{86}NO_3$ (observed *m/z* 664.6599 $[M + H]^+$, calculated for 664.6607).

8.4.2 Methanolysis of Ceramide analog (39)

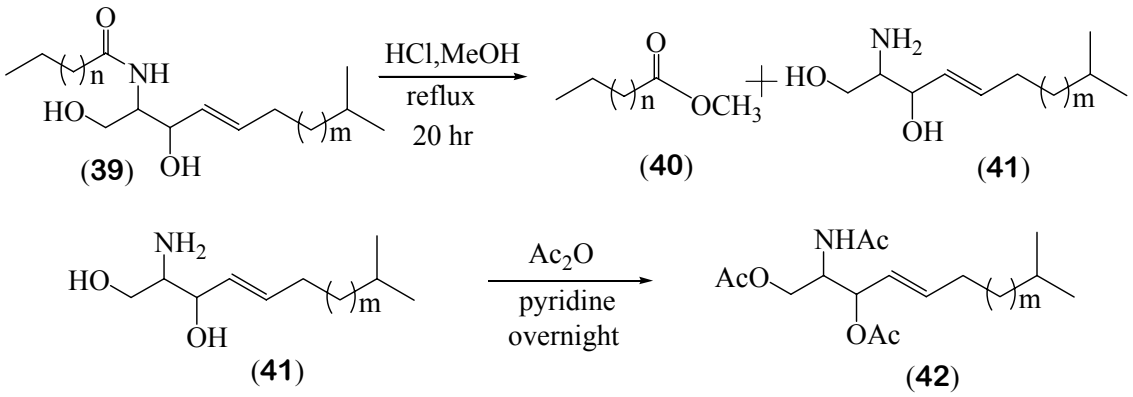

(**39**) (**40**) (**41**) (**41**) (**42**)

Ceramide analog (**39**) (5 mg) was heated with 1.25 M HCl in MeOH (3 mL) at 70 ˚C for 20 h in 5 mL flask. The reaction mixture was extracted with petroleum ether, the extract concentrated *in vacuo* to give fatty acid methyl ester **40** (1.7 mg): ^{1}H NMR ($CDCl_3$, 500 MHz) δ 3.60 (3H, s, OC*H*$_3$), 2.22 (2H, t, *J* = 6.5 Hz), 1.55 (2H, m), 1.18 (br s), 0.81 (3H, t, *J* = 6.7 Hz); ^{13}C NMR ($CDCl_3$, 125 MHz) δ 174.5 (s), 51.7 (q, O*C*H$_3$), 34.4 (t), 32.2 (t), 29.9 (t), 29.8 (t), 29.7 (t), 29.6 (t), 29.5 (t), 29.4 (t), 25.2 (t), 22.9 (t), 14.31 (q, *C*H$_3$); LRFABMS *m*/*z* 383.3 $[M + H]^+$, LREIMS *m*/*z* 382.5 $[M]^+$, HREIMS as $C_{25}H_{50}O_2$ (observed *m*/*z* 382.3804 $[M]^+$, calculated 382.3811).

The MeOH layer was concentrated *in vacuo* to give a long chain base aminodiol (**41**) and then reacted with acetic anhydride in the presence of pyridine (1mL) overnight at room temperature. The reaction mixture was concentrated *in vacuo* to remove pyridine and diluted with CH_2Cl_2 (5 mL) with H_2O (1 mL). The organic layer washed with saturated $NaHCO_3$ solution, H_2O, brine solution and then dried with anhydrous $MgSO_4$.

The filtrate was concentrated *in vacuo* to give protected compound **42** and subjected to silica gel column chromatography using 40% EtOAc in hexane to give protected compound **42** (0.8 mg): ^{1}H NMR ($CDCl_3$, 500 MHz) δ 5.80 (1H, dt, *J* = 7.2, 14.8 Hz), 5.65 (1H, *J* = 9.4 Hz, N*H,*), 5.40 (1H, dd, *J* = 7.6, 15.8 Hz), 5.28 (1H, t, *J* = 6.1 Hz), 3.44 (1H, m), 4.31 (1H, dd, *J* = 6.2, 11.8 Hz), 4.05 (1H, dd, *J* = 3.8, 11.6 Hz), 2.08 (3H, s), 2.07 (3H, s), 2.04 (m), 1.99 (3H, s), 1.58 (br s), 1.52 (1H, m), 1.36 (2H, m), 1.26 (br s), 1.15 (2H, m), 0.87 (6H, d, 6.3 Hz); ^{13}C NMR ($CDCl_3$, 125 MHz) δ 171.2 (s), 170.2 (s), 169.8 (s), 137.7 (d, *C*H), 124.4 (d, *C*H), 74.1 (d, *C*H), 62.8 (t), 50.9 (d, *C*H), 39.3 (t), 32.5 (t), 29.9 (t), 29.8 (t), 29.6 (t), 29.4 (t), 29.1 (t), 28.2 (d, *C*H), 23.6 (q, acetoxy *C*H_3), 22.9 (q, isopropyl *C*H_3), 22.9 (q, isopropyl *C*H_3), 21.3 (q, acetoxy *C*H_3), 21.1 (q, acetoxy *C*H_3); LRFABMS *m/z* 440.3 $[M + H]^+$, HRESIMS as $C_{25}H_{46}NO_5$ (observed *m/z* 440.3372 $[M + H]^+$, calculated 440.3376).

8.4.3 Preparation of MTPA esters for Ceramide analog (39)

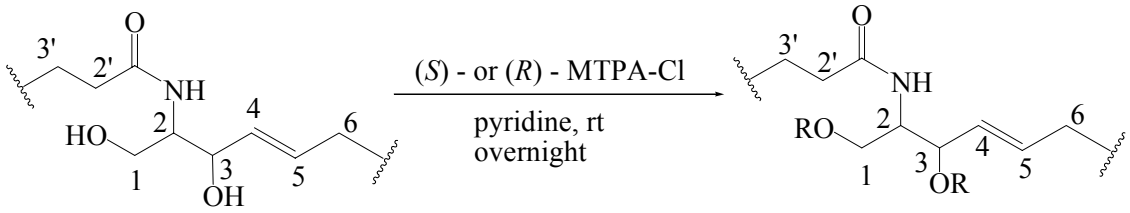

R = (*S*) - MTPA (**43**)
R = (*R*) - MTPA (**44**)

8.4.3.1 (*S*) - MTPA Ester (43)

To a solution of ceramide analog (**39**) (1.5 mg) in pyridine (500 µL) was added (*R*)-MTPA-Cl (30 µL) at room temperature for 16 h and concentrated *in vacuo*. The residue was diluted with EtOAc (4mL)/H_2O (1 mL) and then washed with saturated

$NaHCO_3$ solution, H_2O, brine solution and then dried with anhydrous $MgSO_4$. The filtrate was concentrated *in vacuo* and chromatographed on silica gel by EtOAc/hexane (5:95) to give (*S*) – MTPA ester (**43**) (0.7 mg) as colorless oil: $[\alpha]^{25}_D$ +60.0° (*c* = 0.015, $CHCl_3$); ^{1}H NMR ($CDCl_3$, 500 MHz) δ 7.45 (10H, 2 MTPA's aromatic protons), 5.81 (1H, dt, *J* = 7.9, 13.4 Hz), 5.39 (1H, t, *J* = 7.8 Hz), 5.29 (1H, m), 5.27 (1H, d, *J* = 8.9 Hz, N*H*), 4.55 (1H, m), 4.39 (1H, dd, *J* = 5.2, 11.6 Hz), 4.34 (1H, dd, *J* = 4.0, 11.8 Hz), 3.53 (3H, s), 3.48 (3H, s), 1.99 (m), 1.55 (br s), 1.49 (m), 1.26 (br s), 0.89 (3H, t, *J* = 6.8 Hz), 0.87 (6H, d, *J* = 6.6 Hz).

8.4.3.2 (*R*) - MTPA Ester (44)

Ceramide analog (**39**) (1.5 mg) was reacted with (*S*) – MTPA-Cl (30 μL) as described above and chromatographed to give (*R*) – MTPA ester (**44**) (0.3 mg) as colorless oil: $[\alpha]^{25}_D$ -29.0° (*c* = 0.0165, $CHCl_3$); ^{1}H NMR ($CDCl_3$, 500 MHz) δ 7.46 (10H, 2 MTPA's aromatic protons), 5.90 (1H, dt, *J* = 5.5, 14.6 Hz), 5.42 (1H, t, *J* = 8.5 Hz), 5.39 (1H, m), 5.23 (1H, d, *J* = 9.4 Hz, N*H*), 4.49 (1H, m), 4.27 (1H, dd, *J* = 3.6, 11.5 Hz), 4.20 (1H, dd, *J* = 5.6, 11.3 Hz), 3.53 (3H, s), 3.50 (3H, s), 2.02 (m), 1.56 (br s), 1.49 (m), 1.26 (br s), 1.15 (2H, m), 0.89 (3H, t, *J* = 6.8 Hz), 0.87 (6H, d, *J* = 6.6 Hz).

8.5 Synthesis of Erebusinone (12)

8.5.1 Preparation of Benzyl-3-(benzyloxy)-2-nitrobenzoate (46)

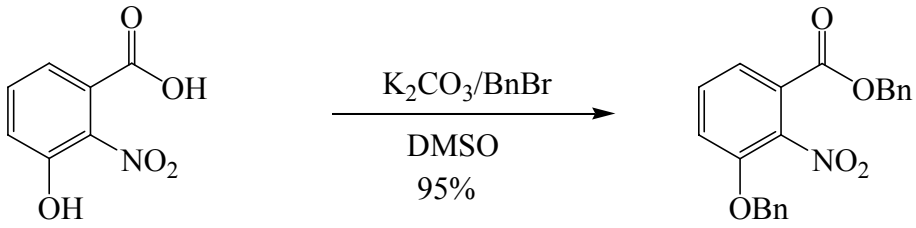

(**45**) (**46**)

To DMSO (100 ml) was added solid K_2CO_3, (9.05 g, 65.5 mmol, 6 eq.). After stirring for 5 min, 3-hydroxy-2-nitrobenzoic acid (**45**) (2.0 g, 10.9 mmol, 1 eq.) was added all at once followed by benzylbromide (7.47g, 43.7 mmol, 4 eq.). The reaction mixture was stirred at room temperature for 3 h and then poured into ice water (300 mL). After cooling, the solution was adjusted to pH 3-4 with HCl (10%) and extracted with CH_2Cl_2 (3 X 100 mL). The organic layer washed with brine (2 X 50 mL), dried with $MgSO_4$ and concentrated. The residue was chromatographed on silica gel by EtOAc/hexane (5:95) to give **46** 3.76g (95% yield) as a white solid: mp 82-83 ˚C; IR ν_{max} 3081, 2931, 1714, 1541, 1454, 1282 cm^{-1}; UV ($CHCl_3$) λ_{max} (log ε) 243 (0.7), 303 (0.44) nm; ^1H NMR ($CDCl_3$, 250 MHz) δ 7.61 (1H, d, J = 7.2 Hz), 7.38 (11H, m), 7.24 (1H, d, J = 8.7 Hz), 5.34 (2H, s), 5.19 (2H, s); ^{13}C NMR ($CDCl_3$, 75 MHz) δ 162.7 (s), 149.8 (s), 141.2 (s),134.9 (s), 134.7 (s), 130.5 (d), 128.7 (d), 128.6 (d), 128.3 (d), 126.9 (d), 123.6 (s), 122.5 (d), 118.6 (d), 71.2 (t), 67.9 (t); HRESIMS $[M + Na]^+$ m/z observed 386.0998 (calculated for $C_{21}H_{17}NO_5Na$ 386.1005).

8.5.2 Preparation of 3-[3-(Benzyloxy)-2-nitrophenyl]-3-oxopropanenitrile (47)

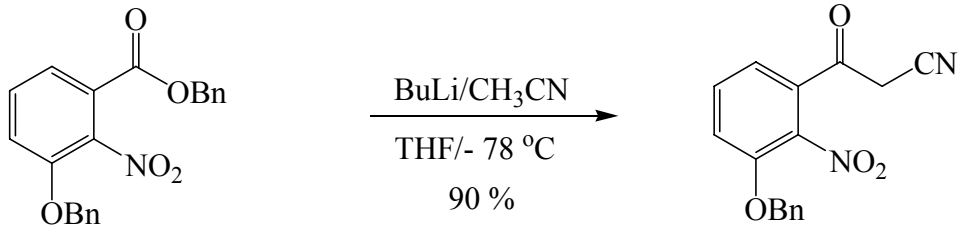

(**46**) (**47**)

Anhydrous neat acetonitrile (1.06 g, 25.8 mmol, 2.5 eq) was added to a solution of n-butyllithium (1.99 g, 31.0 mmol, 3 eq) in THF (100 mL) at –78˚C. After a white suspension formed, the solution of **46** (3.76g, 10.3 mmol, 1 eq) in THF (5 mL) was added into the reaction mixture. The light brown reaction mixture was warmed to – 45 ˚C and then stirred for 2.5 h and the aqueous HCl (10%) was added until pH 4. The reaction mixture was concentrated *in vacuo*. The residue was diluted with dichloromethane (300 mL) and then washed with water (2 X 50 mL) and brine (50 mL) and dried with $MgSO_4$ and the solvent removed *in vacuo*. Flash chromatography eluting with EtOAc/hexane (from10:90 to 20:80) to afford 2.77 g (90% yield) of **47** as a brown solid: mp 160-161 ˚C; IR ν_{max} 3081, 2931, 2220, 1708, 1544, 1449, 1285 cm^{-1}; UV ($CHCl_3$) λ_{max} (log ε) 210 (1.21), 249 (0.30), 313 (0.13) nm; ^1H NMR ($CDCl_3$, 250 MHz) δ 7.54 (1H, t, J = 8.3 Hz), 7.37 (6H, m), 7.26 (1H, d, J = 6.8 Hz), 5.26 (2H, s), 4.00 (2H, s); ^{13}C NMR ($CDCl_3$, 75 MHz) δ 187.8 (s), 149.5 (s), 138.6 (s), 135.5 (d), 131.7 (s), 128.6 (d), 128.3 (d), 127.5 (d), 126.9 (d), 122.3 (d), 120.8 (d), 115.1 (s), 70.7 (t), 31.3 (t); HREIMS $[M]^+$ m/z observed 296.0799 (calculated for $C_{16}H_{12}N_2O_4$ 296.0797).

8.5.3 Preparation of 3-[3-(Benzyloxy)-2-nitrophenyl]-3-hydroxypropanenitrile (48)

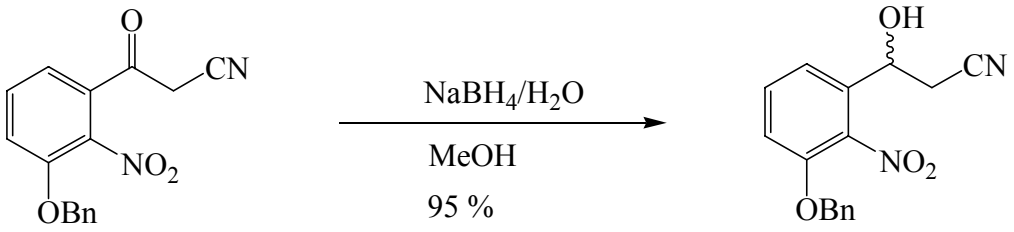

(**47**) (**48**)

To a solution of **46** (300 mg, 1.0 mmol) in MeOH (10 mL) was added slowly a solution of $NaBH_4$ (77 mg, 2.0 mmol), which was prepared with the solution (12 mL, 4:1, methanol and H_2O, pH 9) at 5 ˚C. The reaction mixture was warmed to room temperature and stirred for 3 h. The HCl (10%) solution was added to the reaction mixture until getting pH 4 and then concentrated *in vacuo* and diluted with EtOAc (100 mL). The organic layer was washed with brine and dried with $MgSO_4$ and The residue was chromatographed on silica gel by EtOAc/hexane (10:90) to give 0.29g (95% yield) of **48** as a light brown solid: $[\alpha]^{25}_D$ 0˚ (*c* = 0.193, $CHCl_3$); mp 72-73 ˚C; IR ν_{max} 3389, 2928, 2264, 1630, 1455, 1275 cm^{-1}; UV ($CHCl_3$) λ_{max} (log ε) 244 (0.50) nm; ^1H NMR ($CDCl_3$, 250 MHz) δ 7.47 (1H, t, *J* = 8.1 Hz), 7.36 (7H, m), 7.08 (1H, d, *J* = 8.1 Hz), 5.15 (2H, s), 5.08 (1H, br s), 2.38 (2H, m); ^{13}C NMR ($CDCl_3$, 75 MHz) δ 149.6 (s), 139.4 (s), 135.1 (s), 134.3 (s), 131.6 (d), 128.5 (d), 128.2 (d), 126.9 (d), 118.6 (d), 116.7 (d), 114.1 (s), 71.0 (t), 65.1 (t), 27.2 (d); HRESIMS $[M + Na]^+$ *m/z* observed 321.0841 (calculated for $C_{16}H_{14}N_2O_4Na$ 321.0852).

8.5.4 Preparation of 3-Amino-1-[3-(benzyloxy)-2-nitrophenyl]propan-1-ol (49)

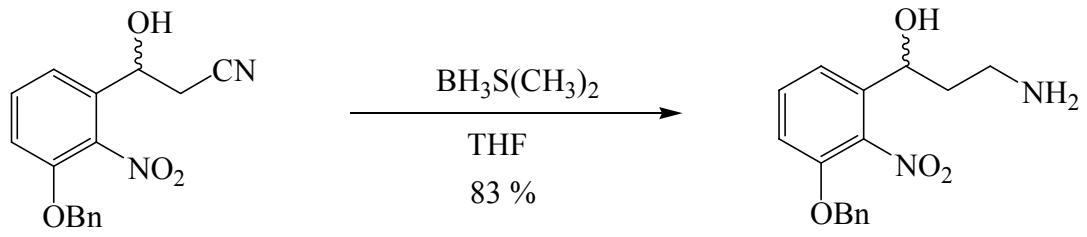

(**48**) (**49**)

To a solution of **48** (288 mg, 0.97 mmol) in THF (5 mL) was added BH_3SMe_2 (183 mg, 2.41 mmol) in THF (10 mL) at 0 ˚C. The reaction mixture was refluxed for 3h and then cooled to room temperature. MeOH (2 mL) followed by 6 N HCl (2 mL) was added to reaction mixture and then refluxed again for additional 0.5h and cooled to room temperature and concentrated under reduced pressure. The residue was partitioned between EtOAc (50 mL) and 1N HCl solution (30 mL). The phases were separated and then aqueous layer was basified with 5 N NaOH and extracted with EtOAc (3 X 50 mL). The combined organic phases were dried with K_2CO_3 and concentrated under reduced pressure. The residue was chromatographed on silica gel by MeOH/CH_2Cl_2 (10:90) to give 292 mg (81% yield) of **49** as a pale brown solid: $[\alpha]^{25}_D$ 0˚ (*c* = 0.210, $CHCl_3$); mp 122-123 ˚C; IR ν_{max} 3320, 3104, 2929,1608, 1525, 1455, 1273 cm^{-1}; UV ($CHCl_3$) λ_{max} (log ε) 245 (0.5) nm; ^1H NMR ($CDCl_3$, 250 MHz) δ 7.23 (m, 7H), 6.85 (1H, d, *J* = 8.2 Hz), 5.06 (2H, s), 4.80 (1H, d, *J* = 8.8 Hz), 3.03 (2H, m), 1.78 (2H, m); ^{13}C NMR ($CDCl_3$, 75 MHz) δ 149.2 (s), 139.8 (s), 137.9 (s), 135.5 (s), 130.8 (d), 128.5 (d), 128.1 (d),126.9 (d), 119.1 (d), 112.5 (d), 70.8 (t), 70.5 (t), 39.9 (t), 38.5 (d); HREIMS $[M]^+$ *m*/*z* observed 302.1261 (calculated for $C_{16}H_{18}N_2O_4$ 302.1267).

8.5.5. Preparation of N-{3-[3-(Benzyloxy)-2-nitrophenyl]-3-hydroxypropyl} acetamide (50)

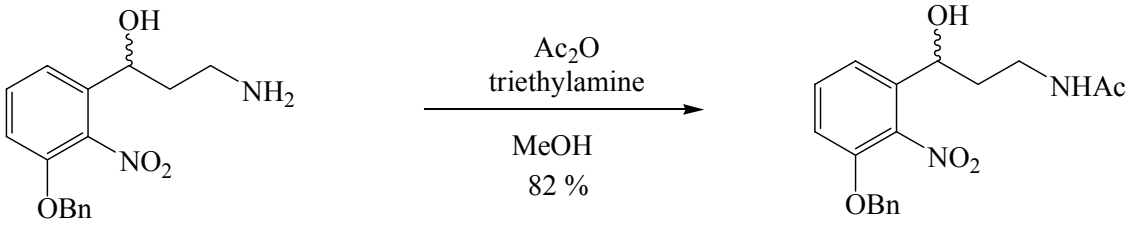

(**49**) (**50**)

To a stirred solution of **49** (136 mg, 0.45 mmol) and triethylamine (68 mg, 0.68 mmol, 1.5 eq) in CH_2Cl_2 (5 mL) was added Ac_2O (55 mg, 0.54 mmol, 1.2 eq) at 0 ˚C. The reaction mixture was stirred at room temperature for overnight and then poured to dilute saturated $NaHCO_3$ solution (5 mL) and the separated organic layer washed with brine and then dried with $MgSO_4$ and concentrated. The residue was chromatographed on silica gel by MeOH/CH_2Cl_2 (1:99) to afford 127 mg (82% yield) of **50** as a pale brown solid: $[\alpha]^{25}_D$ 0˚ (*c* = 0.193, $CHCl_3$); mp 102-103 ˚C; IR ν_{max} 3425, 3264, 3097, 1525, 1449 cm^{-1}; UV ($CHCl_3$) λ_{max} (log ε) 243 (0.36) nm; ^1H NMR ($CDCl_3$, 250 MHz) δ 7.30 (6H, m), 7.18 (1H, d, *J* = 8.2 Hz), 6.93 (1H, d, *J* = 7.9 Hz), 5.93 (1H, br s), 5.14 (2H, s), 4.68 (1H, dd, *J* = 2.3, 9.2 Hz), 4.21 (1H, br s), 3.75 (1H, m), 3.10 (1H, m), 1.99 (3H, s), 1.82 (2H, m); ^{13}C NMR ($CDCl_3$, 75 MHz) δ 171.8 (s), 149.3 (s), 139.9 (s), 137.4 (s), 135.5 (s), 131.2 (d), 128.6 (d), 128.3 (d), 127.0 (d), 118.8 (d), 112.8 (d), 71.0 (t), 66.5 (t), 38.8 (t), 36.4 (t), 23.0 (q); HRESIMS $[M + H]^+$ *m/z* observed 345.1445 (calculated for $C_{18}H_{21}N_2O_5$ 345.1450), $[M + Na]^+$ *m/z* observed 367.1268 (calculated for $C_{18}H_{20}N_2O_5Na$ 367.1270).

8.5.6 Preparation of N-{3-[3-(benzyloxy)-2-nitrophenyl]-3-oxopropyl}acetamide (51)

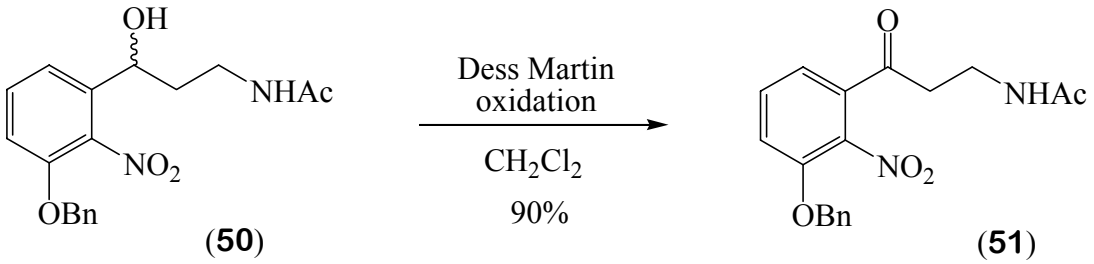

(**50**) (**51**)

To a mixture of Dess-Martin periodinane (360 mg, 0.85 mmol, 3 eq) and pyridine (100 mg, 1.5 eq of Dess-Martin periodinane) in dichloromethane (3 mL) was added a solution of **50** (97 mg, 0.28 mmol) in dichloromethane (1.5 mL) at 0 ˚C and then stirred at room temperature for 2 h. The reaction mixture was diluted with saturated $NaHCO_3$ solution (6 mL) at 5 ˚C and the organic layer was separated and the aqueous layer was extracted with CH_2Cl_2. The combined organic extracts were washed with saturated $Na_2S_2O_3$ (10 mL) and then water (2 X 10 mL) and brine and dried with $MgSO_4$ and concentrated. The residue was chromatographed on silica gel by EtOAc/hexane (80:20) to give 88 mg (92% yield) of **51** as a white solid: mp 73-74 ˚C; IR ν_{max} 3320, 3104, 2929, 1608, 1525, 1455, 1273 cm^{-1}; UV ($CHCl_3$) λ_{max} (log ε) 248 (1.1), 312 (0.47) nm; ^1H NMR ($CDCl_3$, 250 MHz) δ 7.43 (1H, t, J = 8.1 Hz), 7.23 (m, 6H), 7.22 (1H, d, J = 8.1 Hz), 5.17 (2H, s), 3.54 (2H, q, J = 5.6 Hz), 3.14 (2H, t, J = 5.7 Hz), 1.90 (3H,s); ^{13}C NMR ($CDCl_3$, 75 MHz) δ 197.7 (s), 170.4 (s), 150.3 (s), 139.3 (s), 134.8 (s), 131.2 (s), 130.7 (d), 128.7 (s), 128.4 (s), 126.9 (s), 120.6 (s), 118.6 (s), 71.3 (t), 39.7 (t), 34.1 (t), 23.1 (q); HREIMS $[M]^+$ m/z observed 342.1222 (calculated for $C_{18}H_{18}N_2O_5$ 342.1216).

8.5.7. Preparation of Erebusinone, N-[3-(2-amino-3-hydroxyphenyl)-3-oxopropyl] acetamide (12)

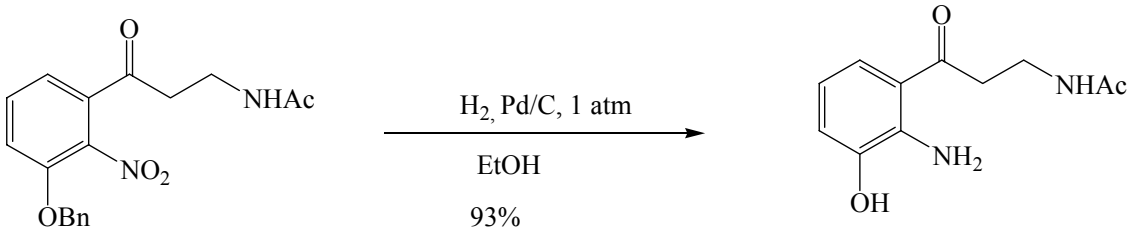

(**51**) Erebusinone (**12**)

A mixture of **51** (30 mg, 0.09 mmol) and 10 % Pd/C (15 mg) in dried ethanol (15 mL) was shaken with hydrogen atmosphere (1 atm) for 3 h. The reaction mixture was filtered to remove the catalyst and then concentrated. The residue was chromatographed on silica gel by MeOH/CH_2Cl_2 (2:98) to give 18.2 mg (93% yield) of erebusinone (**12**) as a bright yellow solid: mp 150-151 ˚C; IR ν_{max} 3488, 3362, 2925, 1619, 1568, 1458, 1221 cm^{-1}; UV (MeOH) λ_{max} (log ε) 231 (3.2), 272 (1.5), 375 (1.1) nm; ^{1}H NMR (MeOH-d_4, 250 MHz) δ 7.28 (1H, dd, J = 8.3, 1.0 Hz), 6.79 (1H, dd J = 7.6, 1.2 Hz), 6.45 (1H, t, J = 7.9 Hz), 3.40 (2H, t, J = 6.5 Hz), 3.12 (2H, t, J = 6.5 Hz), 1.9 (3H, s); ^{13}C NMR (MeOH-d_4, 75 MHz) δ 201.2 (s), 173.5 (s), 146.4 (s), 142.4 (s), 122.8 (s), 118.9 (d), 118.0 (d), 115.8 (d), 39.6 (t), 36.5 (t), 22.7 (q); HREIMS $[M]^+$ m/z observed 222.1007 (calculated for $C_{11}H_{14}N_2O_3$ 222.1004).

8.6 Synthesis of Erebusinonamine (52)

8.6.1 Preparation of *tert*-Butyl 3-[3-(benzyloxy)-2-nitrophenyl]-3-hydroxypropylcarbamate (53)

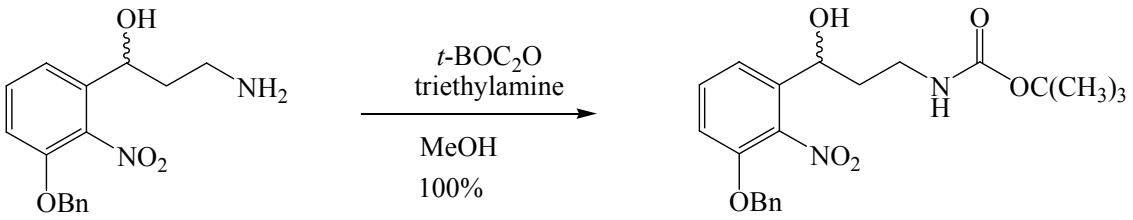

(**49**) (**53**)

To a stirred solution of **42** (2.0 g, 66.15 mmol) and triethylamine (0.67 g, 66.20 mmol, 1 eq) in MeOH (100 mL) was added di-*tert*-butyldicarbonate (2.17 g, 99.20 mmol, 1.5 eq) in MeOH (20 mL) at 0 ˚C. The reaction mixture was stirred at room temperature for 3 h and then concentrated. The crude mixture was diluted with CH_2Cl_2 (50 mL) and washed with saturated $NaHCO_3$ solution (2 X 15 mL) and the separated organic layer washed with brine and then dried with $MgSO_4$ and concentrated to give 2.66 g (100% yield) of **45** as a pale yellow oil which was directly used in the next step without purification: $[\alpha]^{25}_{D}$ 0˚ (*c* = 0.140, $CHCl_3$); IR ν_{max} 3416, 2979, 1686, 1609, 1532, 1368, 1278, 1069 cm^{-1}; UV (MeOH) λ_{max} (log ε) 224 (3.5) nm; ^1H NMR ($CDCl_3$, 250 MHz) δ 7.30 (m, 6H), 7.20 (1H, d, *J* = 8.0 Hz), 6.93 (1H, d, *J* = 8.4 Hz), 5.13 (2H, s), 4.88 (1H, br s), 4.72 (1H, d, *J* = 8.8 Hz), 3.53 (1H, m), 3.07 (1H, m), 1.79 (2H, m), 1.42 (9H, s); ^{13}C NMR ($CDCl_3$, 75 MHz) δ 157.0 (s), 148.9 (s), 139.6 (s), 136.9 (s), 135.1 (s),

130.7 (d), 128.2 (d), 127.7 (d), 126.6 (s), 118.4 (s), 112.4 (s), 79.6 (s), 70.6 (t), 65.8 (d), 39.0 (t), 36.6 (t), 27.8 (q).

8.6.2. Preparation of *tert*-butyl-3-[3-(benzyloxy)-2-nitrophenyl]-3-oxopropyl-carbamate (54)

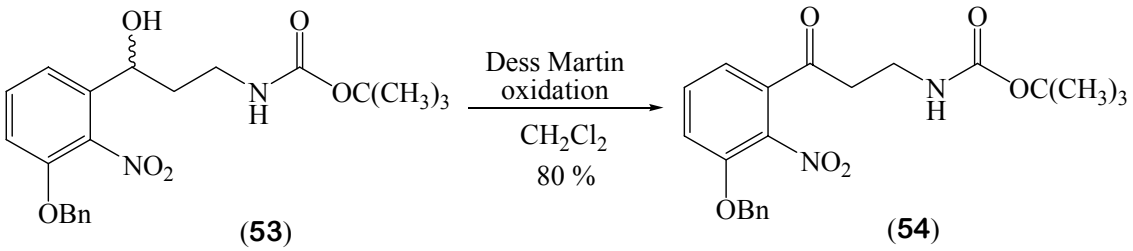

To a mixture of Dess-Martin periodinane (5.27g, 124 mmol, 2 eq.) and pyridine (1.97g, 248 mmol, 2.0 eq of Dess-Martin periodinane) in CH_2Cl_2 (60 mL) was added a solution of **53** (97 mg, 0.28 mmol) in CH_2Cl_2 (30 mL) at 0˚C and then stirred at room temperature for 2h. The reaction mixture was diluted with saturated $NaHCO_3$ solution (60 mL) at 5 ˚C and the organic layer was separated and the aqueous layer was extracted with CH_2Cl_2. The combined organic extracts were washed with saturated $Na_2S_2O_3$ (60 mL) and then H_2O (2 X 30 mL) and brine and dried with $MgSO_4$ and concentrated. The residue was chromatographed on silica gel by EtOAc/hexane (80:20) to give 1.98 g (80%) of **54** as a white solid: mp 66-67 ˚C; IR ν_{max} 3355, 2977, 2928, 1681, 1568, 1514, 1221 cm^{-1}; UV ($CHCl_3$) λ_{max} (log ε) 247 (1.0), 313 (0.4) nm; ^1H NMR ($CDCl_3$, 250 MHz) δ 7.44 (1H, t, J = 8.1 Hz), 7.23 (6H, m), 7.16 (1H, d, J = 7.7 Hz), 5.17 (2H, s), 3.45 (2H, q, J = 5.8 Hz), 3.10 (2H, t, J = 5.5 Hz), 1.39 (9H, s); ^{13}C NMR ($CDCl_3$, 75

MHz) δ 196.9 (s), 155.5 (s), 149.9 (s), 138.9 (s), 134.5 (s), 130.7 (s), 130.3 (d), 128.3 (d), 128.0 (d), 126.5 (d), 120.3 (d), 118.2 (d), 78.9 (s), 70.8 (t), 39.7 (t), 34.8 (t), 27.9 (q); HRESIMS $[M + Na]^+$ *m/z* observed 423.1535 (calculated for $C_{21}H_{24}N_2O_6Na$ 423.1532), $[M + K]^+$ *m/z* observed 439.1271 (calculated for $C_{21}H_{24}N_2O_6K$ 439.1271).

8.6.3 Preparation of 3-amino-1-[3-(benzyloxy)-2-nitrophenyl]propan-1-one hydrochloride (55)

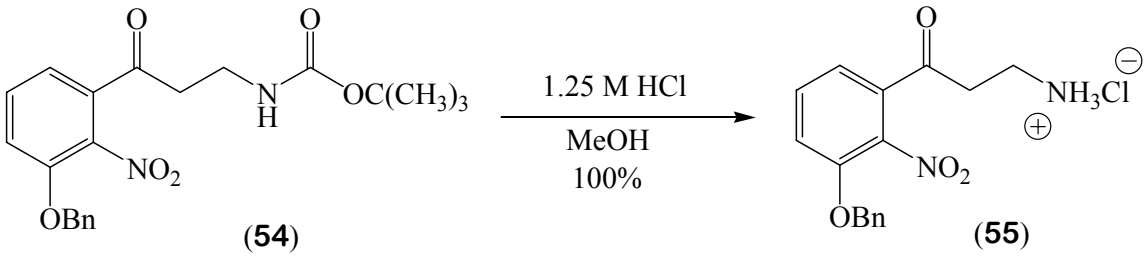

(**54**) (**55**)

To a mixture of *t*-BOC protected compound **54** (0.2g, 0.5 mmol) in MeOH (2 mL) was added HCl solution (7 mL, 1.25 M in MeOH) at 0 ˚C and then stirred at room temperature for 24 h. The reaction mixture was concentrated to give 168 mg (100% yield) of **55** as a white solid which was directly used without any purification for the next step: mp 169-170 ˚C; IR ν_{max} 2957, 2856, 1693, 1539, 1284 cm^{-1}; UV (MeOH) λ_{max} (log ε) 213 (1.1), 250 (0.2), 313 (0.1) nm; ^1H NMR (MeOH-d_4, 250 MHz) δ 7.59 (3H, m), 7.35 (5H, m), 5.22 (2H, s), 3.44 (2H, m), 3.27 (2H, m); ^{13}C NMR (MeOH-d_4, 75 MHz) δ 196.8 (s), 151.5 (s), 140.6 (s), 136.9 (s), 136.9 (s), 132.6 (d), 130.5 (d), 129.6 (d), 129.3 (d), 128.4 (d), 122.5 (d), 120.9 (d), 72.3 (t), 37.9 (t), 35.5 (t); HRESIMS $[M - Cl]^+$ *m/z* observed 301.1187 (calculated for $C_{16}H_{17}N_2O_4$ 301.1188).

8.6.4 Preparation of erebusinonamine, 3-amino-1-[2-amino-3-hydroxyphenyl]-propan-1-one hydrochloride (52)

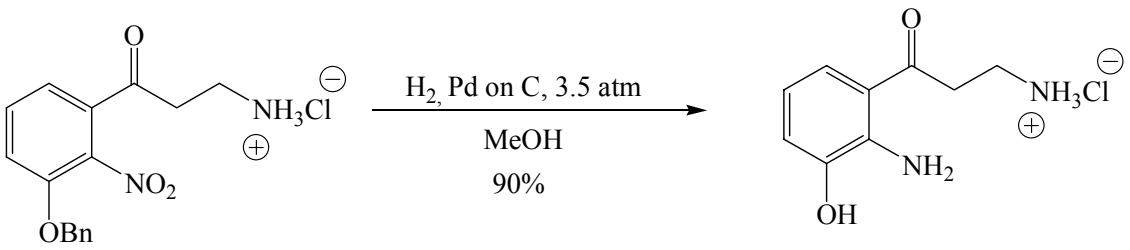

(**55**) Erebusinonamine (**52**)

A mixture of precursor of erebusinonamine (**55**) (66 mg, 0.2 mmol) and 10 % Pd/C (120 mg) in MeOH (50 mL) was shaken with hydrogen atmosphere (3.5 atm) for overnight. The reaction mixture was filtered to remove the catalyst and then concentrated. The residue was chromatographed on silica gel by eluting with $MeOH/CH_2Cl_2/CF_3COOH$ (20:80:0.1) to give 42.5 mg (89.5% yield) of erebusinonamine (**52**) as a brown wet solid: IR ν_{max} 3200, 2925, 1671, 1184 cm^{-1}; UV (MeOH) λ_{max} (log ε) 235 (0.6), 273 (0.2), 381 (0.1) nm; ^1H NMR (MeOH-d_4, 250 MHz) δ 7.18 (1H, d, J = 8.8 Hz), 6.77 (1H, d, J = 7.6 Hz), 6.50 (t, 1H, J = 8.2 Hz), 3.23 (4H, m); ^{13}C NMR (MeOH-d_4, 75 MHz) δ 200.04 (s), 146.9 (s),122.0 (d), 119.3 (s), 118.4 (s),117.4 (d), 114.2 (d), 35.6 (t), 35.1.(t); HRESIMS $[M - Cl]^+$ m/z observed 181.0969 (calculated for $C_9H_{13}N_2O_2$ 181.0977).

REFERENCES

1. Hartwell, J.L., *Lloydia*, **1967**, *30*, 379-436.
2. Ody, P. The Complete Medicinal Herbal,1st Ed., Darling Kindersley Limited, 1993.
3. Barton, D.; Nakanishi, K.; Meth-Cohn, O. Ed., Comprehensive Natural Products Chemistry,1st Ed., Pergman Press, 1999,Vol. 1.
4. Murata, M.; Naoki, H.; Iwashita, T.; Matsunaga, S; Sasaki, M.; Yokoyama, A.; Yasumoto, T. *J. Am. Chem. Soc.* **1993**, *115*, 2060-2062.
5. Nonomura, T.; Sasaki, M.; Matsumori, N.; Murata, M.; Tachibana, K.; Yasumoto, T. *Angew. Chem. Int. Ed. Engl.* **1996**, *35,* 1675-1678.
6. Wani, M.C.; Taylor, H.L.; Wall, M.E.; McPhail, A.T. *J. Am. Chem. Soc.* **1971**, *93*, 2325-2327
7. Scheuer, P.J. In *Chemistry of Marine Natural Products*; 1st Ed.; Academic Press, 1973.
8. Scheuer, P.J. In *Marine Natural Products*: *Chemical and Biological Perspectives*; Academic Press, New York, 1978-1983, Vol. I-V.
9. Fenical, W.H. *Science* **1982**, *215*, 923-928.
10. Scheuer, P.J. In *Biomedical Importance of Marine Organisms*; Fauntin, D., Ed.; Memories of the California Academy of Sciences, San Francisco, 1988, Vol. 13, 37-40.
11. Paul, V.J. In *Biomedical Importance of Marine Organisms*; Fauntin, D., Ed.; Memories of the California Academy of Sciences, San Francisco, 1988, Vol. 13, 23-27.

12. Paul, V.J. In *Ecological Roles of Marine Natural Products*; Paul, V.J., Ed., Ithaca, New York, Comstock Publishing, 1992, pp 164-188.
13. Pawlik, J.R. *Chem. Rev*. **1993**, *93*, 1911-1922.
14. Faulkner, D.J. *Nat. Prod. Rep*. **1984**, *1*, 551-598.
15. Faulkner, D.J. *Nat. Prod. Rep*. **1984**, *1*, 251-280.
16. Faulkner, D.J. *Nat. Prod. Rep*. **1986**, *3*, 1-33.
17. Faulkner, D.J. *Nat. Prod. Rep*. **1987**, *4*, 539-576.
18. Faulkner, D.J. *Nat. Prod. Rep*. **1988**, *5*, 613-663.
19. Faulkner, D.J. *Nat. Prod. Rep*. **1990**, *7*, 269-309.
20. Faulkner, D.J. *Nat. Prod. Rep*. **1991**, *8*, 97-147.
21. Faulkner, D.J. *Nat. Prod. Rep*. **1992**, *9*, 323-364.
22. Faulkner, D.J. *Nat. Prod. Rep*. **1993**, *10*, 497-539.
23. Faulkner, D.J. *Nat. Prod. Rep*. **1994**, *11*, 355-394.
24. Faulkner, D.J. *Nat. Prod. Rep*. **1995**, *12*, 223-269.
25. Faulkner, D.J. *Nat. Prod. Rep*. **1996**, *13*, 75-125.
26. Faulkner, D.J. *Nat. Prod. Rep*. **1997**, *14*, 259-302.
27. Faulkner, D.J. *Nat. Prod. Rep*. **1998**, *15*, 113-158.
28. Faulkner, D.J. *Nat. Prod. Rep*. **1999**, *16*, 155-198.
29. Faulkner, D.J. *Nat. Prod. Rep*. **2000**, *17*, 7-55.
30. Faulkner, D.J. *Nat. Prod. Rep*. **2001**, *18*, 1-49.
31. Faulkner, D.J. *Nat. Prod. Rep*. **2002**, *19*, 1-48.
32. Burris, J.E. *BioSci.*, **1996**, *46*, 235-237.
33. Fenical, W.; Jensen, P.R. In *Marine Biotechnology*, Attaway, D.H., Zaborsky, O.R.,

Eds., Plenum Press, New York, 1993, Vol. 1, pp 419-457.

34. Cragg, G.M.; Newman, D.J.; Snader, K.M. *J. Nat. Prod*. **1997**, *60*, 62-60.
35. Adams, M.E.; Swanson, G. TINS Neurotoxins supplement, 2nd Ed, Elsevier, 1996.
36. Cimino, G.; Ghiselin, M.T. In *Marine Chemical Ecology*, McClintock, J.B., Baker, B.J. Eds., CRC Press, Boca Raton, FL, 2001, 115-154.
37. Pears, V.; Pears, J.; Buchsbaum, M.; Buchsbaum, R. *Living Invertebrates*, Blackwell Scientific Publications, Boston, MA, 1987, p 847.
38. Santavy, D.L.; Willenz, P.; Colwell,R.R. *Applied Env. Micro*. **1990**, *56*, 1750-1762.
39. Bewley, C.A.; Holland, N.D.; Faulkner, D.J. *Experientia* **1996**, *52*, 716-722.
40. Friedlander, P. *Chem. Ber.* **1909**, *42*, 765-770.
41. Bergmann, W.; Feeny, R.J. *J. Org. Chem*. **1951**, *16,* 981-987.
42. Bergmann, W.; Burke.D.C. *J. Org. Chem.* **1955**, *20*, 1051-1057.
43. Mastrianni, D.M.; Tung, N.M.; Tenen, D.G. *Am. J. Med*. **1992**, *82*, 286-295.
44. Whitley, R.J.; Alford, C.A.; Hirsch, M.S. *N. Engl. J. Med*. **1986**, 144-149.
45. Skoldenberg, B.; Forsgren, M.; Alestig, K. *Lancet*. **1984**, 707-711.
46. Pettit, G.R.; Herald, C.L.; Doubek, D.L.; Arnold, E.; Clardy, J. *J. Am. Chem. Soc.* **1982**, *104*, 6846-4848.
47. Pluda, J.M.; Cheson, B.D.; Phillips, P.H. *Oncology*, **1996**, *10*, 740-742.
48. Haygood, M.G.; Schmidt, E.W.; Davidson, S.K.; Faulkner, D.J. *J. Mol. Microbiol. Biotechnol.* **1999**, *1*, 33-43.
49. Ireland, C.M.; Copp, B.R.; Foster, M.P.; McDonald, L.A.; Radisky, D.C.; Swersey, J.C. In *Marine Biotechnology*, Attaway, D.H.; Zaborsky, O.R. Eds., Plenum Press: New York, 1993, Vol. 1, pp 1-43.

50. Rinehart, K.L.; Holt, T.G.; Fregeau, N.L.; Stroh, J.G.; Keifer, P.A.; Sun, F.; Li, L.H.; Martin, D.G. *J. Org. Chem.* **1990**, *55*, 4512-4515.

51. Wright, A.E.; Forleo, D.A.; Gunawardana, F.P.; Gunasekera, S.P.; Koehn, F.E.; McConnell, O.J. *J. Org. Chem.* **1990**, *55*, 4508-4512.

52. Weinheimer, A. J.; Spraggins, R.L. *Tetrahedron Lett*. **1969**, 5785-5188.

53. Okuda, R. K.; Klein, D.; Kinnel, R.B.; Li, M.; Scheuer, P.J. *Pure Appl. Chem*. **1982**, *54*, 1907-1914 and reference therein.

54. Baker, B.J.; Okuda, R.K.; Yu, P. T.K.; Scheuer, P.J. *J. Am. Chem. Soc*. **1985**, *107*, 2976-2977.

55. Suzuki, M.; Morita, Y.; Yanagisawa, A.; Noyori, R.; Baker, B.J.; Scheuer, P.J *J. Am. Chem. Soc*. **1986**, *108*, 5021-5022.

56. Baker, B.J.; Scheuer, P.J.; Shoolery, J.M. *J. Am. Chem. Soc*., **1988**, *110*, 965-966.

57. He, H.; Kulanthaivel, P.; Baker, B.J. *Tetrahedron Lett*. **1994**, *35*, 7189-7192.

58. Amsler, C.D.; Iken, K.B.; McClintock, J.B.; Baker, B.J. In *Marine Chemical Ecology*, McClintock, J.B.; Baker, B.J., Eds., CRC Press, Boca Raton, FL, 2001, 267-300.

59. Dayton, P.K.; Robilliaird, G.A.; Paine, R.T.; Dayton, L.B. *Ecol. Monog.* **1974**, *44*, 105-128.

60. Moon B.H.; Baker, B.J.; McClintock, J.B. *J. Nat. Prod*. **1998**, *61*, 116-118.

61. Moon B.H.; Park, Y.C.; Baker, B.J.; McClintock, J.B. *Tetrahedron* **2000**, 9057-9062.

62. Pearse, V.; Pearse, J.; Bushsbaum, M.; Buschsbaum, R. In *Living Invertebrates,* The Blackwood Press, Pacific Grove, CA, 1987, 71-90.

63. Kashman, Y.; Groweiss, A.; Lidor, R.; Blasberger, D.; Carmely, S. *Tetrahedron* **1985**, *41*, 1905-1914.

64. Copp, B.R.; Fulton, K.F.; Perry, N.B.; Blunt, J.W.; Munro, M.H.G. *J. Org. Chem.* **1994**, *59*, 8233 -8238.

65. Yang, A.; Baker, B.J.; Grimwade, J.E.; Leonard, A.C.; McClintock, J.B. *J. Nat. Prod.* **1995**, *58,* 1596-1599.

66. Trimurtulu, G.; Faulkner, D.J.; Perry, N.B.; Ettouati, L.; Litaudon, M.; Blunt, J.W.; Munro, M.H.G.; Jameson, G.B. *Tetrahedron,* **1994**, *50,* 3993-4000.

67. Jayatilake, G.S.; Baker, B.J.; McClintock, J.B. *Tetrahedron Lett.* **1997**, *38*, 7507-7510.

68. Molinski, T.F.; Faulkner, D.J. *J. Org. Chem.* **1987**, *52,* 296-298.

69. Molinski, T.F.; Faulkner, D.J. *Tetrahedron Lett.* **1988**, *29,* 2137-2138.

70. Moon B.H. Ph.D. Dissertation., Florida Institute of Technology, Melbourne, FL 1997.

71. Perry, N.B.; Blunt, J.W.; Munro, M.H.G. *J. Nat. Prod.* **1987**, *50*, 307-308.

72. Copp, B.R.; Wassvik, C.M.; Lambert, G.; Page, M.J. *J. Nat. Prod.* **2000**, *63*, 1168-1169.

73. Rice, J.M.; Dudek, G.O. *J. Am. Chem. Soc*. **1967**, *89*, 2719-2725.

74. Naya, Y.; Kishida, K.; Sugiyama, M.; Murata, M.; Miki, W.; Ohinishi, M.; Nakanish, K. *Experientia* **1988,** *44*, 50-52.

75. Buckingham, J. In *Dictionary of Organic Compounds*, 5th Ed., Chapman and Hall, 1982, Vol. 3, 3091.

76. Mclintock, J.B.; Baker, B.J.; Slattery, M.; Hamann, M.; Kopitzke, R.; Heine, J. *J.*

Chem. Ecol. **1994**, *20,* 859-870.

77. Jayatilake, G.S.; Thornton, M.P.; Leonard, A.C.; Grimwade, J.E.; Baker, B.J. *J. Nat. Prod.* **1996**, *59,* 293-296.

78. Thornton, M.P., MS Thesis, Florida Institute of Technology, Melbourne, FL 1995.

79. Becker, E.D.; Miles, H.T.; Bradley, R.B. *J. Am. Chem. Soc.* **1965**, *87*, 5575-5582.

80. Pouchert, C.J. In *The Aldrich Library of NMR Spectra*, 2nd Ed., Aldrich Chemical Company, INC., 1983, Vol. 2, 693, 710.

81. Pouchert, C.J. In *The Aldrich Library of NMR Spectra*, 2nd Ed., Aldrich Chemical Company, INC., 1983, Vol. 2, 694.

82. Pouchert, C.J. In *The Aldrich Library of NMR Spectra*, 2nd Ed., Aldrich Chemical Company, INC., 1983, Vol. 2, 746.

83. Baker, B.J.; Kopitzke, R.W.; Yoshida, W.Y.; McClintock, J.B. *J. Nat. Prod.* **1995**, *58,* 1459-1462.

84. McClintock, J.B.; Baker, B.J.; Hamann, M.T.; Yoshida, W.Y.; Slattery, M.; Heine, J.N.; Bryan, P.J.; Jayatilake, G.S.; Moon, B.H. *J. Chem. Ecol.* **1994**, *20,* 2539-2549.

85. Pouchert, C.J. In *The Aldrich Library of NMR Spectra*, 2nd Ed., Aldrich Chemical Company, INC., 1983, Vol. 2, 664.

86. Ohtani, I.; Kusumi, T.; Kashman, Y.; Kakisawa, H. *J. Am. Chem. Soc.* **1991**, *113*, 4092-4096.

87. Dale, J.A.; Mosher, H.S. *J. Am. Chem. Soc.* **1973**, *95*, 512-519.

88. Ohtani, I.; Kusumi, T.; Kashman, Y.; Kakisawa, H. *J. Org. Chem.* **1991**, *56*, 1296-1298.

89. Kusumi, T.; Fujita, Y.; Ohtani, I.; Kakisawa, H. *Tetrahedron Lett.* **1991**, *32*, 2923-

2926.

90. Cahn, R.S.; Ingold, D.K.; Prelog, V. *Experientia* **1956**, *12,* 81.

91. Nakanishi, K. In *Biomedical Importance of Marine Organisms*, Fauntin, D.G., Ed., California Academy of Science Press, San Francisco, 1988, pp 59-67.

92. Robert, A.W.; Rose, M.E. *Tetrahedron* **1979**, *35*, 2169-2173.

93. Fleming, F.F.; Huang, A.; Sharief, V.A.; Pu Y. *J. Org. Chem.* **1999**, *64*, 2830-2834.

94. Osby, J.O.; Heinzman, S.W.; Ganem, B. *J. Am. Chem. Soc.* **1986**, *108*, 67-72.

95. Yoon, N.M.; Brown, H.C. *J. Am. Chem. Soc.* **1968**, *90*, 2927-2938.

96. Sleath, P.R.; Noar, J.B.; Eberlein, G.A.; Bruice, T.C. *J. Am. Chem. Soc.* **1985**, *107*, 3328-3338.

97. Brown, H.C.; Chandrasekharn, J. *J. Org. Chem.* **1983**, *48*, 644-648.

98. Kisfaludy, I.; Mohacsi, M.; Low, M.; Drexler, F. *J. Org. Chem.* **1979**, *44*, 654-656.

99. Dess, D.B.;Martin, J.C. *J. Org. Chem.* **1983**, *48*, 4155-4156.

100. Ponnusamy, E.; Fotadar, U.; Spisni, A.; Fiat, D. *Synthesis,* **1986**, 48-53.

101. Stahl, G.L.; Walter, R.; Smith, C.W. *J. Org. Chem.* **1983**, *43*, 2285-2286.

102. Mitscher, L.A.; Leu, R.-P.; Bathala, M.S.; Wu, W.-N.; Beal, J.L. *J. Nat. Prod.* **1972**, *35*, 157-166.

103. Cimino, G.; de Giulio, A.; de Rosa, S.; de Stefano, S.; Puliti, R.; Mattia, C.A.; Mazzarella, L. *J. Nat. Prod.* **1985**, *48*, 523-528.

104. Fujii, T.; Saito, T.; Mori, S. *Chem. Pharm. Bull.* **1990**, *38*, 2146-2150.

105. Ackermann, D.; List, P.H. *Hoppe-Seyler's Z. Physiol. Chem.* **1960**, *318*, 281.

106. Cafieri, F.; Fattorusso, E.; Mangoni, A.; Taglialatela-Scafati, O. *Tetrahedron Lett.* **1995**, *36*, 7893-7896.

107. Chehade, C.C.; Dias, R.L.A.; Berlinck, R.G.S.; Gerreira, A.G.; Costa, L.V.; Rangel M.; Malpezzi, E.L.A.; de Freitas, J.C.; Hajdu, E. *J. Nat. Prod.* **1997**, *60*, 729-731.

108. Bourguet-Kondracki, M.-L.; Martin, M.-T.; Vacelet, J.; Guyot, M. *Tetrahedron Lett.* **2001**, *42*, 7257-7259.

109. Bergmann, W.; Burke, D.C. *J. Org. Chem.* **1956**, *21*, 225-228.

110. Bergmann, W.; Feeney, R.J. *J. Am. Chem. Soc*. **1950**, *72*, 2809-2810.

111. Searle, P.A.; Molinski, T.F. *J. Org. Chem.* **1995**, *60*, 4296-4298.

112. Isono, K. *J. Antibiot.* **1988**, *41*, 1711-1739.

113. Isono, K. *Pharmacol. Ther.* **1991**, *52*, 269-286.

114. Isono, K.; Uramoto, M.; Kusakabe, H.; Miyato, N.; Koyama, T.; Ubukata, M.; Sethi, S.; McCloskey, J.A. *J. Antibiot.* **1984**, *37*, 670-672.

115. Takahasi, E.; Beppu, T. *J. Antibiot.* **1982**, *32*, 930-947.

116. Hattori, T.; Adachi, K.; Shizuri, Y. *J. Nat. Prod.* **1998**, *61*, 823-826.

117. Chakrabarty, M.; Batabyal, A.; Barua, A.K. *J. Nat. Prod.* **1994**, *57*, 393-395.

118. Shin J.; Seo, Y. *J. Nat. Prod.* **1995**, *58*, 948-953.

APPENDICES

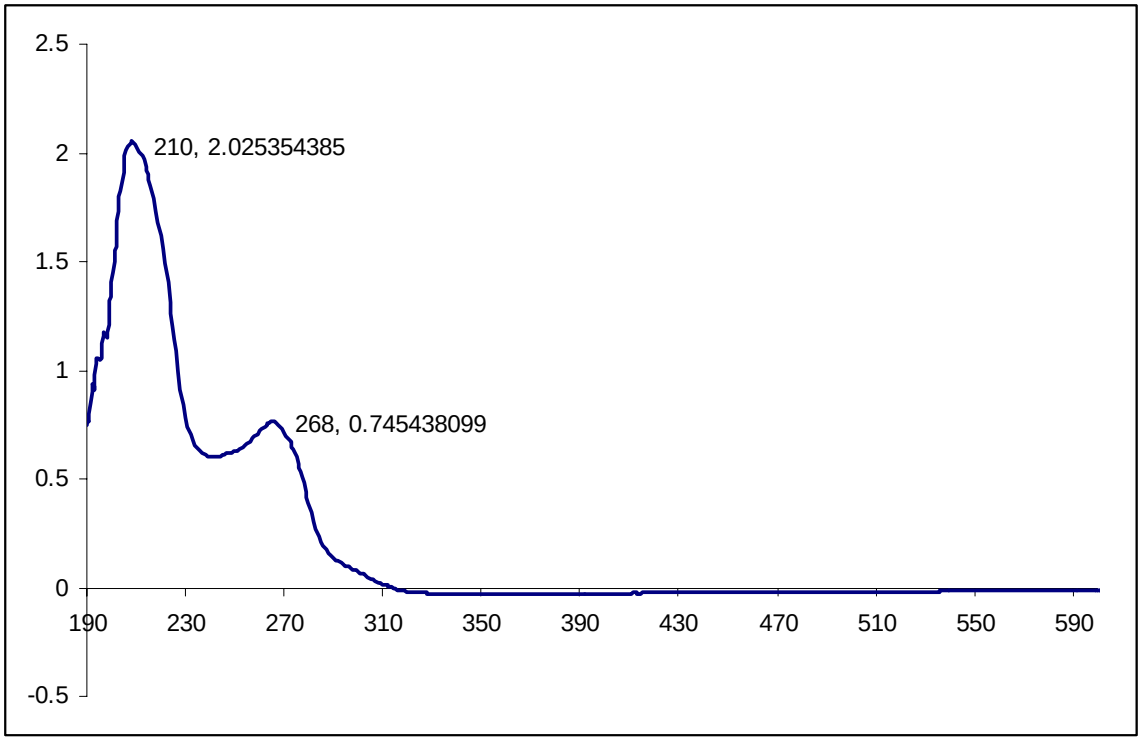

Figure 69. UV spectrum of purine analog (**23**) in MeOH.

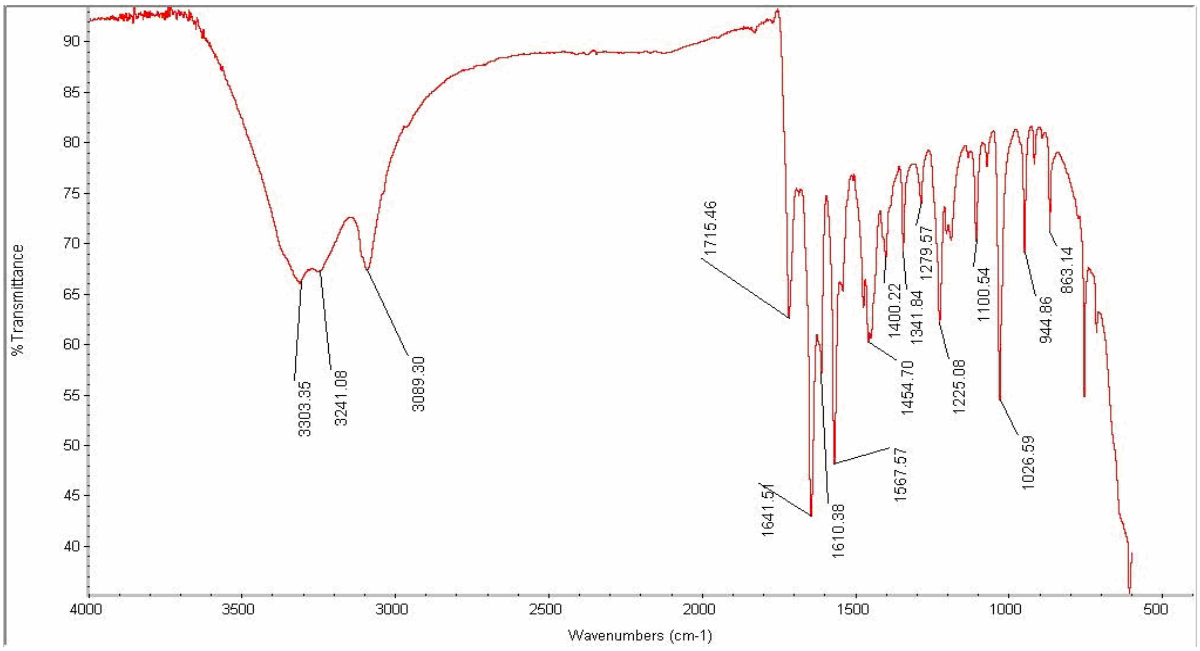

Figure 70. IR spectrum of purine analog (**23**).

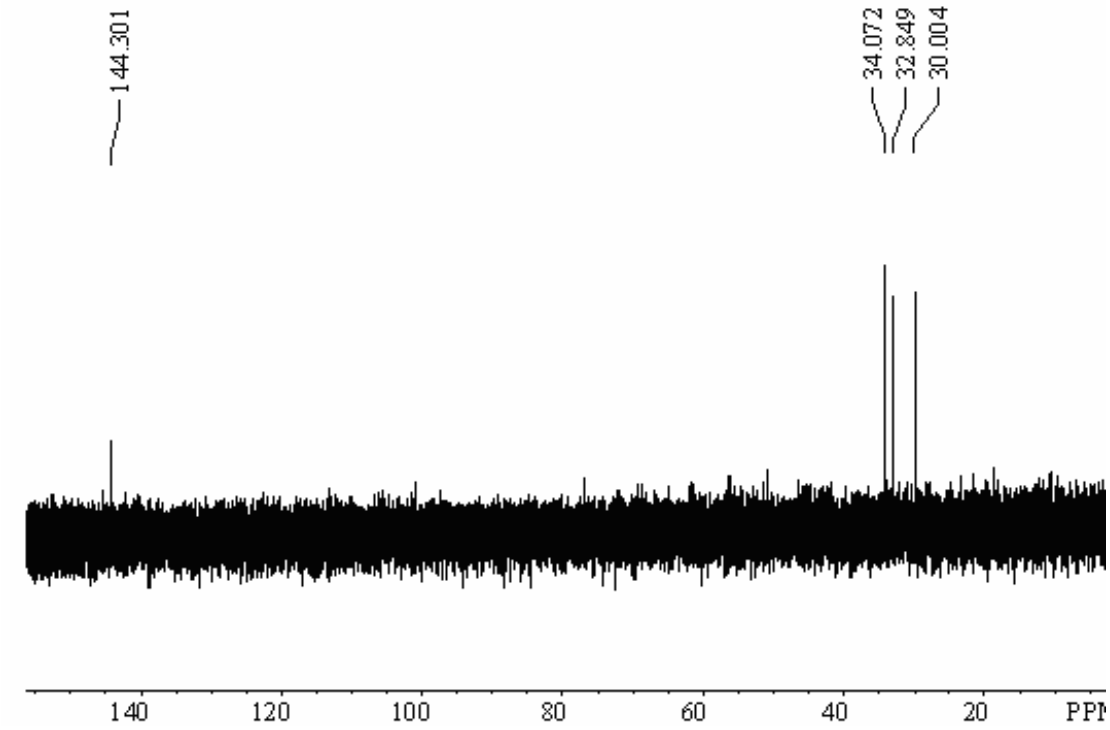

Figure 71. DEPT-135 spectrum of purine analog (**23**) (125 MHz, DMSO-d_6).

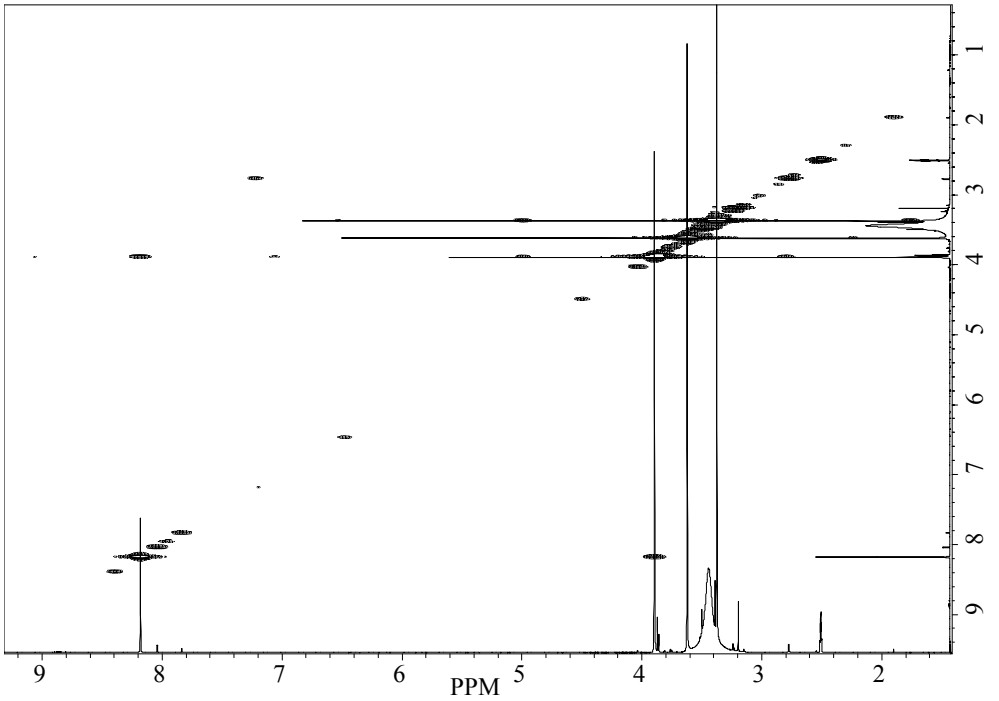

Figure 72. gCOSY spectrum of purine analog (**23**) (500 MHz, DMSO-d_6).

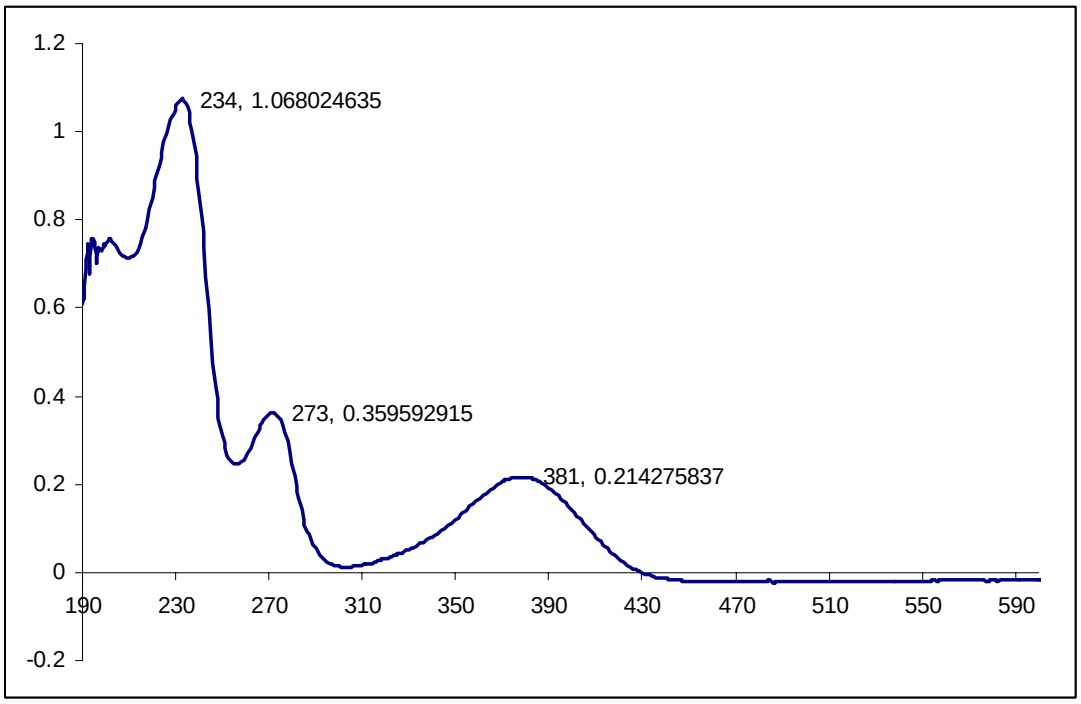

Figure 73. UV spectrum of 3-hydroxykynurenine (**24**) in MeOH.

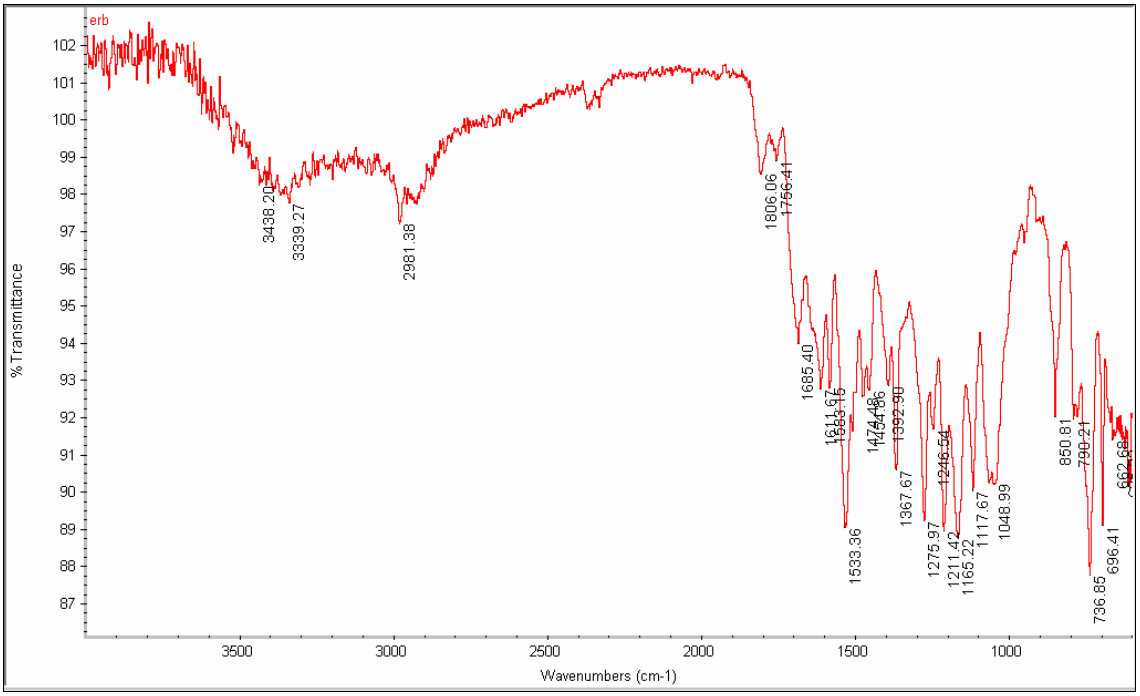

Figure 74. IR spectrum of 3-hydroxykynurenine (**24**).

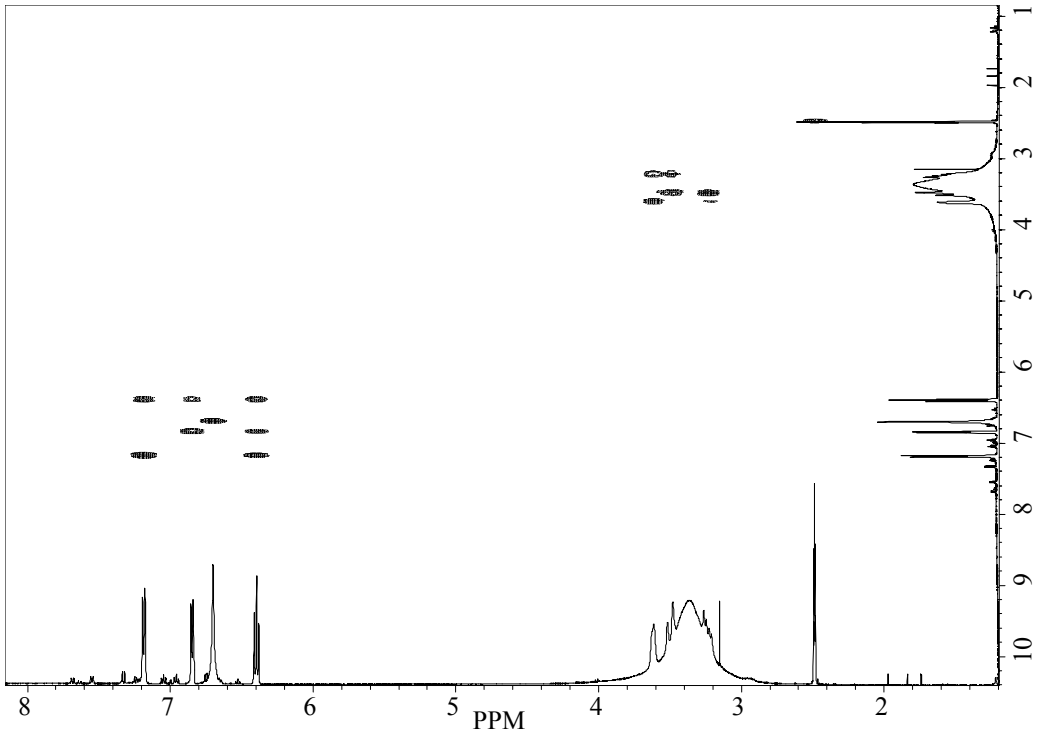

Figure 75. gCOSY spectrum of 3-hydroxykynurenine (**24**) (500 MHz, DMSO-d_6).

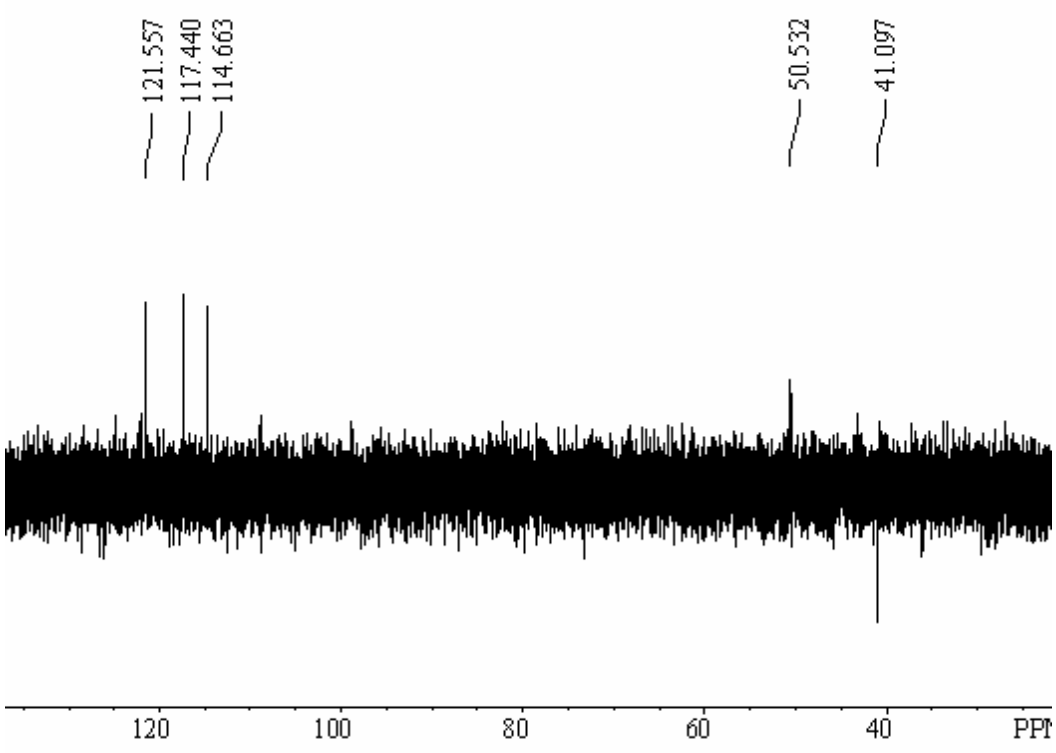

Figure 76. DEPT-135 spectrum of 3-hydroxkynurenine (**24**) (125 MHz, DMSO-d_6).

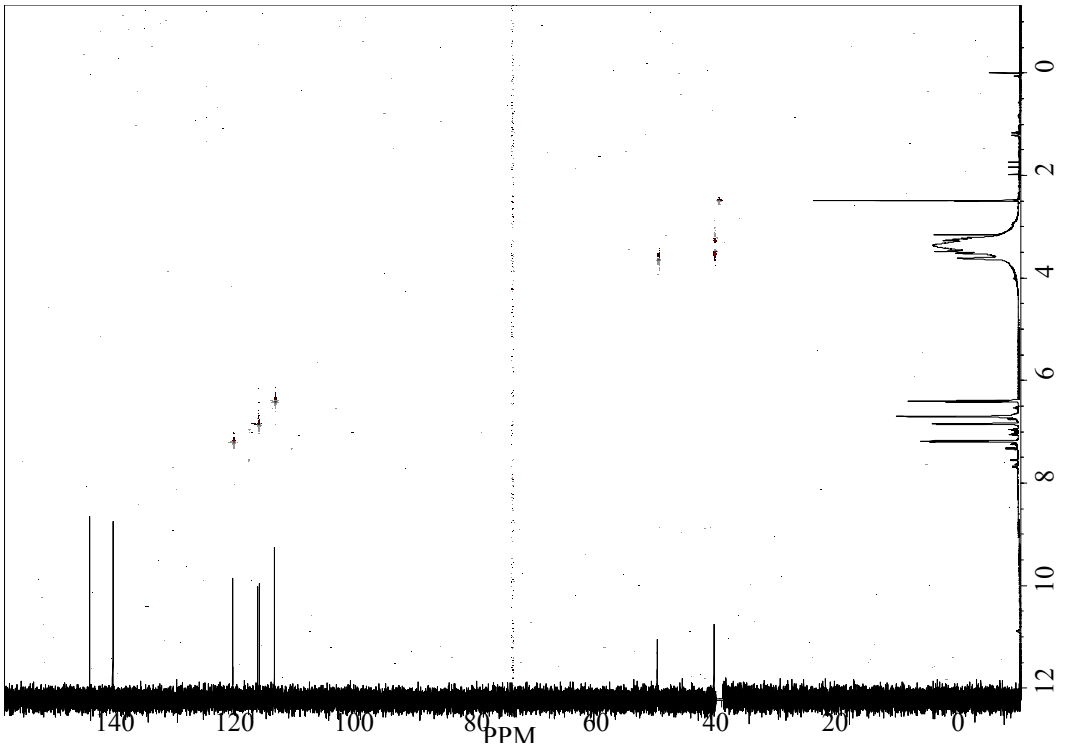

Figure 77. gHSQC spectrum of 3-hydroxykynurenine (**24**) (500 MHz, DMSO-d_6).

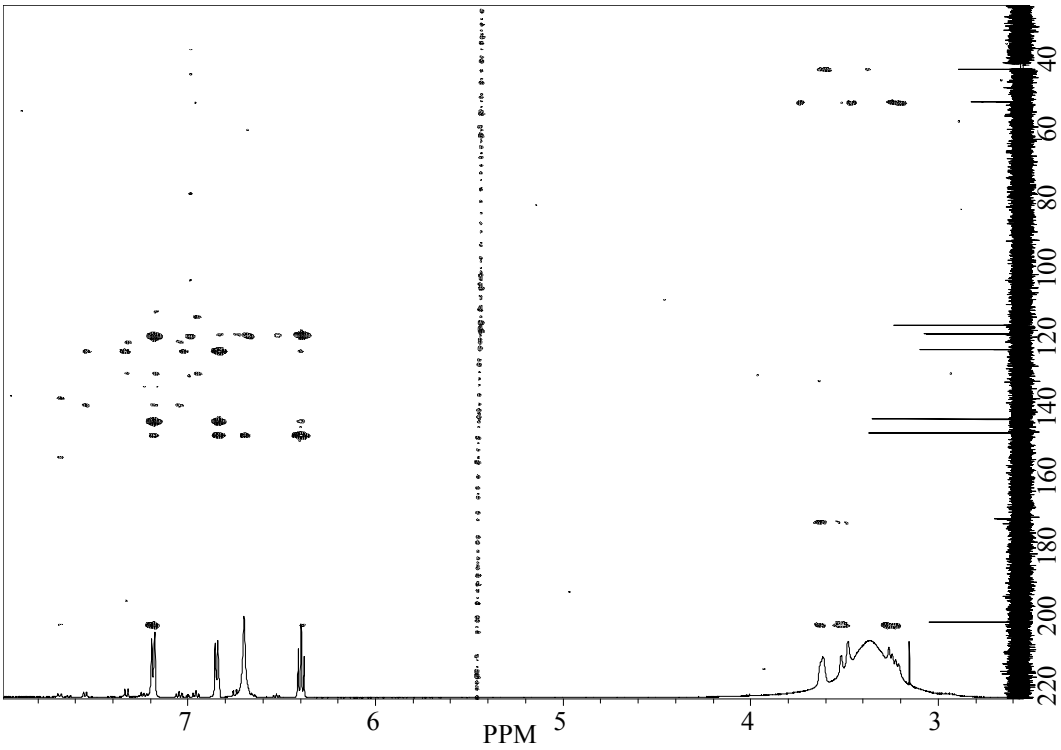

Figure 78. gHMBC spectrum of 3-hydroxykynurenine (**24**) (500 MHz, DMSO-d_6).

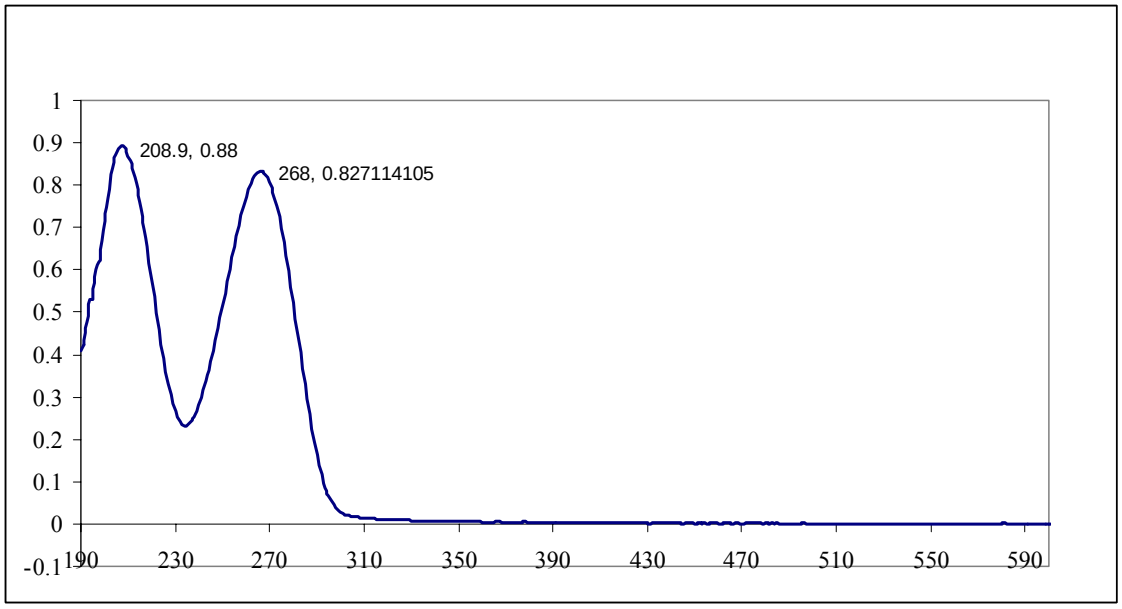

Figure 79. UV spectrum of 5-methyl-2'-deoxycytidine (**25**) in MeOH.

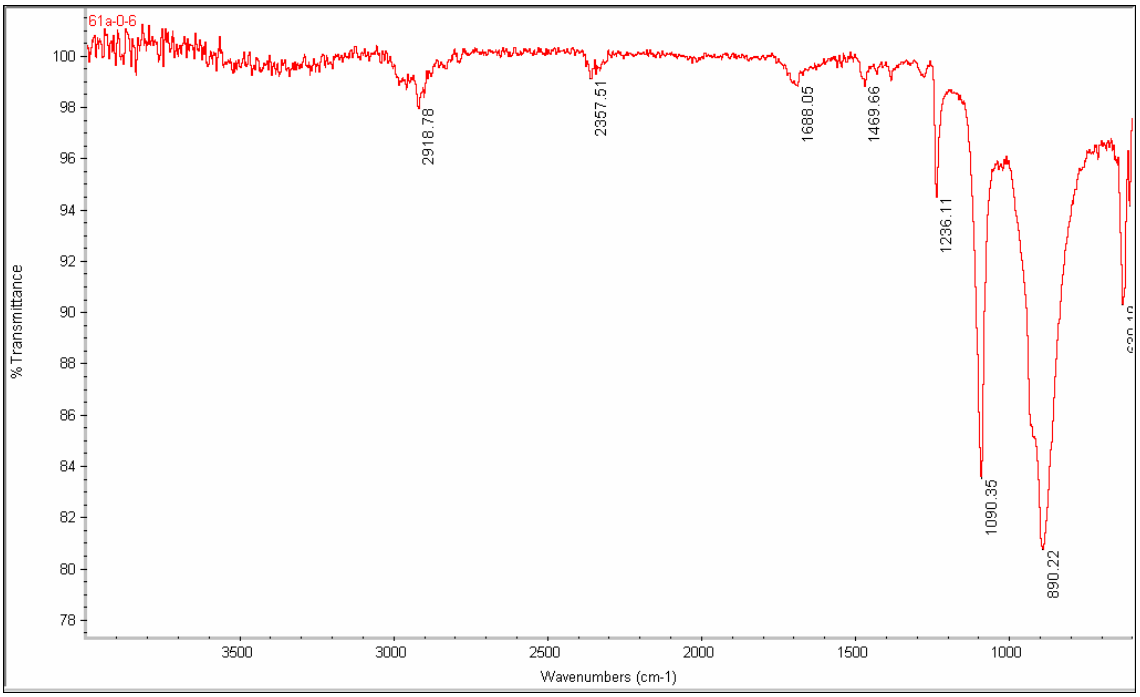

Figure 80. IR spectrum of 5-methyl-2'-deoxycytidine (**25**).

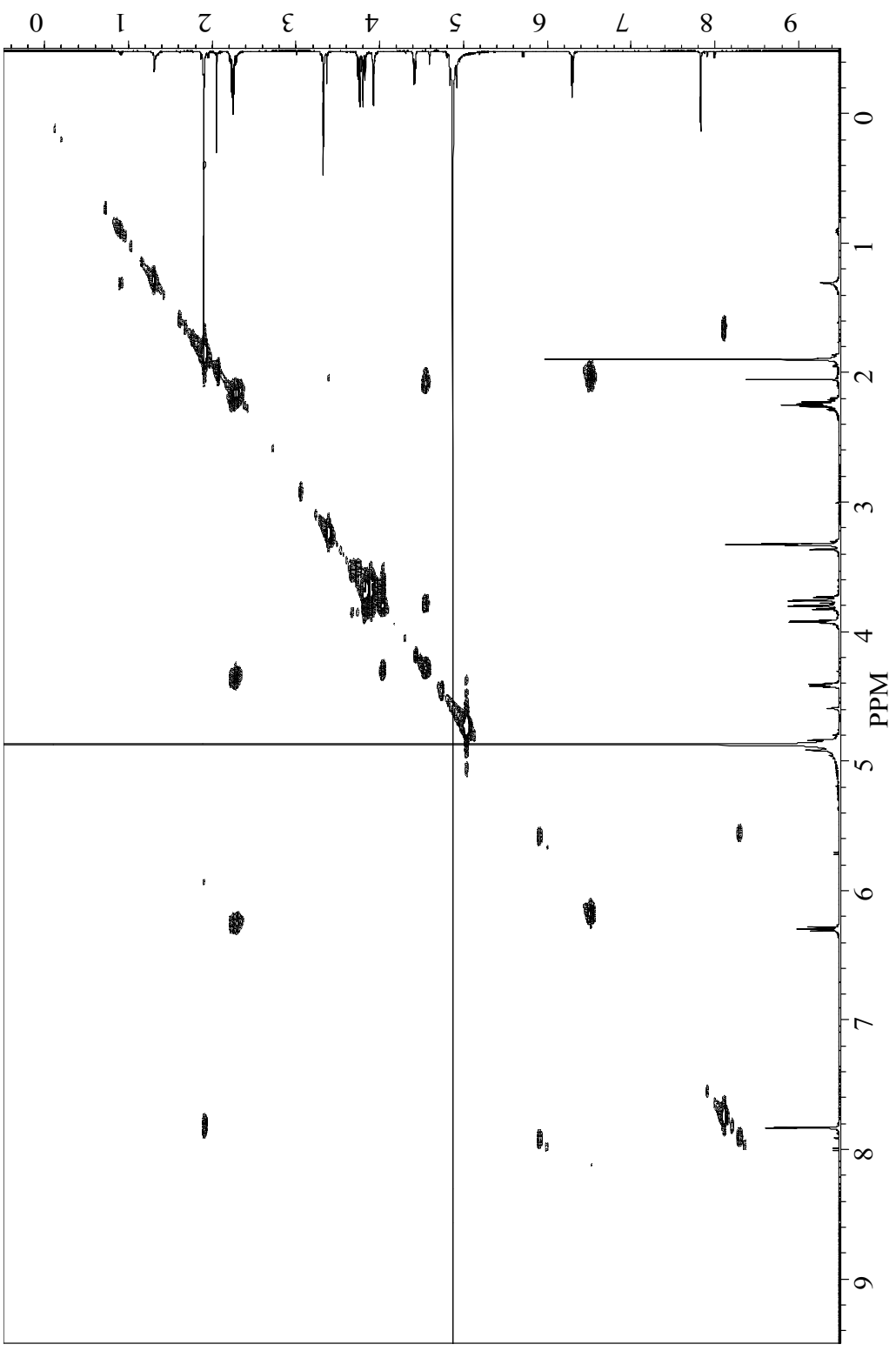

Figure 81. gCOSY spectrum of 5-methyl-2'-deoxycytidine (**25**) (500 MHz, MeOH-d_4).

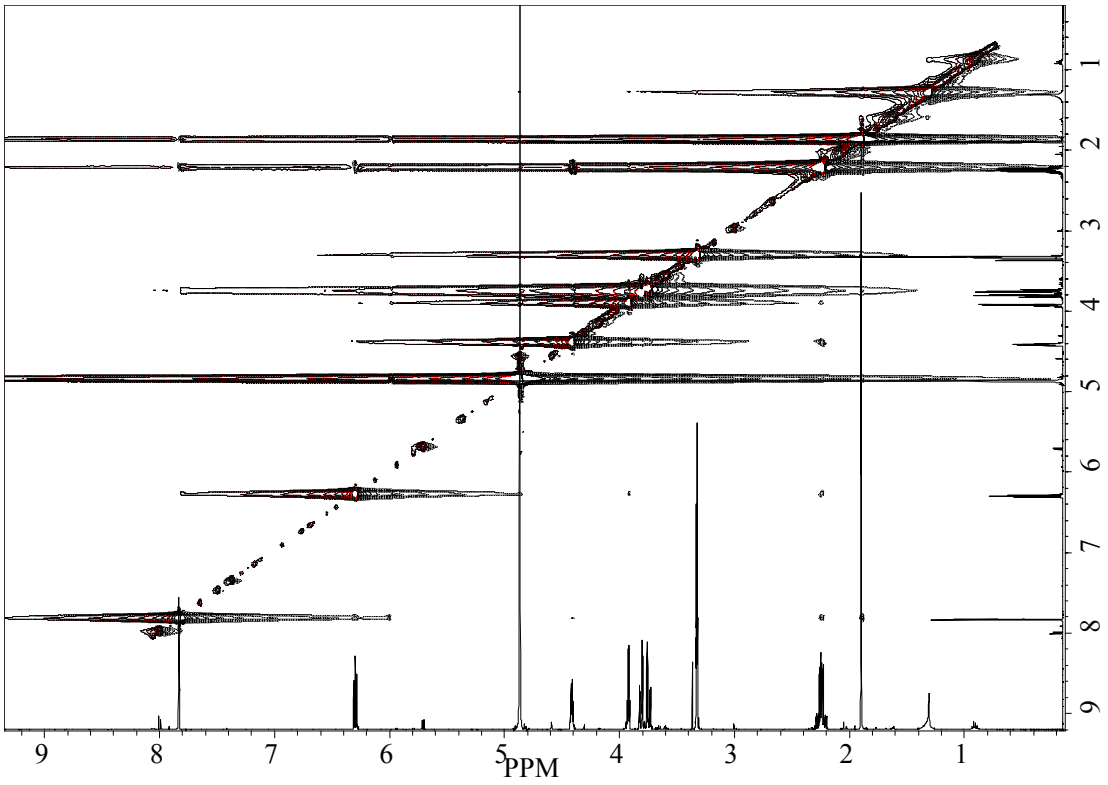

Figure 82. ROESY spectrum of 5-methyl-2'-deoxycytidine (**25**) (500 MHz, MeOH-d_4).

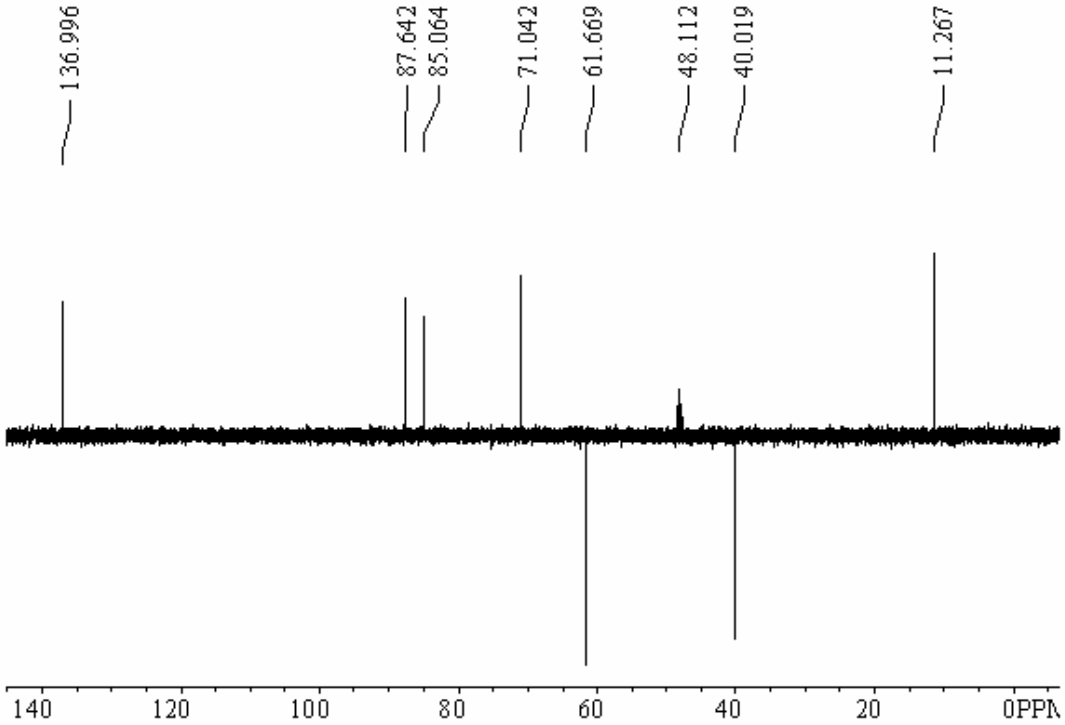

Figure 83. DEPT-135 spectrum of 5-methyl-2'-deoxycytidine (**25**) (125 MHz, MeOH-d_4).

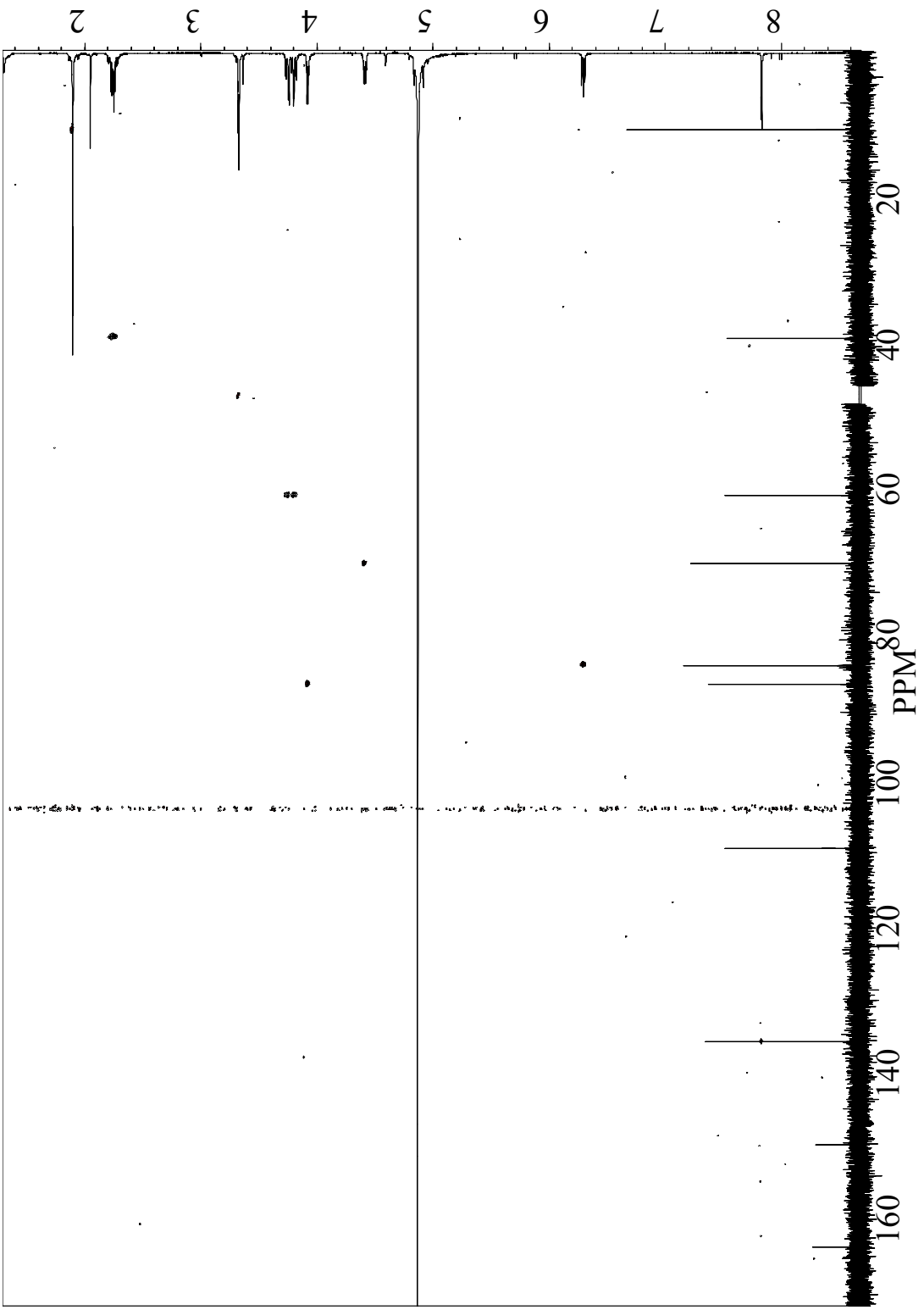

Figure 84. gHSQC spectrum of 5-methyl-2'-deoxycytidine (**25**) (500 MHz, MeOH-d_4).

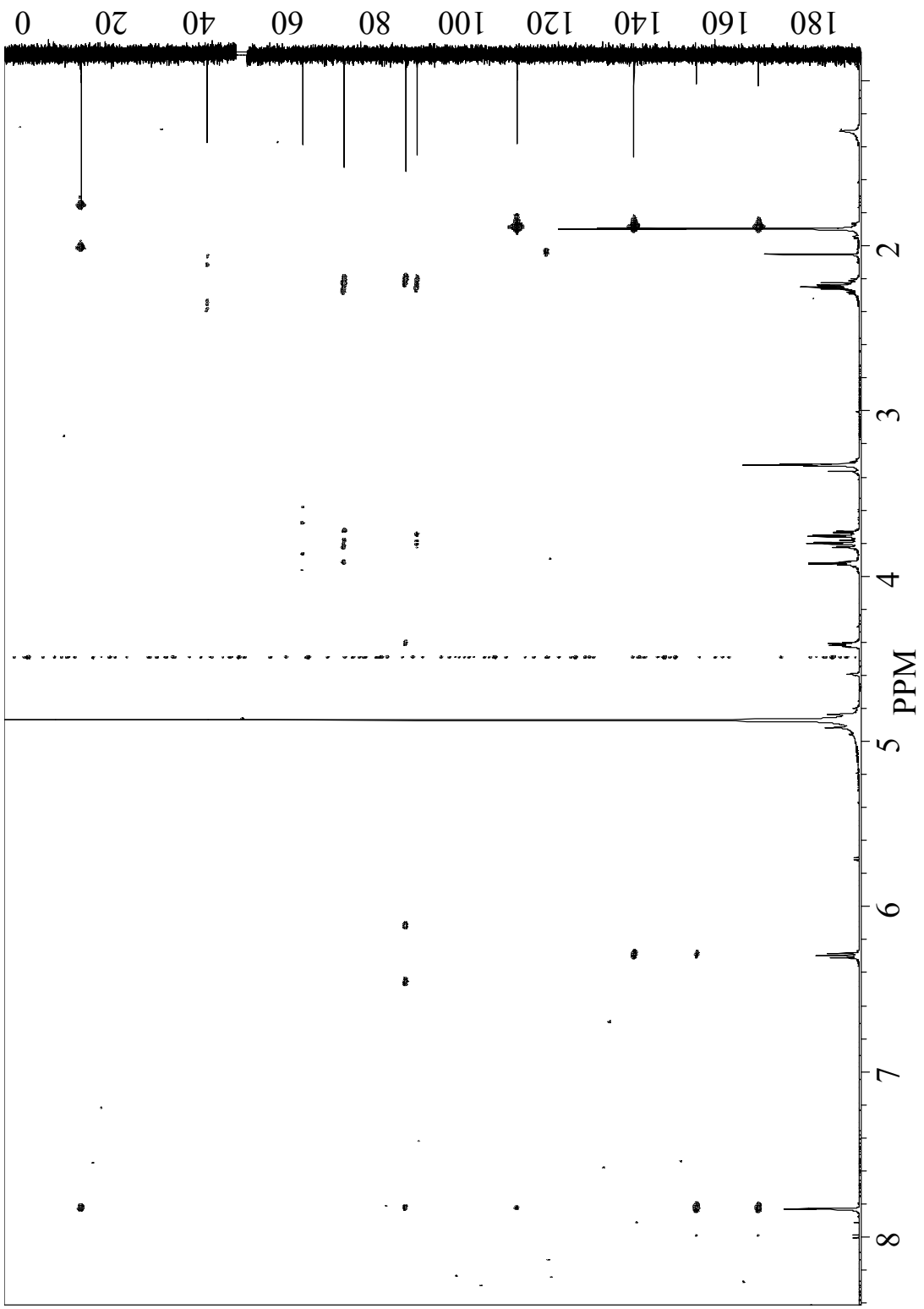

Figure 85. gHMBC spectrum of 5-methyl-2'-deoxycytidine (**25**) (500 MHz, MeOH-d_4).

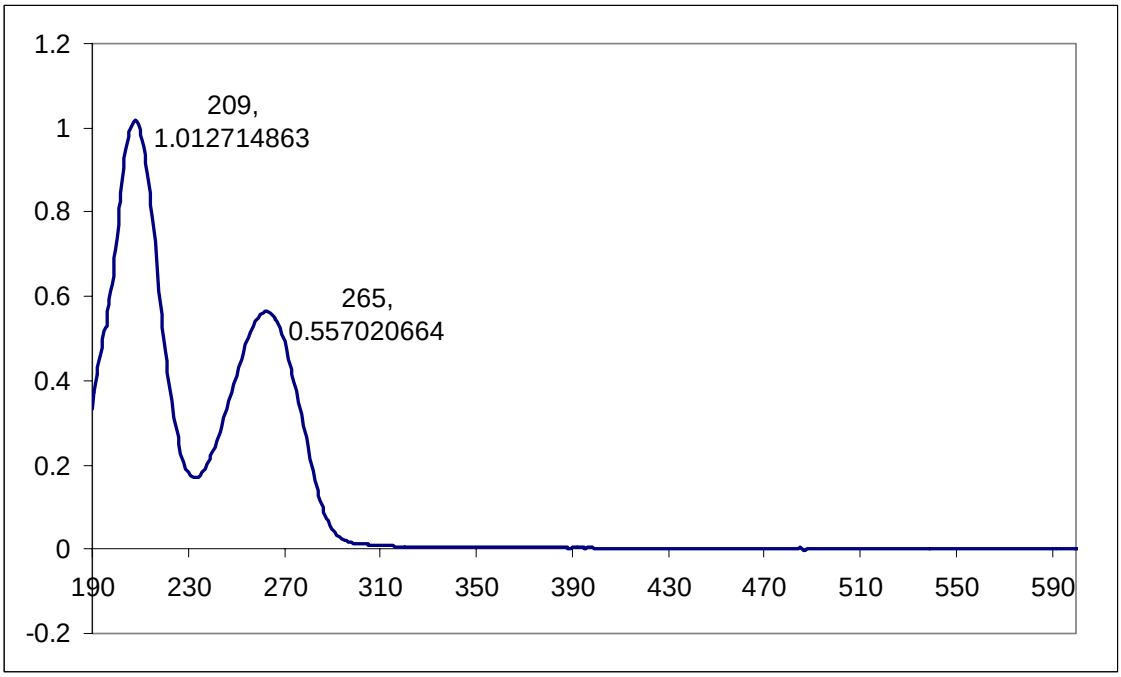

Figure 86. UV spectrum of uridine (**28**) in MeOH.

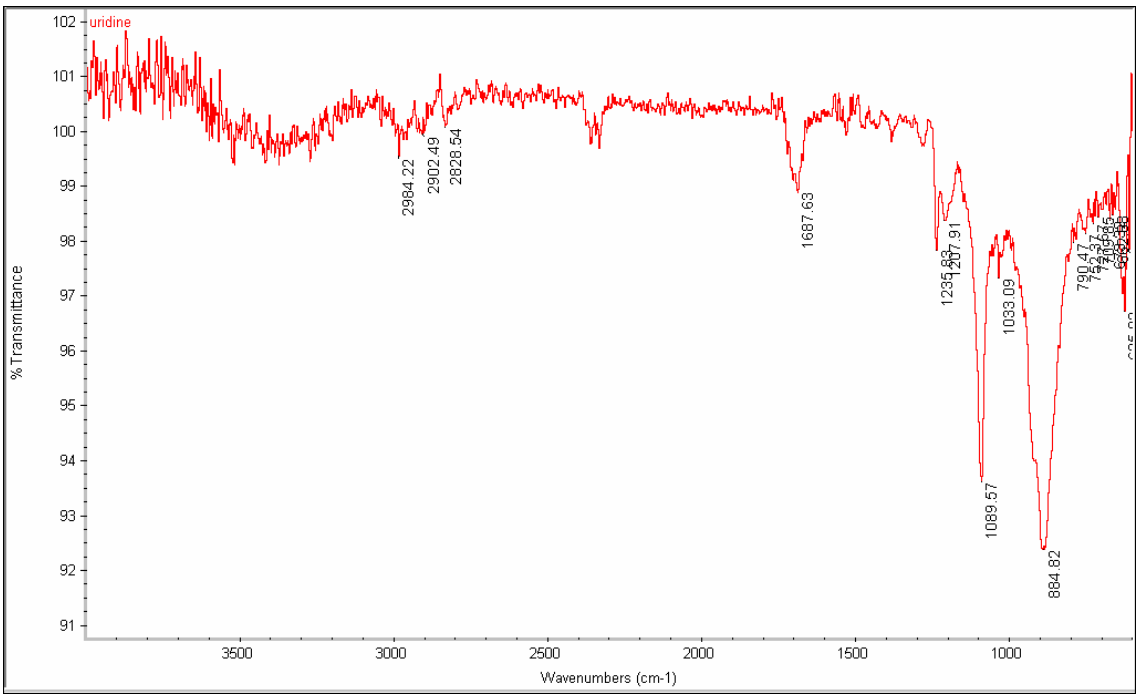

Figure 87. IR spectrum of uridine (**28**).

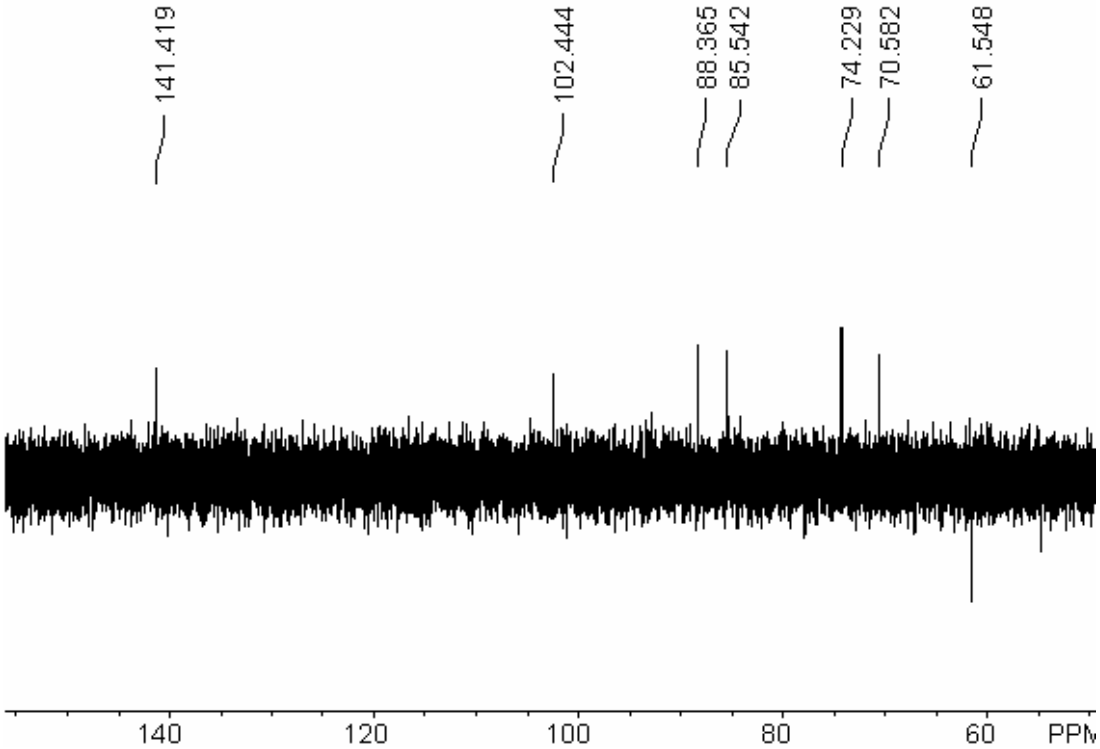

Figure 88. DEPT-135 spectrum of uridine (**28**) (125 MHz, DMSO-d_6).

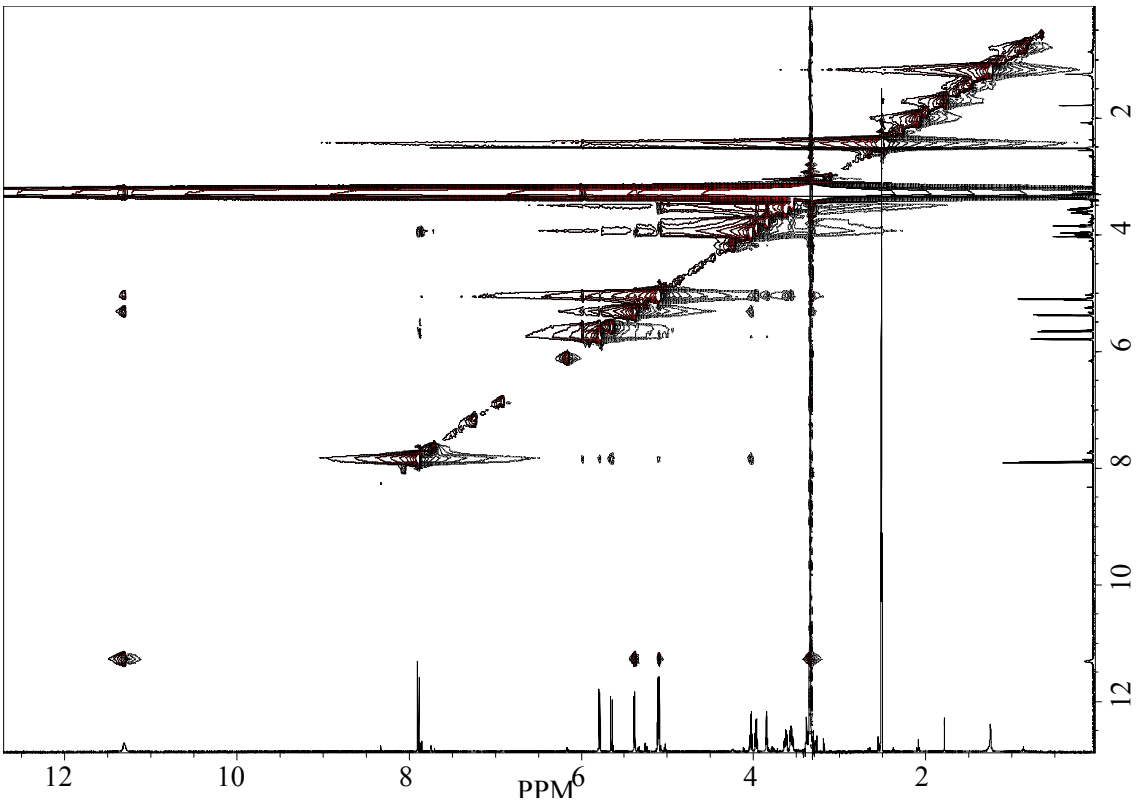

Figure 89. ROESY spectrum of uridine (**28**) (500 MHz, DMSO-d_6).

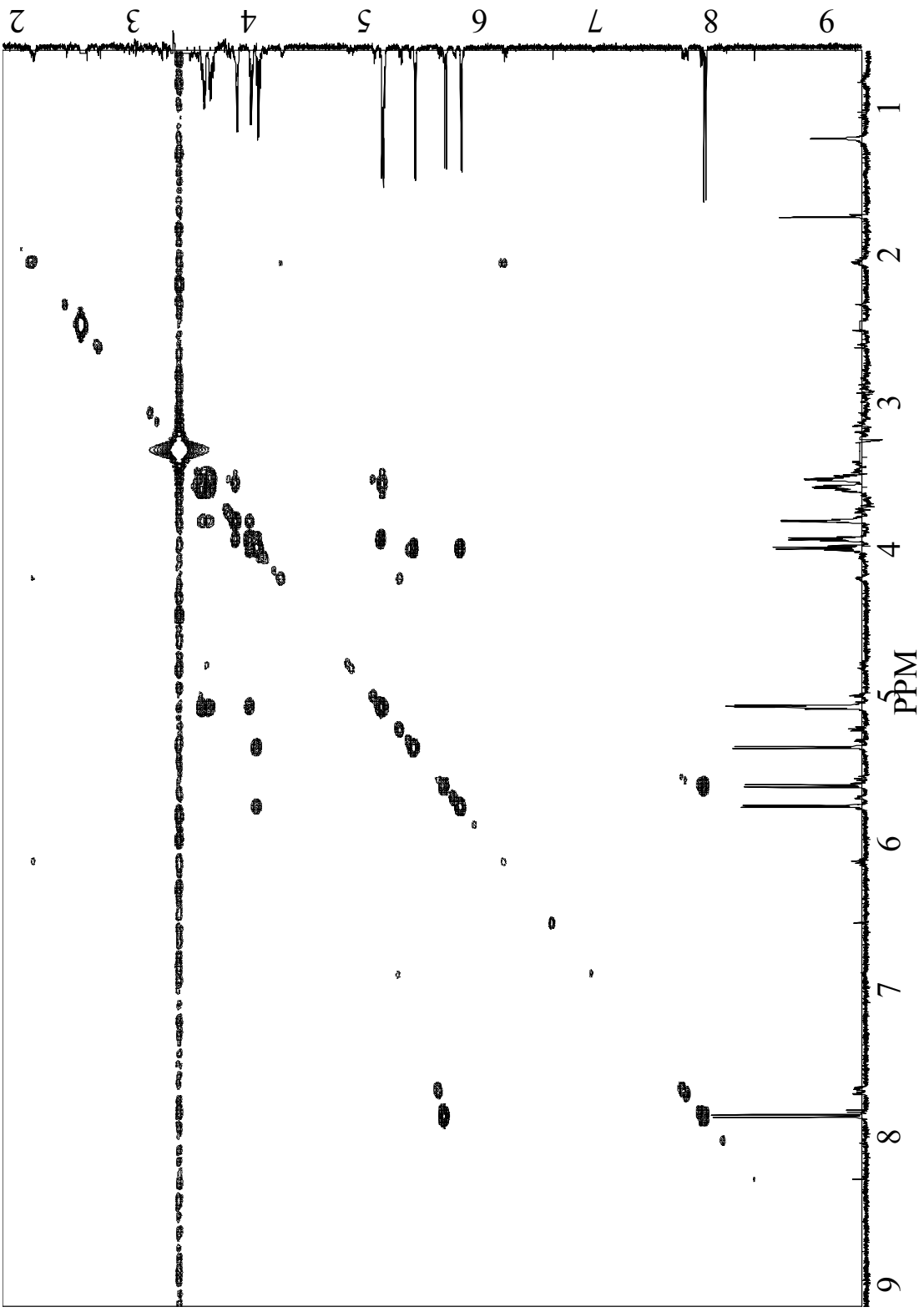

Figure 90. gCOSY spectrum of uridine (**28**) (500 MHz, DMSO-d_6).

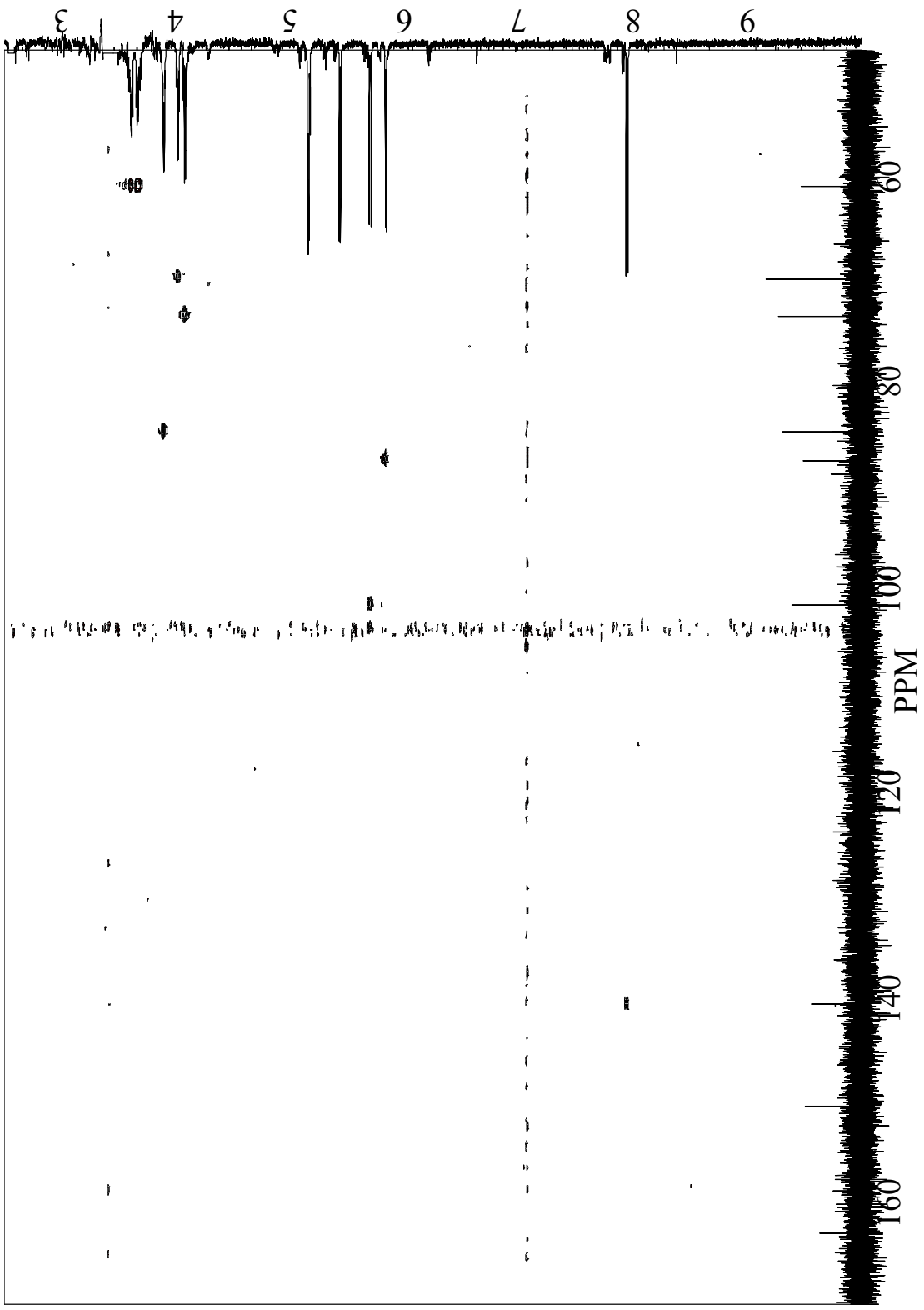

Figure 91. gHSQC spectrum of uridine (**28**) (500 MHz, DMSO-d_6).

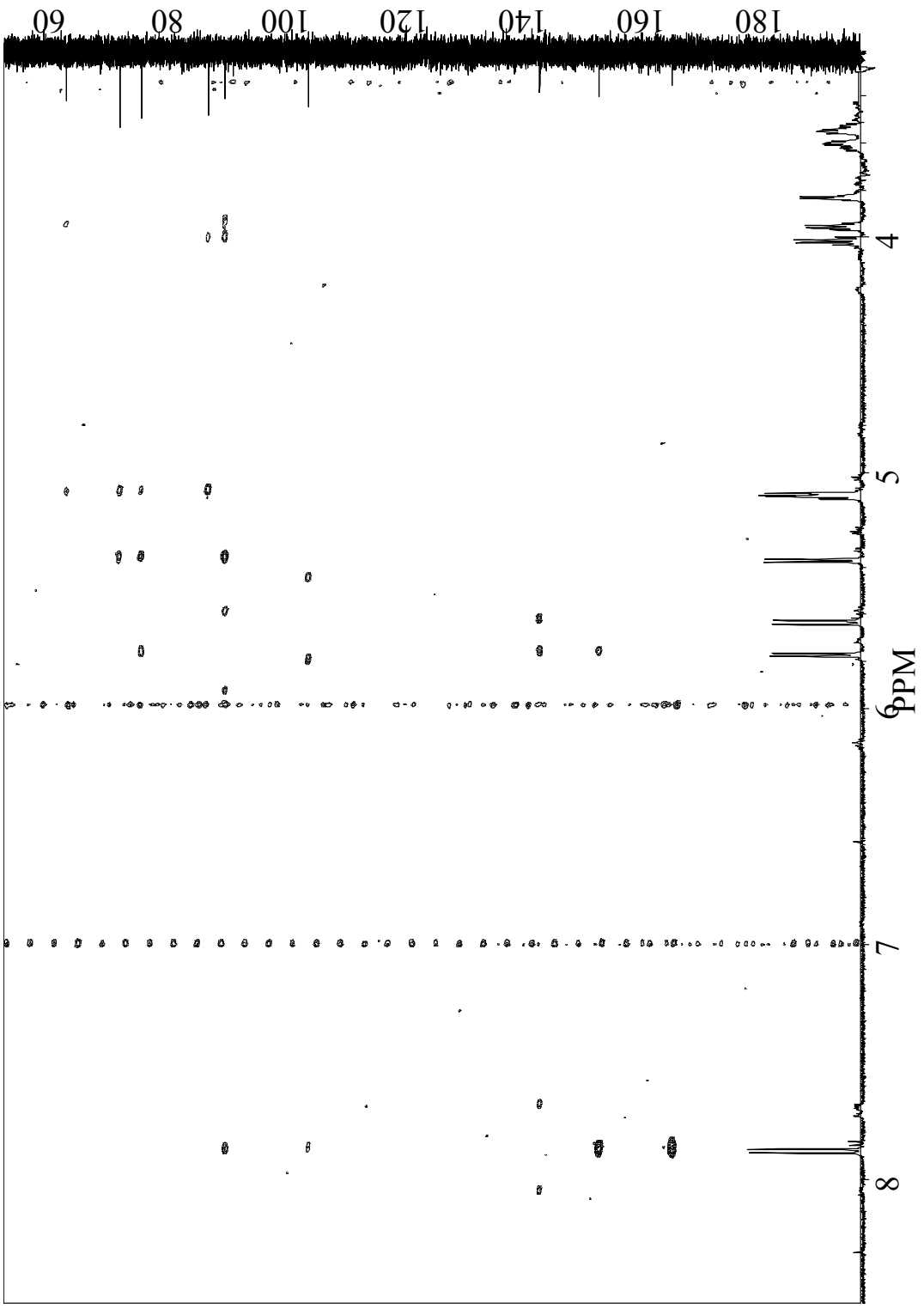

Figure 92. gHMBC spectrum of uridine (**28**) (500 MHz, DMSO-d_6).

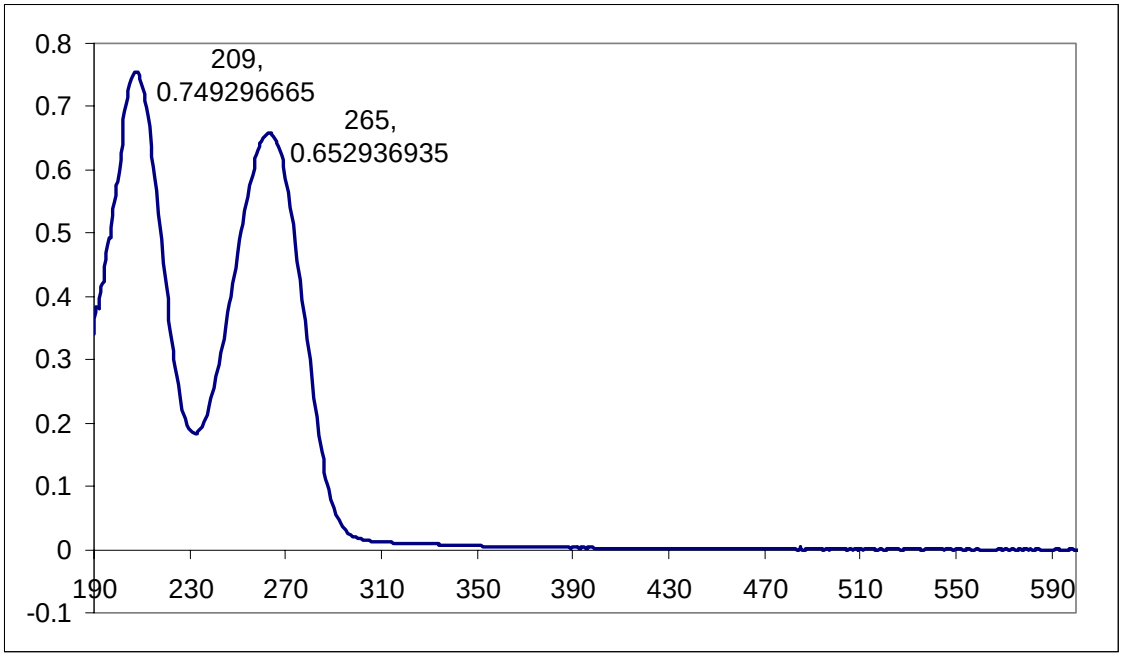

Figure 93. UV spectrum of 2-deoxycytidine (**31**) in MeOH.

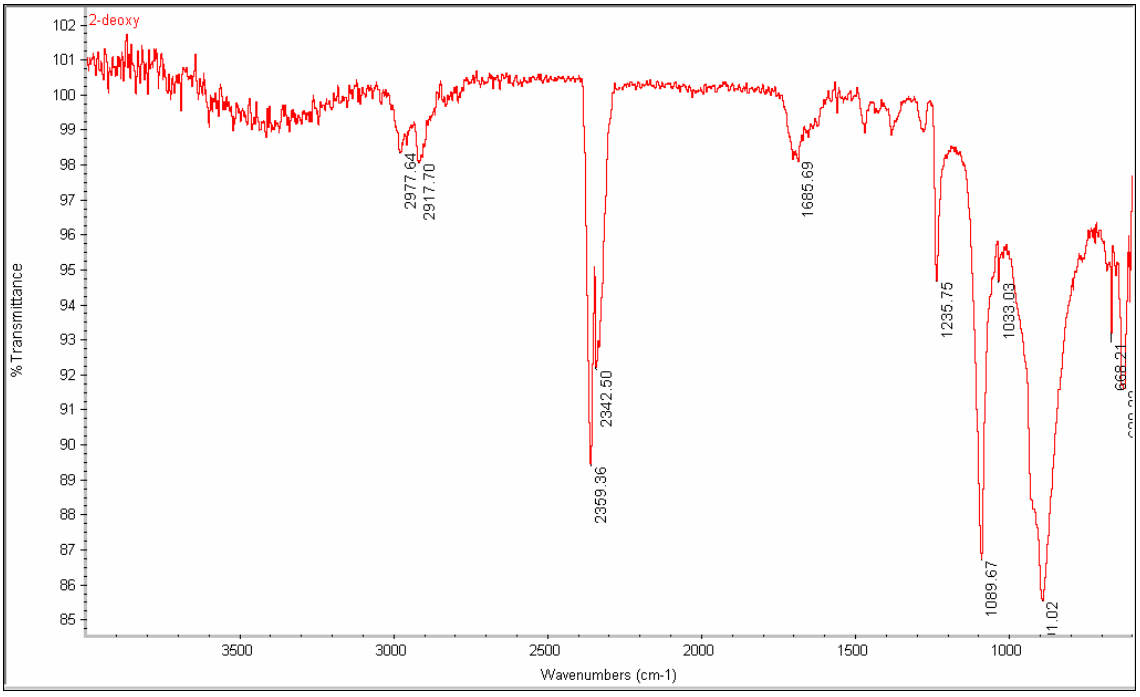

Figure 94. IR spectrum of 2-deoxycytidine (**31**).

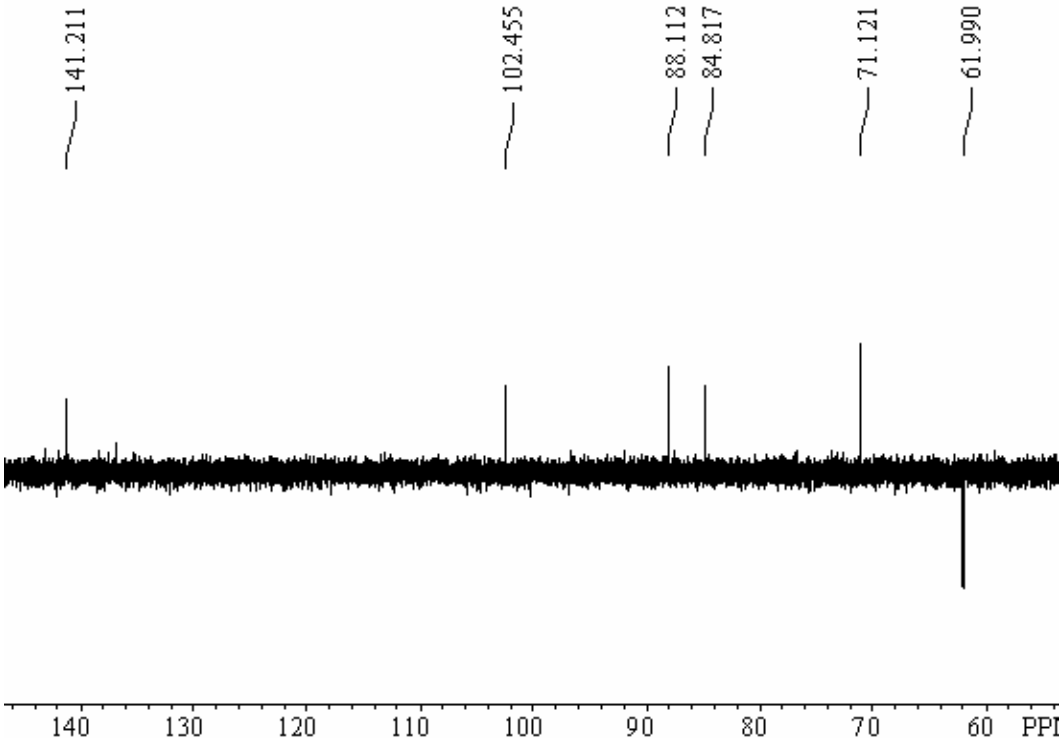

Figure 95. DEPT-135 spectrum of 2-deoxycytidine (**31**) (125 MHz, DMSO-d_6).

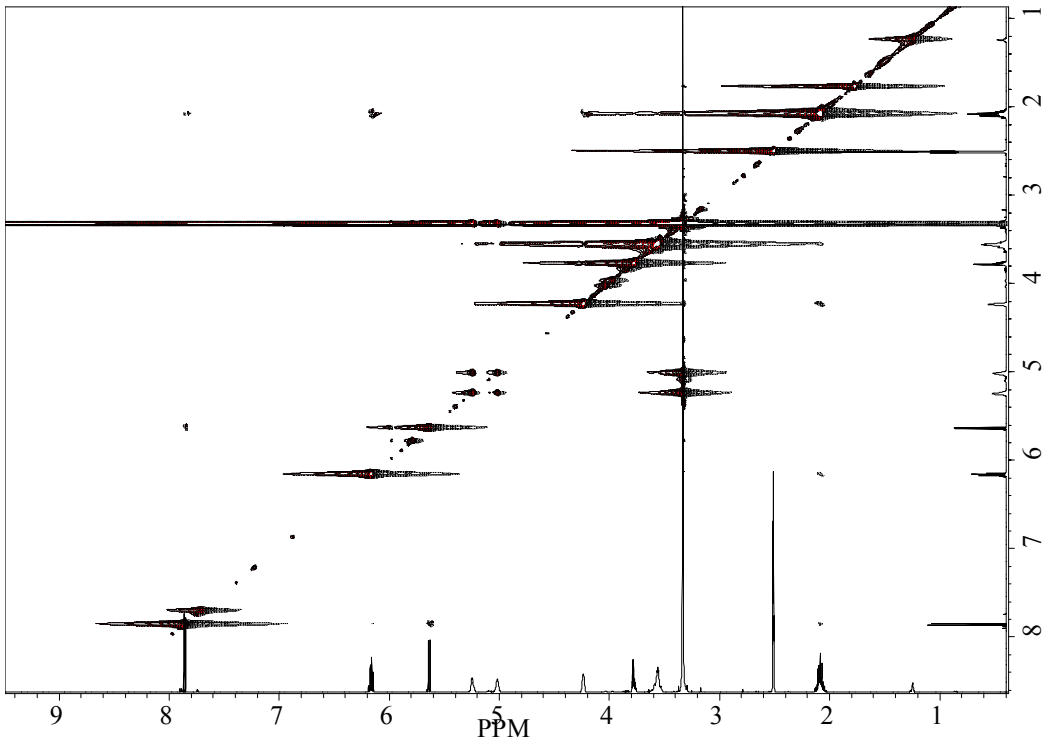

Figure 96. ROESY spectrum of 2-deoxycytidine (**31**) (500 MHz, DMSO-d_6).

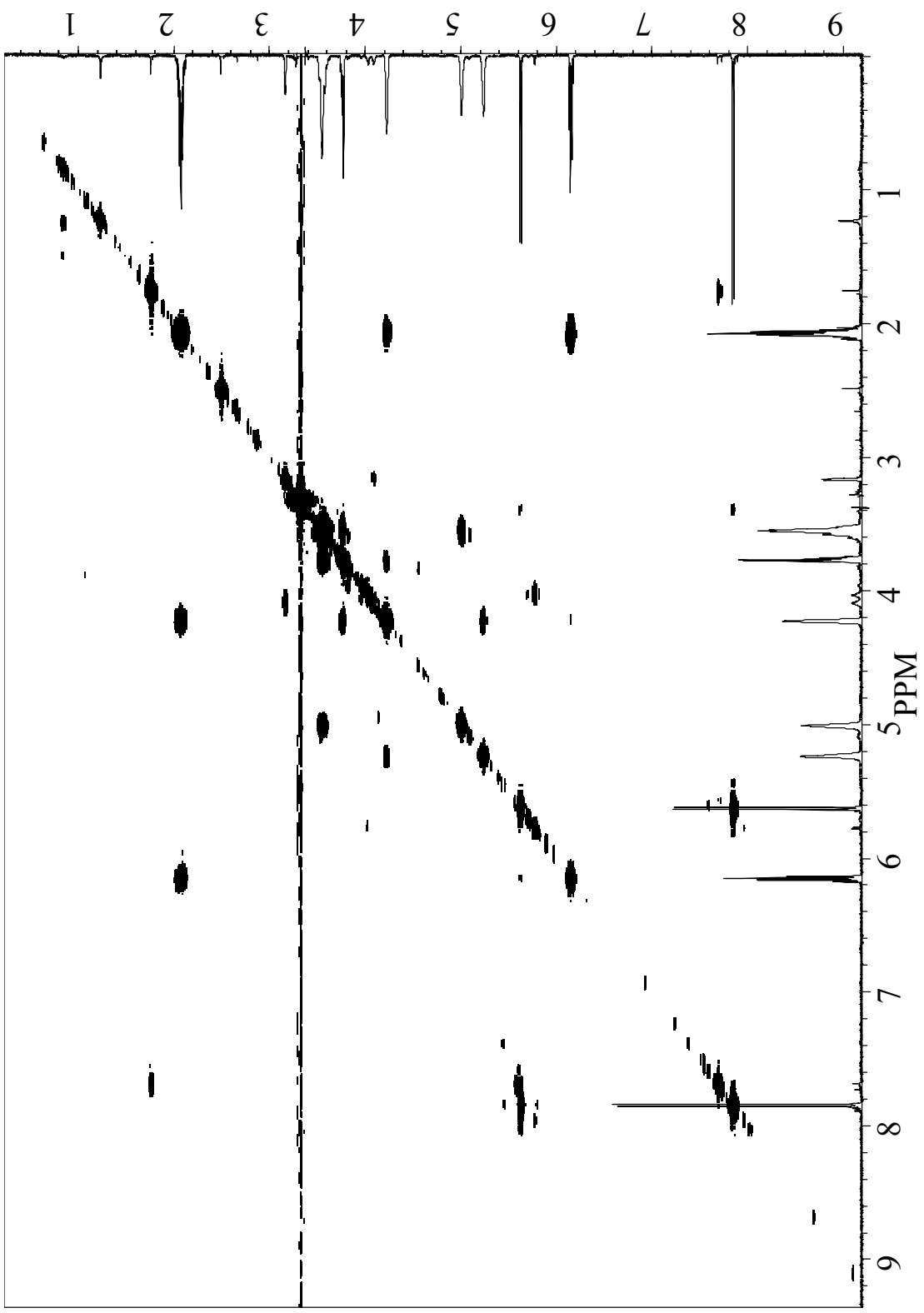

Figure 97. gCOSY spectrum of 2-deoxycytidine (**31**) (500 MHz, DMSO-d_6).

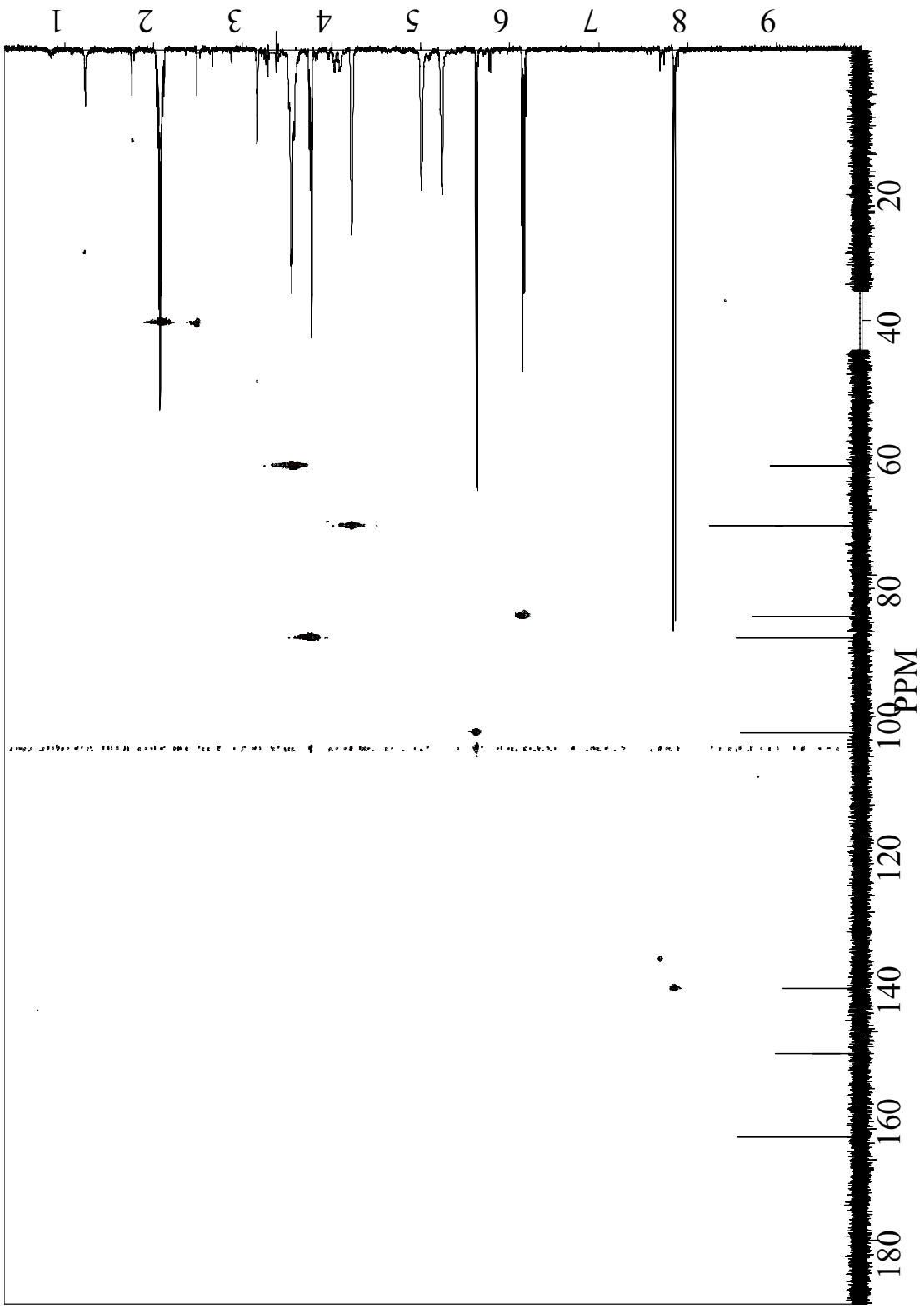

Figure 98. gHSQC spectrum of 2-deoxycytidine (**31**) (500 MHz, DMSO-d_6).

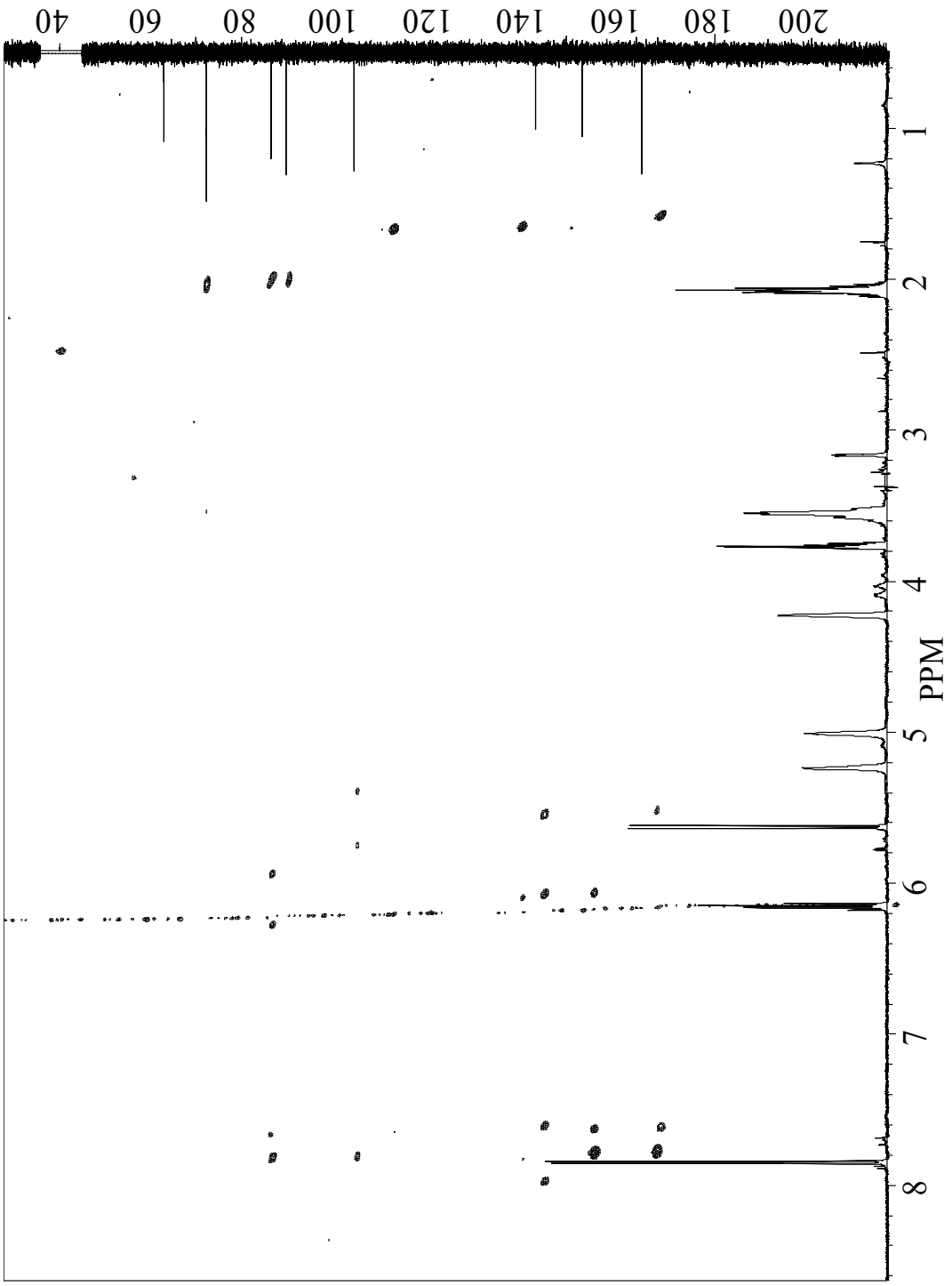

Figure 99. gHMBC spectrum of 2-deoxycytidine (**31**) (500 MHz, DMSO-d_6).

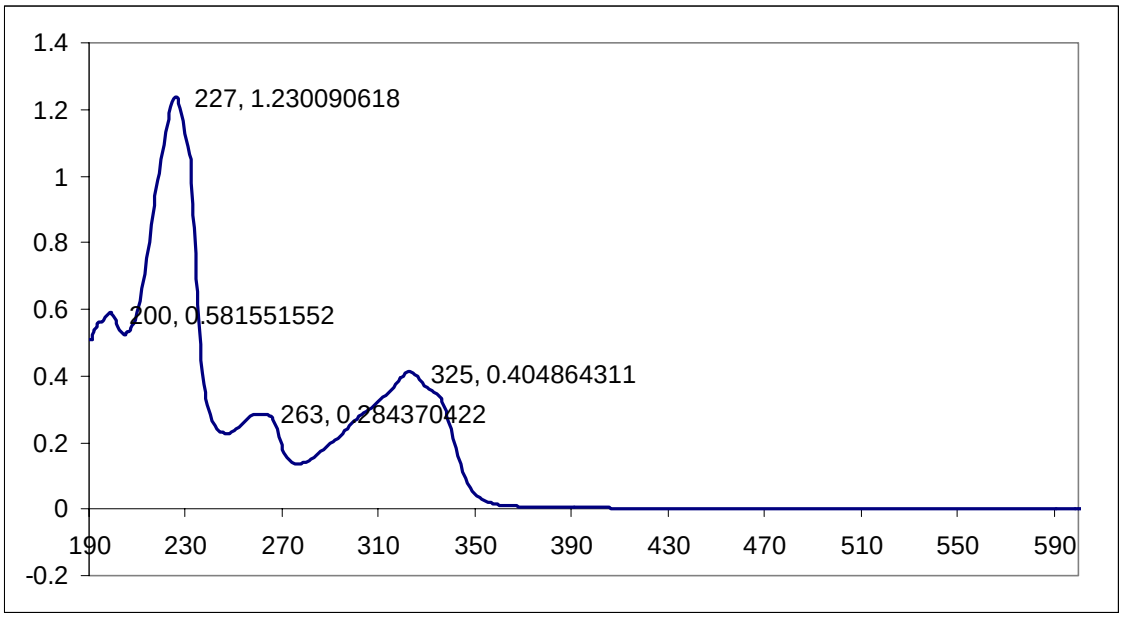

Figure 100. UV spectrum of 4, 8-dihydroxyquinoline (**33**) in MeOH.

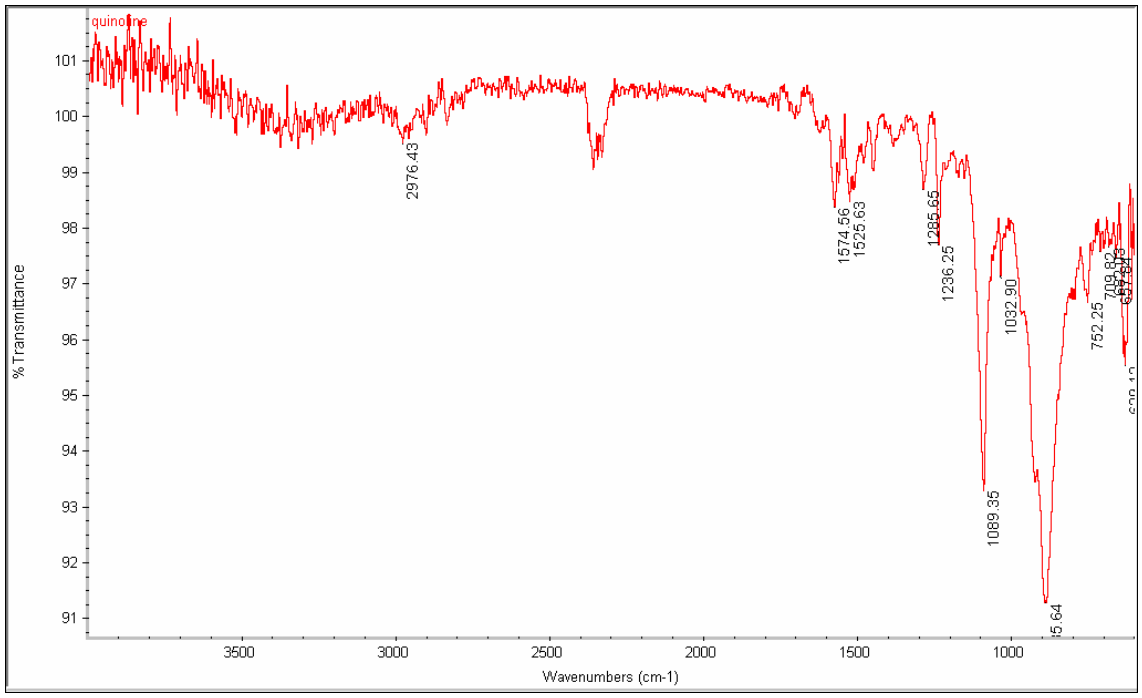

Figure 101. IR spectrum of 4, 8-dihydroxyquinoline (**33**).

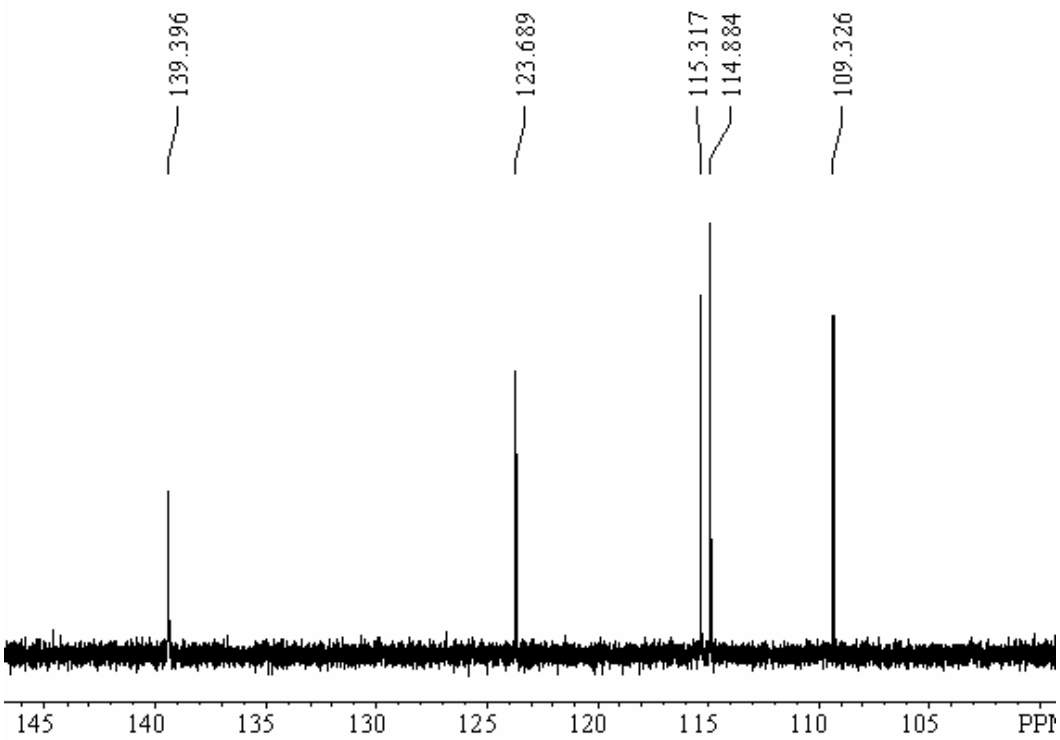

Figure 102. DEPT-135 spectrum of 4, 8-dihydroxyquinoline (**33**) (125 MHz, DMSO-d_6).

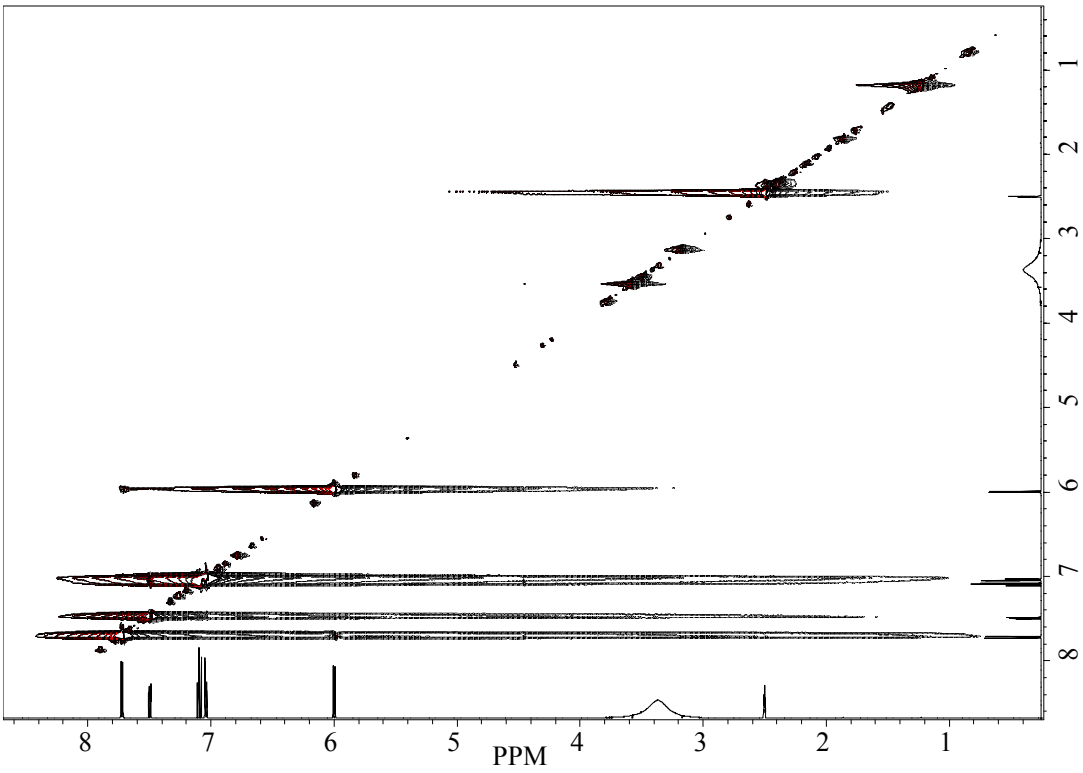

Figure 103. ROESY spectrum of 4, 8-dihydroxyquinoline (**33**) (500 MHz, DMSO-d_6).

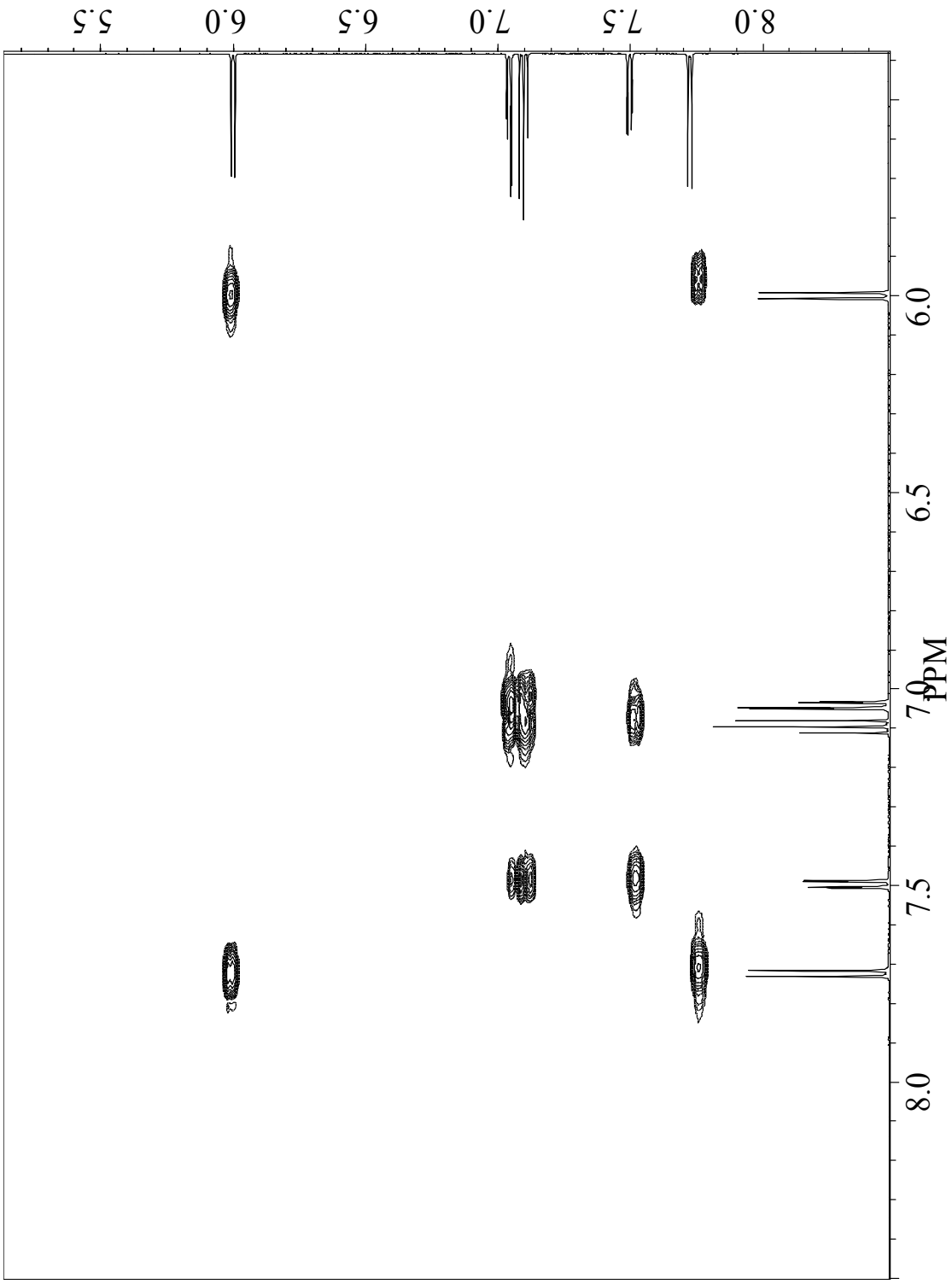

Figure 104. gCOSY spectrum of 4, 8-dihydroxyquinoline (**33**) (500 MHz, DMSO-d_6).

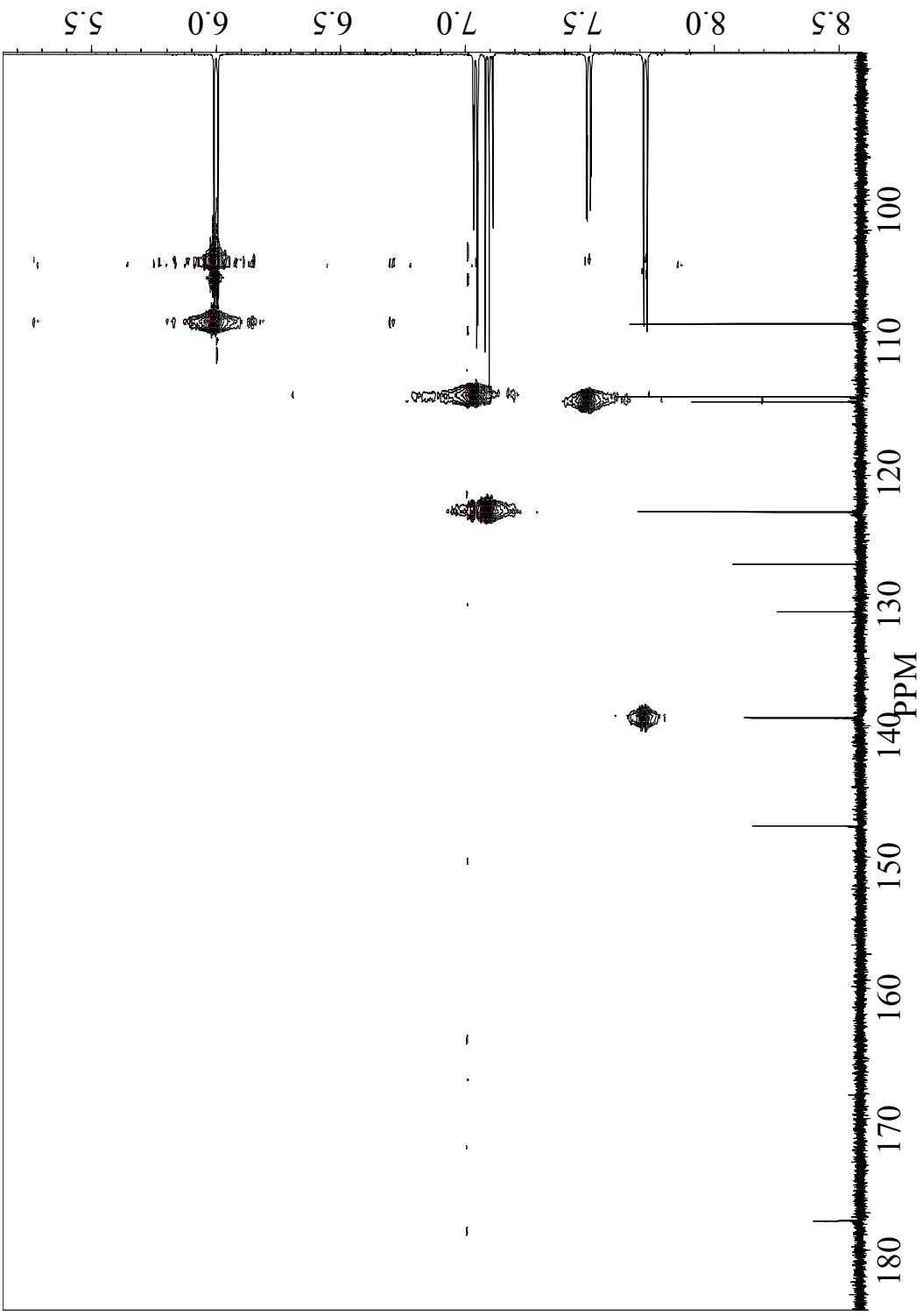

Figure 105. gHSQC spectrum of 4, 8-dihydroxyquinoline (**33**) (500 MHz, DMSO-d_6).

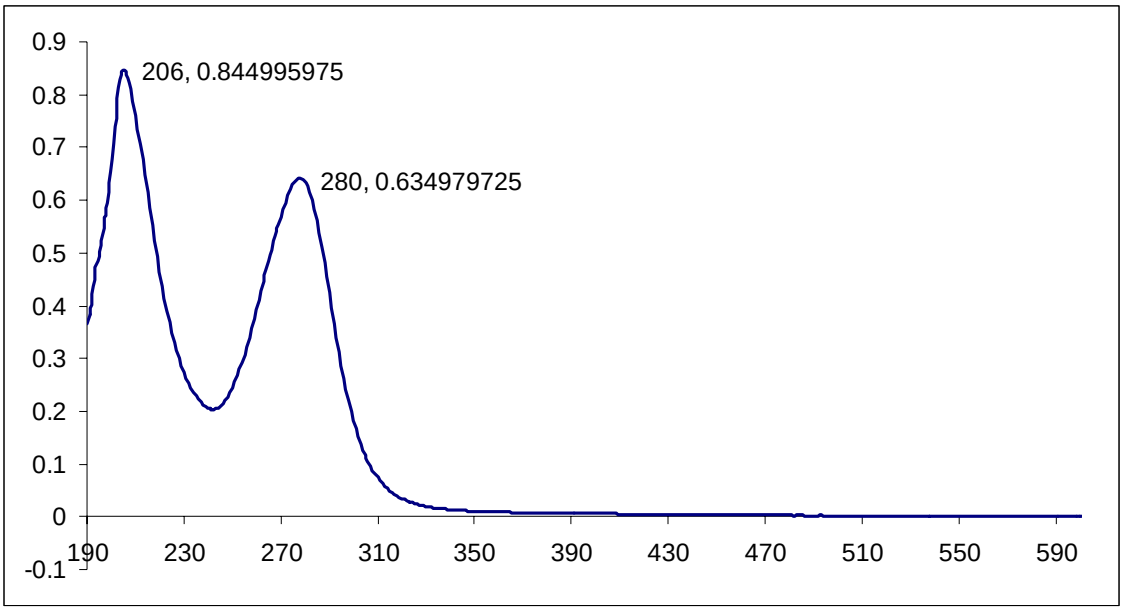

Figure 106. UV spectrum of homarine (**37**) in MeOH.

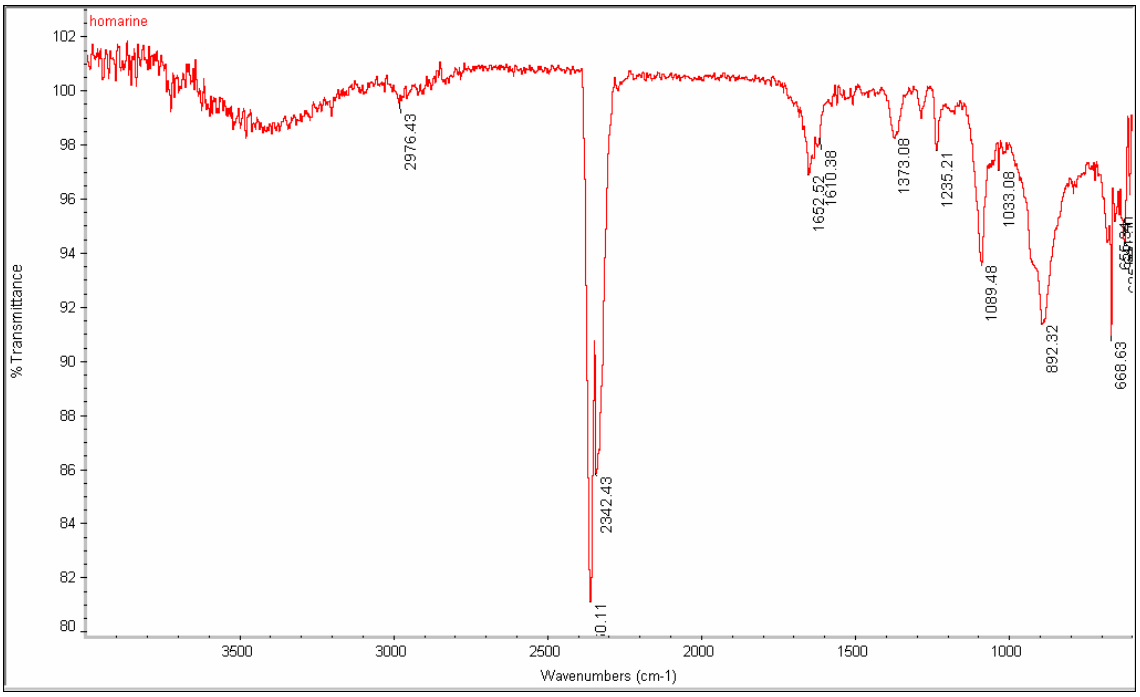

Figure 107. IR spectrum of homarine (**37**).

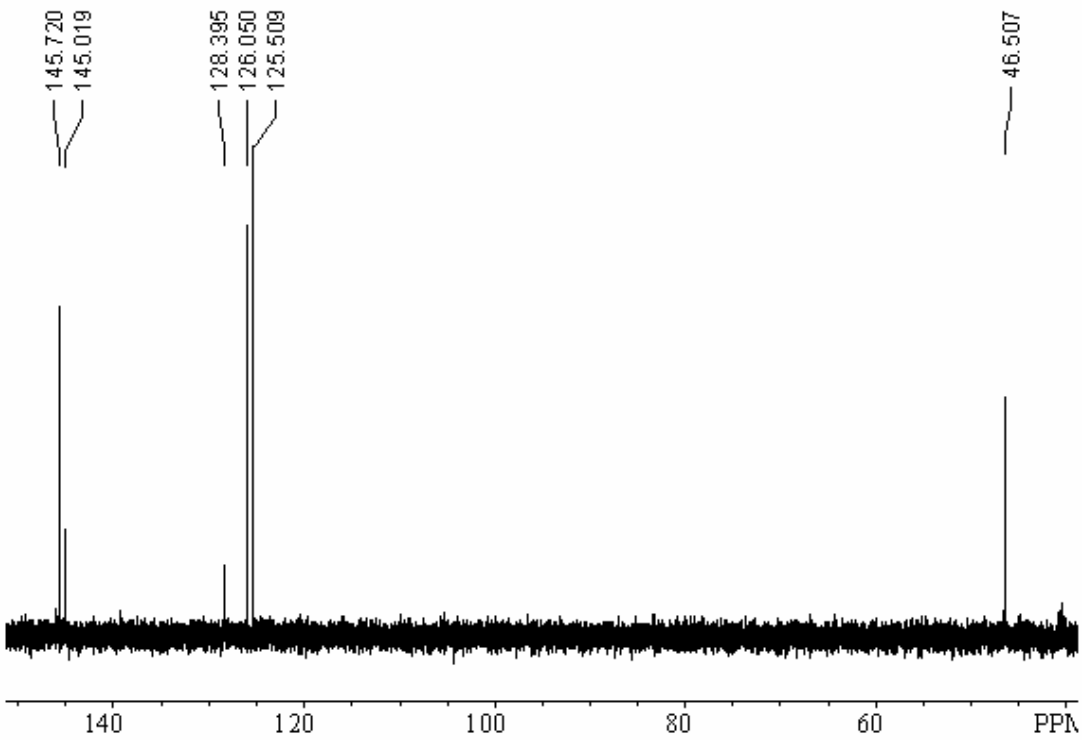

Figure 108. DEPT-135 spectrum of homarine (**37**) (125 MHz, DMSO-d_6).

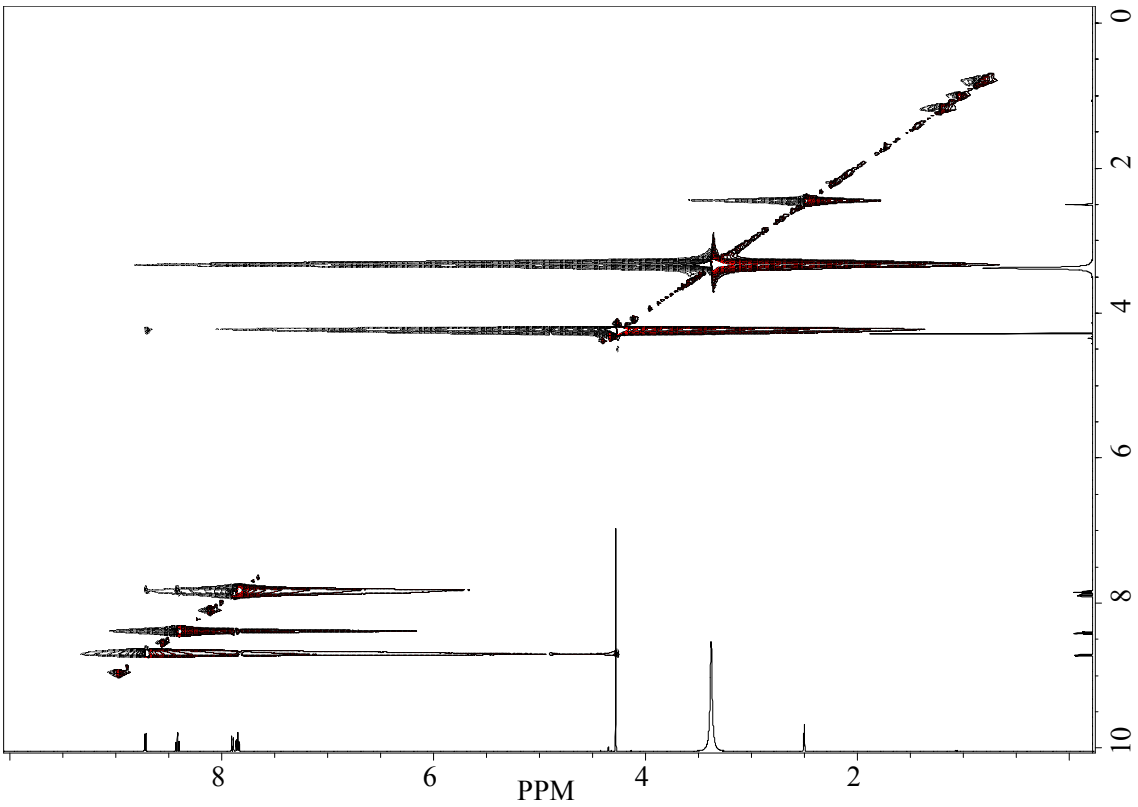

Figure 109. ROESY spectrum of homarine (**37**) (500 MHz, DMSO-d_6).

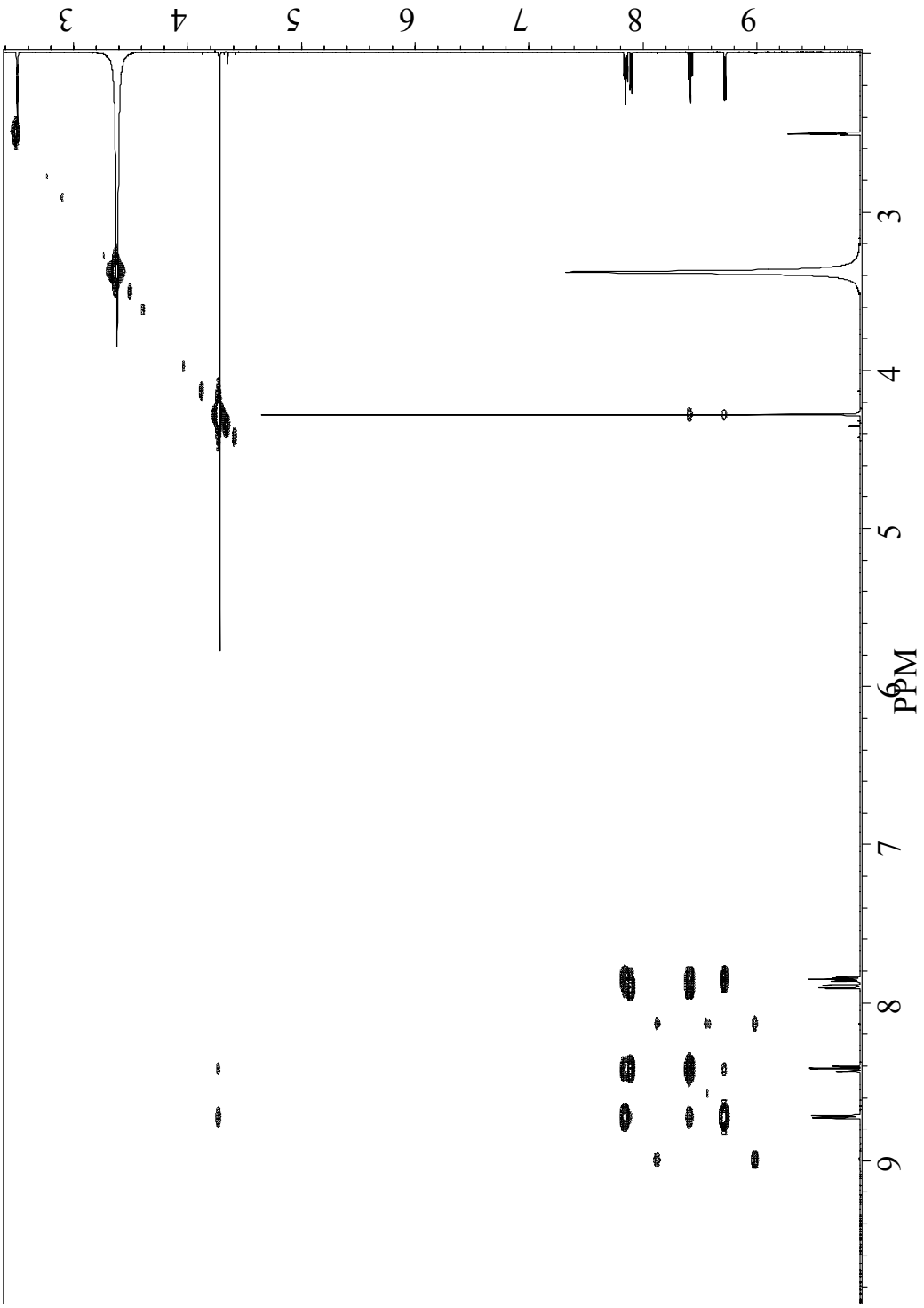

Figure 110. gCOSY spectrum of homarine (**37**) (500 MHz, DMSO-d_6).

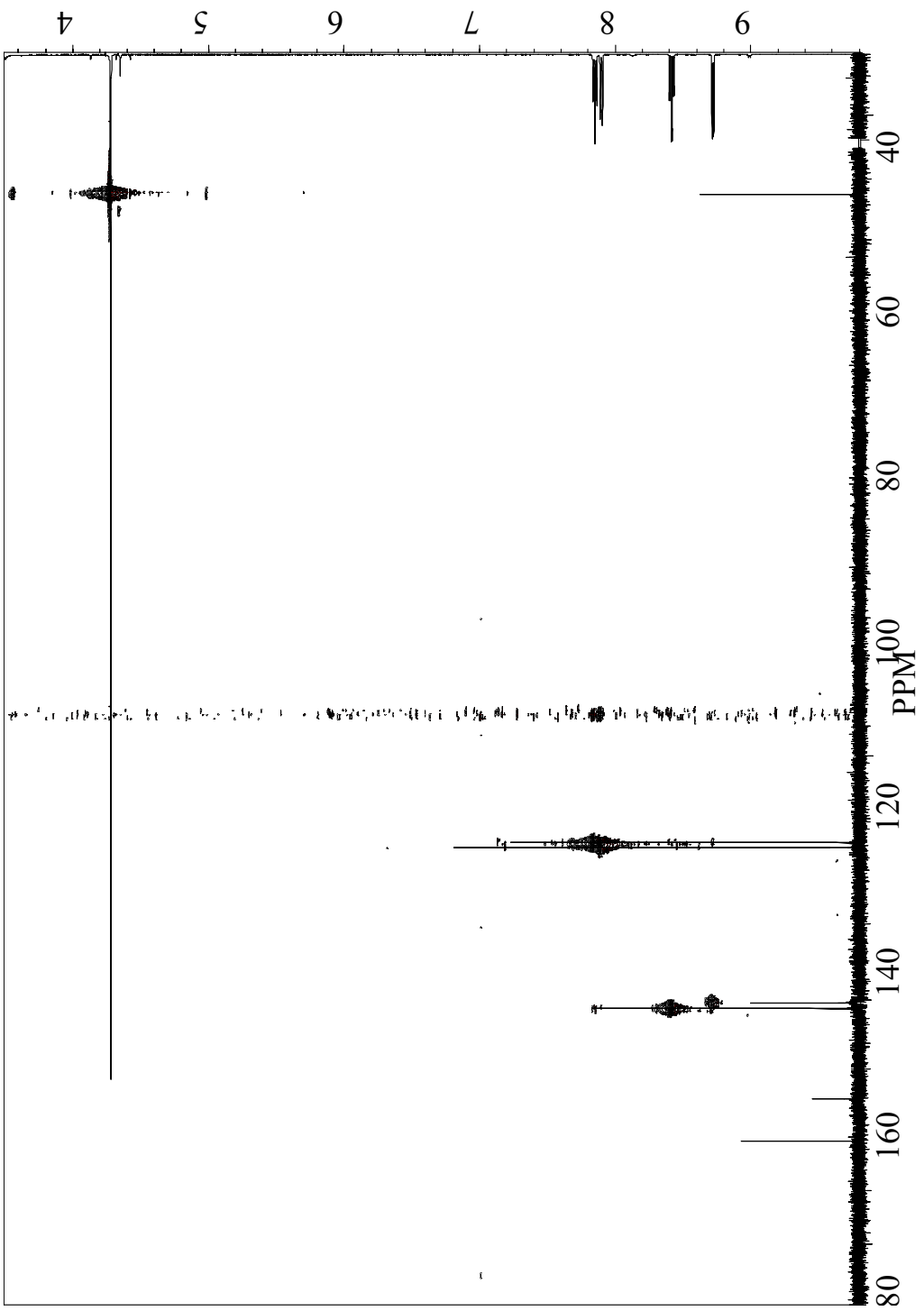

Figure 111. gHSQC spectrum of homarine (**37**) (500 MHz, DMSO-d_6).

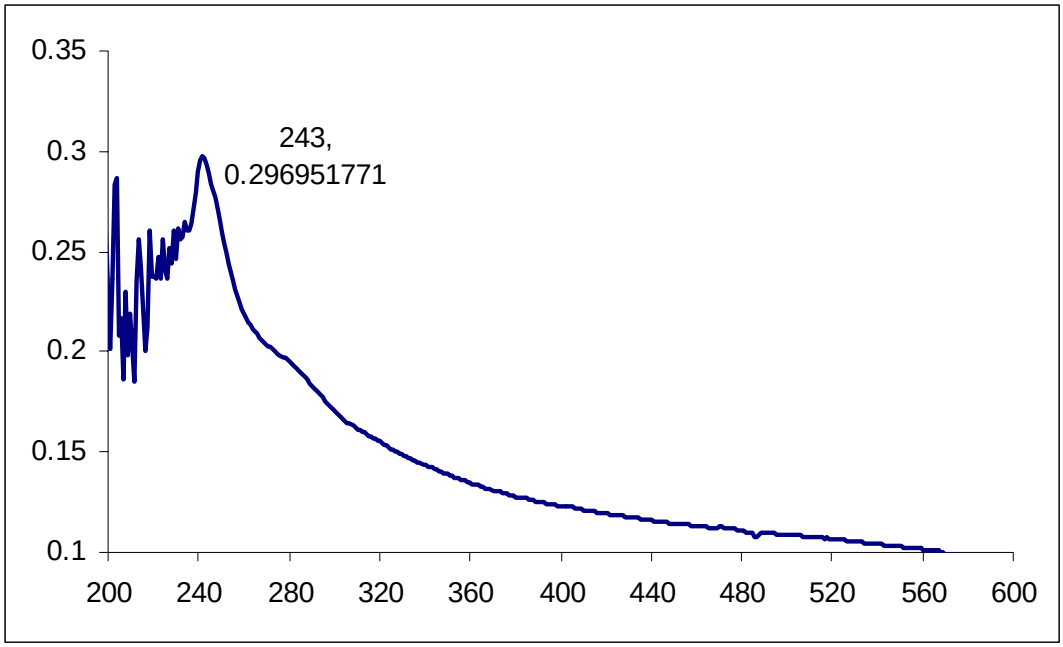

Figure 112. UV spectrum of ceramide analog (**39**) in $CHCl_3$.

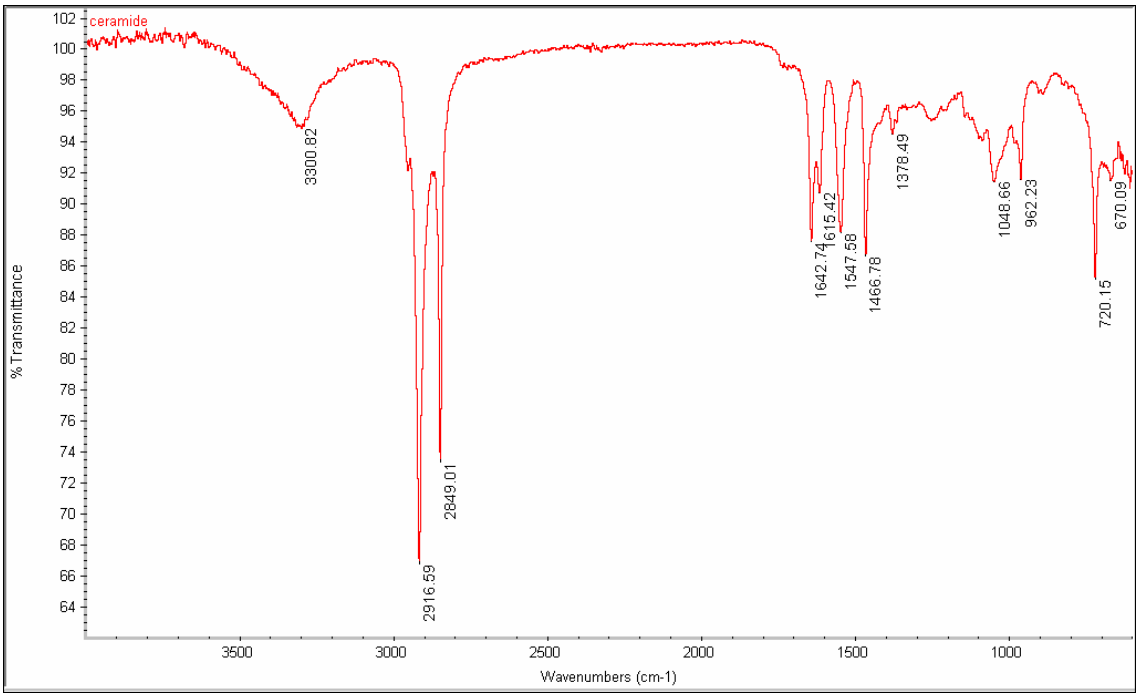

Figure 113. IR spectrum of ceramide analog (**39**).

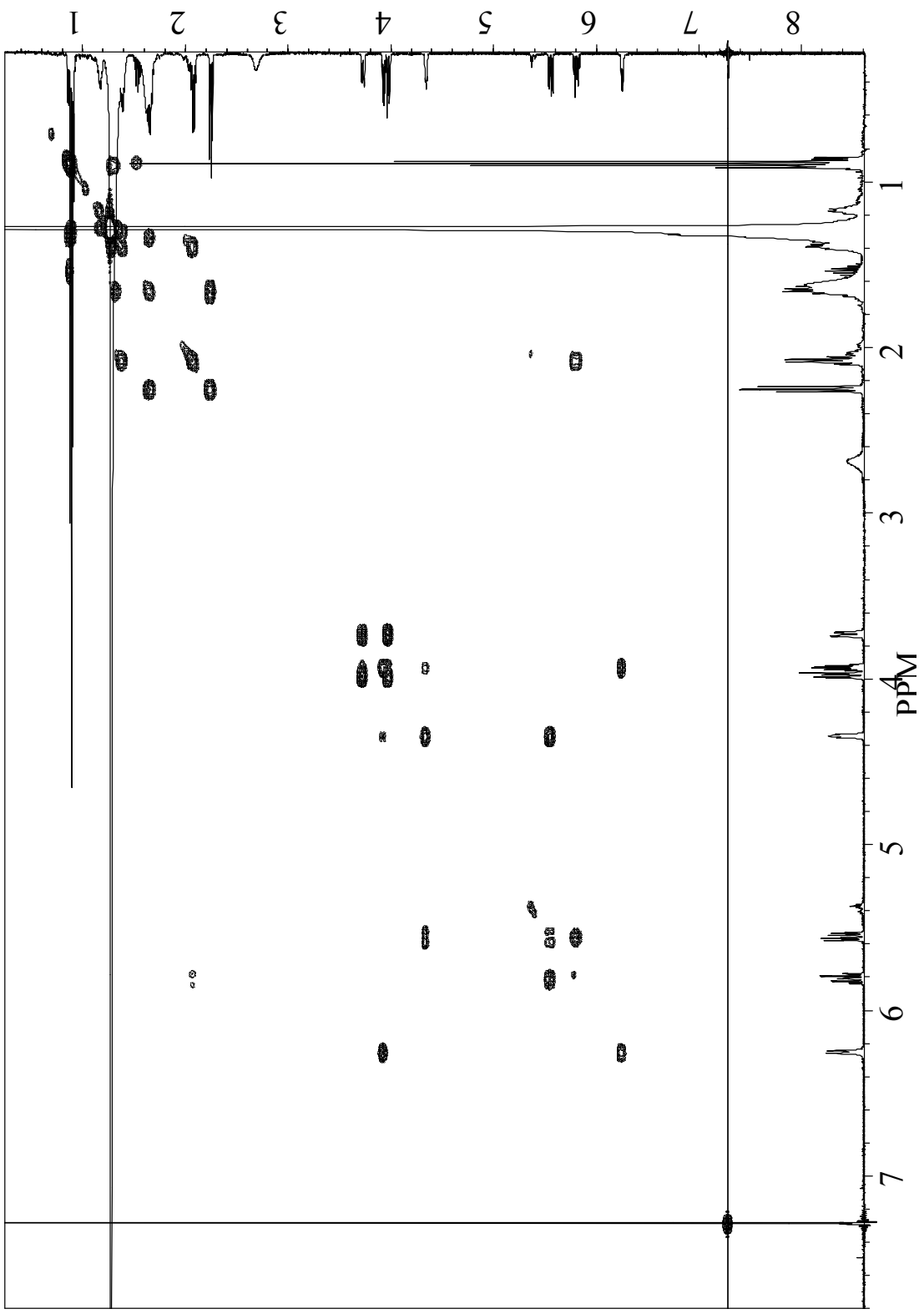

Figure 114. gCOSY spectrum of ceramide analog (**39**) (500 MHz, $CDCl_3$).

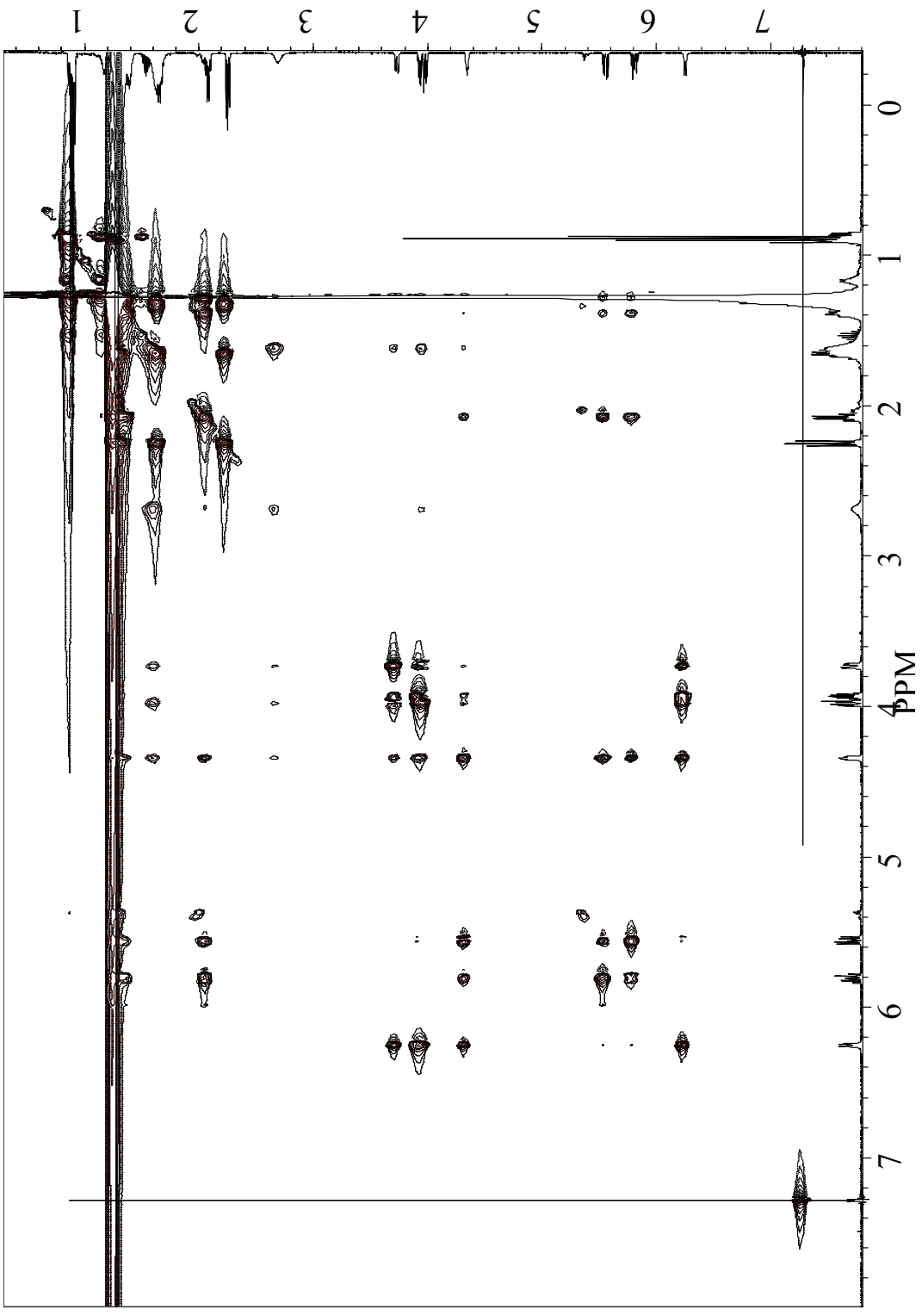

Figure 115. TOCSY spectrum of ceramide (**39**) (500 MHz, $CDCl_3$).

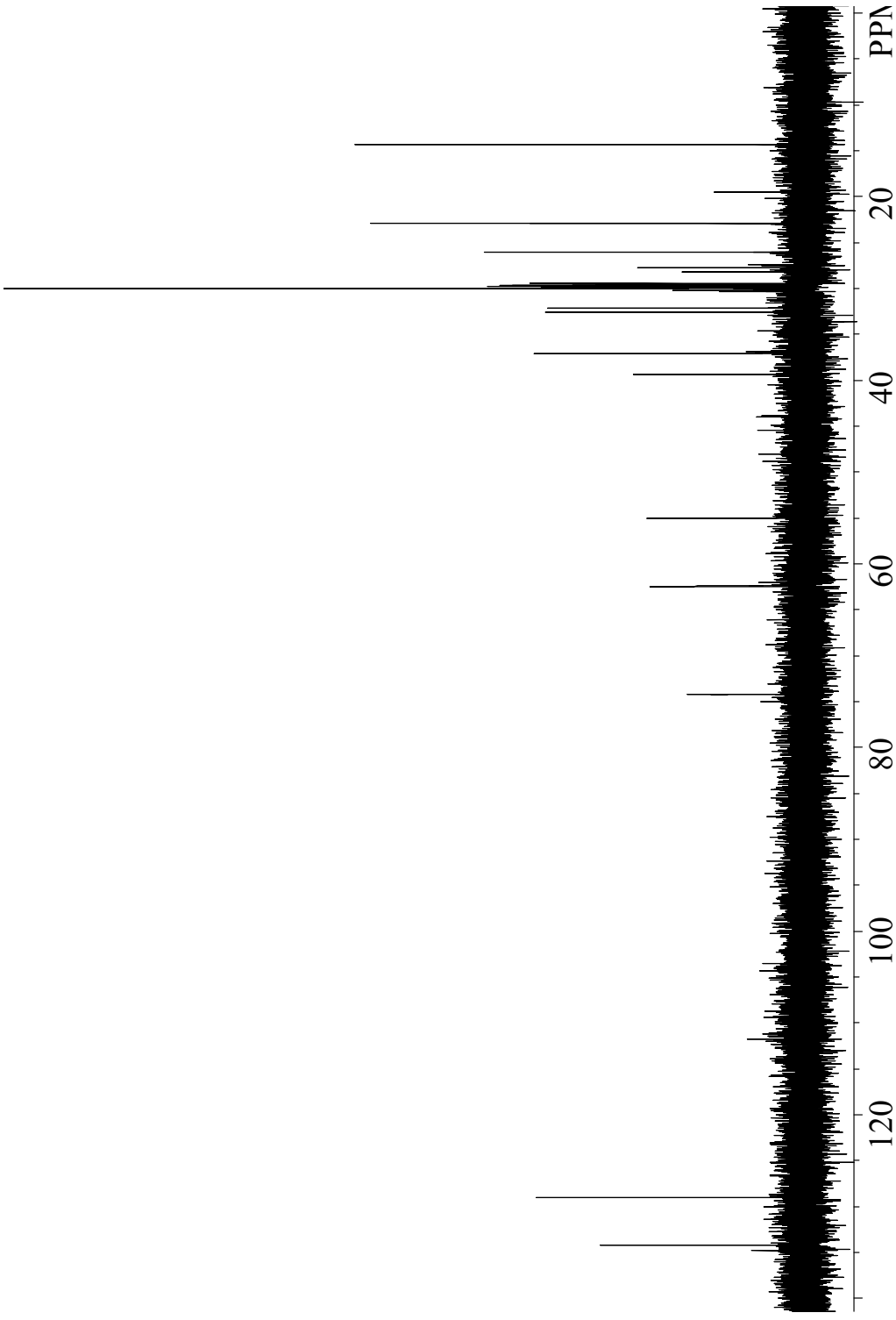

Figure 116. DEPT-45 spectrum of ceramide analog (**39**) (125 MHz, $CDCl_3$).

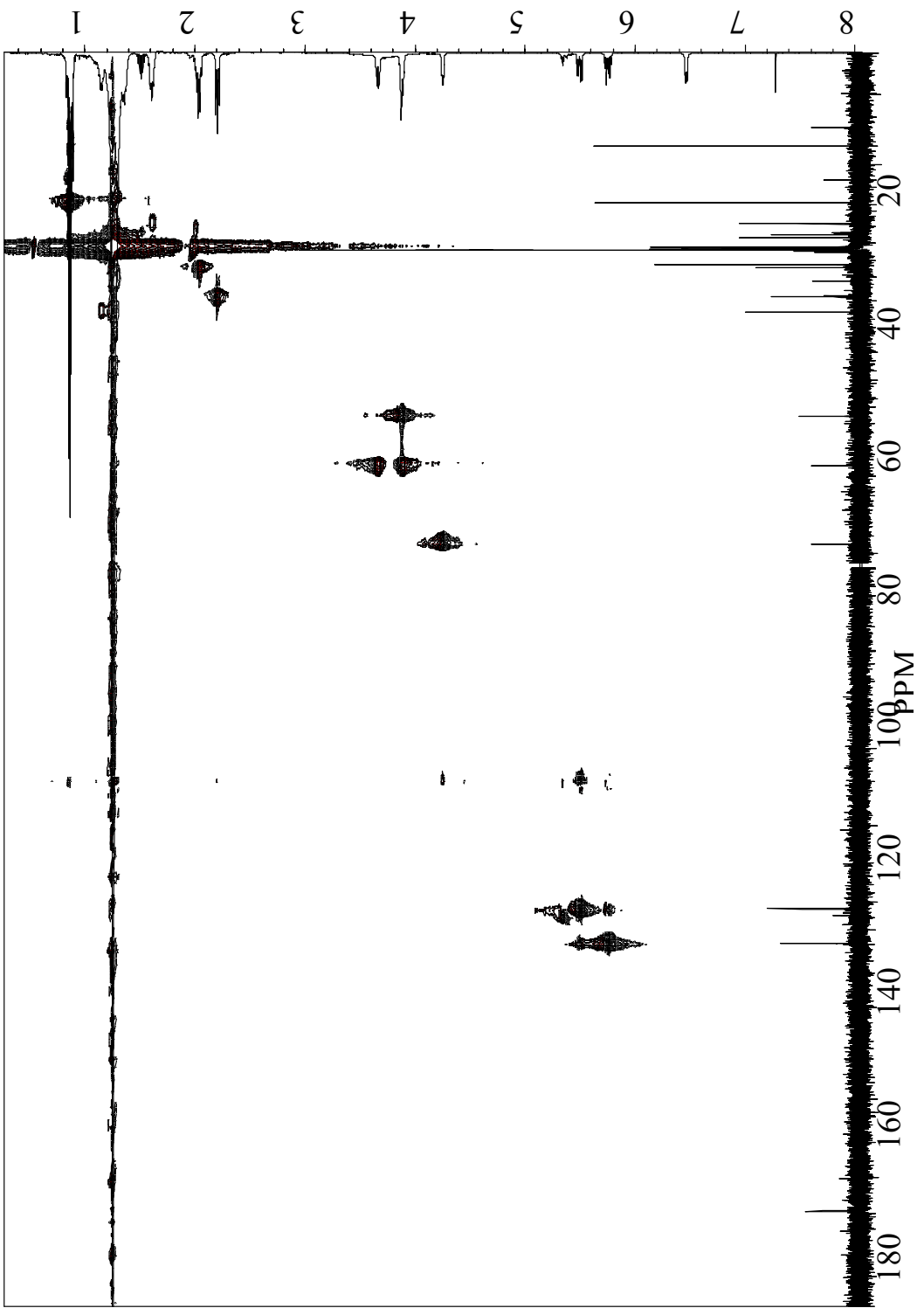

Figure 117. gHSQC spectrum of ceramide analog (**39**) (500 MHz, $CDCl_3$).

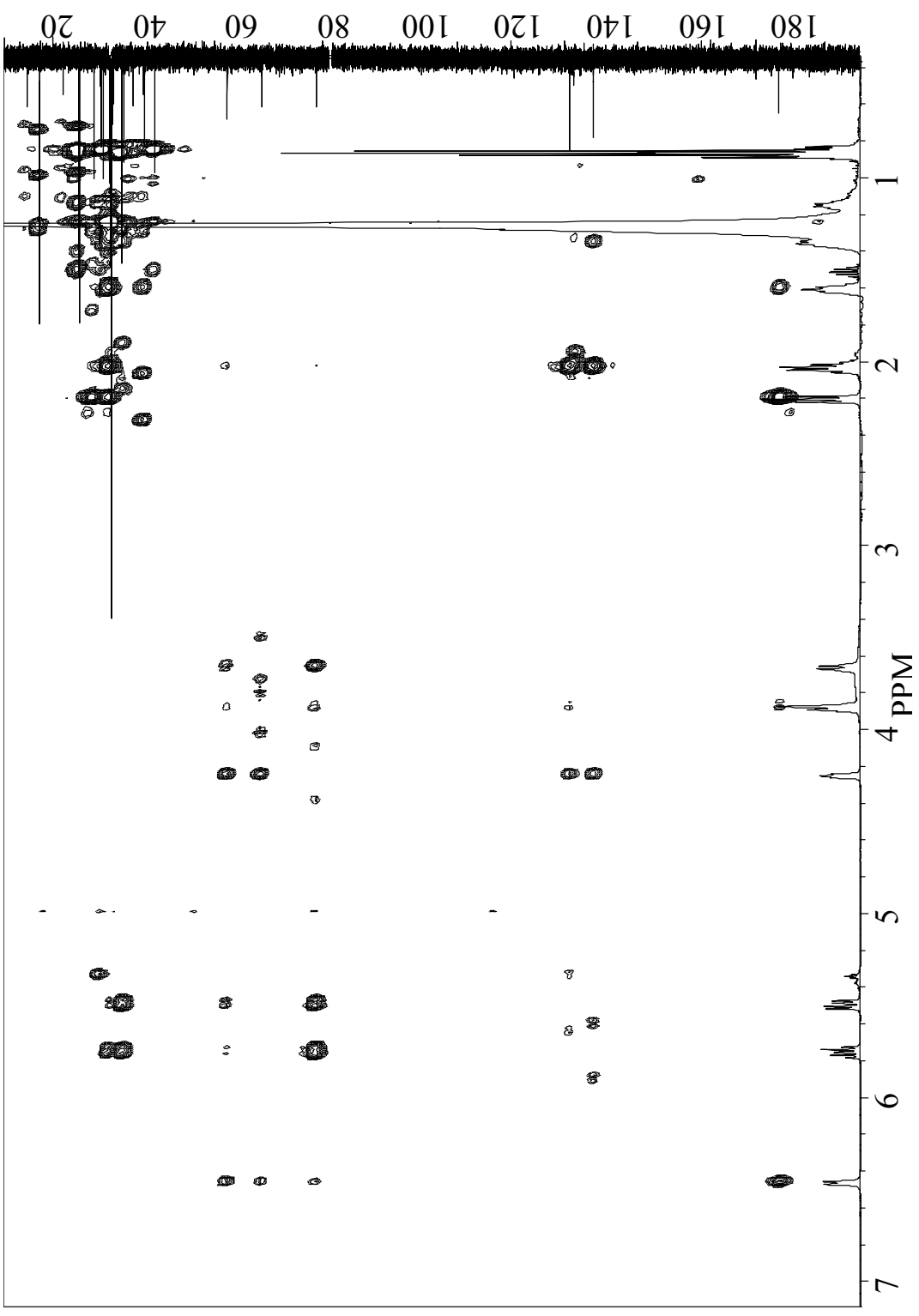

Figure 118. gHMBC spectrum of ceramide analog (**39**) (500 MHz, $CDCl_3$).

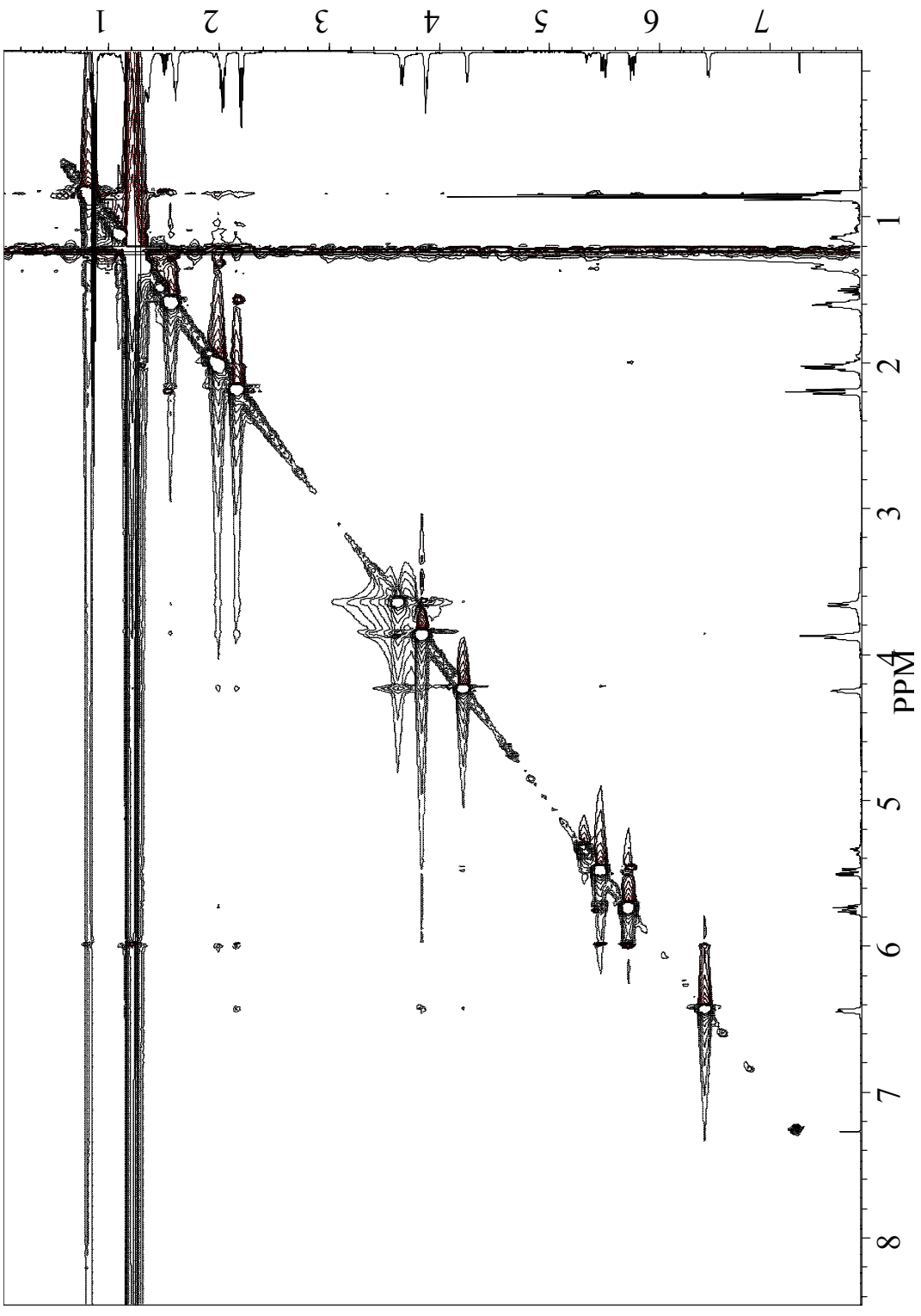

Figure 119. NOESY spectrum of ceramide analog (**39**) (500 MHz, $CDCl_3$).

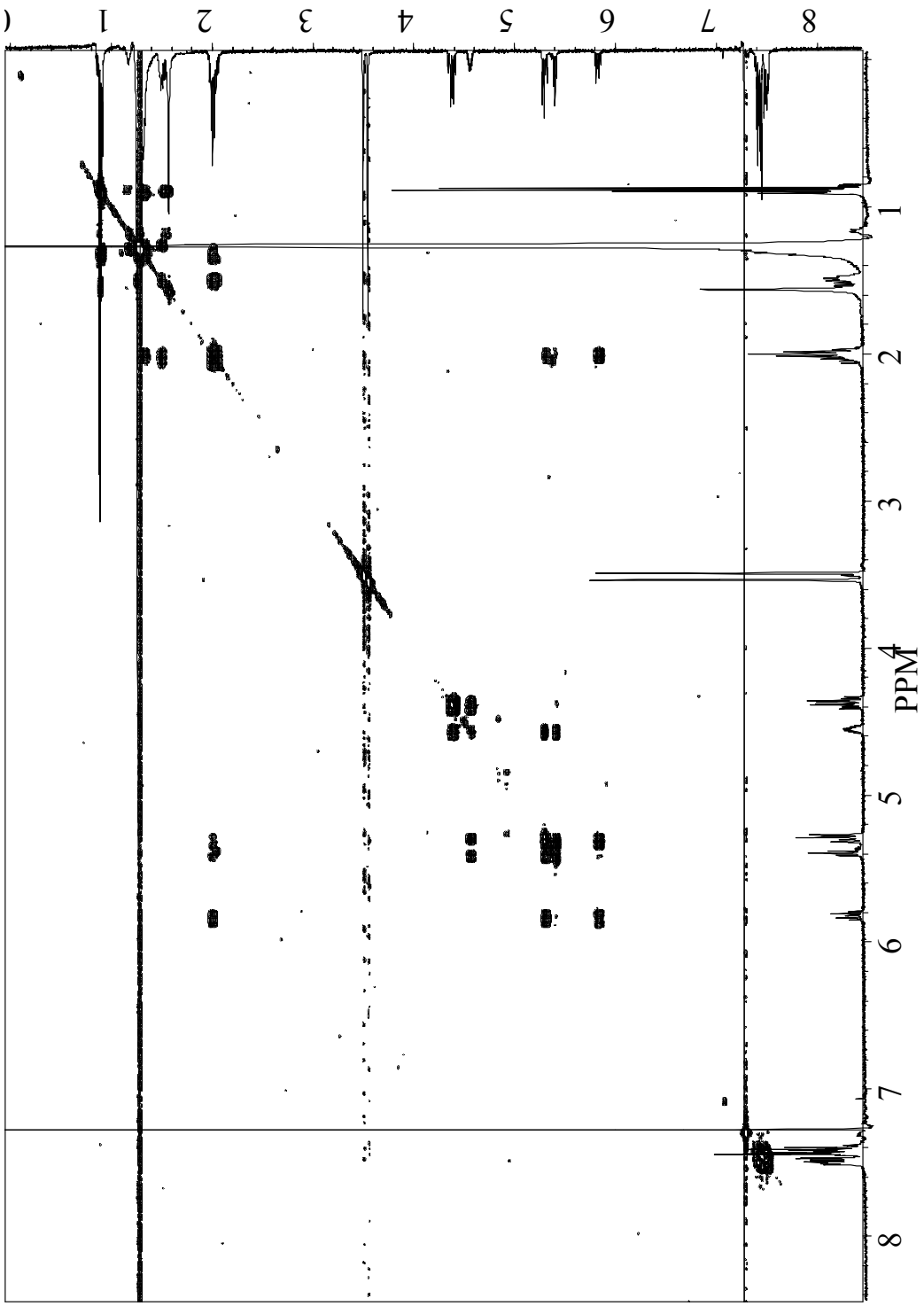

Figure 120. gCOSY spectrum of (*S*)-MTPA ester (**43**) (500 MHz, $CDCl_3$).

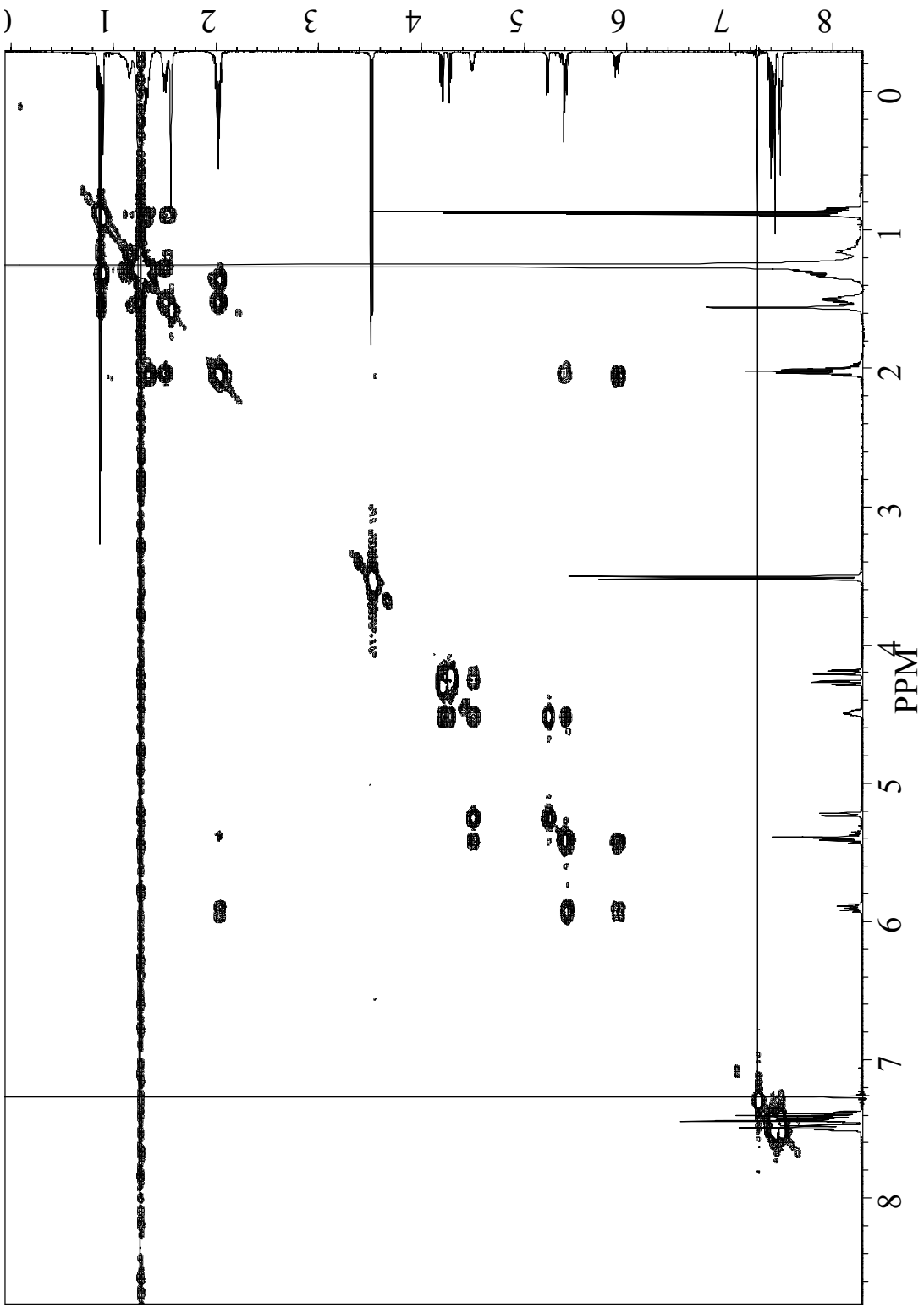

Figure 121. gCOSY spectrum of (*R*)-MTPA ester (**44**) (500 MHz, $CDCl_3$).

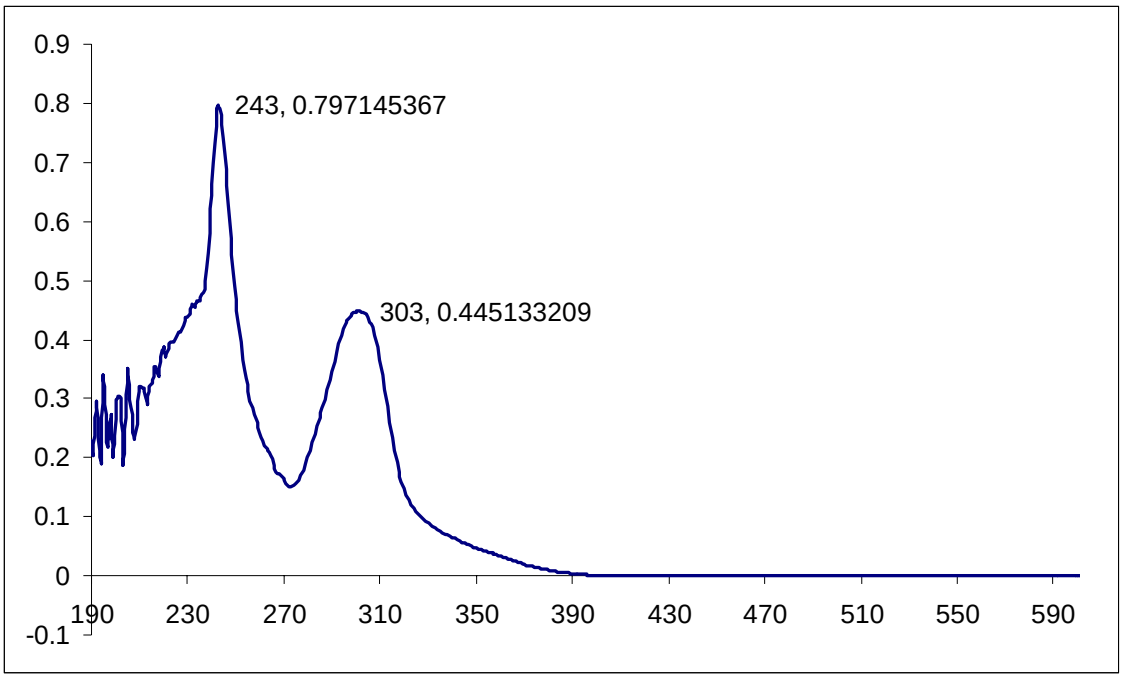

Figure 122. UV spectrum of benzyl-3-(benzyloxy)-2-nitrobenzoate (**46**) in $CHCl_3$.

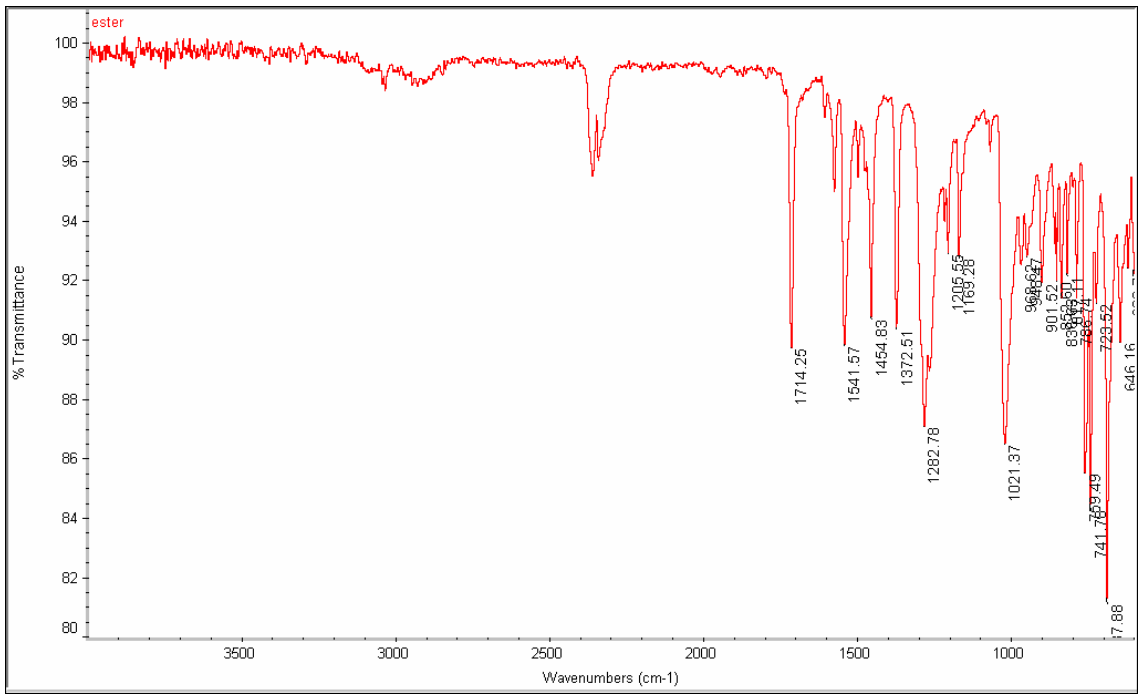

Figure 123. IR spectrum of benzyl-3-(benzyloxy)-2-nitrobenzoate (**46**).

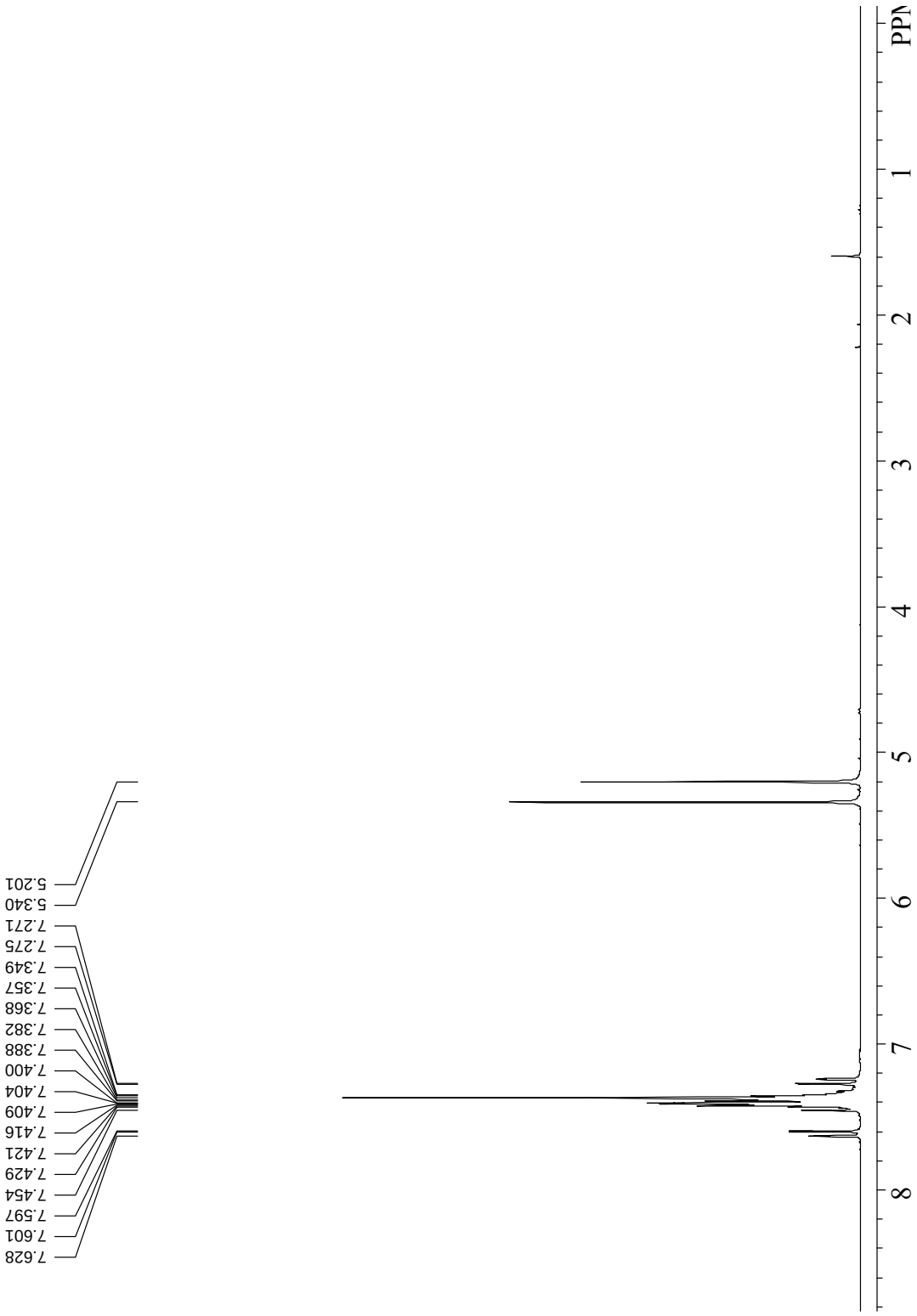

Figure 124. ^{1}H NMR spectrum of benzyl-3-(benzyloxy)-2-nitrobenzoate (**46**) (250 MHz, $CDCl_3$).

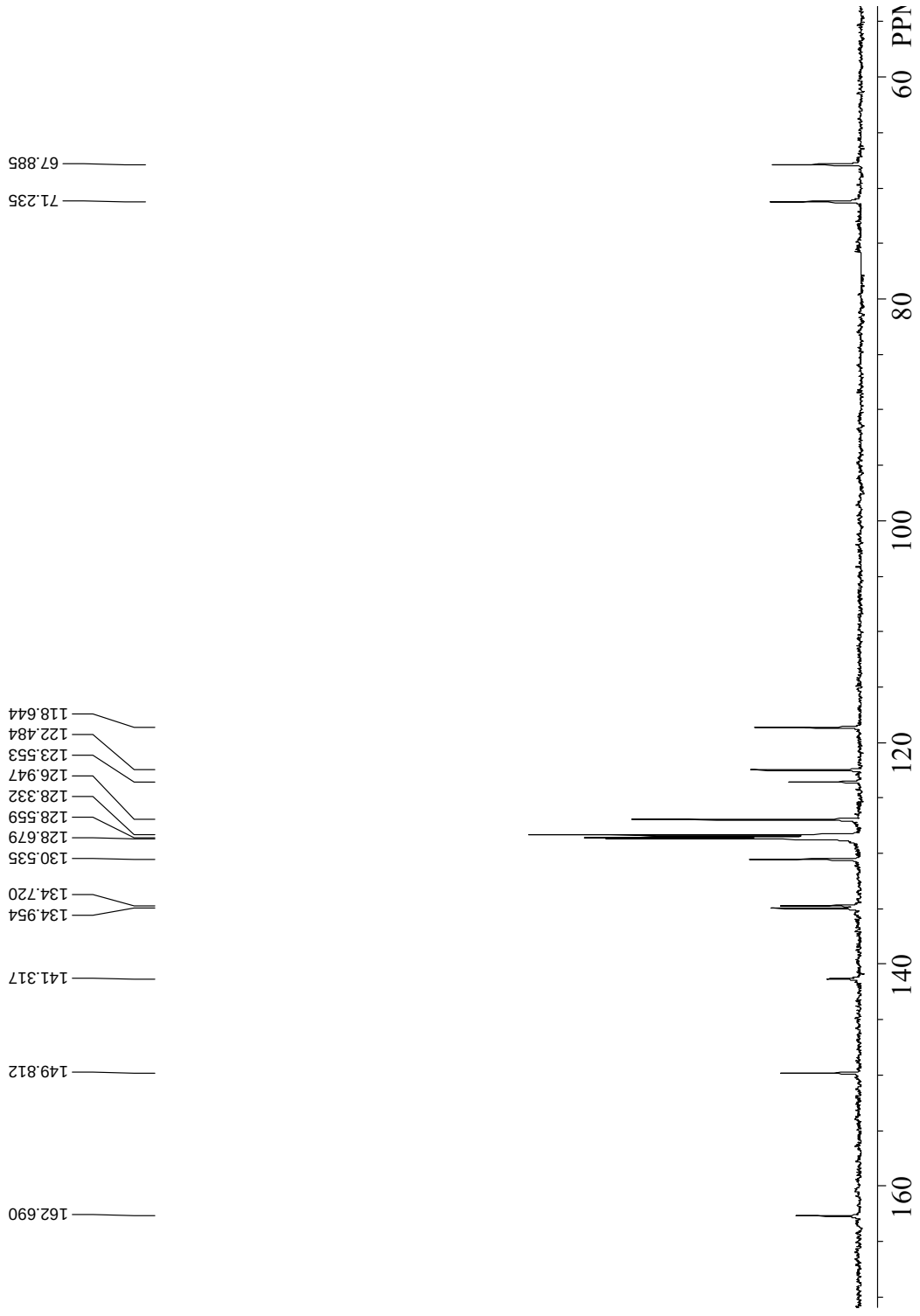

Figure 125. ^{13}C NMR spectrum of benzyl-3-(benzyloxy)-2-nitrobenzoate (**46**) (75 MHz, $CDCl_3$).

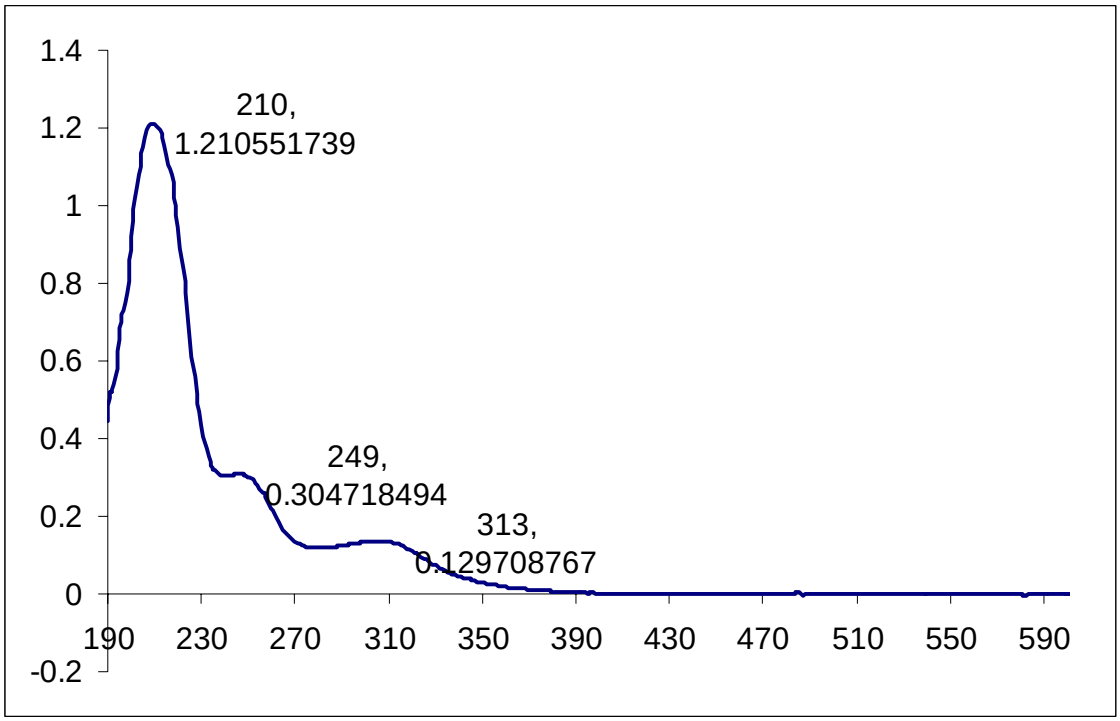

Figure 126. UV spectrum of 3-[3-(benzyloxy)-2-nitrophenyl]-3-oxopropanenitrile (**47**) in $CHCl_3$.

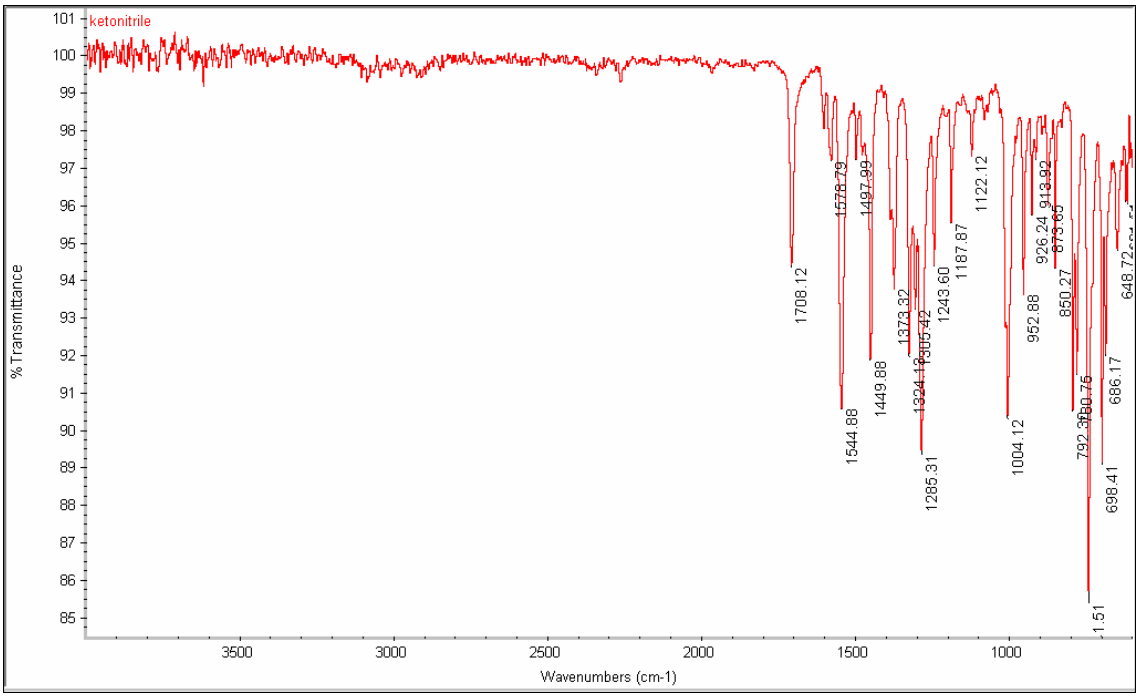

Figure 127. IR spectrum of 3-[3-(benzyloxy)-2-nitrophenyl]-3-oxopropanenitrile (**47**).

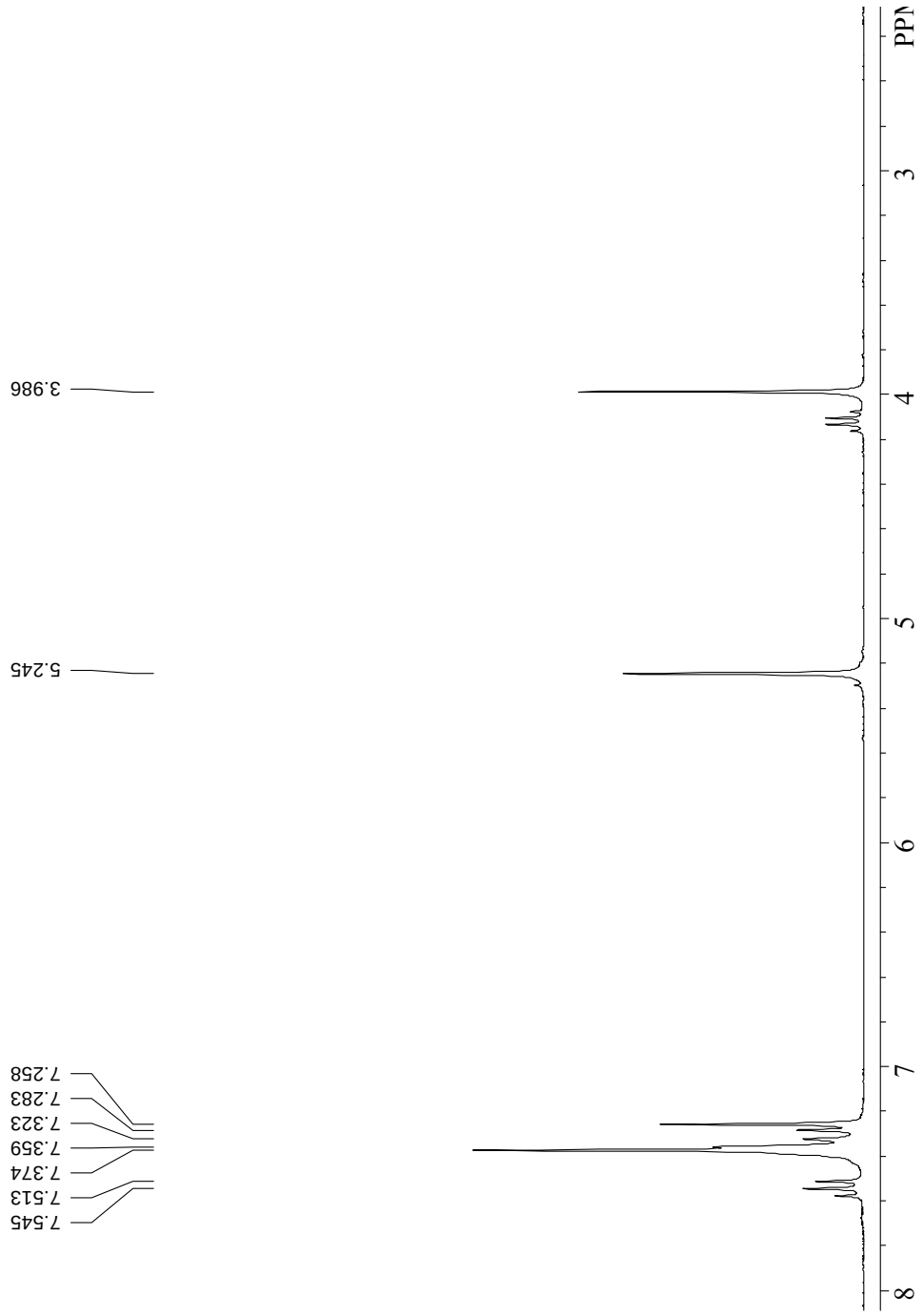

Figure 128. ^{1}H NMR spectrum of 3-[3-(benzyloxy)-2-nitrophenyl]-3-oxopropanenitrile (**47**) (250 MHz, $CDCl_3$).

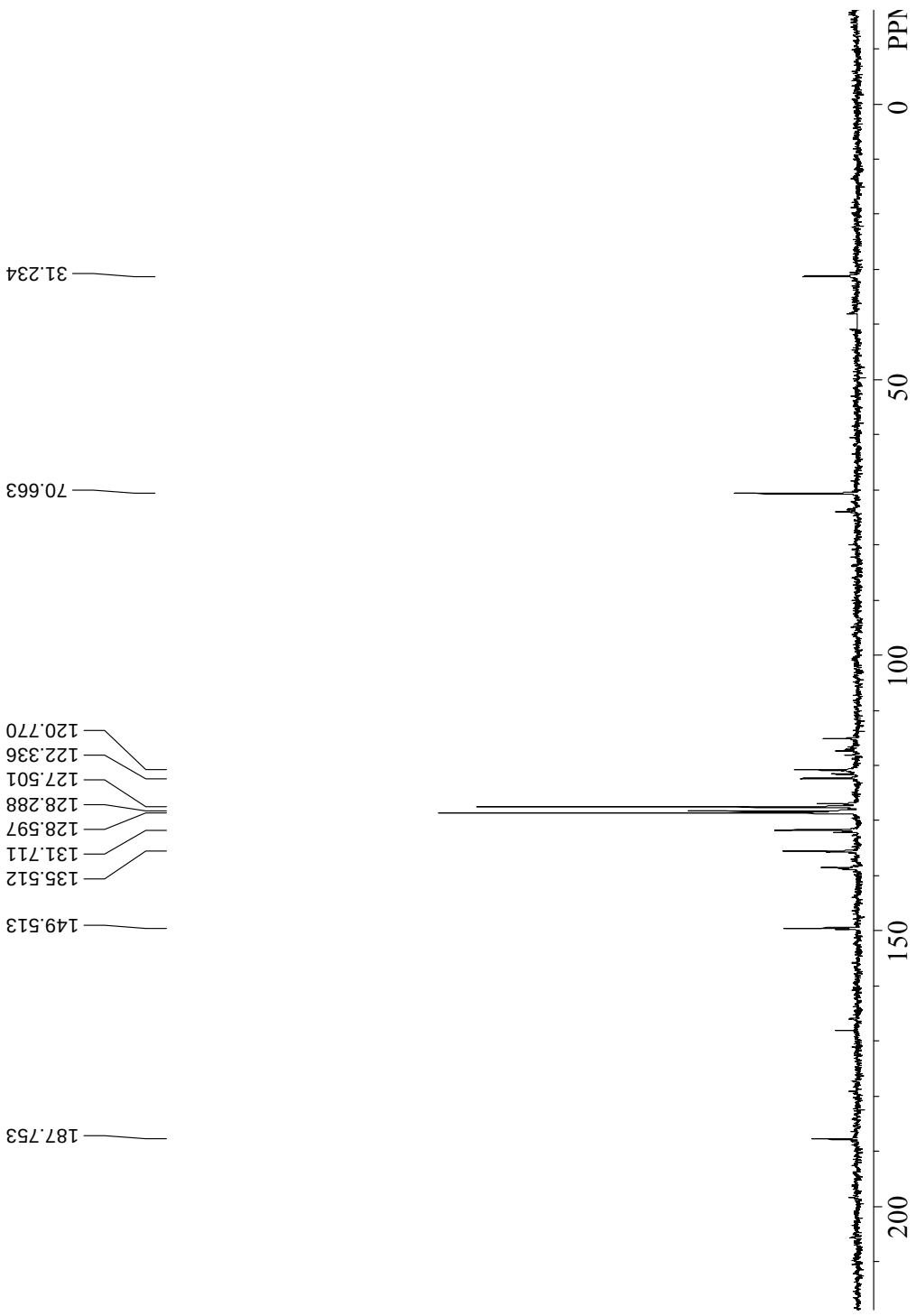

Figure 129. ^{13}C NMR spectrum of 3-[3-(benzyloxy)-2-nitrophenyl]-3-oxopropanenitrile (**47**) (250 MHz, $CDCl_3$).

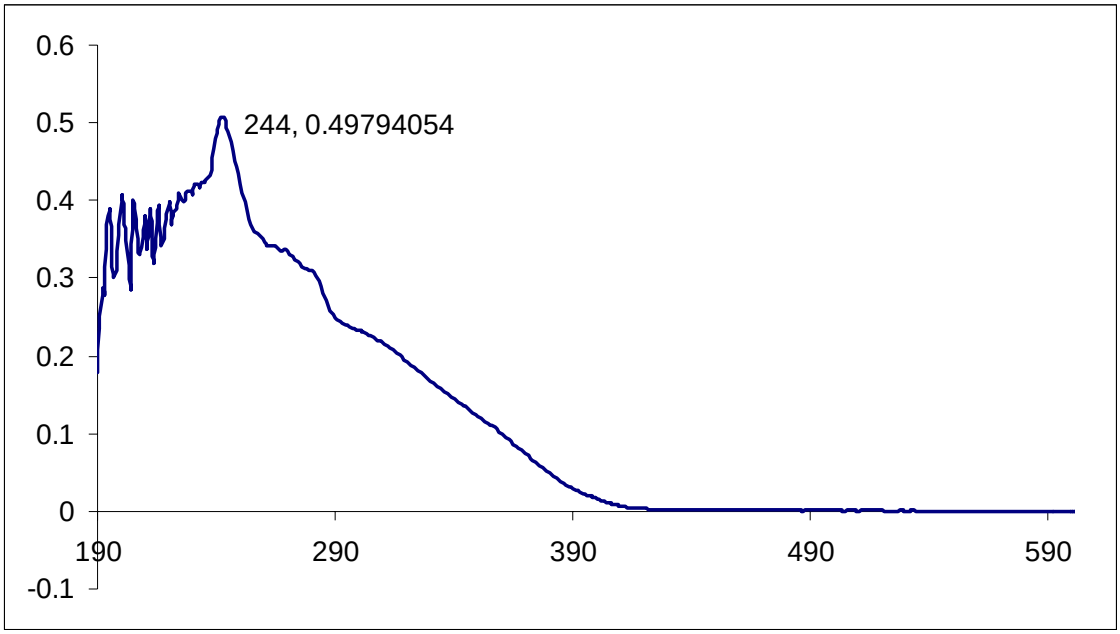

Figure 130. UV spectrum of 3-[3-(benzyloxy)-2-nitrophenyl]-3-hydroxypropanenitrile (**48**) in $CHCl_3$.

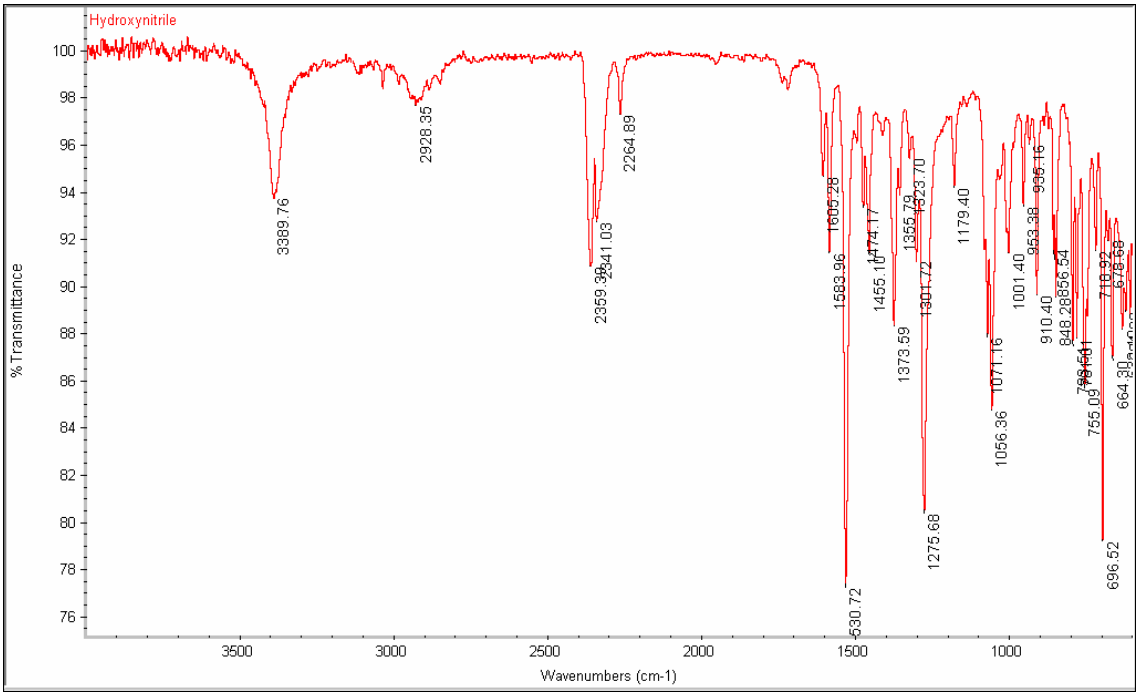

Figure 131. IR spectrum of 3-[3-(benzyloxy)-2-nitrophenyl]-3-hydroxypropanenitrile (**48**).

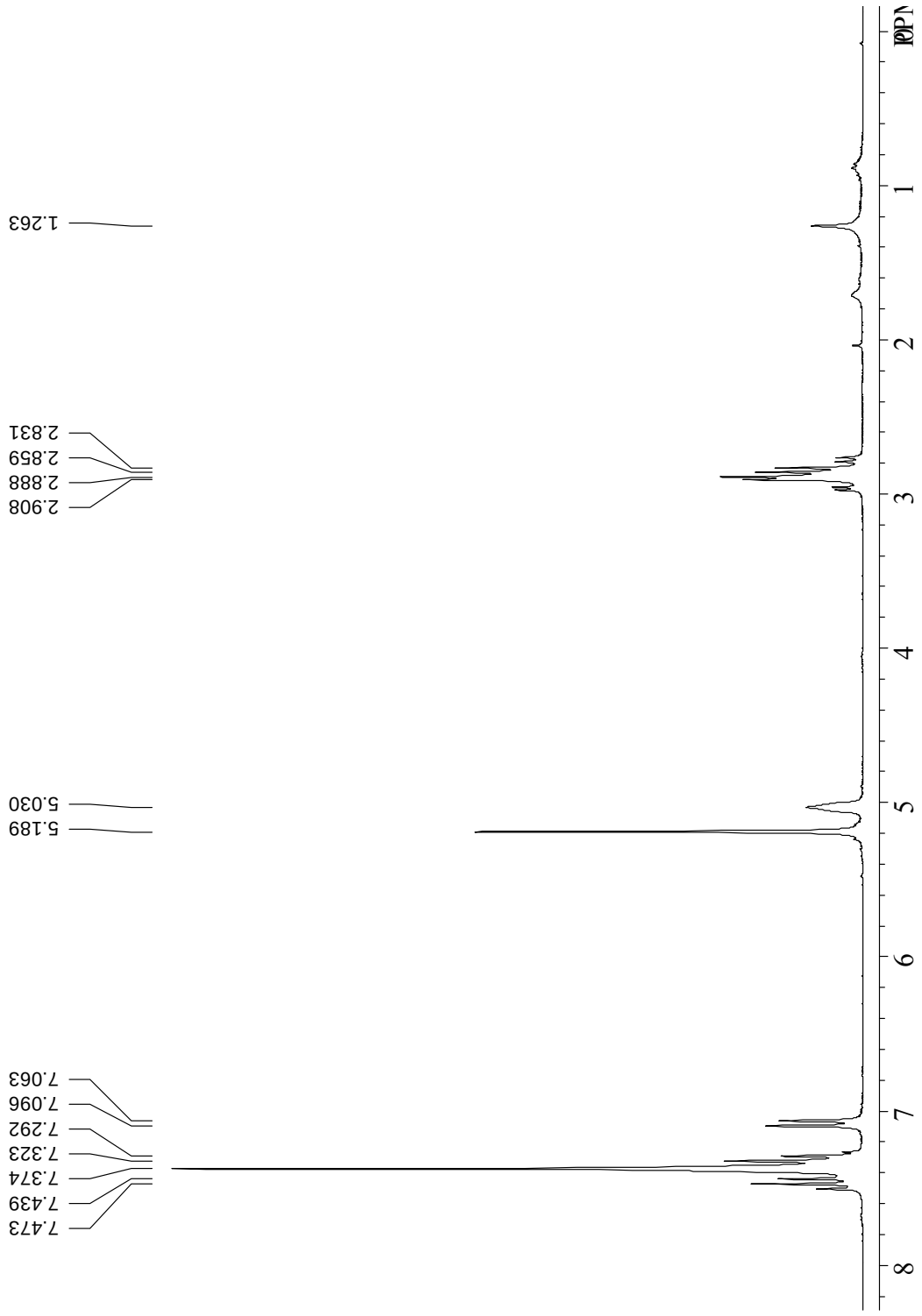

Figure 132. ^{1}H NMR spectrum of 3-[3-(benzyloxy)-2-nitrophenyl]-3-hydroxypropanenitrile (**48**) (250 MHz, $CDCl_3$).

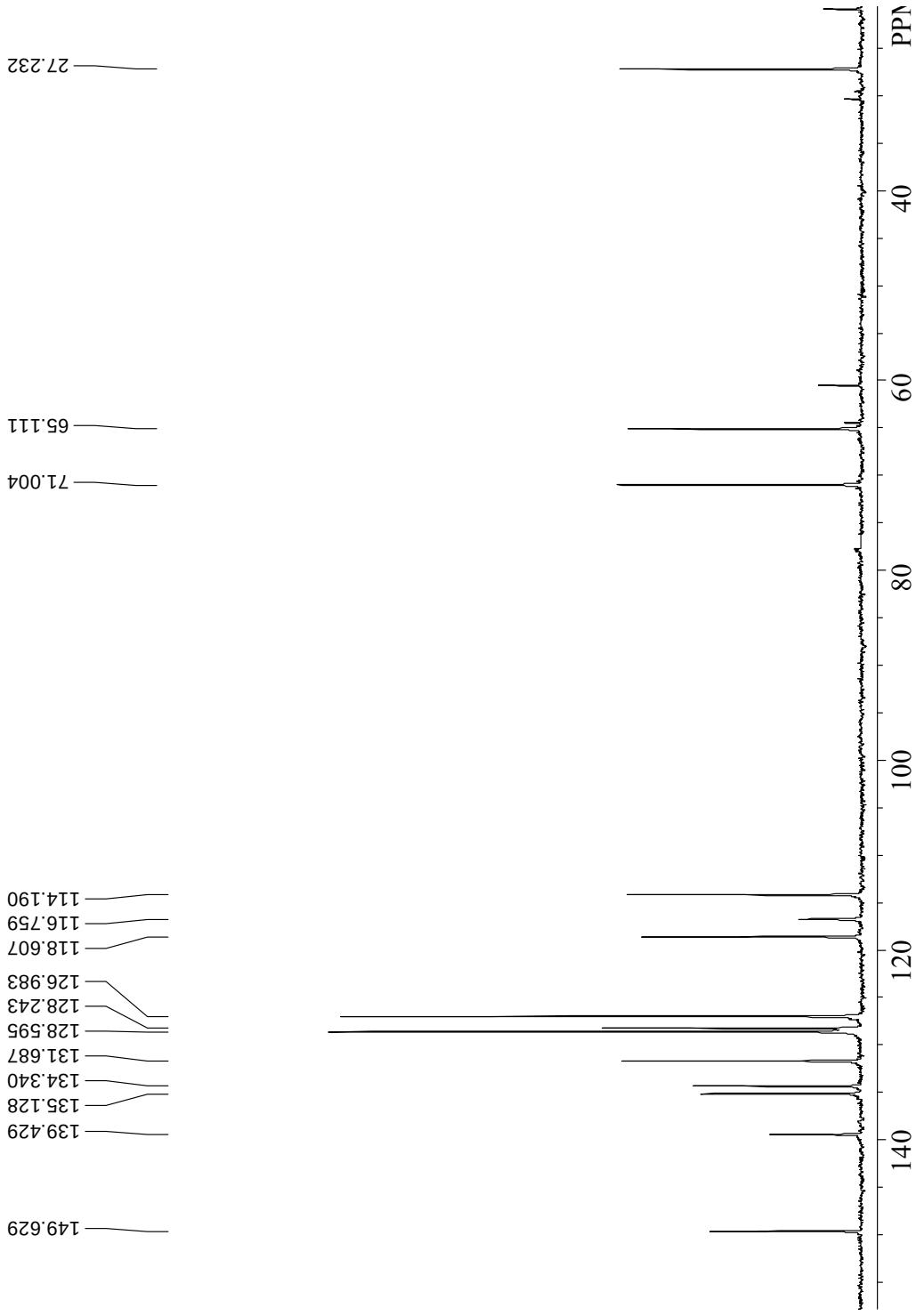

Figure 133. ^{13}C NMR spectrum of 3-[3-(benzyloxy)-2-nitrophenyl]-3-hydroxypropanenitrile (**48**) (75 MHz, $CDCl_3$).

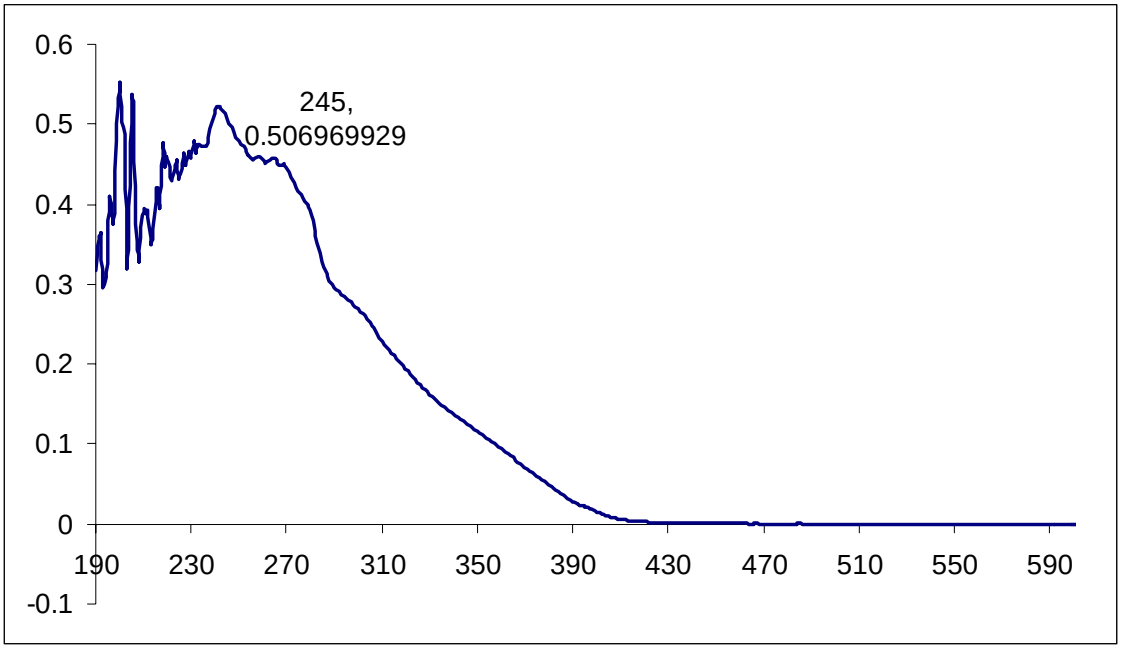

Figure 134. UV spectrum of 3-amino-1-[3-(benzyloxy)-2-nitrophenyl]propan-1-ol (**49**) in $CHCl_3$.

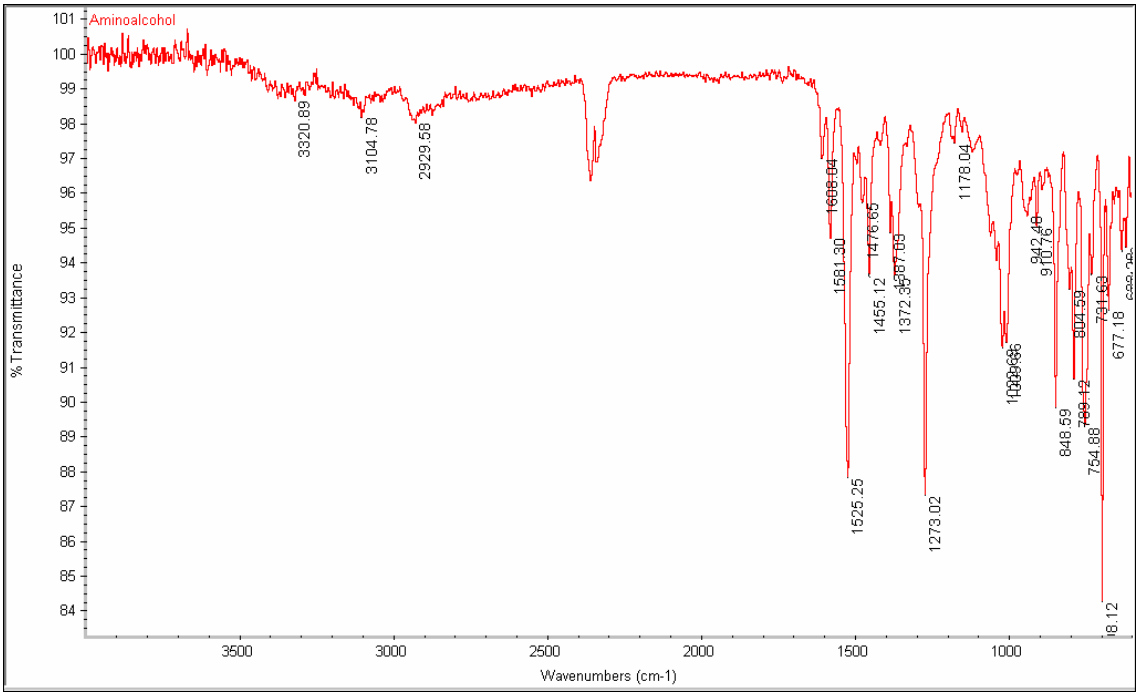

Figure 135. IR spectrum of 3-amino-1-[3-(benzyloxy)-2-nitrophenyl]propan-1-ol (**49**).

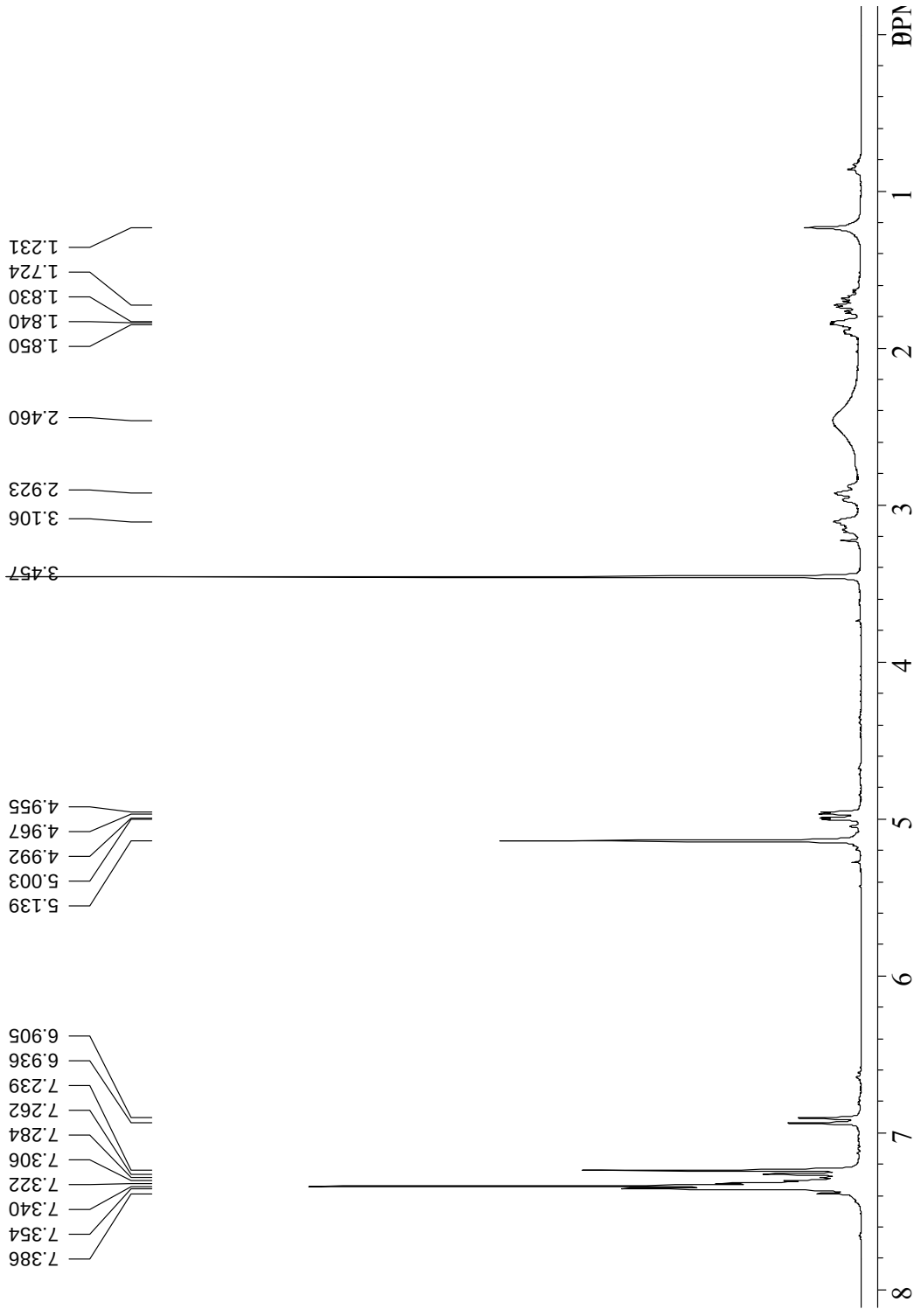

Figure 136. ^{1}H NMR spectrum of 3-amino-1-[3-(benzyloxy)-2-nitrophenyl]propan-1-ol (**49**) (250 MHz, $CDCl_3$).

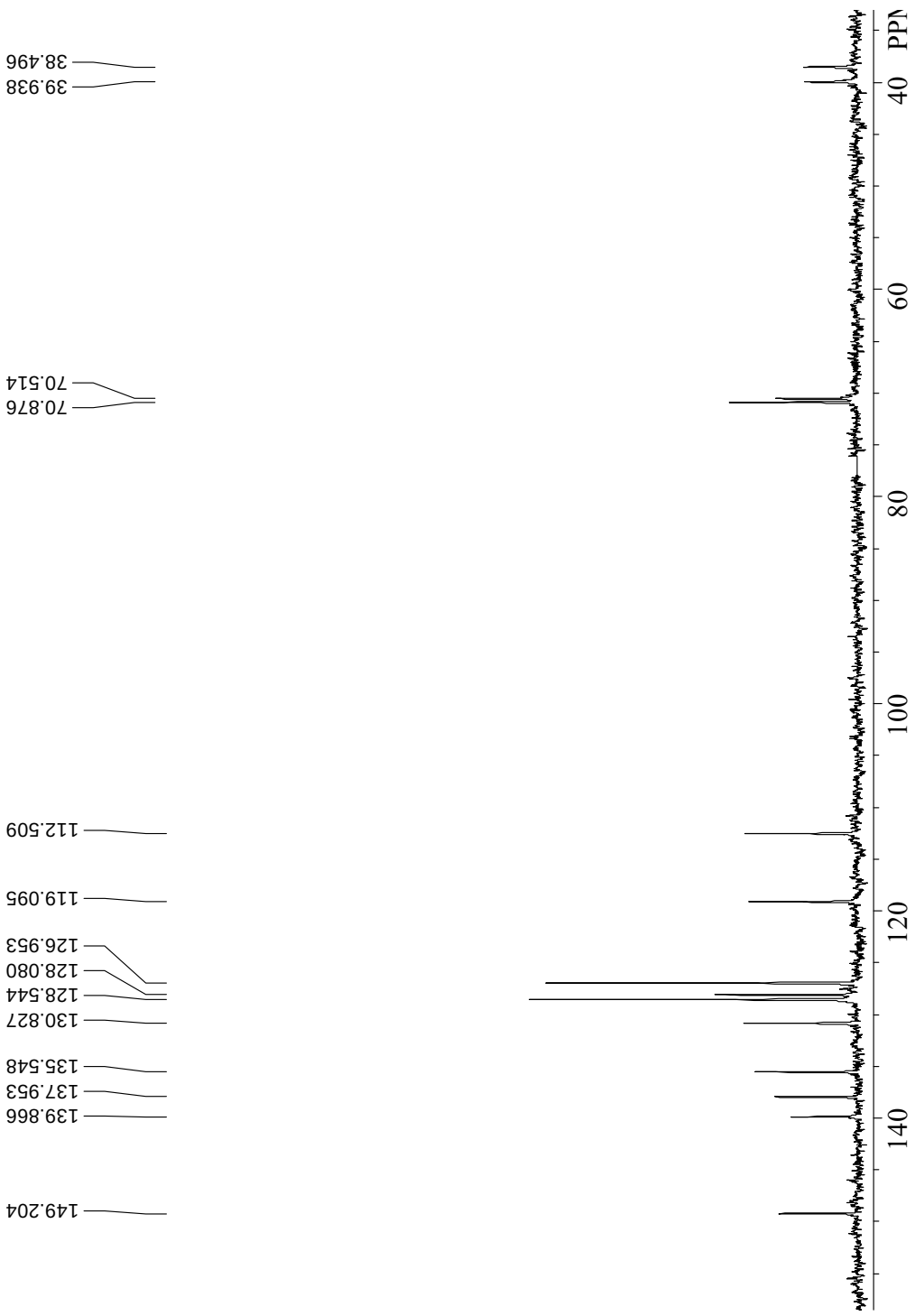

Figure 137. ^{13}C NMR spectrum of 3-amino-1-[3-(benzyloxy)-2-nitrophenyl]propan-1-ol (**49**) (75 MHz, $CDCl_3$).

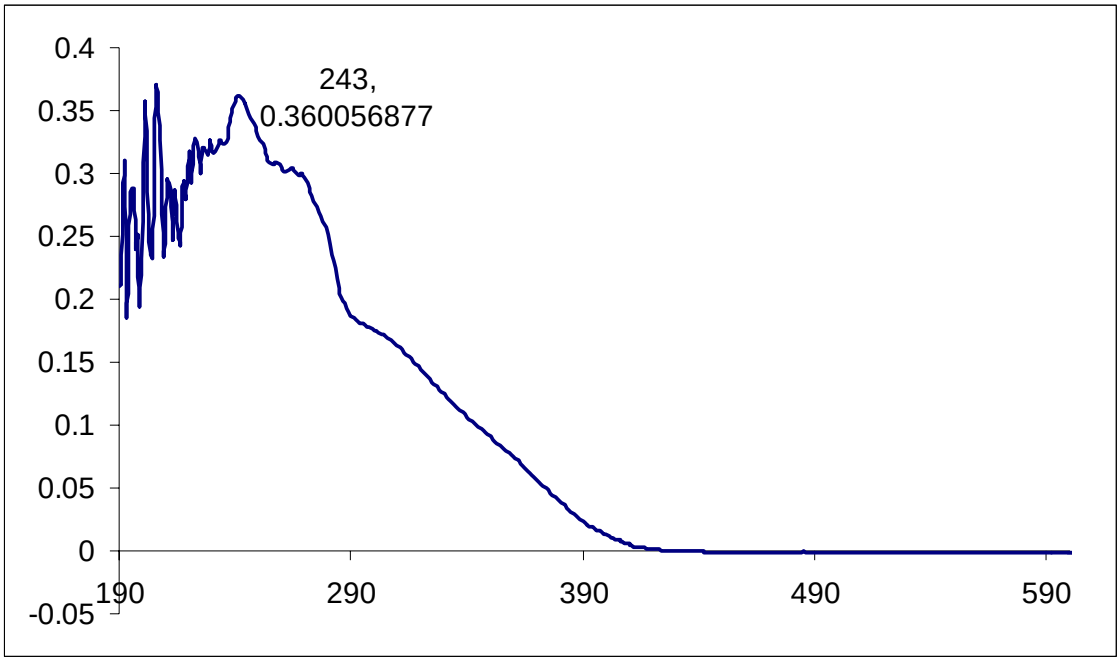

Figure 138. UV spectrum of N-{3-[3-(benzyloxy)-2-nitrophenyl]-3-hydroxypropyl}acetamide (**50**) in $CHCl_3$.

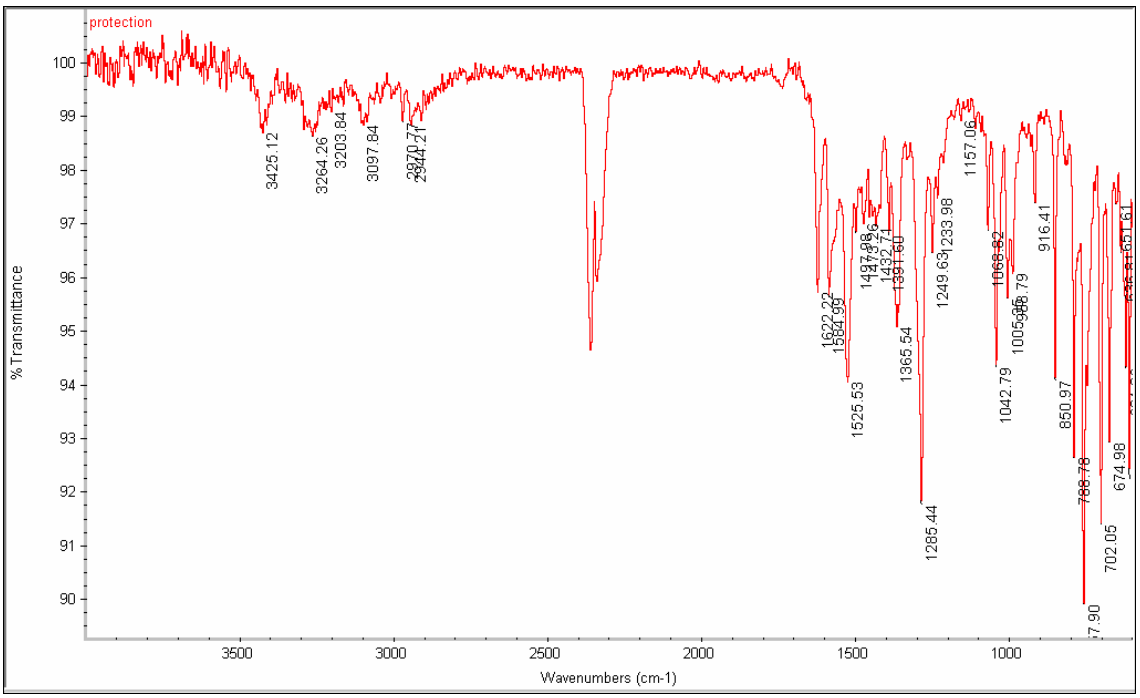

Figure 139. IR spectrum of N-{3-[3-(benzyloxy)-2-nitrophenyl]-3-hydroxypropyl}acetamide (**50**).

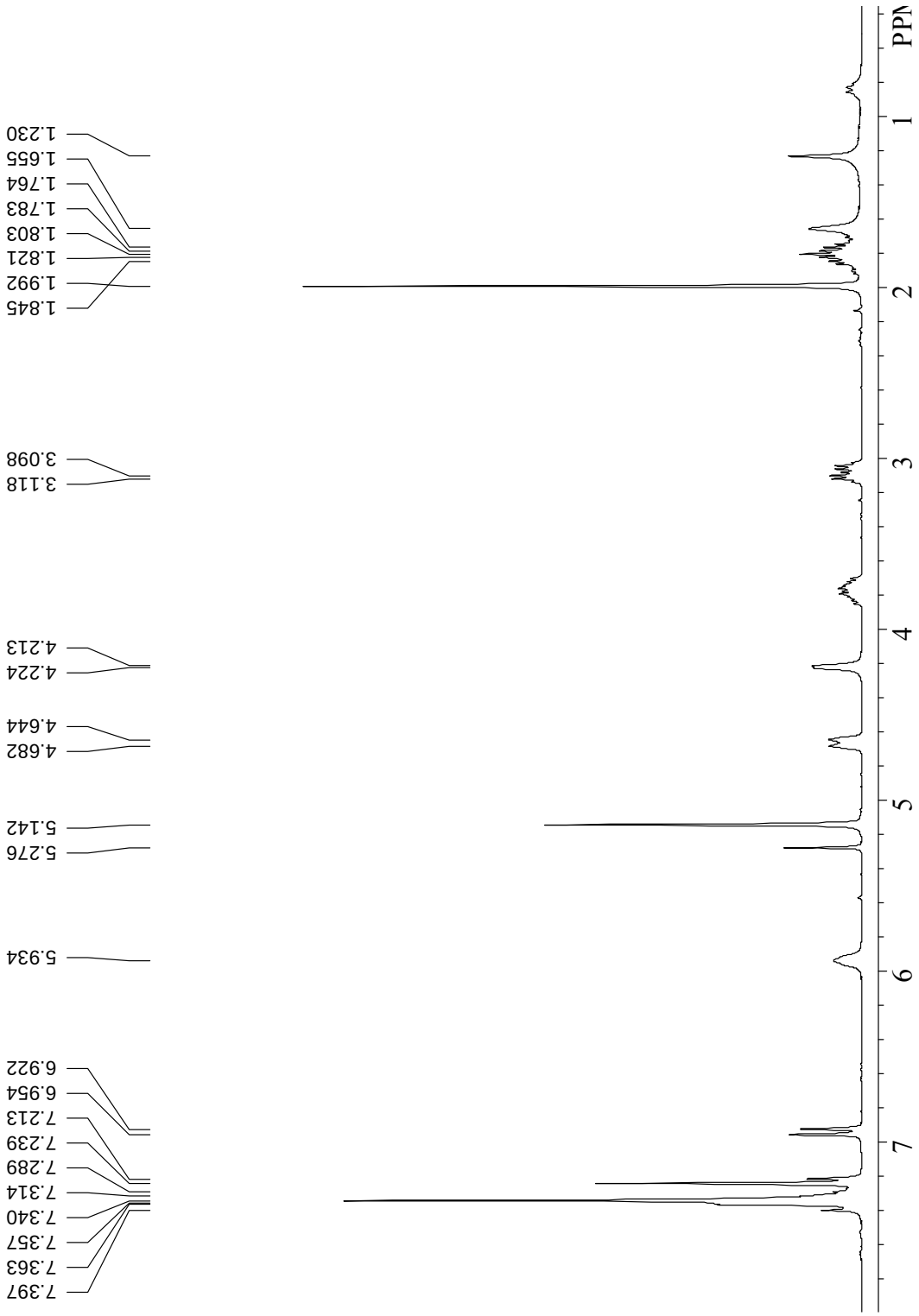

Figure 140. ^{1}H NMR spectrum of N-{3-[3-(benzyloxy)-2-nitrophenyl]-3-hydroxypropyl}acetamide (**50**) (250 MHz, $CDCl_3$).

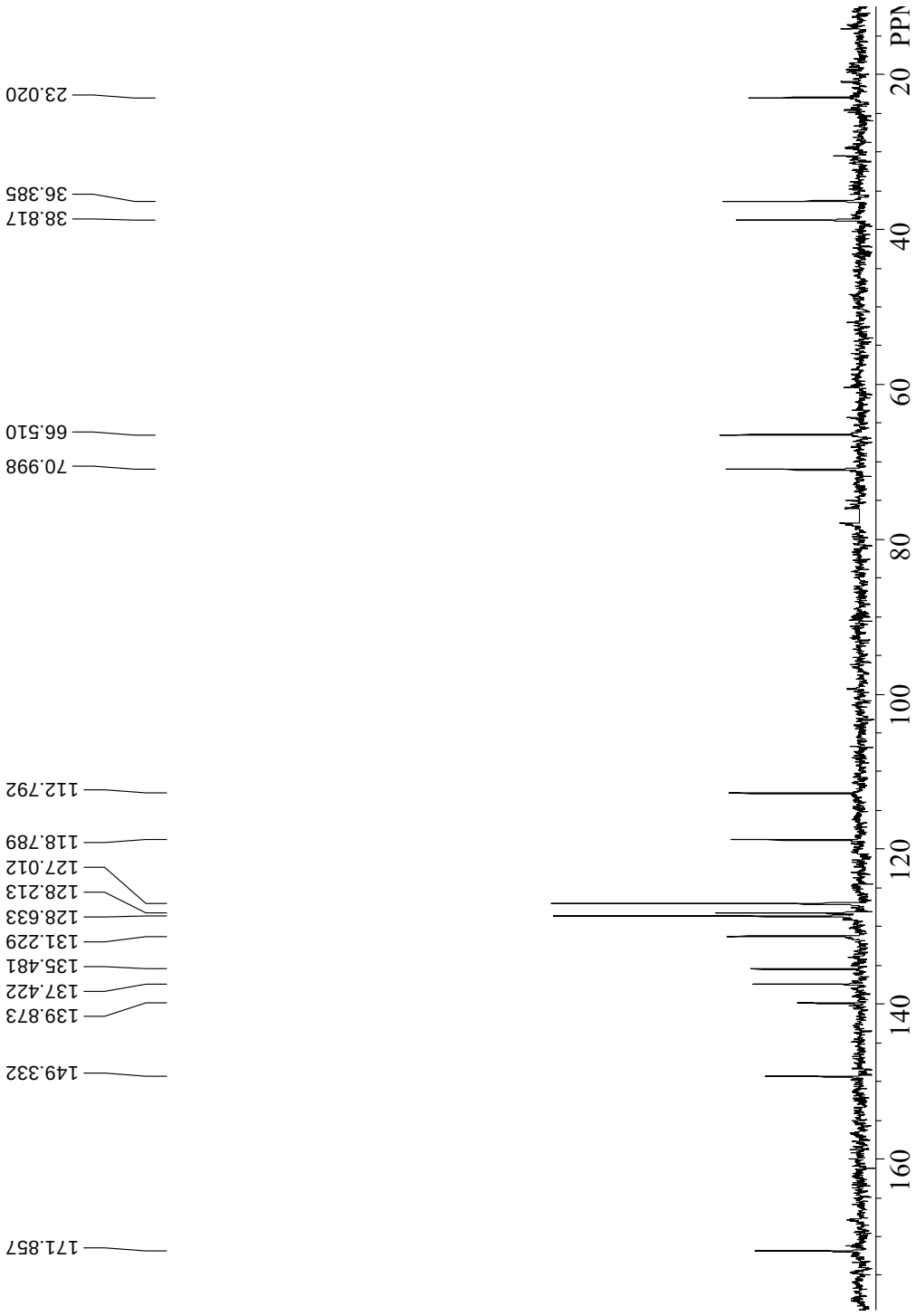

Figure 141. ^{13}C NMR spectrum of N-{3-[3-(benzyloxy)-2-nitrophenyl]-3-hydroxypropyl}acetamide (**50**) (75 MHz, $CDCl_3$).

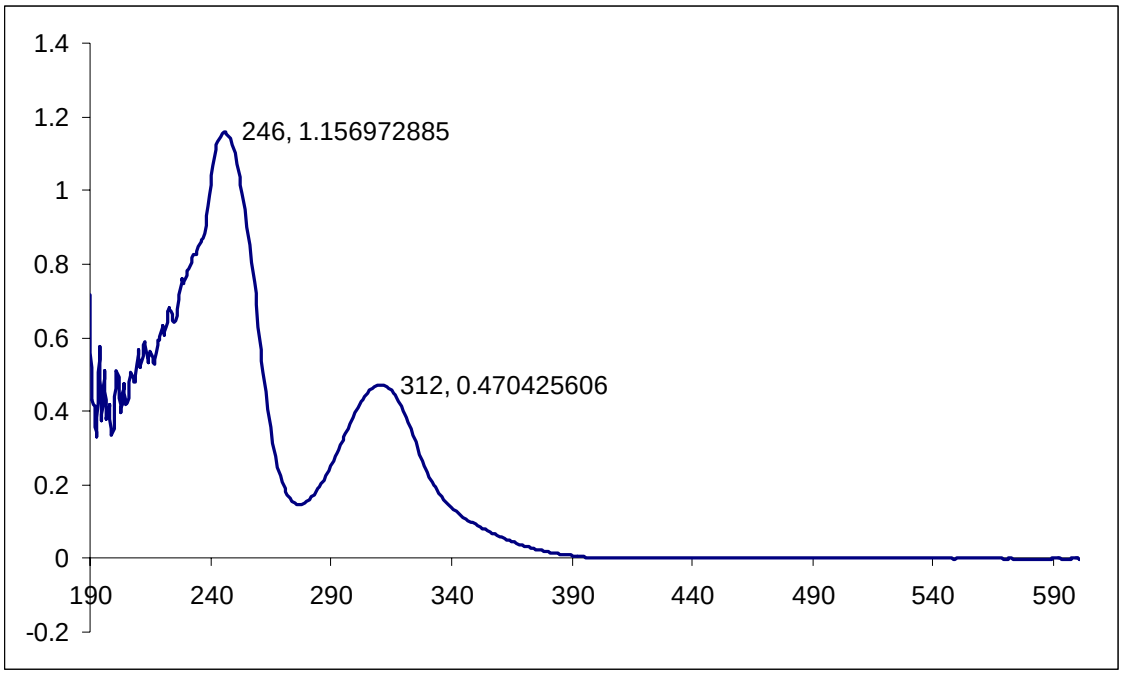

Figure 142. UV spectrum of N-{3-[3-(benzyloxy)-2-nitrophenyl]-3-oxoypropyl}acetamide (**51**) in $CHCl_3$.

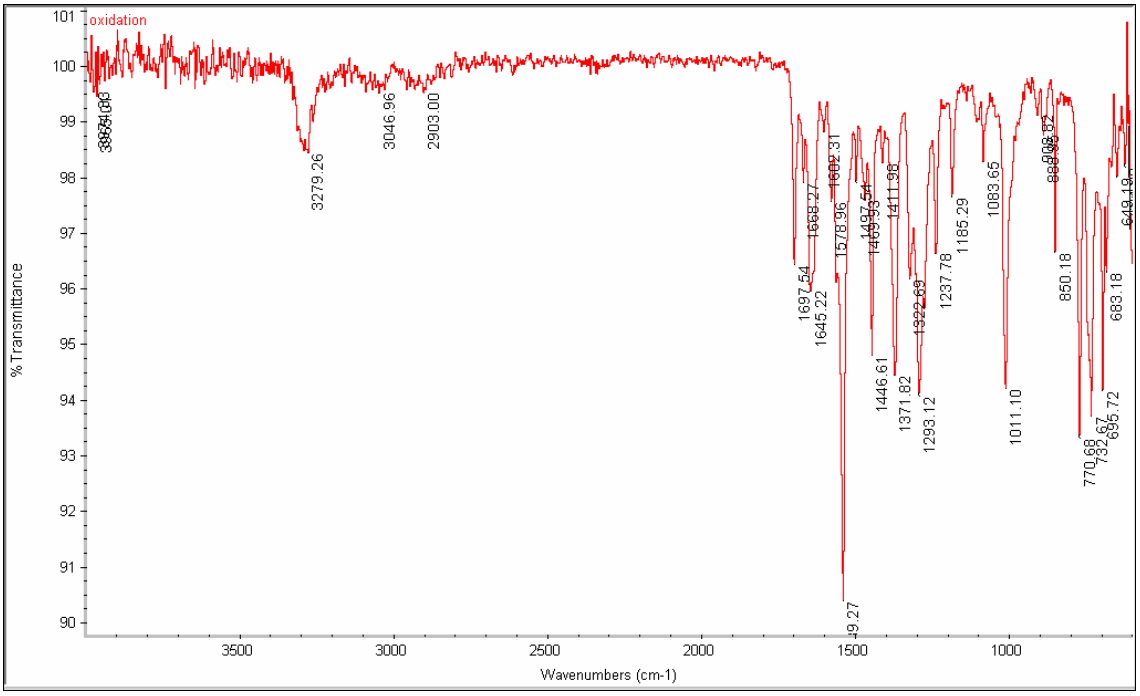

Figure 143. IR spectrum of N-{3-[3-(benzyloxy)-2-nitrophenyl]-3-oxopropyl}acetamide (**51**).

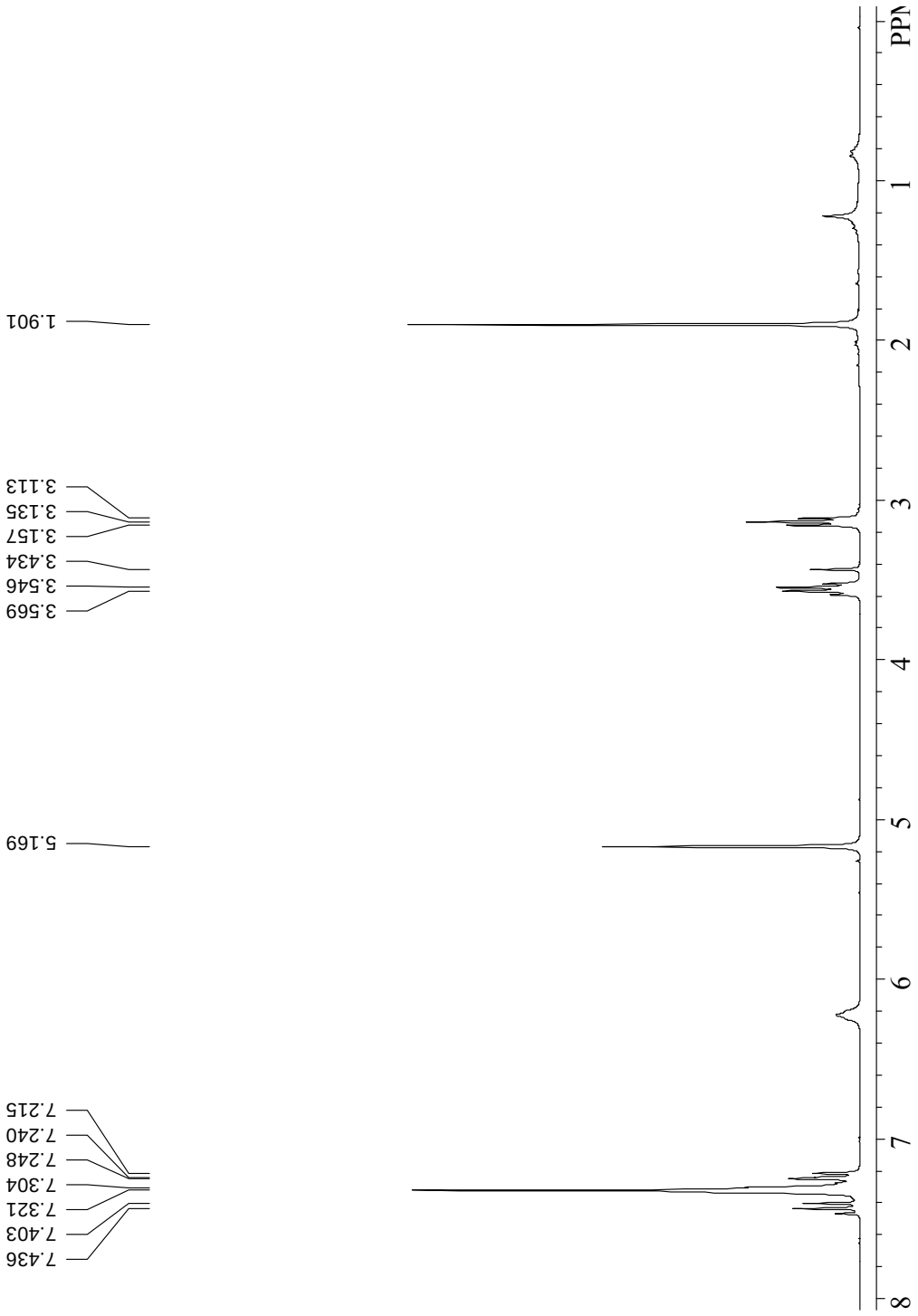

Figure 144. ^{1}H NMR spectrum of N-{3-[3-(benzyloxy)-2-nitrophenyl]-3-oxoypropyl}acetamide (**51**) (250 MHz, $CDCl_3$).

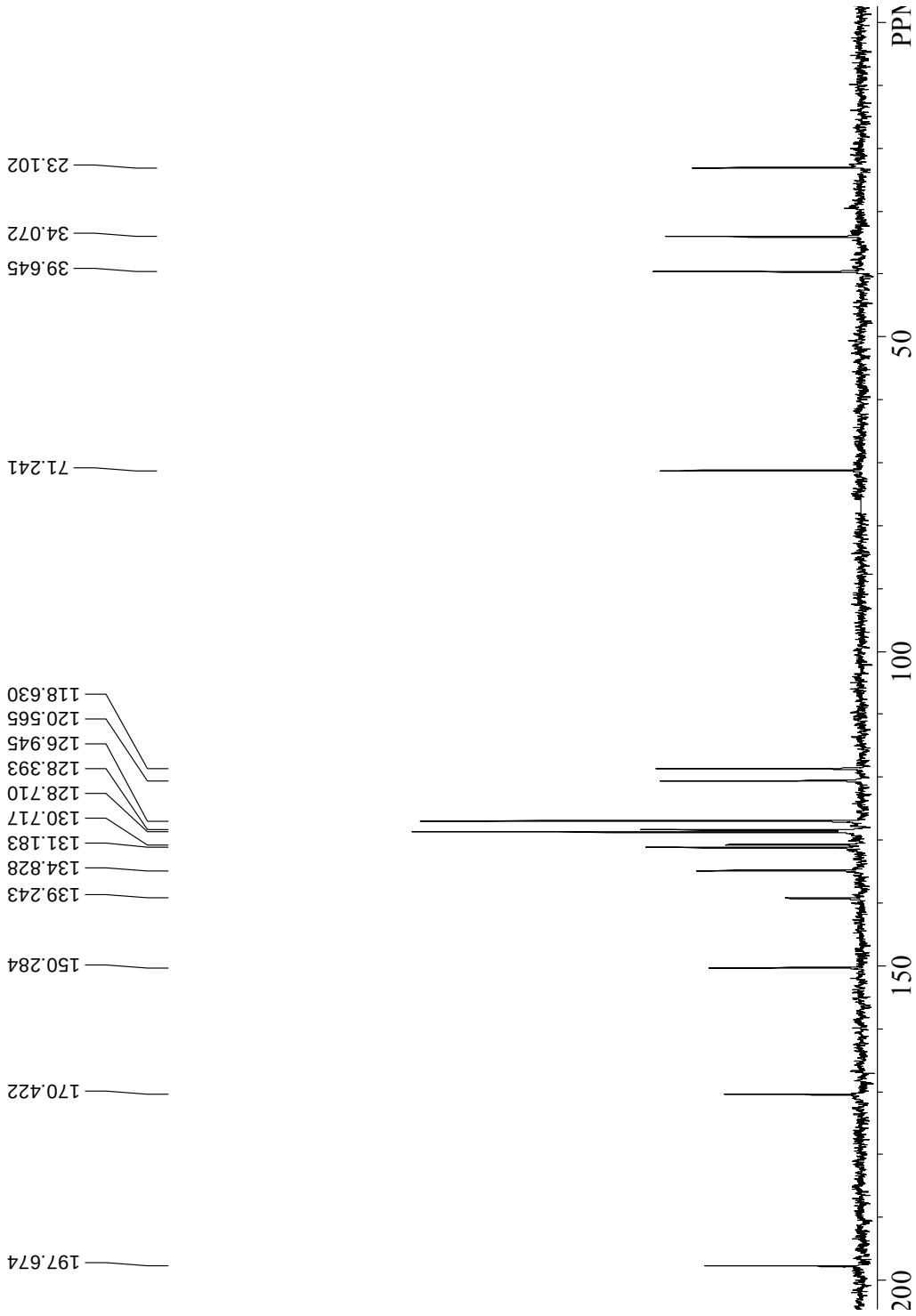

Figure 145. ^{13}C NMR spectrum of N-{3-[3-(benzyloxy)-2-nitrophenyl]-3-oxoypropyl}acetamide (**51**) (75 MHz, $CDCl_3$).

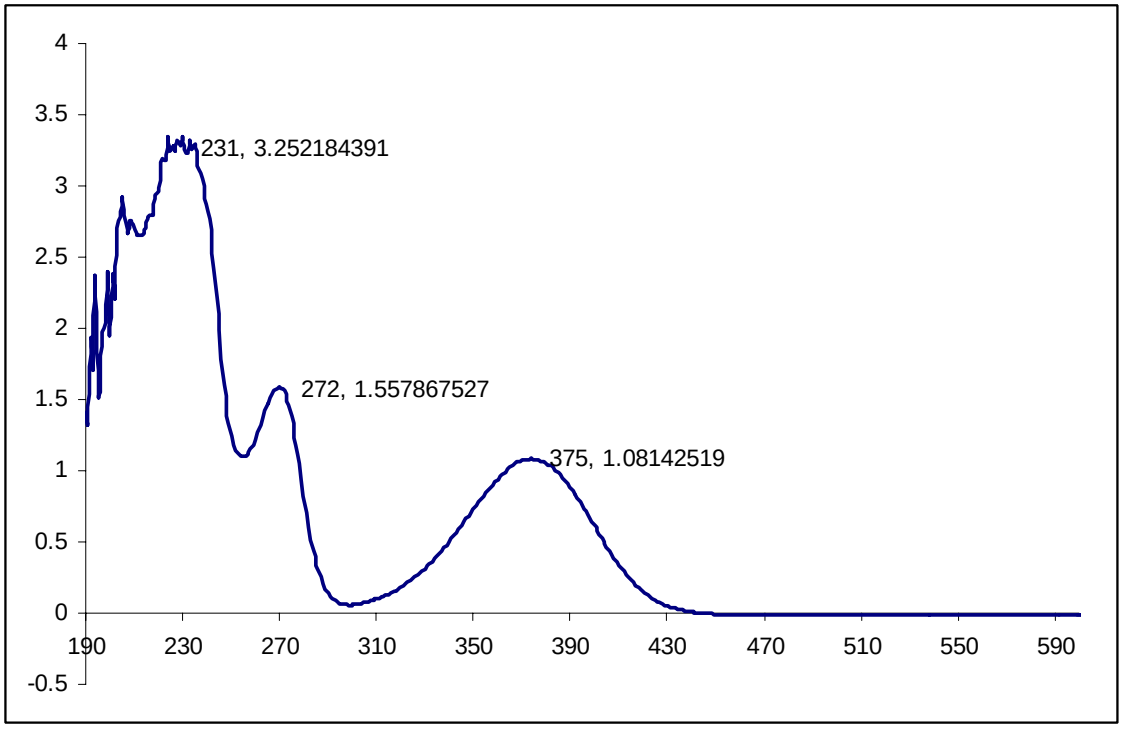

Figure 146. UV spectrum of erebusinone (**12**) in MeOH.

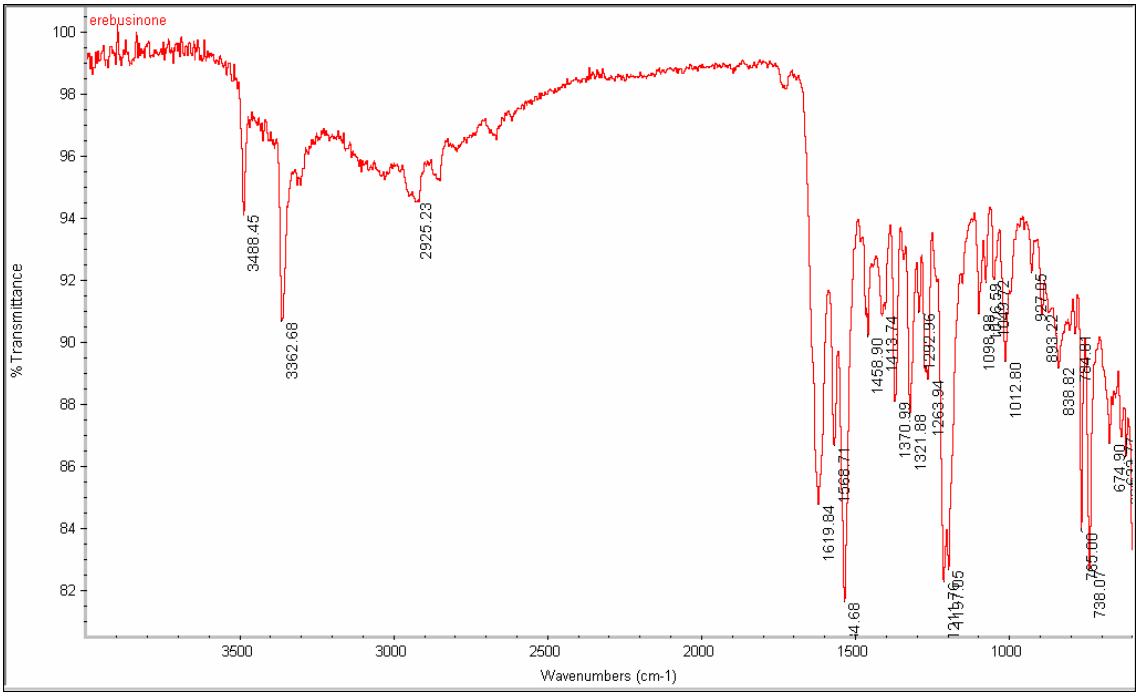

Figure 147. IR spectrum of erebusinone (**12**).

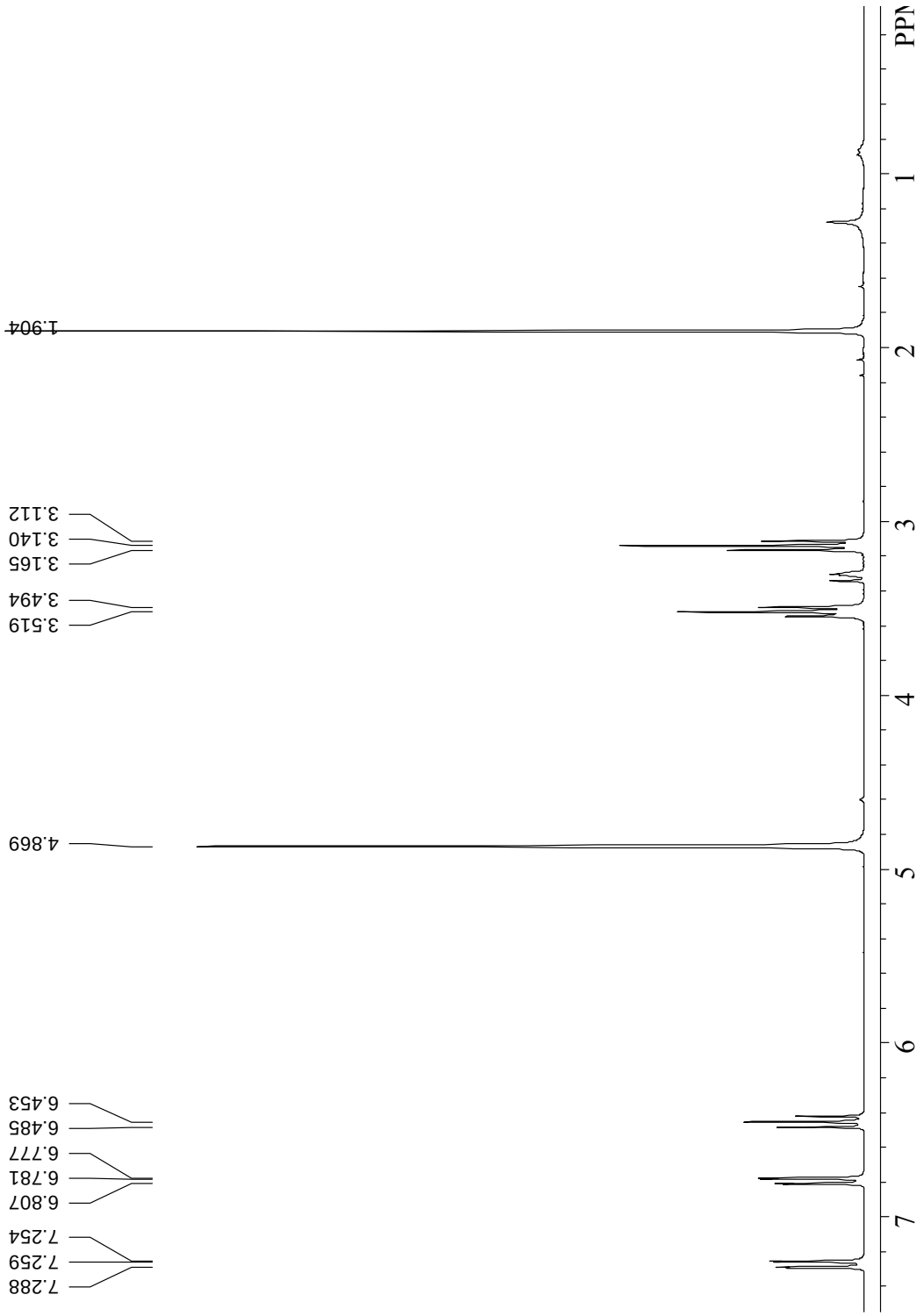

Figure 148. ^{1}H NMR spectrum of erebusinone (**12**) (250 MHz, MeOH-d_4).

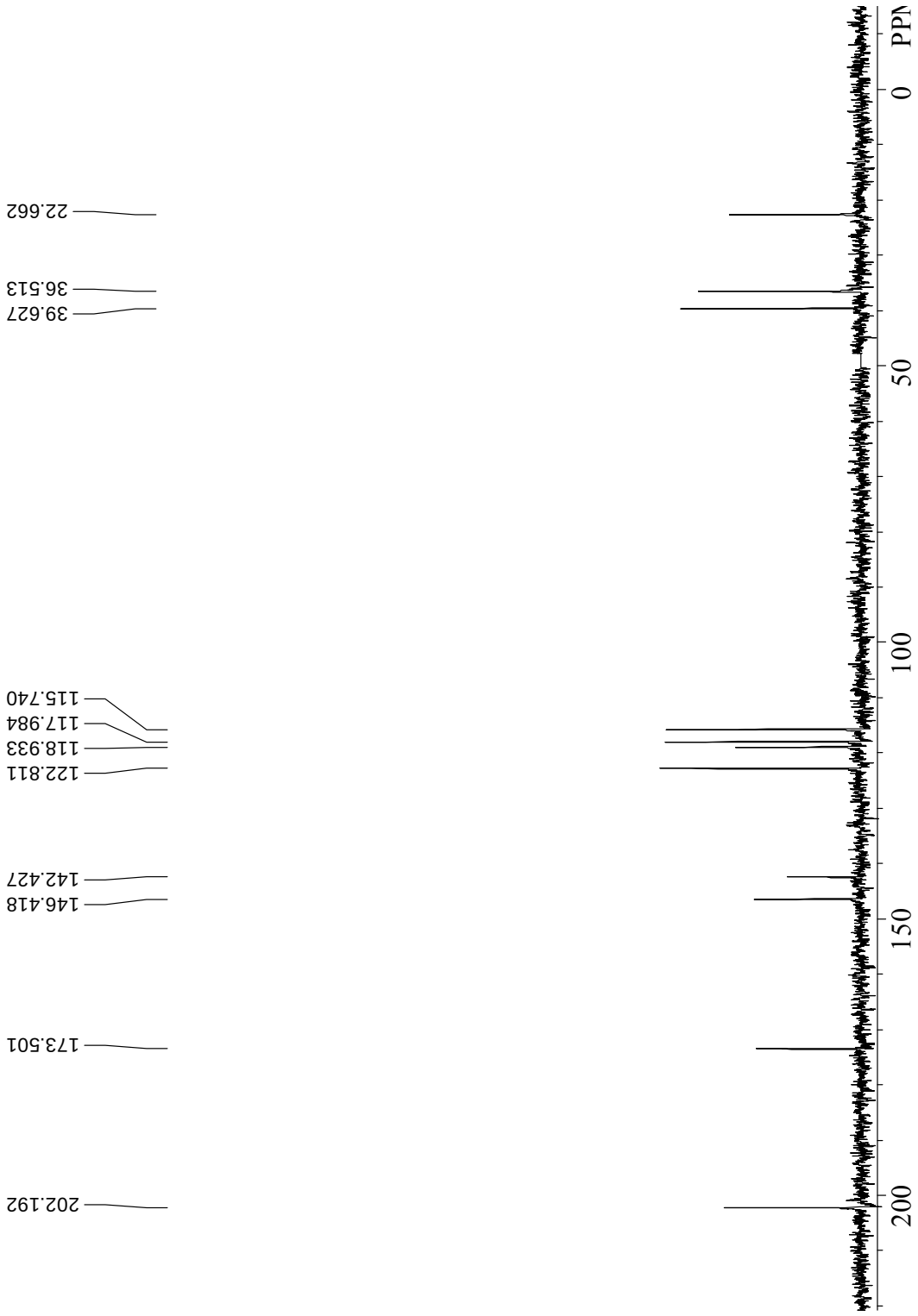

Figure 149. ^{13}C NMR spectrum of erebusinone (**12**) (75 MHz, MeOH-d_4).

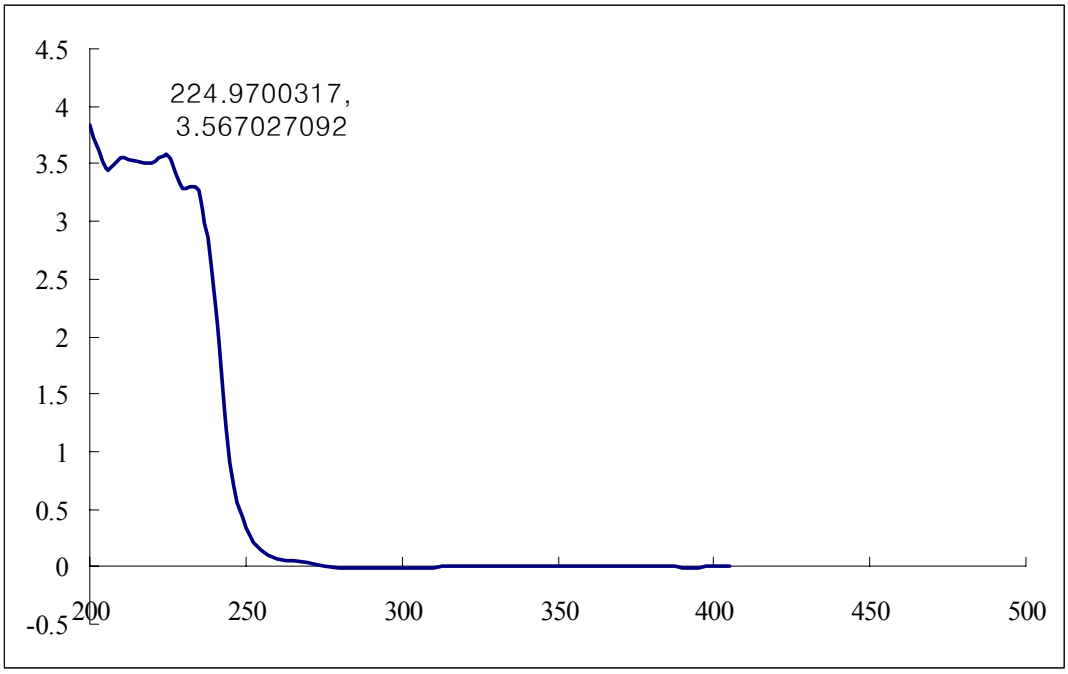

Figure 150. UV spectrum of *tert*-butyl-3-[3-(benzyloxy)-2-nitrophenyl]-3-hydroxypropylcarbamate (**53**).

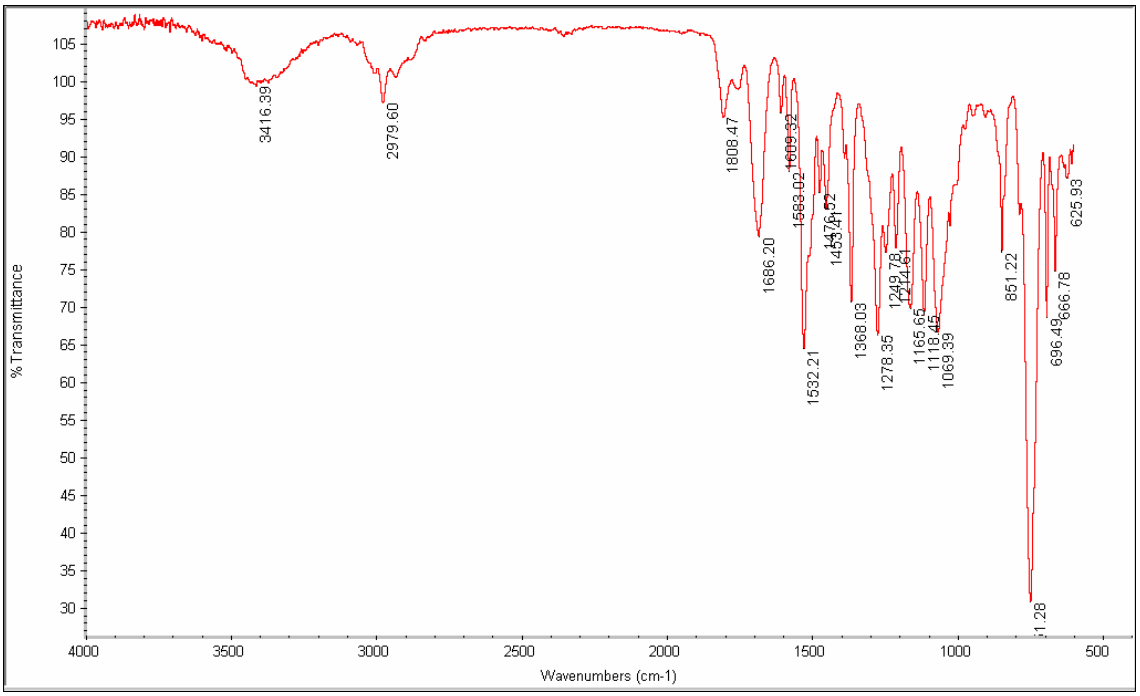

Figure 151. IR spectrum of *tert*-butyl-3-[3-(benzyloxy)-2-nitrophenyl]-3-hydroxypropylcarbamate (**53**).

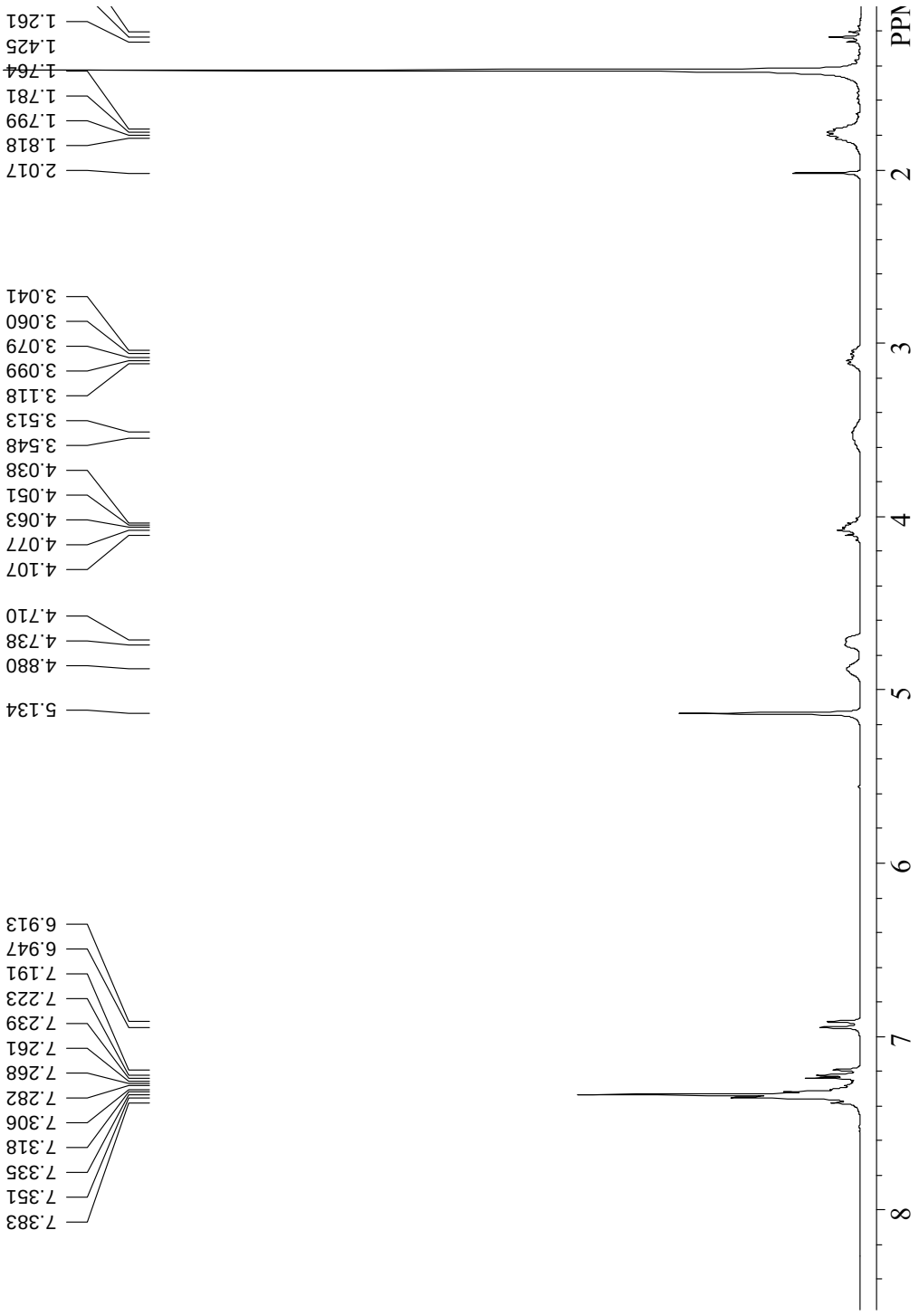

Figure 152. ^{1}H NMR spectrum of *tert*-butyl-3-[3-(benzyloxy)-2-nitrophenyl]-3-hydroxypropylcarbamate (**53**) (250 MHz, $CDCl_3$).

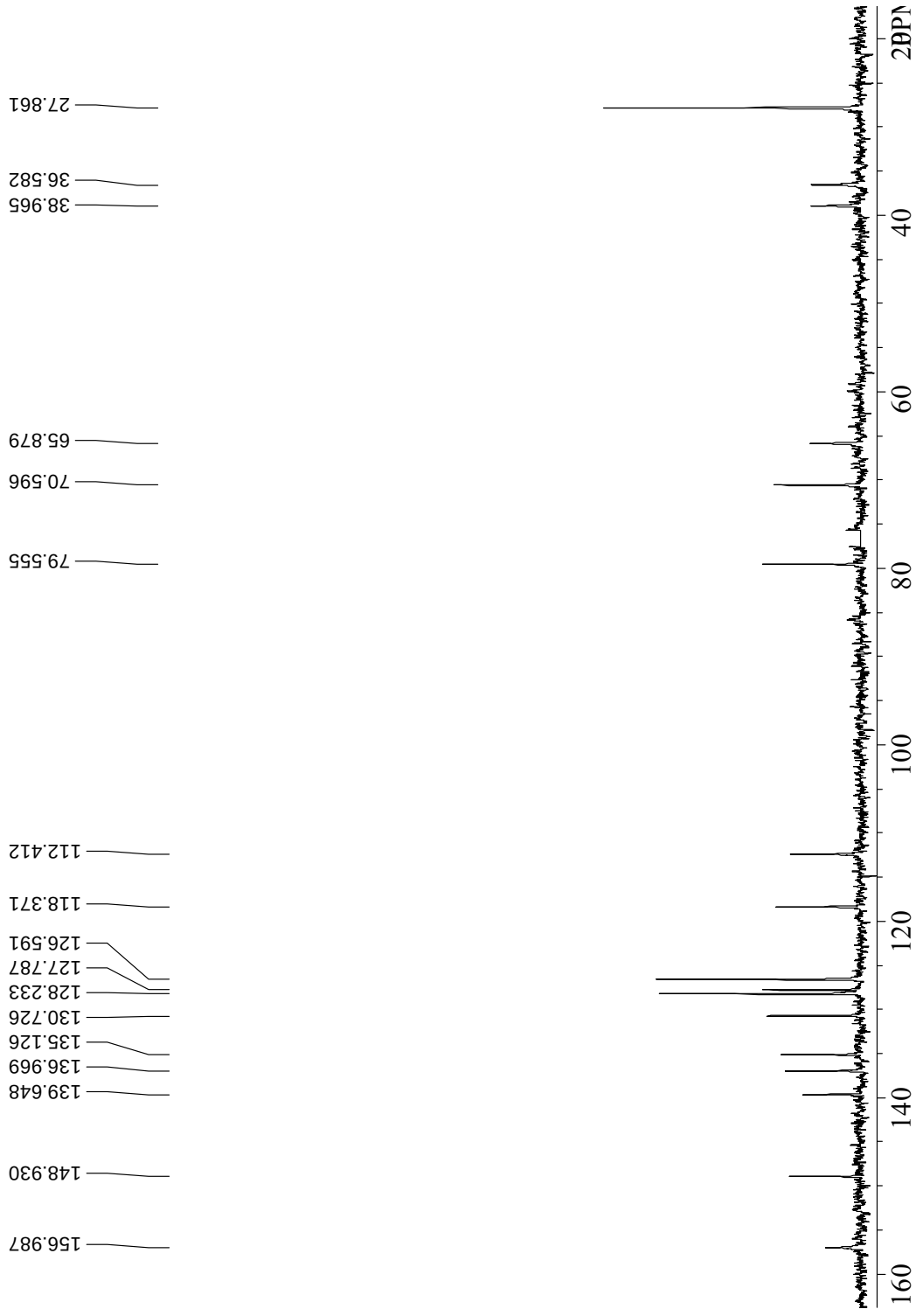

Figure 153. ^{13}C NMR spectrum of *tert*-butyl-3-[3-(benzyloxy)-2-nitrophenyl]-3-hydroxypropylcarbamate (**53**) (75 MHz, $CDCl_3$).

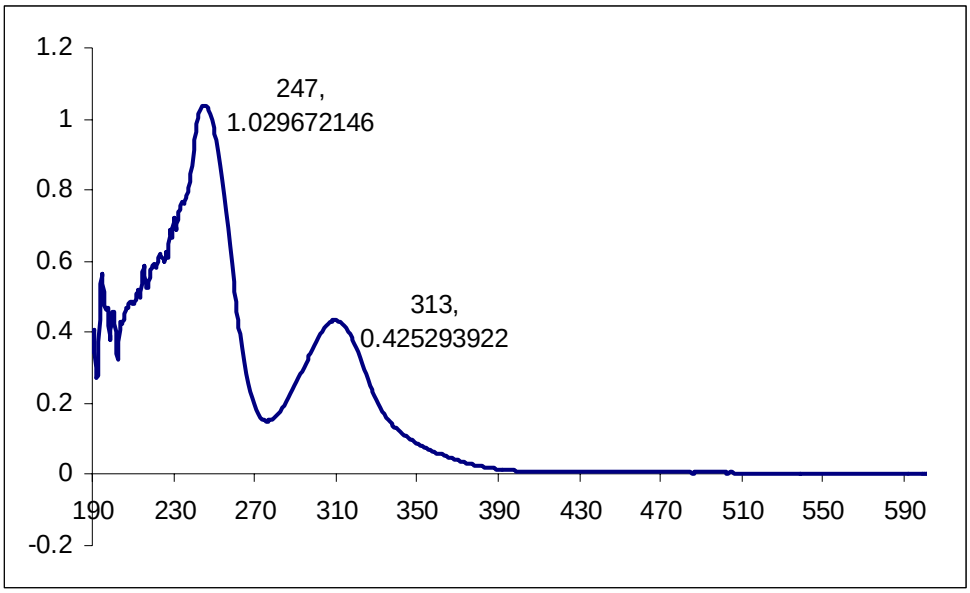

Figure 154. UV spectrum of *tert*-butyl-3-[3-(benzyloxy)-2-nitrophenyl]-3-oxopropylcarbamate (**54**) in $CHCl_3$.

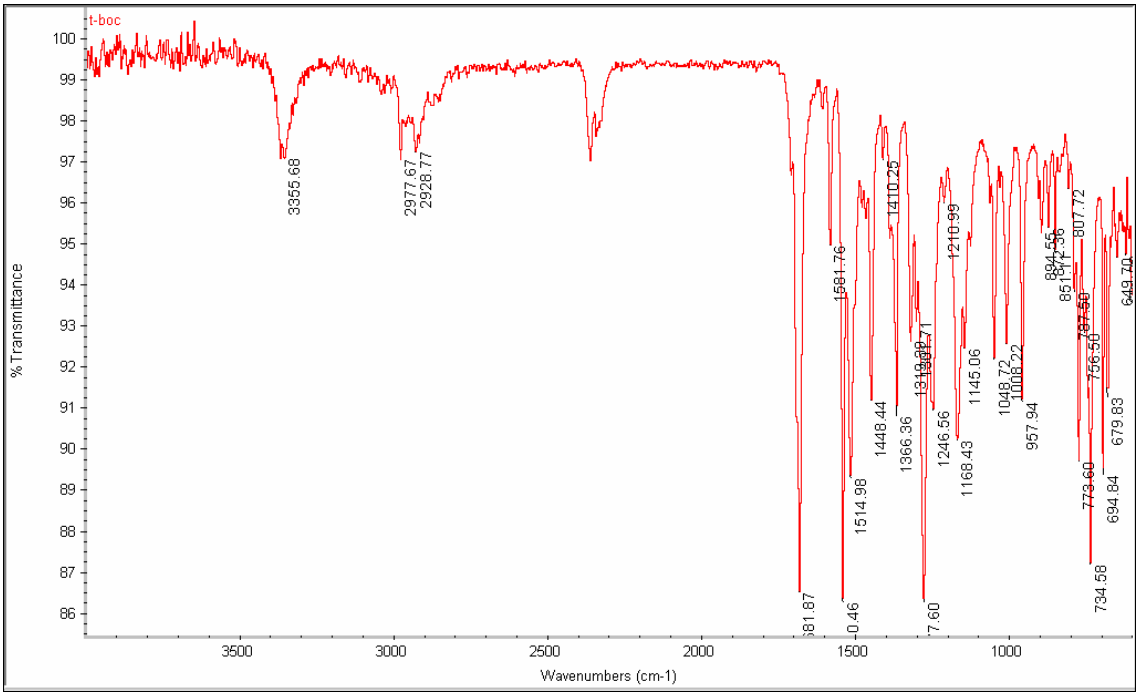

Figure 155. IR spectrum of *tert*-butyl-3-[3-(benzyloxy)-2-nitrophenyl]-3-oxopropylcarbamate (**54**).

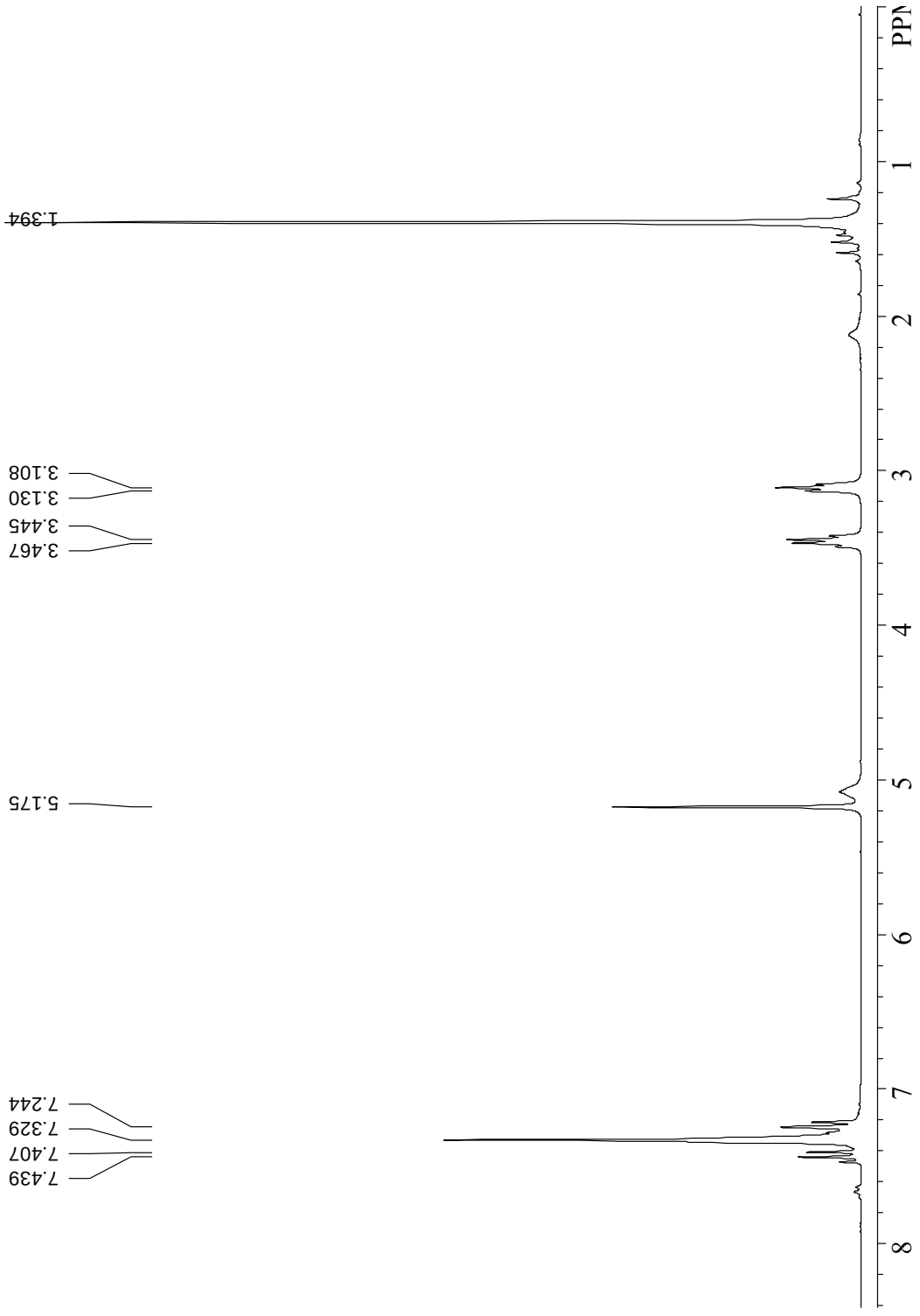

Figure 156. ^{1}H NMR spectrum of *tert*-butyl-3-[3-(benzyloxy)-2-nitrophenyl]-3-oxopropylcarbamate (**54**) (250 MHz, $CDCl_3$).

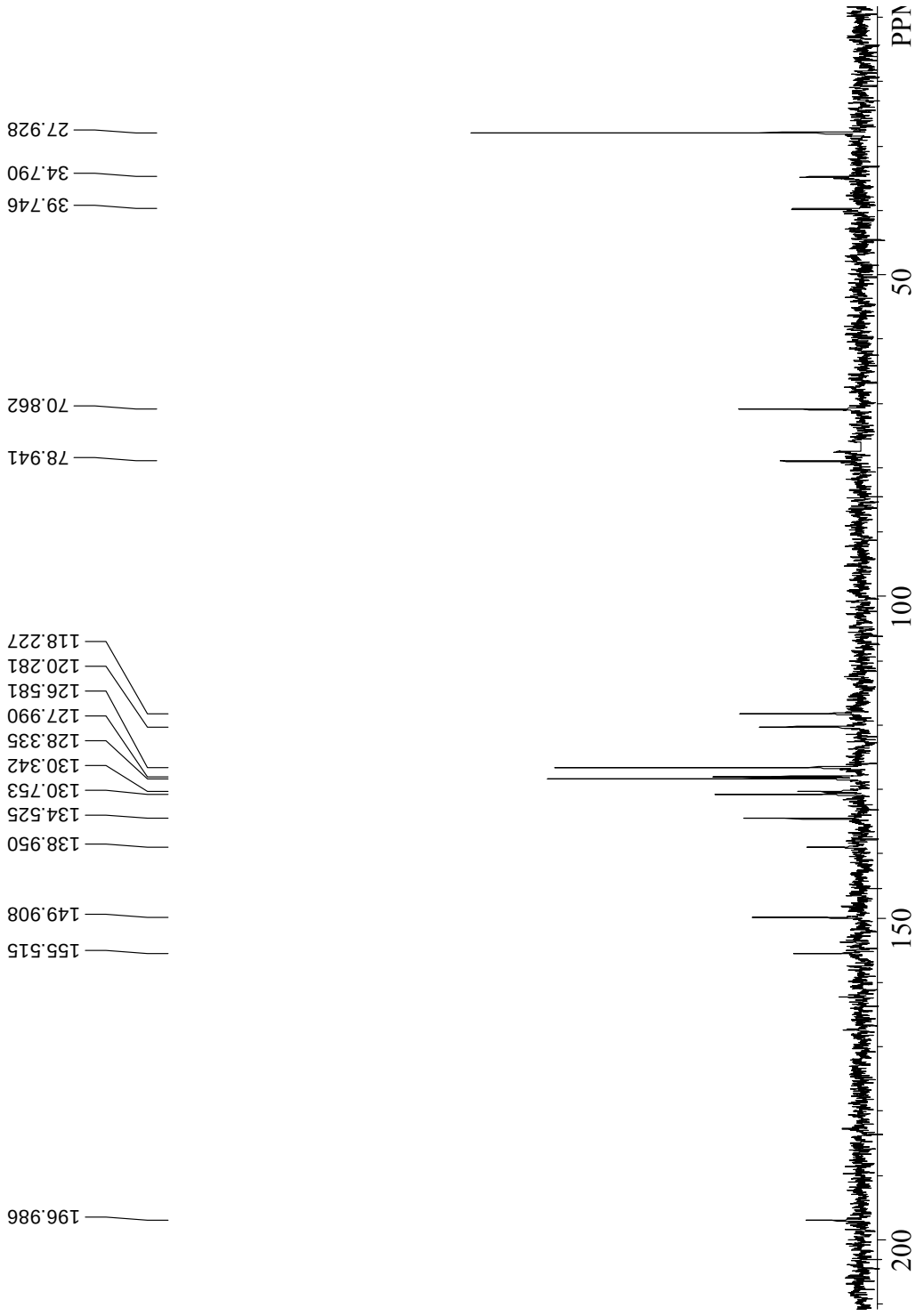

Figure 157. ^{13}C NMR spectrum of *tert*-butyl-3-[3-(benzyloxy)-2-nitrophenyl]-3-oxopropylcarbamate (**54**) (75 MHz, $CDCl_3$).

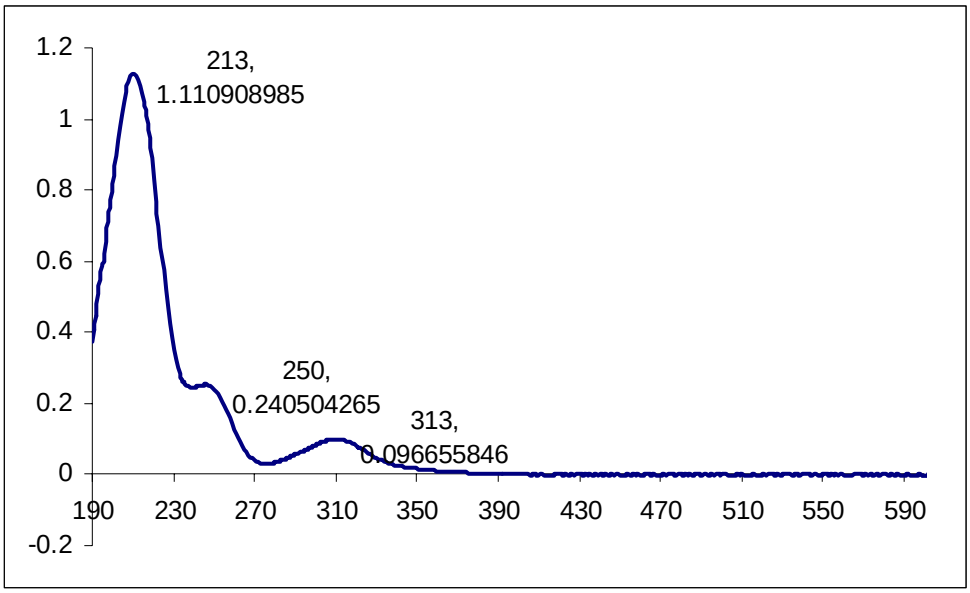

Figure 158. UV spectrum of 3-amino-1-[3-(benzyloxy)-2-nitrophenyl]propan-1-one hydrochloride (**55**) in MeOH.

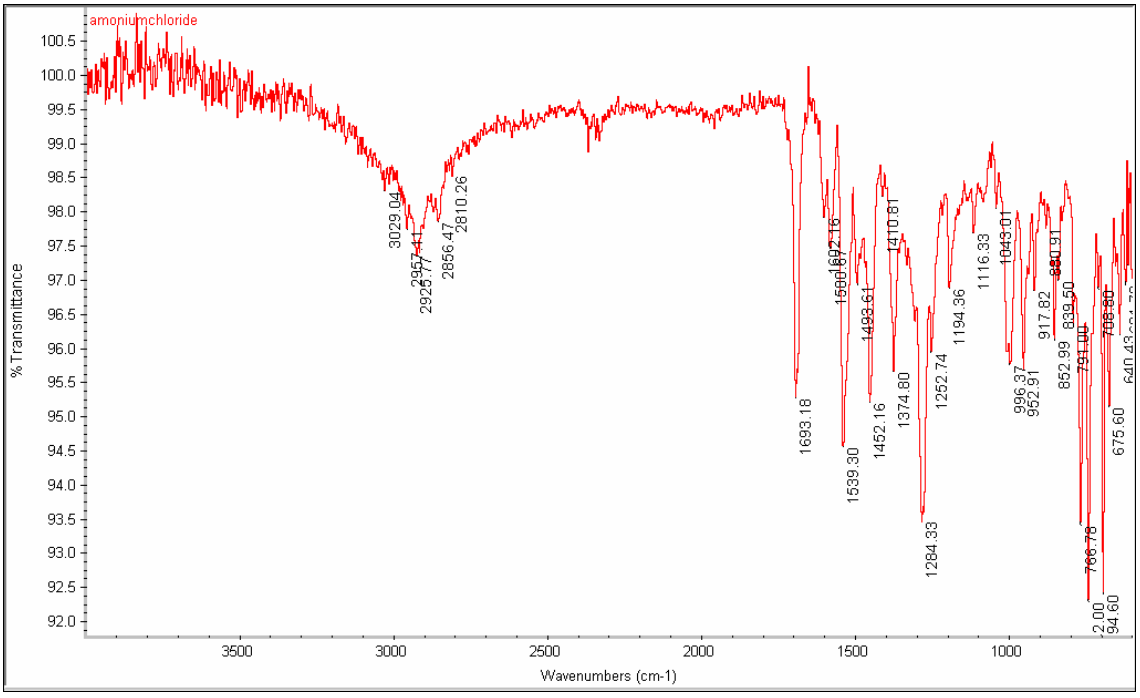

Figure 159. IR spectrum of 3-amino-1-[3-(benzyloxy)-2-nitrophenyl]propan-1-one hydrochloride (**55**).

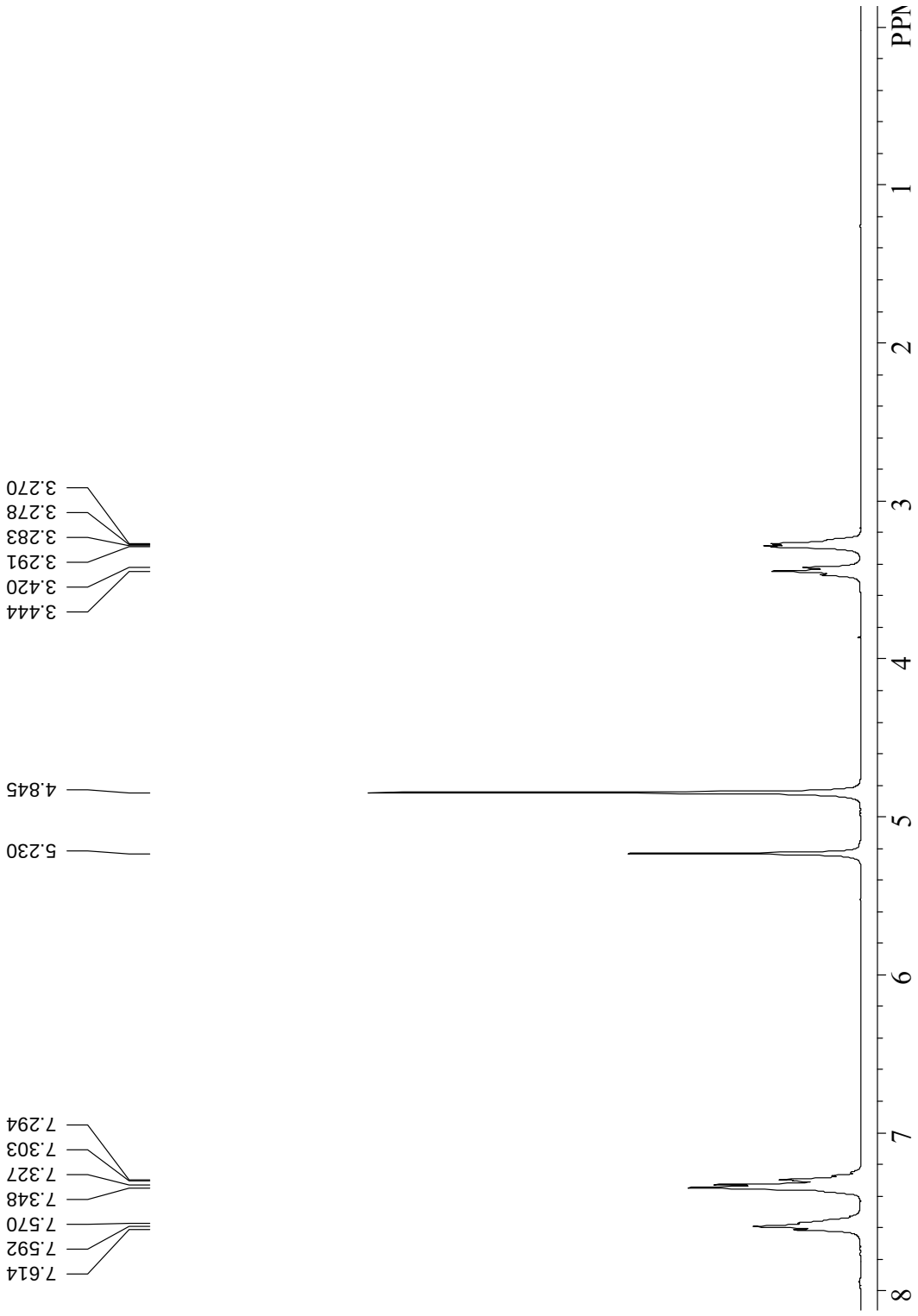

Figure 160. ^{1}H NMR spectrum of 3-amino-1-[3-(benzyloxy)-2-nitrophenyl]propan-1-one hydrochloride (**55**) (250 MHz, MeOH-d_4).

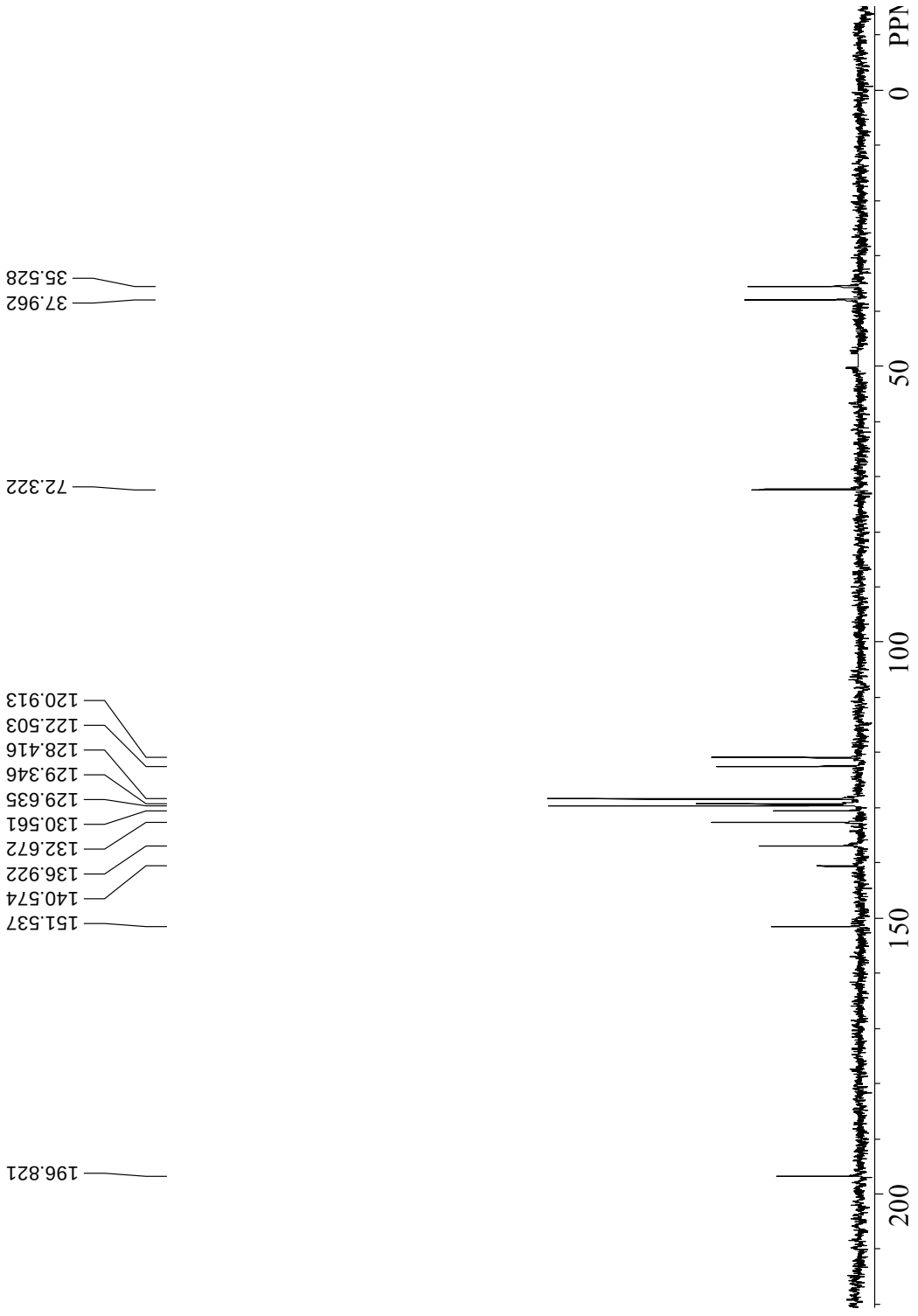

Figure 161. ^{13}C NMR spectrum of 3-amino-1-[3-(benzyloxy)-2-nitrophenyl]propan-1-one hydrochloride (**55**) (75 MHz, MeOH-d_4).

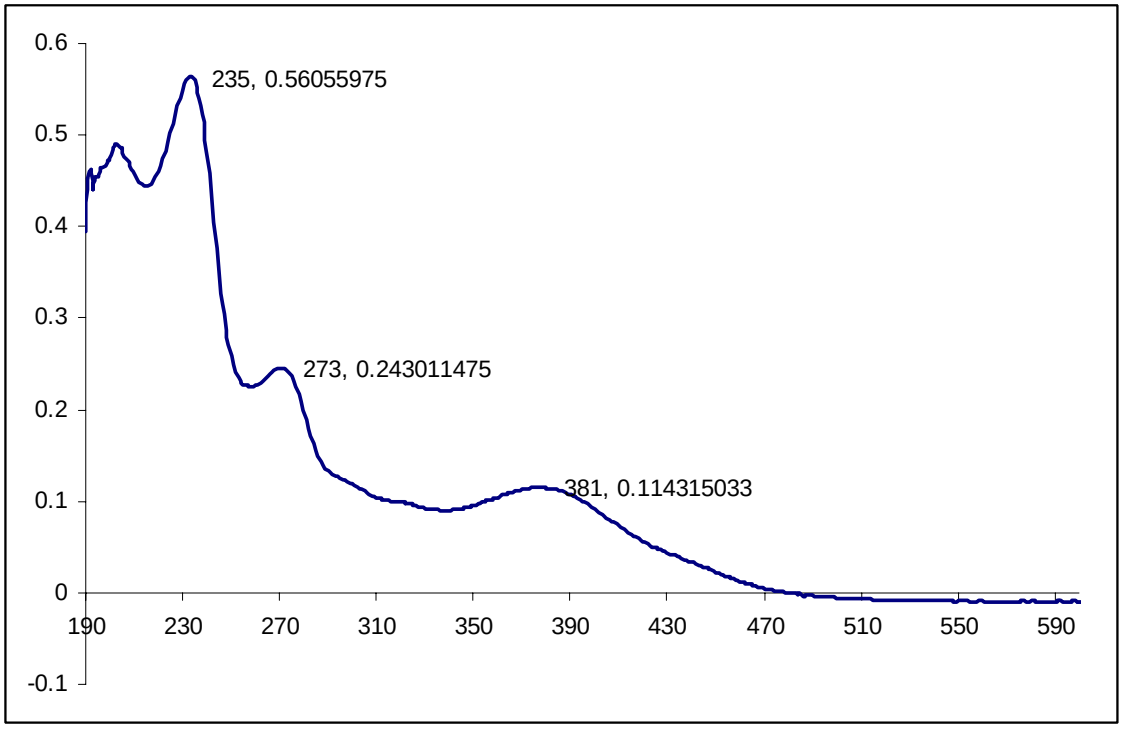

Figure 162. UV spectrum of erebusinonamine (**52**) in MeOH.

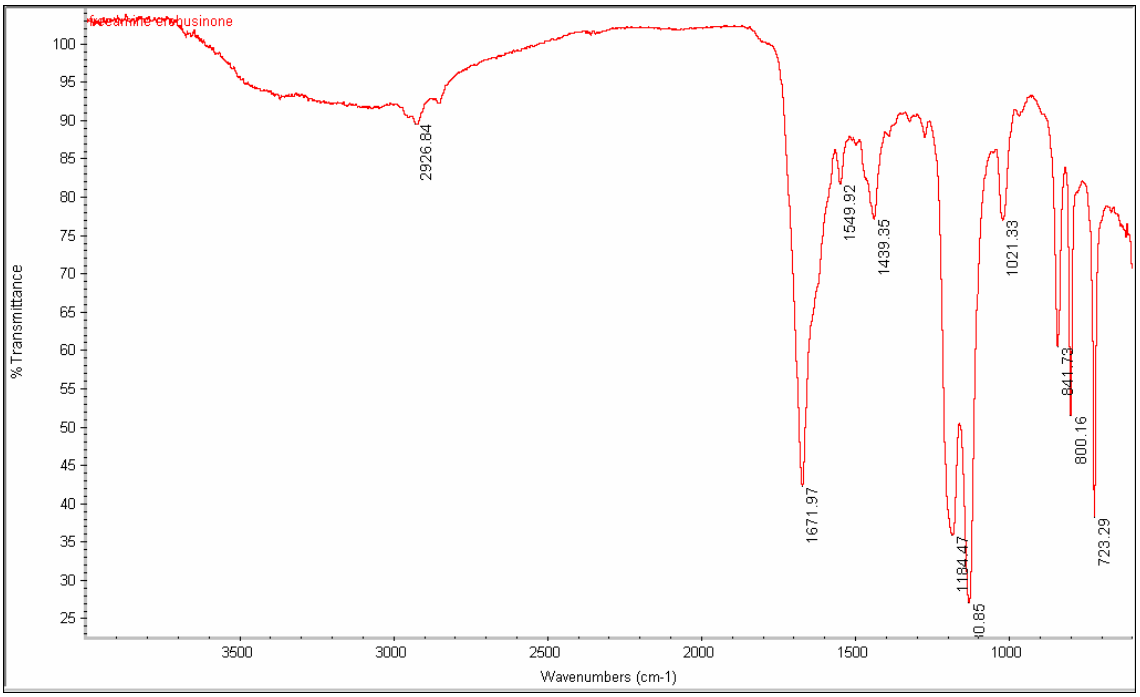

Figure 163. IR spectrum of erebusinonamine (**52**).

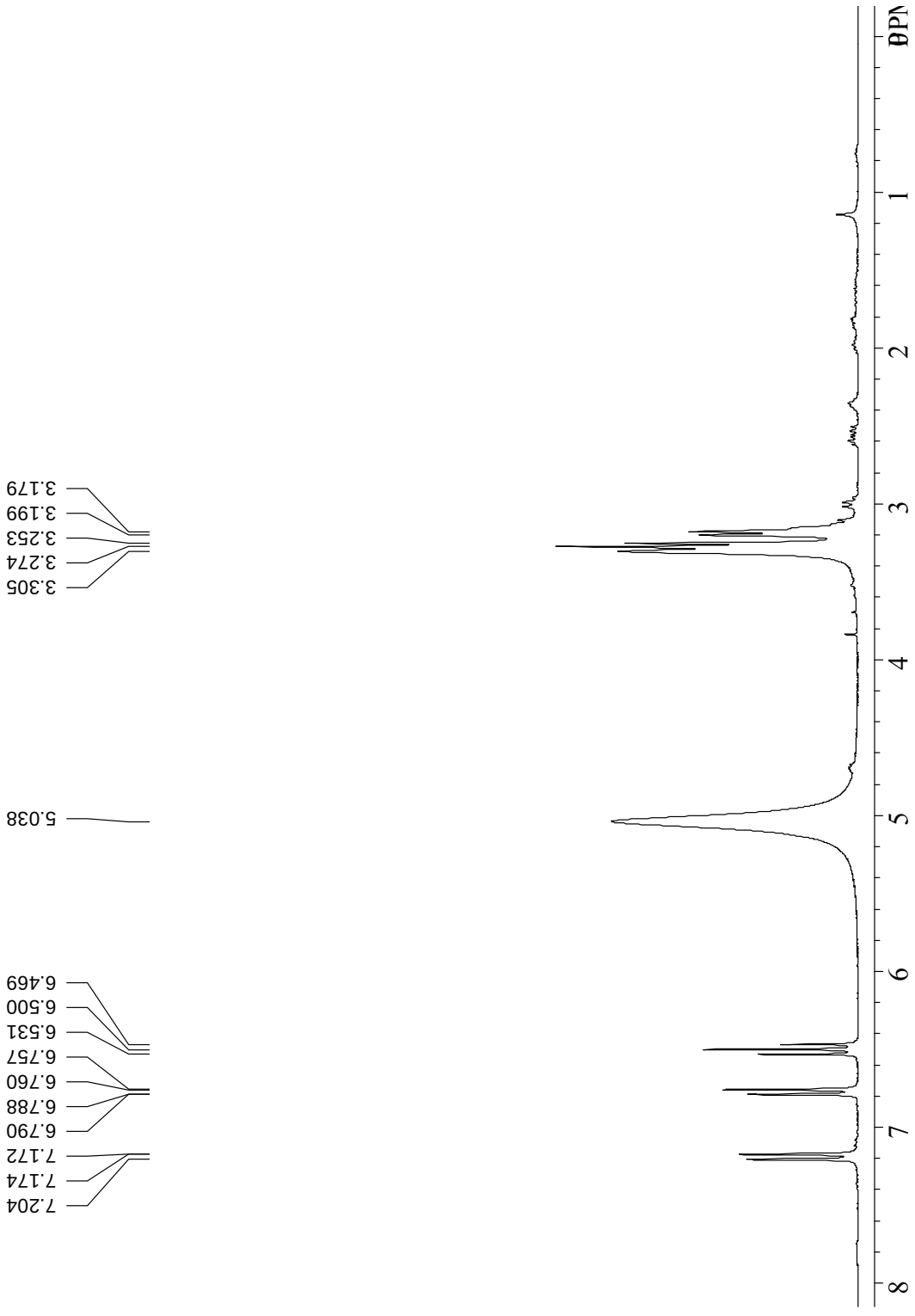

Figure 164. ^{1}H NMR spectrum of erebusinonamine (**52**) (250 MHz, MeOH-d_4).

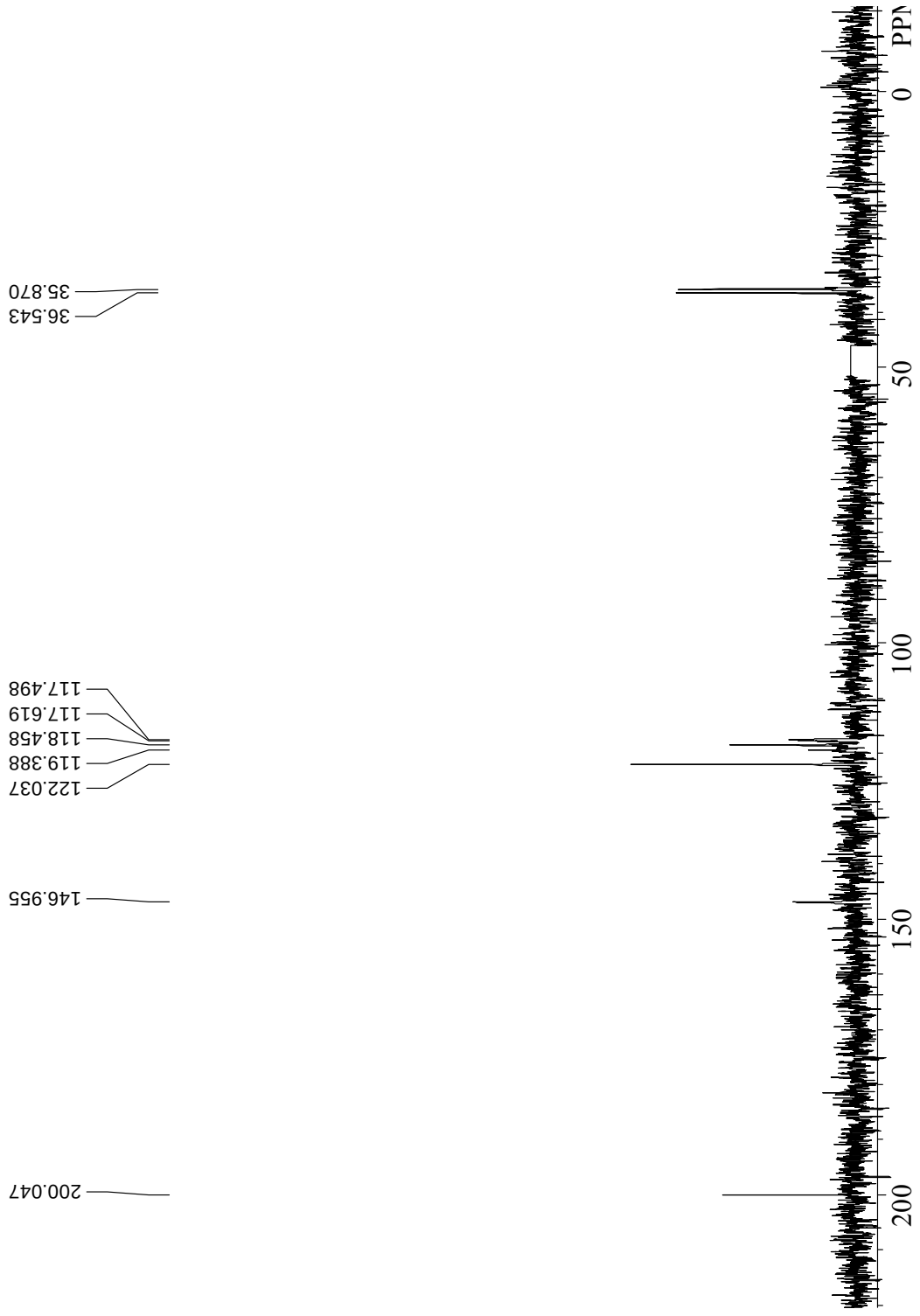

Figure 165. ^{13}C NMR spectrum of erebusinonamine (**52**) (75 MHz, MeOH-d_4).

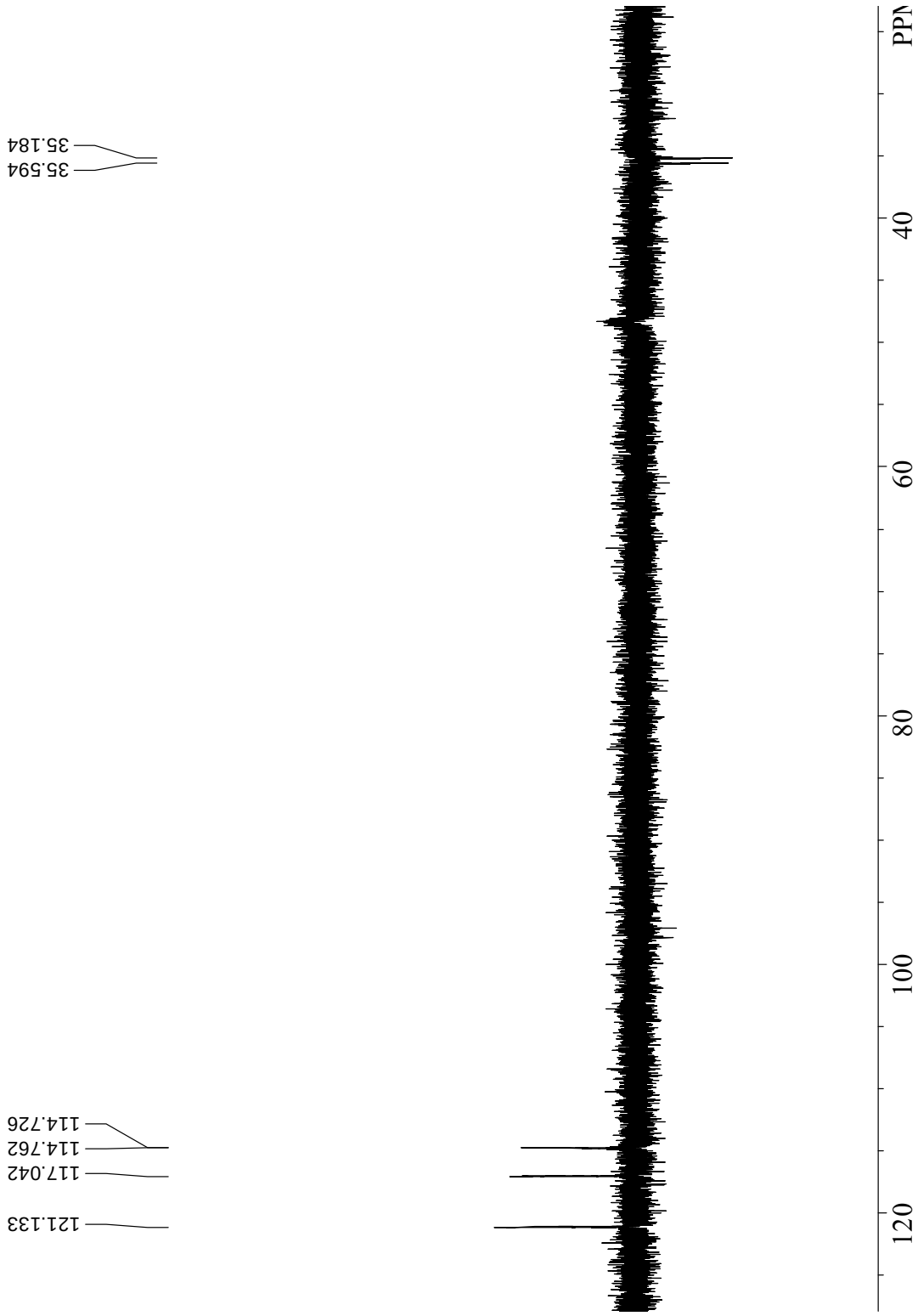

Figure 166. DEPT-135 spectrum of erebusinonamine (**52**) (125 MHz, MeOH-d_4).

ABOUT THE AUTHOR

Young Chul Park received a M.S. with honors in chemistry from Dankook University, Seoul, Korea in the year 1990. He then worked in Korea for 8 years on natural products chemistry and also on total synthesis of natural products at Esung pharmaceutical company. He joined the Department of Chemistry at Florida Institute of Technology in 1999 for his Ph.D. program under the supervision of Dr. Bill J. Baker. His research is based on the isolation of secondary metabolites from Antarctic marine organisms and total synthesis of natural products. He relocated along with his supervisor Dr. Bill J. Baker to Department of Chemistry, University of South Florida in 2001 to continue his Ph.D. program. He has coauthored two publications in *Tetrahedron* and *J. Nat. Prod*. He also gave several presentations at international meetings of the American Chemical Society and the American Society of Pharmacognosy in 2003.